frontiers | Research Topics

Strategies for mitigating zoonotic influenza outbreaks: a comprehensive preparedness approach

Edited by
Sneha Vishwanath, Hazel Stewart and Sankaran Sandhya

Published in
Frontiers in Public Health

ISSN 1664-8714
ISBN 978-2-8325-6865-1
DOI 10.3389/978-2-8325-6865-1

Generative AI statement
Any alternative text (Alt text) provided alongside figures in the articles in this ebook has been generated by Frontiers with the support of artificial intelligence and reasonable efforts have been made to ensure accuracy, including review by the authors wherever possible. If you identify any issues, please contact us.

About Frontiers

Frontiers is more than just an open access publisher of scholarly articles: it is a pioneering approach to the world of academia, radically improving the way scholarly research is managed. The grand vision of Frontiers is a world where all people have an equal opportunity to seek, share and generate knowledge. Frontiers provides immediate and permanent online open access to all its publications, but this alone is not enough to realize our grand goals.

Frontiers journal series

The Frontiers journal series is a multi-tier and interdisciplinary set of open-access, online journals, promising a paradigm shift from the current review, selection and dissemination processes in academic publishing. All Frontiers journals are driven by researchers for researchers; therefore, they constitute a service to the scholarly community. At the same time, the *Frontiers journal series* operates on a revolutionary invention, the tiered publishing system, initially addressing specific communities of scholars, and gradually climbing up to broader public understanding, thus serving the interests of the lay society, too.

Dedication to quality

Each Frontiers article is a landmark of the highest quality, thanks to genuinely collaborative interactions between authors and review editors, who include some of the world's best academicians. Research must be certified by peers before entering a stream of knowledge that may eventually reach the public - and shape society; therefore, Frontiers only applies the most rigorous and unbiased reviews. Frontiers revolutionizes research publishing by freely delivering the most outstanding research, evaluated with no bias from both the academic and social point of view. By applying the most advanced information technologies, Frontiers is catapulting scholarly publishing into a new generation.

What are Frontiers Research Topics?

Frontiers Research Topics are very popular trademarks of the *Frontiers journals series*: they are collections of at least ten articles, all centered on a particular subject. With their unique mix of varied contributions from Original Research to Review Articles, Frontiers Research Topics unify the most influential researchers, the latest key findings and historical advances in a hot research area.

Find out more on how to host your own Frontiers Research Topic or contribute to one as an author by contacting the Frontiers editorial office: frontiersin.org/about/contact

Strategies for mitigating zoonotic influenza outbreaks: a comprehensive preparedness approach

Topic editors
Sneha Vishwanath — University of Cambridge, United Kingdom
Hazel Stewart — University of Cambridge, United Kingdom
Sankaran Sandhya — On a sabbatical, Bangalore, India

Citation
Vishwanath, S., Stewart, H., Sandhya, S., eds. (2025). *Strategies for mitigating zoonotic influenza outbreaks: a comprehensive preparedness approach*. Lausanne: Frontiers Media SA. doi: 10.3389/978-2-8325-6865-1

Dr. Sneha Vishwanath declares that she is named on 6 patents related to influenza and coronavirus vaccines, affiliated with the University of Cambridge.

Table of contents

05 Editorial: Strategies for mitigating zoonotic influenza outbreaks: a comprehensive preparedness approach
Sneha Vishwanath, Hazel Stewart and Sankaran Sandhya

08 Toward One Health: a spatial indicator system to model the facilitation of the spread of zoonotic diseases
Daniel Jato-Espino, Fernando Mayor-Vitoria, Vanessa Moscardó, Fabio Capra-Ribeiro and Leticia E. Bartolomé del Pino

25 Epidemiology and phylodynamics of multiple clades of H5N1 circulating in domestic duck farms in different production systems in Bangladesh
Ariful Islam, Mohammad Enayet Hossain, Emama Amin, Shariful Islam, Monjurul Islam, Md Abu Sayeed, Md Mehedi Hasan, Mojnu Miah, Mohammad Mahmudul Hassan, Mohammed Ziaur Rahman and Tahmina Shirin

38 Protocol for establishing a model for integrated influenza surveillance in Tamil Nadu, India
Rizwan S. Abdulkader, Varsha Potdar, Gulam Mohd, Joshua Chadwick, Mohan Kumar Raju, S. Devika, Sumit Dutt Bharadwaj, Neeraj Aggarwal, Neetu Vijay, C. Sugumari, T. Sundararajan, V. Vasuki, N. Bharathi Santhose, C. A. Mohammed Razik, Vinoth Madhavan, N. C. Krupa, Nandhini Prabakaran, Manoj V. Murhekar and Nivedita Gupta

46 Coverage and impact of influenza vaccination among children in Minhang District, China, 2013–2020
Zhaowen Zhang, Liming Shi, Nian Liu, Biyun Jia, Kewen Mei, Liping Zhang, XuanZhao Zhang, Yihan Lu, Jia Lu and Ye Yao

55 A semi-empirical risk panel to monitor epidemics: multi-faceted tool to assist healthcare and public health professionals
Aida Perramon-Malavez, Mario Bravo, Víctor López de Rioja, Martí Català, Sergio Alonso, Enrique Álvarez-Lacalle, Daniel López, Antoni Soriano-Arandes and Clara Prats

68 The effectiveness of intervention measures on MERS-CoV transmission by using the contact networks reconstructed from link prediction data
Eunmi Kim, Yunhwan Kim, Hyeonseong Jin, Yeonju Lee, Hyosun Lee and Sunmi Lee

84 Enhancing mass vaccination programs with queueing theory and spatial optimization
Sherrie Xie, Maria Rieders, Srisa Changolkar, Bhaswar B. Bhattacharya, Elvis W. Diaz, Michael Z. Levy and Ricardo Castillo-Neyra

97 Investigation of human infection with H5N6 avian influenza cases in Sichuan Province from 2014 to 2024: a retrospective study
Lijun Zhou, Zhirui Li, Xingyu Zhou, Lin Zhao, Huanwen Peng, Xunbo Du, Jianping Yang, Fengmiao Hu, Shuang Dong, Baisong Li, Guidan Liu, Hongyu Tang, Xiao Lei, Xiaojuan Wang, Shunning Zhao, Ping Zhou, Heng Yuan and Chongkun Xiao

109 Epidemiological trends of influenza A and B in one hospital in Chengdu and national surveillance data (2019–2024)
Xiang Li, Chenlijie Yang, Lu Chen, Jian Ma and Zhongliang Hu

120 Exploring influenza vaccination coverage and barriers to influenza vaccine uptake among preschool children in Fuzhou in 2022: a cross-sectional study
Haimei Jia, Wenyan Gao, Xun Huang, Qinghua Wang, Yonghan Huang, Liang Chen, Desi Zheng, Yinchuan Zhang and Lifei Xu

130 Highly pathogenic avian influenza: pandemic preparedness for a scenario of high lethality with no vaccines
Cristina Possas, Ernesto T. A. Marques, Alessandra Oliveira, Suzanne Schumacher, Marilda M. Siqueira, John McCauley, Adelaide Antunes and Akira Homma

frontiers | Frontiers in Public Health

TYPE Editorial
PUBLISHED 03 September 2025
DOI 10.3389/fpubh.2025.1685224

OPEN ACCESS

EDITED AND REVIEWED BY
Marc Jean Struelens,
Université Libre de Bruxelles, Belgium

*CORRESPONDENCE
Sneha Vishwanath
✉ sv446@cam.ac.uk
Hazel Stewart
✉ hs623@cam.ac.uk
Sankaran Sandhya
✉ sandhyagovind@gmail.com

RECEIVED 13 August 2025
ACCEPTED 20 August 2025
PUBLISHED 03 September 2025

CITATION
Vishwanath S, Stewart H and Sandhya S (2025) Editorial: Strategies for mitigating zoonotic influenza outbreaks: a comprehensive preparedness approach.
Front. Public Health 13:1685224.
doi: 10.3389/fpubh.2025.1685224

Editorial: Strategies for mitigating zoonotic influenza outbreaks: a comprehensive preparedness approach

Sneha Vishwanath[1]*, Hazel Stewart[2]* and Sankaran Sandhya[3]*

[1]Department of Veterinary Medicine, University of Cambridge, Cambridge, United Kingdom, [2]Department of Pathology, University of Cambridge, Cambridge, United Kingdom, [3]Independent Researcher, Bengaluru, India

KEYWORDS

zoonotic influenza, pandemic preparedness and response, one-health approach, epidemiological studies, mathematical modeling, public health education, surveillance

Editorial on the Research Topic
Strategies for mitigating zoonotic influenza outbreaks: a comprehensive preparedness approach

Introduction

The spillover of zoonotic influenza viruses into human populations and non-reservoir hosts such as cows, seals, and other animals continues to pose a significant threat to global public health. The emergence of strains like H5N1, H5N6, and H7N9 has not only disrupted societies but also tested—and at times overwhelmed—public health systems worldwide. With a growing human population, encroachment into wildlife habitats, climate change, and intensified human-animal interactions, the frequency and impact of zoonotic spillovers is expected to increase. To counter this looming threat, it is essential that we move beyond traditional, reactive approaches and adopt a robust, forward-looking preparedness strategy.

A key pillar in combating zoonotic influenza outbreaks is the One Health approach, which recognizes the interdependence of human, animal, and environmental health. This approach must form the foundation of any preparedness plan.

Key strategies under the one-health approach to mitigate zoonotic influenza outbreaks.

Surveillance and early detection

Effective surveillance is vital for early detection and timely containment of zoonotic influenza outbreaks. Advancements in genomic sequencing, digital health systems, and data-sharing platforms have enabled real-time monitoring of viral mutations and disease burden, as evidenced during the COVID-19 pandemic. Possas et al., advocate for a shift from reactive approaches to a globally coordinated surveillance system which utilizes our

advancements in technology. This is particularly relevant given the potential emergence of high-lethality influenza pandemics without available vaccines. Such surveillance systems must be integrated across veterinary, agricultural, and public health sectors. Early warning signals from poultry, swine, or wild birds can offer critical lead time for human health systems to prepare and respond.

For instance, a case study in India advocates the importance of integrating surveillance within existing public health frameworks. Abdulkader et al., detailed a comprehensive model in the Indian state of Tamil Nadu that combines clinical and epidemiological data with molecular diagnostics for effective early detection and response.

Similarly, a retrospective study by Zhou et al., on H5N6 outbreaks in Sichuan, China (2014–2024) highlights the importance of environmental surveillance in live poultry markets, farms, and migratory bird habitats, noting that human cases although rare were often fatal due to delayed treatment and co-morbidities.

Risk assessment and modeling of transmission

Each zoonotic spillover—regardless of its initial scale—warrants rigorous risk assessment and modeling to forecast its trajectory within human populations and ecosystems. Islam et al., examined H5N1 transmission patterns in Bangladesh's domestic duck farming systems, highlighting the need for tailored surveillance and control strategies. Integrating local and national data sources, as shown by Li et al., ensures accurate assessment of non-seasonal influenza activity.

Modeling tools have also emerged as essential components of early warning systems. Perramon-Malavez et al., introduced a simplified tool adapted from the Moving Epidemic Method (MEM), predicting epidemic thresholds 6–7 days in advance for Influenza using the Effective Potential Growth (EPG) index. Jato-Espino et al., presented a spatial indicator system integrating ecological, environmental, and socio-economic data to identify high-risk transmission zones and support targeted interventions.

Controlling transmission

Once human infections begin, transmission can be curtailed through two major approaches: (1) Isolation and quarantine, and (2) Vaccination campaigns. Isolation and quarantine, especially in the early stages of outbreaks, remain effective in the absence of vaccines. Kim et al., used machine learning to simulate the spread of MERS-CoV and found that targeted quarantining of cases and contacts outperformed mass isolation strategies in both efficiency and effectiveness. A strategy that could be extrapolated to zoonotic influenza outbreak. Once vaccines become available, population-wide immunization is the most efficient strategy. Xie et al., recommend optimizing vaccination site placements by minimizing queue times—a crucial lesson from the COVID-19 experience. Long wait times can deter participation and erode public trust.

In addition, computational advances have enabled the development of broadly protective vaccine antigens, as discussed by Possas et al., offering hope for variant-proof vaccine designs for Influenza.

Public awareness and education

Public awareness is central to both prevention and control. Understanding zoonotic transmission pathways and the importance of vaccines is critical to public cooperation. Jia et al., highlight that low influenza vaccine coverage in children is often due to structural and informational gaps. They advocate for better parental education, easier access to vaccines at local clinics, and public awareness campaigns. Zhang et al., demonstrated that, even with low vaccination rates among children in Shanghai's Minhang District, vaccination efforts still prevented 6–17% of influenza cases and had substantial indirect benefits. This stresses the importance of community engagement and education in achieving high coverage and reducing disease burden.

To confront the growing threat of zoonotic influenza outbreaks, we must embrace a paradigm shift from reactive to proactive preparedness. By integrating the One Health approach across surveillance, modeling, transmission control, and public education, we can build resilient systems capable of early detection, rapid response, and sustainable prevention. Global health security hinges on our ability to anticipate and adapt. Coordinated action, investment in research, surveillance infrastructure and inclusive public health strategies will be vital. Our preparedness today will determine our resilience tomorrow.

Author contributions

SV: Writing – original draft, Writing – review & editing. HS: Writing – original draft, Writing – review & editing. SS: Writing – original draft, Writing – review & editing.

Conflict of interest

The authors declare that the research was conducted in the absence of any commercial or financial relationships that could be construed as a potential conflict of interest.

Generative AI statement

The author(s) declare that no Gen AI was used in the creation of this manuscript.

Any alternative text (alt text) provided alongside figures in this article has been generated by Frontiers with the support of artificial intelligence and reasonable efforts have been made to ensure accuracy, including review by the authors wherever possible. If you identify any issues, please contact us.

Publisher's note

frontiers | Frontiers in Public Health

TYPE Technology and Code
PUBLISHED 29 June 2023
DOI 10.3389/fpubh.2023.1215574

OPEN ACCESS

EDITED BY
Juarez Antonio Simões Quaresma,
Federal University of Pará, Brazil

REVIEWED BY
Taif Shah,
Kunming University of Science and Technology, China
Jay Paul Graham,
University of California, Berkeley, United States

*CORRESPONDENCE
Daniel Jato-Espino
djato@universidadviu.com

RECEIVED 04 May 2023
ACCEPTED 14 June 2023
PUBLISHED 29 June 2023

CITATION
Jato-Espino D, Mayor-Vitoria F, Moscardó V, Capra-Ribeiro F and Bartolomé del Pino LE (2023) Toward One Health: a spatial indicator system to model the facilitation of the spread of zoonotic diseases.
Front. Public Health 11:1215574.
doi: 10.3389/fpubh.2023.1215574

Toward One Health: a spatial indicator system to model the facilitation of the spread of zoonotic diseases

Daniel Jato-Espino[1]*, Fernando Mayor-Vitoria[1], Vanessa Moscardó[1], Fabio Capra-Ribeiro[1,2] and Leticia E. Bartolomé del Pino[1]

[1]GREENIUS Research Group, Universidad Internacional de Valencia—VIU, Calle Pintor Sorolla, Valencia, Spain, [2]School of Architecture, College of Art and Design, Louisiana State University, Baton Rouge, LA, United States

Recurrent outbreaks of zoonotic infectious diseases highlight the importance of considering the interconnections between human, animal, and environmental health in disease prevention and control. This has given rise to the concept of One Health, which recognizes the interconnectedness of between human and animal health within their ecosystems. As a contribution to the One Health approach, this study aims to develop an indicator system to model the facilitation of the spread of zoonotic diseases. Initially, a literature review was conducted using the Preferred Reporting Items for Systematic Reviews and Meta-Analyses (PRISMA) statement to identify relevant indicators related to One Health. The selected indicators focused on demographics, socioeconomic aspects, interactions between animal and human populations and water bodies, as well as environmental conditions related to air quality and climate. These indicators were characterized using values obtained from the literature or calculated through distance analysis, geoprocessing tasks, and other methods. Subsequently, Multi-Criteria Decision-Making (MCDM) techniques, specifically the Entropy and Technique for Order of Preference by Similarity to Ideal Solution (TOPSIS) methods, were utilized to combine the indicators and create a composite metric for assessing the spread of zoonotic diseases. The final indicators selected were then tested against recorded zoonoses in the Valencian Community (Spain) for 2021, and a strong positive correlation was identified. Therefore, the proposed indicator system can be valuable in guiding the development of planning strategies that align with the One Health principles. Based on the results achieved, such strategies may prioritize the preservation of natural landscape features to mitigate habitat encroachment, protect land and water resources, and attenuate extreme atmospheric conditions.

KEYWORDS

geographic information system, multi-criteria decision-making, green infrastructure, indicators, one health, systematic literature review

1. Introduction

Zoonotic diseases pose a significant public health concern, with over 70% of emerging diseases being transmitted from animals to humans and 60% of human infectious diseases being shared with animals (1). This means that zoonotic diseases have played a role in recent outbreaks, including Ebola and coronavirus pandemics, as well as in well-known foodborne illnesses. These

diseases can be transmitted not only through direct contact with animals or vectors, or the ingestion of animal products, but also through the consumption of contaminated vegetables grown in areas where domestic or wild animal manure or irrigation water is used (2).

The transmission of zoonotic diseases is a complex and multifactorial process, making it difficult to manage and predict due to the interconnected elements involved. Therefore, an interdisciplinary approach is necessary; focusing not only on disease surveillance but also on the development of predictive models (3).

The concept of One Health is crucial for today's sustainable human development. One Health is "an approach that recognizes people's health, closely connected to the health of animals and our shared environment" (4). The recurrence of outbreaks of emerging and re-emerging zoonotic diseases has emphasized the importance of the One Health approach, which acknowledges the interconnectedness of human, animal, and environmental health (5, 6). Achieving One Health requires a comprehensive understanding of the complex interactions and feedback between these systems and the identification of interventions that can promote positive outcomes for all (7). However, measuring progress toward One Health goals remains challenging, and various initiatives have employed different indicator systems to address this issue (8–10).

There is an ongoing debate on the most effective way to measure progress toward One Health goals (11–14), but there is a clear relationship between contagious diseases and spatial configurations and conditions (15, 16). The exponential growth of human population has disrupted the interface between humans, animals, and the environment through increased urbanization and the expansion of livestock and agricultural areas (17). These processes lead to the fragmentation of wildlife habitats that increase interspecies friction and the spread of pathogens. For example, it has been argued that certain infectious diseases are exacerbated by factors such as rapid urbanization, large migrant workers populations, climate change, ecological changes, and policies like deforestation (18).

Spatial assessment of disease susceptibility or transmissibility is crucial for the One Health approach as it helps identify areas where zoonotic diseases are more likely to occur and spread. Understanding the relationship between different spatial configurations and the spread of pathogens is essential to reduce the transmission of infectious diseases (17, 19, 20). However, it is a complex and challenging subject.

The number of publications examining the relationship between spatial configuration and the spread of infectious diseases increased from 100 in 2000 to over 700 publications in 2017 (20). This highlights the growing interest in this field and the motivation behind conducting a systematic literature review to better understand what had been done previously.

Previous research has addressed this issue from different perspectives. There is a general trend toward interdisciplinary strategies (17), although the focus has often been on program implementation rather than contextual research (21). More specifically, the analysis diverges in multiple directions. The interest in modeling methodologies has been of particular interest, but different approaches have been taken. Some authors have incorporated census data, land use information, and population mobility into their model design (22), while others have examined multiple cases to understand how mathematical models can generate robust evidence and shape effective public health policies at local and global levels (23). Recent research shows a notable trend toward automation and the development of more complex models.

Significant research has attempted to understand how proximity to Green Infrastructure (GI), which refers to a network of natural and semi-natural areas, can help improve human health (24). Other studies have focused on zoonoses related to ecosystems, assessing their impact on human health while examining the existing evidence of ecological responses to global changes (25). Recent studies have emphasized the need for a holistic approach within the concept of One Health to predict and prevent future pandemics (26, 27). Some models have considered different spatial conditions (28), while others have focused on specific species (29). An important percentage analyzed specific outbreaks in detail (e.g. (30–33),). In these cases, the proliferation of Geographic Information Systems (GIS) has contributed to a better understanding of the role of space in pathogen spillover (34, 35). For more details, refer to (36–39).

In general, the study of previous research has provided insights into the strong relationship between the spread of diseases and various spatial conditions. However, we could not find any studies specifically addressing how these spatial conditions could represent susceptibility or weaknesses that contribute to the faster, stronger, or broader spread of zoonotic diseases. Apart from the previously mentioned approaches, some authors have worked on developing indicators to better understand One Health conditions (8, 9, 40), but they used qualitative research based on binary logic, were conducted at the regional/national scale, or were somehow not holistic and complex enough to capture all the conditions prevailing in the area. In other words, to address a given area using the One Health framework, holistic tools to assess its spatial susceptibility need to be developed.

This research helps to fill this knowledge gap by developing a spatial indicator system that models the facilitation of zoonotic diseases spread, providing insights into a region's contribution to One Health. The proposed indicator system takes a multidimensional approach for One Health, incorporating indicators of human, animal, and environmental health, as well as their interactions. We apply this indicator system to the region of Valencia, Spain, which exhibits diverse ecosystems and land uses including agriculture, urban areas, and natural areas. The novelty of this research lies in the development of a practical tool for measuring a region's contribution to One Health.

As mentioned earlier, One Health requires collaboration among different sectors and stakeholders (41–43). This case study aims to provide policymakers, researchers, and practitioners with a practical tool for monitoring progress toward One Health goals and identifying areas for intervention and improvement. Furthermore, our study seeks to evaluate the usefulness and validity of the proposed indicator system by comparing its results with infectious disease records in the case study area and assessing the potential role of GI in achieving One Health.

This document is structured as follows: first, we review the literature on One Health and indicator systems. Second, we describe the methodology employed to develop the indicator system and apply it to the region of Valencia, Spain. Third, we present the results of our case study and evaluate the utility and validity of the proposed indicator system. Finally, we discuss the implications of our findings and provide recommendations for future research.

2. Materials and methods

The steps for designing and applying the proposed indicator system are depicted in Figure 1. A systematic literature review was first conducted to gain insights into the breadth of prior research on using indicators for One Health goals. The outcomes of the literature review were used to select a list of indicators that encompassed aspects related to animal, human, and environmental health. GIS and Multi-Criteria Decision-Making (MCDM) methods were employed to characterize, weight, and aggregate the shortlisted indicators. This resulted in a composite index that reflects the contributions of a region's spatial context to One Health. These index values were then compared with the area covered by GI to assess its impact on One Health.

2.1. Selection of indicators

The indicators were selected based on the results of a literature review conducted according to the Preferred Reporting Items for Systematic Reviews and Meta-Analyses (PRISMA) statement (44). The literature review aimed to answer the research question: are there any indicators or metrics that have been consistently used to address One Health issues? Finding an answer to this question should result in a set of indicators ranked by their frequency of use in previous research. The inclusion criteria for the review were as follows:

- The publications are original research articles.
- The articles are indexed in the Scopus, Web of Science or PubMed databases.
- The year of publication of the documents is equal to or later than 2004.
- The articles are published in English.

Review articles, conference papers, and books were excluded from the eligible items to focus on original research contributions that utilized indicators to address the One Health initiative. The search included the Scopus, Web of Science, and PubMed databases because of their extensive journal coverage, temporal range, and relevance to medical research, respectively (45). The time frame was limited to 2004 onwards, aligning with the year when the term One Health was coined (46, 47). The documents had to be written in English because of its consideration as the language of science (48).

The search query included the terms "one health," and either "indicator*" or "metric*" in the title, abstract, or keywords of the documents. Additional specific terms related to different facets of the One Health concept, particularly those with spatial implications, were also incorporated into the search query. Eq. (1) presents the search query used in the Scopus database.

TITLE-ABS-KEY ["one health" AND ("indicator*" OR "metric*")] AND ["agricultur*" OR "air" OR "biodiversity" OR "climate change*" OR "disease*" OR "ecologic*" OR "ecosystem*" OR "epidemi*" OR "food" OR "forest*" OR "habitat" OR "land use*" OR "livestock" OR "pollution" OR "population" OR "soil" OR "urban*" OR "warming" OR "water" OR "wildlife"] AND LIMIT-TO (DOCTYPE, "ar")] AND [LIMIT-TO (PUBYEAR, 2022–2004) AND LIMIT-TO (LANGUAGE, "English"]. (1)

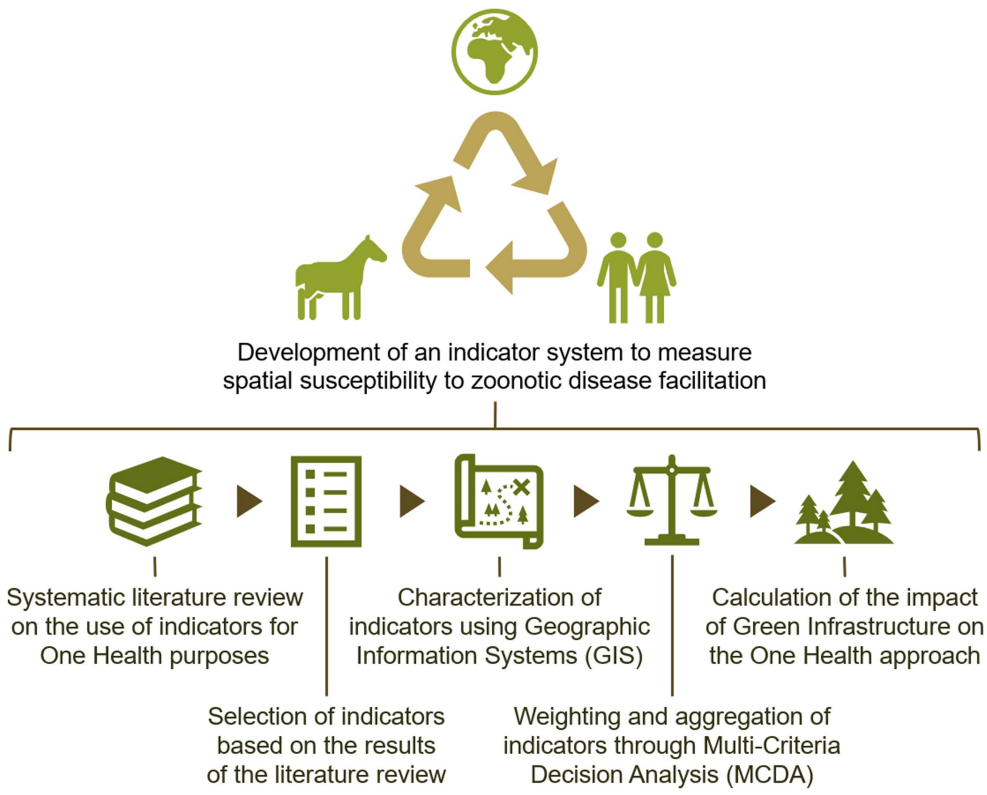

FIGURE 1
Components of the indicator system to measure the facilitation of the spread of zoonotic diseases.

The results from the databases were combined to eliminate duplicates. Aside from the fields returned directly from the query (authors, year, title, abstract, and keywords), a few others were added manually to gather more specific information. One of these fields was used to track the reasons for discarding initially eligible articles. This could be for a variety of reasons, including the article being a review that is not labeled as such, misinterpretation of search query terms (e.g., "one's health" instead of "one health"), or the absence of suggested indicators. Invalid documents could be identified through reading the abstracts or full texts.

Six additional fields were related to the dimensions of One Health. Three fields indicated whether articles emphasized animal, human, or environmental health, while the other three fields recorded the specific terms used for each dimension. Two binary fields were included to indicate whether the articles considered GI and whether they had a spatial component. Another pair of fields compiled the indicators proposed in the papers and derived from reading them.

The screened documents were processed to generate frequency counts from the words contained in some fields, particularly keywords, and indicators, as well as the binary data on the dimensions of One Health and the presence of GI and spatial approaches. After reclassification and standardization, this analysis revealed the main trends found in the articles and created a hierarchy of the most frequently recurring indicators for modeling One Health.

2.2. Processing of indicators

Due to the orientation of the study on the role of spatial planning in the facilitation of zoonotic disease spread, the indicators were designed in a way that allowed them to be characterized using GIS. This involved applying geoprocessing tools to conduct spatial analyses regarding densities, distances, or algebraic operations. The resulting maps were then used to calculate descriptive statistics (mean or sum) per administrative unit through zonal calculations.

The outputs of this characterization process enabled the creation of a matrix of m indicators assessed with x_{ij} values across n administrative units. This arrangement resembles an MCDM problem, where multiple alternatives are evaluated depending on a set of criteria (49). MCDM problems broadly consist of two steps: weighting of criteria (indicators) and assessment of alternatives (administrative units) across the weighted criteria (50). Given the multiple branches that stem from the concept of One Health, the selection of indicators aimed to capture different aspects of environmental, human, and animal health.

2.2.1. Weighting of indicators

The weighting of indicators was performed using the Entropy Method (EM), which was proposed by Zeleny (51) to objectively calculate the weights of criteria in decision-making processes. The importance of a criterion is assumed to be proportional to the amount of information it provides about the alternatives. The idea is to give more weight to the criterion that can better discriminate the other options, i.e., the criterion that shows greater diversity when evaluating the other options. The higher the entropy (E_j), the lower the diversity ($1 - E_j$).

In this study, the EM was employed to determine the weights of indicators based on their differentiation. Indicators that exhibited more distinct values across the administrative units contained more information and had lower entropy (52). This implies large weights for indicators with low entropy values and vice versa. For example, if all administrative units had very similar values (e.g., from 0.5 to 0.6) regarding a particular indicator, that indicator would be given a low weight. Conversely, if another indicator exhibited a wide range of values (e.g., from 0.1 to 0.9) across the administrative units, it would be assigned a higher weight.

To enable a proper comparison of the index dimensions within the decision-making matrix a max-min transformation was applied to normalize the values x_{ij} of the m indicators across the n administrative units, as shown in Eq. (2). Transformation ensured that the indicator values were on a comparable scale.

$$r_{ij} = \begin{cases} \dfrac{x_{ij} - \min x_j}{\max x_j - \min x_j}, \textit{for benefit indicators} \\ \dfrac{\max x_j - x_{ij}}{\max x_j - \min x_j}, \textit{for cost indicators} \end{cases} \quad (2)$$

where $\max x_j$ and $\min x_j$ are the maximum and minimum values among the alternatives for indicator j. The entropy E_j of each indicator was determined from the normalized values r_{ij} as formulated in Eq. (3).

$$E_j = -\frac{\sum_{i=1}^{n} f_{ij} \cdot \ln f_{ij}}{\ln n} (i = 1, \ldots, n, j = 1, \ldots, m) \quad (3)$$

where $f_{ij} = r_{ij} / \sum_{i=1}^{n} r_{ij}$. For the applicability of the method, the entire term $f_{ij} \cdot \ln f_{ij}$ is set to 0 if $f_{ij} = 0$. To give more importance to those indicators that contain more information, the weights w_j were computed as defined in Eq. (4).

$$w_j = \frac{1 - E_j}{m - \sum_{j=1}^{m} E_j}, \sum_{j=1}^{m} w_j = 1, (j = 1, \ldots, m) \quad (4)$$

2.2.2. Ranking of administrative units

Once the weights were determined, the Technique for Order of Preference by Similarity to Ideal Solution (TOPSIS) (53) was utilized to aggregate them and generate a composite measure of each administrative unit's contribution to One Health. Here, TOPSIS was used to evaluate the proximity of a set of alternatives (administrative units in this case) to an ideal solution in terms of One Health.

The ideal administrative unit represents a theoretical scenario with the best scores for all the indicators related to the facilitation of zoonotic disease spread. In practice, this scenario is highly unlikely, as it should usually be the case that the highest values of the indicators are distributed over several administrative units. Therefore, TOPSIS calculates the distance between these real solutions and the ideal solution through a series of steps. Again, the first one was to normalize the decision-making matrix. In this case, a vector normalization as shown in Eq. (5) is proposed for the TOPSIS method (54).

$$r_{ij} = \frac{x_{ij}}{\sqrt{\sum_{j=1}^{m} x_{ij}^2}} \quad (5)$$

The weights w_j yielded by Eq. (4) were then multiplied by the normalized values r_{ij} in Eq. (5) to result in a set of normalized weighted values v_{ij}. These were in turn used to determine the positive (A^+) and negative (A^-) ideal solutions through Eqs. (6) and (7), respectively.

$$A^+ = \left\{\left(\max v_{ij} \mid j \in J\right), \left(\min v_{ij} \mid j \in J'\right), i = 1,2,\ldots,m\right\} = \left\{v_1^+, v_2^+, \ldots, v_n^+\right\} \quad (6)$$

$$A^- = \left\{\left(\min v_{ij} \mid j \in J\right), \left(\max v_{ij} \mid j \in J'\right), i = 1,2,\ldots,m\right\} = \left\{v_1^-, v_2^-, \ldots, v_n^-\right\} \quad (7)$$

where J and J' represent indicators that are beneficial and harmful to the spread of zoonotic diseases, respectively. The distances (d_i^+ and d_i^-) from the actual administrative units to these ideal solutions were calculated by applying Eqs. (8) and (9).

$$d_i^+ = \sqrt{\sum_{j=1}^{n} \left(v_{ij} - v_j^+\right)^2} \quad (8)$$

$$d_i^- = \sqrt{\sum_{j=1}^{n} \left(v_{ij} - v_j^-\right)^2} \quad (9)$$

Finally, the Relative Closeness (RC_i) from the administrative units to the ideal solution was computed using Eq. (10). The higher the value of RC_i, the more susceptible the administrative unit is to zoonoses (the less it contributes to One Health), and vice versa.

$$RC_i = \frac{d_i^-}{d_i^- + d_i^+} \quad (10)$$

2.3. Correlation between the number of infectious diseases and Green Infrastructure

The validity of the values of RC_i obtained from Eq. (10) was assessed by comparing them with the records of infectious disease counts in the case study area. This comparison was conducted using Pearson's r correlation coefficient (55) since both variables were quantitative (continuous). The presence of a statistically significant association was determined at a significance level (α) of 0.05. Therefore, the proposed indicator system was considered valid if it exhibited a strong positive correlation with the infectious disease count, and the value of p obtained from Pearson's r was less than α.

Moreover, the results were also analyzed in terms of their relationship with Green Infrastructure (GI). The potential benefits of GI for the three pillars of One Health have been discussed in previous literature (24). GI can be defined as "a strategically planned network of natural and semi-natural areas with other environmental features designed and managed to deliver a wide range of ecosystem services. It incorporates green spaces (or blue if aquatic ecosystems are concerned) and other physical features in terrestrial (including coastal) and marine areas" (56).

The correlation between One Health and GI was determined by the correlation coefficient between these values of RC_i and the area covered by GI in each administrative unit. The latter was determined based on the following classes in the Corine Land Cover (CLC) (57): 1.4 (artificial, non-agricultural vegetated areas), 2 (agricultural areas), 3.1 (forest), 3.2 (shrub and/or herbaceous vegetation associations), 4 (wetlands), and 5.1 (inland waters). These categories allowed for differentiation between artificial (class 1.4) and natural and semi-natural (classes 2, 3.1, 3.2, 4, and 5) GI.

3. Results and discussion: a case study in the Valencian Community (Spain)

The indicator system was tested in the 33 counties of the Valencian Community as shown in Figure 2. The Valencian Community is located in eastern Spain and has a predominantly Mediterranean, arid, and semi-arid climate. Regions with Mediterranean ecosystems, like the Valencian Community, are known to experience high levels of environmental degradation due to biophysical factors such as wildfires, drought, erosion, as well as social factors such as tourism, urbanization, and deforestation (58, 59).

In terms of biophysical factors, it is noteworthy that 17% of the forest area in the region has experienced at least one wildfire, 29% suffers from serious erosion problems, and 46% is at risk of desertification. In addition, the effects of climate change significantly affect the regularity of precipitation, which can have implications for areas prone to desertification (58, 60).

Concerning social factors, the region is characterized by a dominance of the service sector, which accounts for more than 65% of total employment, and tourism activities, such as real estate, gastronomy, and transportation, which have an employment rate of over 12% and contribute 15% to the GDP (61, 62). In particular, the Valencian Community has cultivated a tourism model focused on second homes linked to construction that has resulted in serious environmental impacts, high space requirements, and an unsustainable approach (63).

All these activities have been boosted by lax political guidelines and favorable economic incentives, leading to land degradation (58) (EVR, 2020). Thus, insufficient budgetary resources further contribute to the challenge of meeting the goal of recovering 15% of degraded ecosystems. Besides, other studies indicate that the Valencian Community has primarily focused on reforestation projects with limited impact on biodiversity, while neglecting medium and long-term-ecological restoration projects (64, 65).

3.1. Selection of indicators

The systematic literature review conducted following the PRISMA statement produced the results presented in Figure 3, which shows the number of records removed at each step. The search query formulated

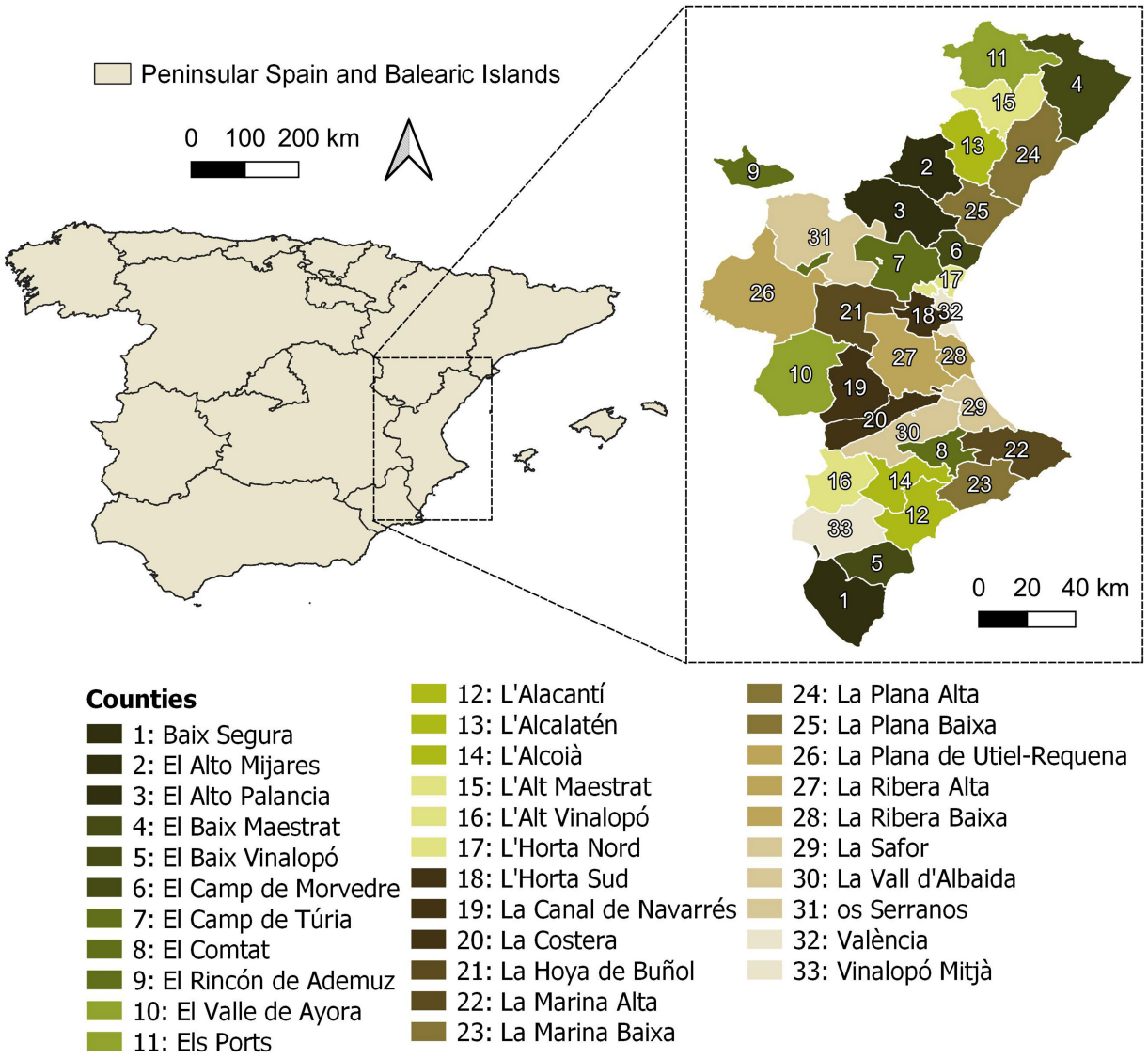

FIGURE 2
Situation map of the Valencian community and geographical extent of its counties.

in Eq. (1) initially returned 463 records from the three databases considered. This number gradually decreased through the different steps of the PRISMA statement until a final number of 99 articles was obtained for data analysis.

The extraction of information from these articles allowed for the identification of several indicators that could potentially influence the spread of diseases impacting human, animal, and environmental health. The vast majority of these indicators were not used as direct metrics to model spatial facilitation of disease spread but were instead discussed as factors that may affect One Health. Table 1 compiles the list of indicators extracted from the review and provides the main references that supported their use as surrogates for aspects that go against the One Health concept (9, 14, 40, 66–161).

Certainindicators were discarded due to limited data availability, low frequency, and/or the impossibility to characterize them spatially. Based on the frequency of the indicators found to be valid, the list in Table 2 was compiled for subsequent calculations. The first subset of indicators (from I_1 to I_8) focused on population demographics (either human or animal) and socioeconomic aspects such as health facility density, education level, and financial resources. Another group consisted of indicators related to land use (from I_9 to I_{13}). The interactions between animal and human populations and water bodies were addressed in the indicators ranging from I_{13} to I_{18}. The final group of indicators pertained to environmental conditions, including air quality (I_{19} and I_{20}) and climate (I_{21} and I_{22}).

The rationale behind the influence of these indicators on One Health is outlined below. The impact of Antimicrobial Resistance (AMR) and its implications for One Health has been linked to reduced accessibility to adequate healthcare and human health (I_1) as well as veterinary (I_2) professionalism (83). Moreover, high population densities (I_3, I_6, I_7 and I_8) can contributeto the spread of zoonotic diseases and increased intra-interactions within and between

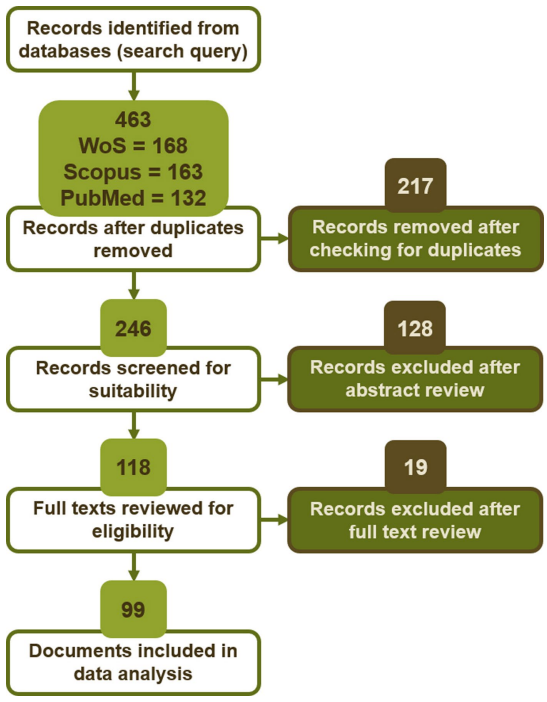

FIGURE 3
Number of records retained and removed after each step of the systematic literature review.

populations and ecosystems (81). In the case of human populations, factors such as poverty (I_5) can support the evolution of pathogen life cycles, while education (I_4) can aid in controlling global zoonotic pathogens (75).

The impact of agriculture (I_9) is associated with freshwater, which serves as a common drinking source for wildlife (69), as reflected in I_{17}. Agricultural runoff can be a source of pollution, especially if antibiotics are utilized in farming practices (68). The use of agrochemicals in agriculture contributes to reduced biodiversity and promotes mutation among microbial populations in soil and water bodies (I_{13}) (162). Other forms of anthropogenic land use changes such as deforestation (I_{10}) are linked to the increased adaptability of disease vectors and the creation of the conditions for increased interactions at the wildlife-human interface (163). I_{11} and I_{12} relate to aspects like the role of hunted animals as carriers of bacteria with specific resistance traits (92) and livestock movement as a contributing factor to the emergence of zoonotic diseases (164).

Increased global connectivity between humans and animals (either livestock or wildlife; I_{14} and I_{16}) has been identifiedas a source of acceleratedand exacerbated AMR (70). Surface water (streams, rivers, lakes, and ponds) used as drinking water for dairy cattle can serve as a source of pathogens (72) (I_{18}), posingbilateral implications for farm animals and humans (I_{15}) due to the dissemination and maintenance of resistance genes in the environment (165).

The impact of air pollution (I_{19} and I_{20}) is indirect as it stems from its contribution to biodiversity decline (166), which in turn has been argued to increase human exposure to zoonotic pathogens (167). Moisture resulting from precipitation (I_{21}) results in dense vegetation that provides suitable conditions for vector proliferation (168). Floods caused by heavy rainfall also increase the risk of waterborne diseases (169). Temperature (I_{22}) is proportional to vector distribution and disease risk too. High temperatures promote increased activity of mosquitoes, ticks, and sandflies, while they can lead to the migration of rodents into human habitats (170, 171).

3.2. Processing of indicators

Some indicators in Table 2 were obtained directly as single values per administrative unit, while others were available as either vector (point or polygon) or raster layers. These data had to be processed to express them as a single value per administrative unit. The indicators in point format were processed to obtain densities per county. Instead, polygon data were used to determine the proportion of the area corresponding to the indicators covered by the counties.

The indicators related to the interactions between point and polygon layers (I_{14}, I_{16}, and I_{17}) were determined through a three-step process: transform the point layer into a raster using a Kernel density function (shape = quartic, radius = 25 km), calculate the interaction of the gridded density and the polygon layer by multiplication, and aggregate the values per county by taking the median of the interaction values per raster unit into a polygon layer.

Apart from these general procedures, two indicators required specific calculations. Deforestation (I_{10}) was determined based on the variations in class 3.1 (Forests) in the 2006, 2012, and 2018 CLC maps in the Valencian Community. The CLC map was also used to characterize water and soil pollution (I_{13}), which was computed by assigning scores depending on the land cover classes (172).

Figure 4 shows various steps in the processing of indicators as an example. Figure 4A depicts the location of health and veterinary centers in the study area, which were used to obtain their density per county (I_1 and I_2). Figure 4B applies the aforementioned scores for water and soil pollution to the different land covers in the study area. Figures 4C,D represent the presence of wild animals and livestock areas in the region along with the human population values per county, which were the inputs used to characterize I_{14} and I_{15}. The values per county for each indicator considered (I_1-I_{22}) are provided as Supplementary material.

3.2.1. Weighting of indicators

The application of the EM algorithm according to Eqs. (2)–(4) resulted in the weights shown in Figure 5. These weights indicate the importance of various indicators for this study. Some indicators were found to have reduced importance (weights less than 0.025 out of 1): including healthcare facilities (for humans or animals), temperature, and NOx concentration, deforestation, hunting territory, and water and soil pollution. According to the EM principle, these variables are not sufficiently discriminatory among the counties in the Valencian Community, indicating that most counties are relatively homogeneous in relation to these indicators.

Instead, the indicators related to human and animal populations and their interactions obtained the highest weights. In particular, the presence of wildlife and humans was identified as the two most important indicators. This highlights the significance of distinct habitats and the risks associated with phenomena such as urban sprawl. The next most important indicators were also aligned with this focus, involving domestic and farm animals and their interactions

TABLE 1 List of proposed or derivable indicators from the systematic literature review on metrics used to address One Health.

Indicators proposed or derivable	Reference(s)
Crops; Agriculture	(66–68)
Hunting spaces, human-wildlife interface; and crops-animals-water interface	(69–71)
Exposure of farm animals to water pollution	(72–74)
Income *per capita*; access to water supply	(40, 75)
Wildlife population	(76, 77)
Soil pollution	(78, 79)
Cardiovascular diseases; diabetes	(80)
Poverty; livestock movement; and population density	(75, 81, 82)
Climate change; extreme weather, healthcare facilities; and education	(83, 84)
Hiking trails; parks	(85)
Seabirds	(86–88)
Social inequalities	(70)
Domestic animals	(89, 90)
Animal bites	(91)
Habitat overlap; wildlife-livestock interactions	(92)
Deforestation	(75, 93)
Bird migration	(71)
Dog abandonment	(94, 95)
Sewage water	(96, 97)
Rainfall, temperature; humidity; and air pollution	(98–101)
Farm outbreaks; rural areas	(102)
Human-livestock interface	(103–105)
Human-bird interface	(106)
Insects-farms interface	(107)
None (at least in the terms that can be useful for this study)	(9, 14, 72, 108–161)

TABLE 2 List of indicators to model spatial susceptibility to zoonotic diseases.

ID	Indicator	Type	Format
I_1	Density of health centers (no./km^2)	Cost	Point
I_2	Density of veterinary centers (no./km^2)	Cost	Point
I_3	Human population density (no./km^2)	Benefit	Value
I_4	Share of illiterate population (%)	Benefit	Value
I_5	Average income per consumption unit (€)	Cost	Value
I_6	Density of domestic animals (/km^2)	Benefit	Value
I_7	Density of farm animals (no./km^2)	Benefit	Value
I_8	Density of wild animals (no./km^2)	Benefit	Point
I_9	Agricultural land (%)	Benefit	Polygon
I_{10}	Deforestation (%)	Benefit	Polygon
I_{11}	Livestock (%)	Benefit	Polygon
I_{12}	Hunting territory (%)	Benefit	Polygon
I_{13}	Water and soil pollution (score)	Benefit	Polygon
I_{14}	Humans * Wild animals (score)	Benefit	Polygon/Point
I_{15}	Humans * Livestock (score)	Benefit	Polygon
I_{16}	Wild animals * Livestock (score)	Benefit	Point/Polygon
I_{17}	Wild animals * Water bodies (score)	Benefit	Point/Polygon
I_{18}	Livestock * Water bodies (score)	Benefit	Polygon
I_{19}	Average concentration of NOx (μg/m^3)	Benefit	Grid polygon
I_{20}	Average concentration of POD6 wheat (mmol/m^2)	Benefit	Grid polygon
I_{21}	Total precipitation (mm)	Benefit	Raster
I_{22}	Mean temperature (° C)	Benefit	Raster

with wildlife, humans, and water bodies, with the latter also being represented by precipitation. The ozone uptake by wheat was also identified as an important environmental indicator due to its impact on food safety.

Apart from the rationale behind them, all of these indicators with the highest weights exhibited spatial variability among the counties in the study area. In addition, they accounted for the three dimensions of One Health. Among them, animal-related variables were the most important (I_6-I_8, I_{14}-I_{18}), followed by those focused on humans (I_3, I_{14}, and I_{15}) and the environment (I_{17}, I_{20}, and I_{21}).

3.2.2. Ranking of administrative units

The use of Eqs. (5)–(10) following the steps of the TOPSIS method resulted in the map shown in Figure 6A. The results are consistent with the significance of indicators associated with humans and wildlife (Figure 5), as well as the distribution of these populations (Figure 4A). According to this map, the primary focus of disease spread is observed in the county of València (Figure 2), where the region's capital is situated, highlighting the implications of population movement in this area.

The second county in the ranking of zoonotic disease susceptibility was el Baix Segura, located in the southern of the Valencian Community. Although the human population density is not as high in this county, it attained the highest scores in terms of wildlife-livestock-water interactions. Instead, counties in the western and northern regions exhibited lower susceptibility. As can be seen from the results provided as Supplementary material, these counties only obtained high scores in indicators of lesser importance (Figure 5), such as illiterate population (I_4), average income per consumption unit (I_5), or hunting territory (I_{12}).

Overall, the results presented in Figure 6A are instructive in terms of indicating hotspots linked to susceptibility to infectious diseases.

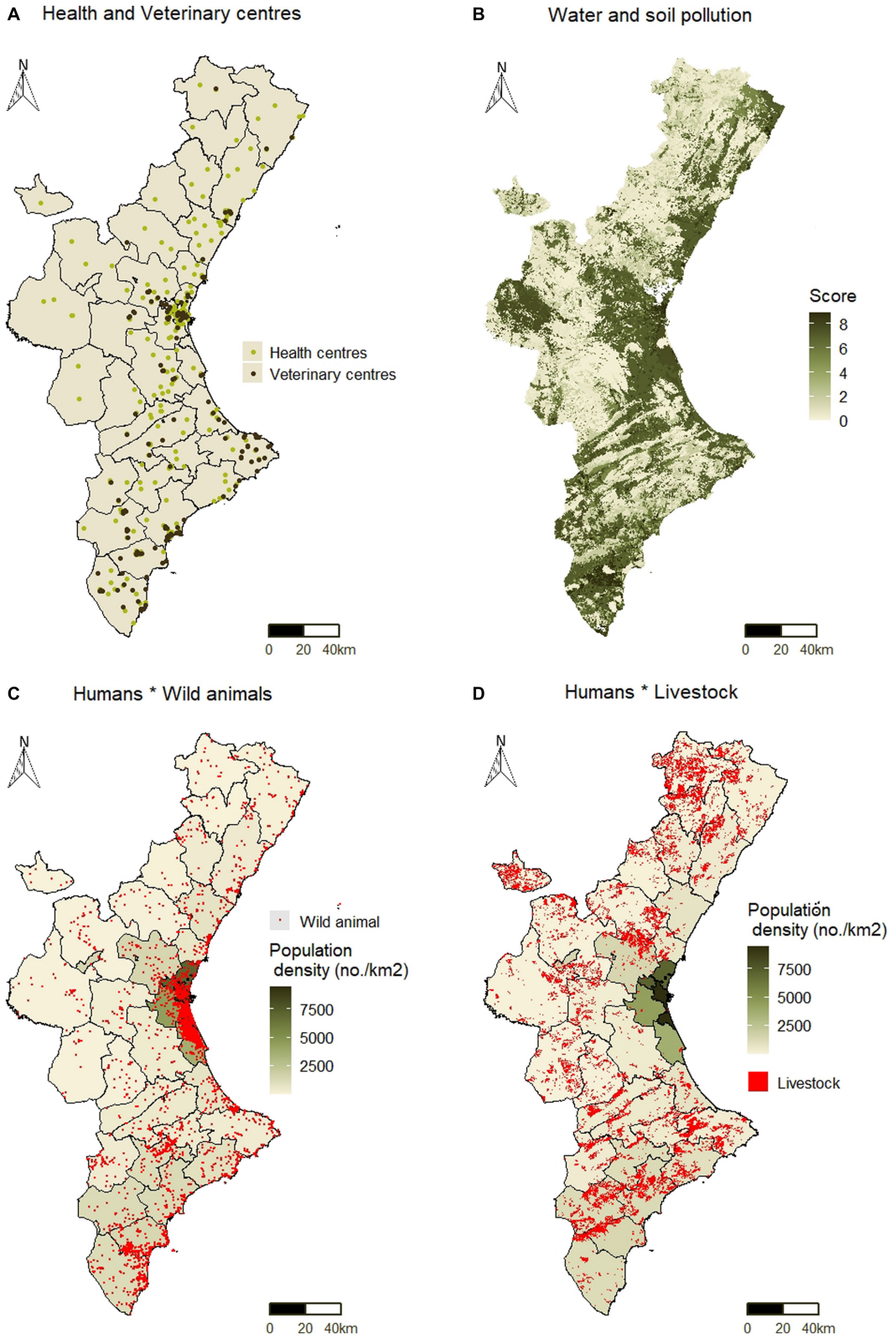

FIGURE 4
Processing of indicators before their calculation per county **(A)** Health and veterinary centers (I_1 and I_2); **(B)** Water and soil pollution (I_{13}); **(C)** Interaction between human population and wildlife (I_{14}); and **(D)** Interaction between human population and livestock (I_{15}).

The indicator system based on the EM and TOPSIS methods enables the derivation of discriminative results, highlighting substantial differences between the most critical counties and the others. Consequently, this facilitates the implementation of strategies to strengthen One Health through measures aimed at safeguarding the interface between humans, animals, and the environment.

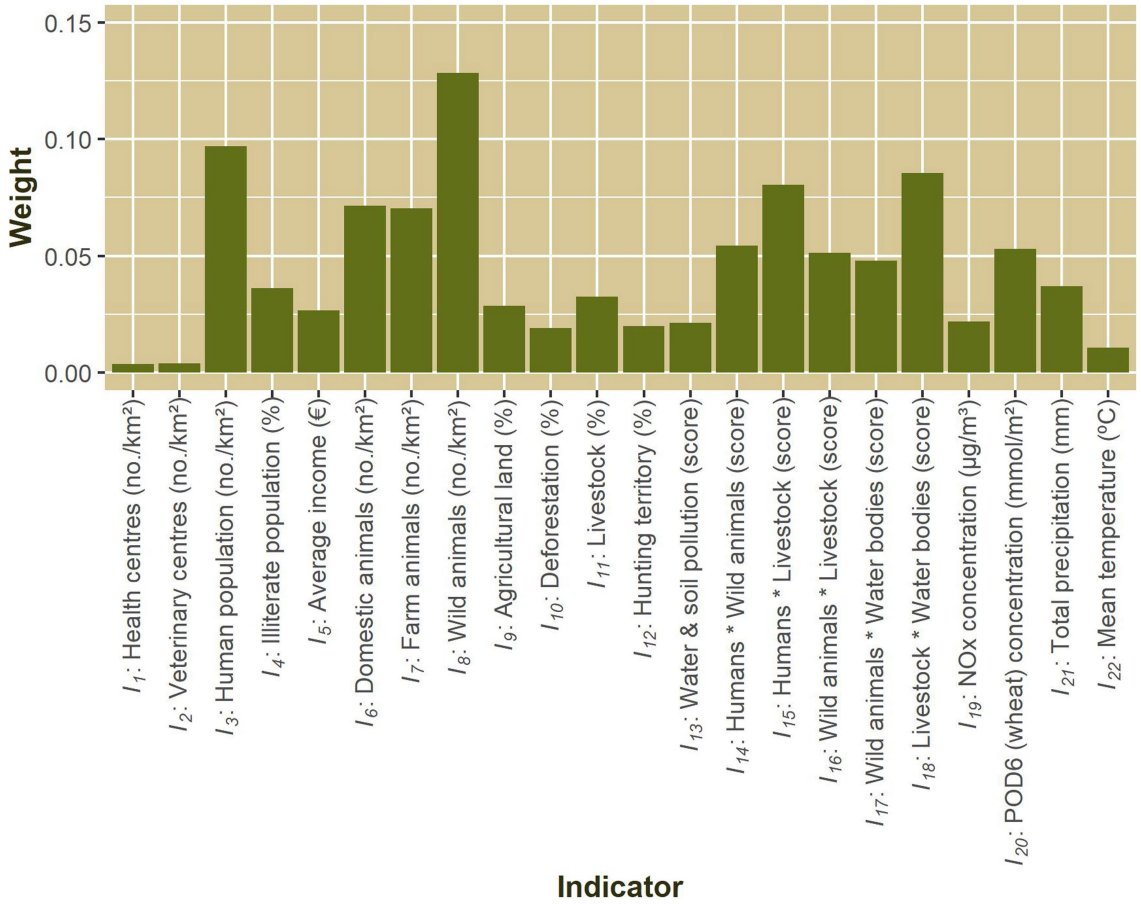

FIGURE 5
Weights obtained for the proposed indicators using the Entropy Method (EM).

3.3. Correlation between the number of infectious diseases and green infrastructure

The Valencian Animal Identification Registry (RIVIA in Spanish) provides a report on the cases notified in 2021 for the following diseases: Leishmaniosis, Ehrlichiosis, Dirofilariosis, Leptospirosis, Toxoplasmosis, and Babesiosis. Figure 6B shows how these cases are distributed across the counties in the Valencian Community.

Figure 7A demonstrates that the value of Pearson's r obtained between disease density (number of records per county area) and the values of RC_i was 0.72 (value of $p < 0.05$). This strong and positive correlation coefficient reinforces the effectiveness of the proposed indicator system in representing a region's susceptibility to the emergence of infectious diseases.

A similar analysis was carried out to examine the relationship between RC_i and the proportion of artificial (Figure 6C) and natural and semi-natural GI (Figure 6D) in the study area. Again, the p values were below the significance level of 0.05 in both cases, while the values of Pearson's r obtained were 0.78 (Figure 7B) and −0.73 (Figure 7C), respectively. These results indicate that more developed and urbanized counties exhibit a higher susceptibility to the emergence of infectious diseases, while the presence of natural and semi-natural areas may contribute to the One Health initiative.

4. Discussion

The results obtained in this study address some key demands in the field of landscape epidemiology, including the incorporation of spatial interactions between individuals and environmental gradients in large-scale studies (173). Spatial dimensions such as distances between humans, animals, and environments have been found to be associated with both directly and indirectly transmitted infectious diseases (174). Overall, the spatial processing of indicators proposed in this study aligns with these premises.

The results are also consistent with the notion that urbanization contributes to increased encounters with wildlife, leading to challenges in infectious disease epidemiology due to amplified and faster spread (175). Although the interface between human and wildlife populations (I_{14}) carries moderate weight, wild animals (I_8) and human population (I_3) were identified as the two most important indicators according to Figure 5.

Other authors have emphasized that land urbanization, rather than population urbanization is a key driver of infectious disease morbidity and mortality (176). This does not necessarily contradict the results obtained in this study but underscores the importance of using appropriate metrics. Population density goes beyond population size by considering how the accumulation of people and animals can facilitate disease transmission.

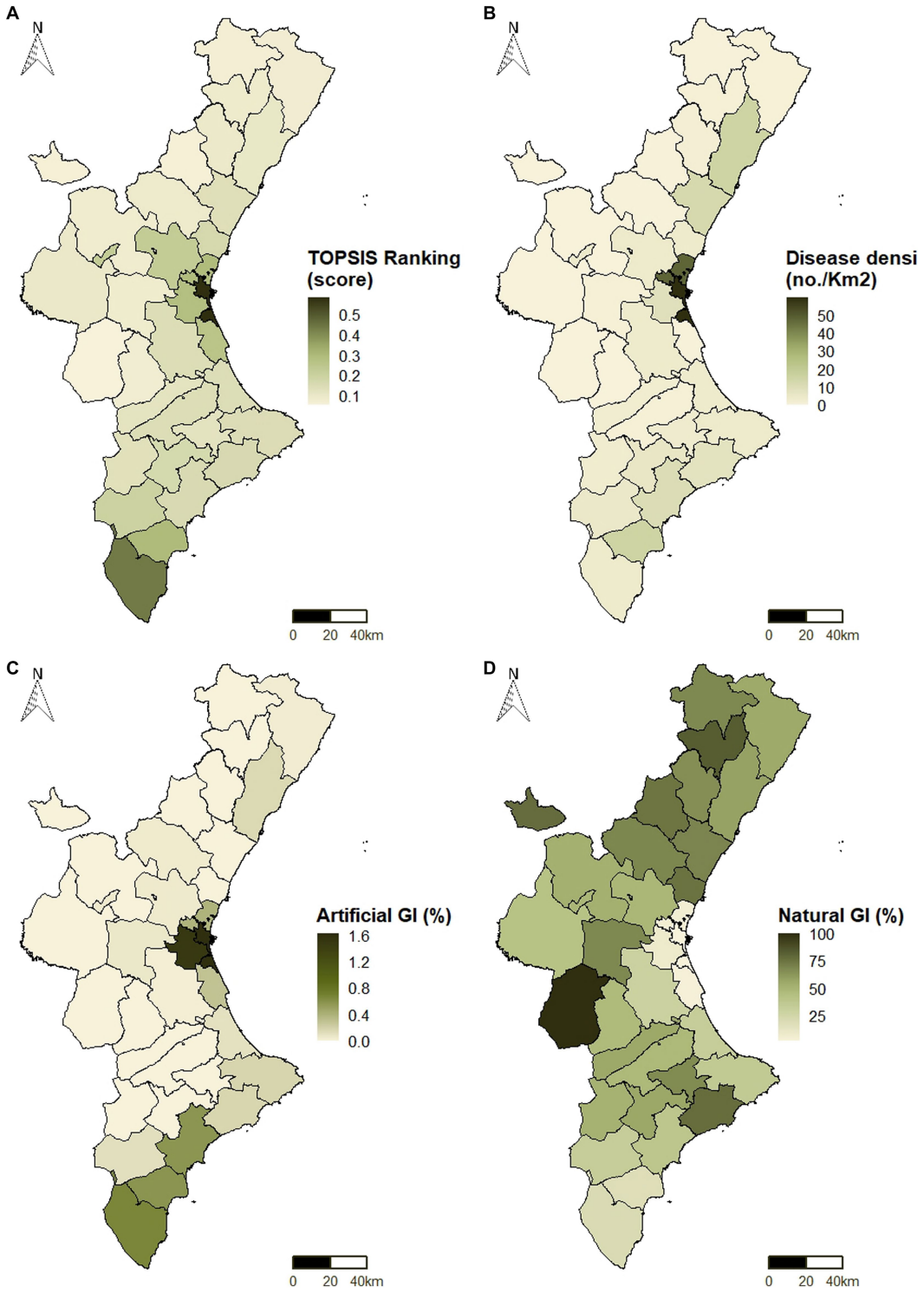

FIGURE 6
(A) Susceptibility to zoonoses according to the indicator system; **(B)** Infectious disease density (cases/km^2); **(C)** Proportion of artificial GI (%); and **(D)** Proportion of natural and semi-natural GI (%).

Urbanization promotes the occurrence of zoonoses through demographic growth and density, socioeconomic inequalities, increased movement of people and animals, and land use change (177). All these factors are included in the list of indicators presented in Table 1. The results in Figure 7 would be supported by this line of thought, since considering these aspects together correlates positively with the number of infectious diseases and the presence of natural and semi-natural GI, while correlating negatively with artificial GI in more urbanized areas.

The role of GI is linked to biodiversity, which is a crucial factor to consider when pursuing One Health goals. Zoonotic pathogens are

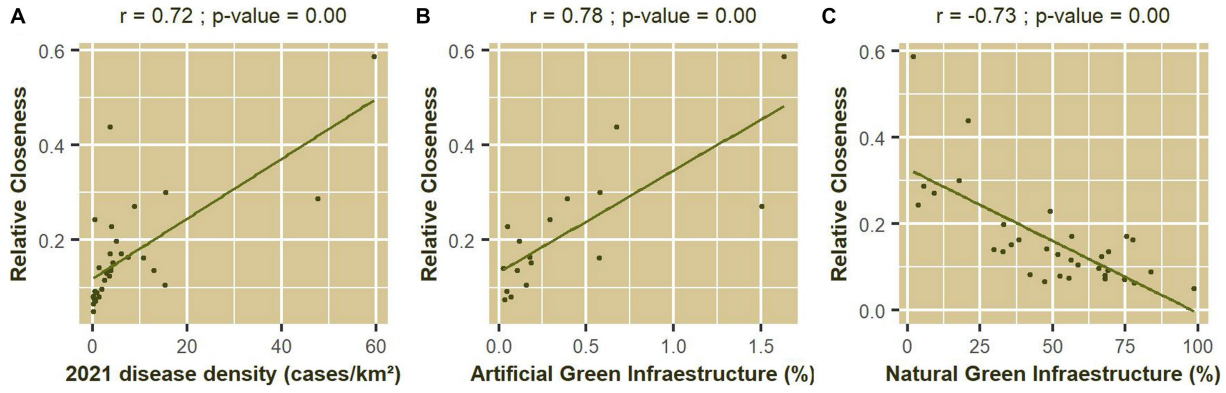

FIGURE 7
Correlation coefficient between the results of applying the indicator system to the Valencian Community and **(A)** Infectious disease density reported in 2021 (cases/km^2); **(B)** Proportion of artificial GI (%); and **(C)** Proportion of natural and semi-natural GI (%).

more likely to originate from specific taxa that often reproduce due to human influences, i.e., in urbanized areas lacking biodiversity values (167). This may explain the lower susceptibility to infectious diseases in counties with higher proportions of natural and semi-natural GI. Notably, the provision of suitable habitats for vector and zoonotic reservoir populations is one of the regulating ecosystem services supported by GI (178).

Therefore, the results of the indicator system can support the development of planning strategies aimed at promoting the principles of One Health. Strategies could focus on the implementation of natural GI, as the presence of these areas showed a negative correlation with zoonoses. Preserving and/or restoring natural landscape features can help minimize habitat encroachment, improve land and water quality, and mitigate extreme atmospheric conditions. Instead, artificial green spaces, commonly found in urban areas, showed a positive correlation with zoonoses. This is associated with urban sprawl and its effects on increased interactions between populations through greater movement of people, animals, and wildlife between developed and undeveloped areas.

Although these conclusions stem from validated results, this investigation had some limitations that constrain its impact. First, the data used to characterize certain indicators were site-specific, which hampers the usability of the indicator system in other parts of the world where such data may be lacking. Second, the methodology behind the indicator system could benefit from automation, which would result in a web-based application where users only need to input the data to obtain the composite metric of zoonotic disease susceptibility, while calculating the GIS and MCDA tasks would be in the background. Finally, this indicator system may have limitations in modeling diseases transmitted by vectors such as ticks or mosquitoes, whose distribution and survival are influenced by complex dynamics determined by climatic and seasonal factors, as well as by the presence of specific hosts, with certain conditions being favorable for some species but not for others (179, 180).

5. Summary and concluding remarks

This research consisted of the development, application, and validation of an indicator system to model spatial susceptibility to zoonotic disease facilitation, thus providing an indirect measurement of contributions to the One Health initiative. The study focused on the counties of the Valencian Community (Spain) as a case study. The methods used to achieve this goal included a systematic literature review, the combination of GIS and MCDM techniques, and the use of statistical testing.

The systematic literature review resulted in the identification of 22 spatial indicators that encompassed population, land use, and atmospheric variables. These indicators represented the risks associated with direct or indirect interactions at the interfaces between humans, wildlife, livestock, and ecosystems, thereby addressing the three pillars of the One Health approach: human, animal, and environmental health.

Processing these indicators using GIS and MCDM methods resulted in a composite metric for zoonotic disease susceptibility. The results showed that the indicators concerning human and animal populations and their interactions are the most important ones, underlining the relevance of controlling urban sprawl to mitigate habitat encroachment. The impact of urbanization was also further supported by the county level analysis, with the highest susceptibility to zoonotic diseases observed in the county corresponding to the capital and most populated city in the region.

This trend was confirmed by the strong positive correlation between the results of the indicator system and the presence of artificial GI. Conversely, the association with natural and semi-natural GI exhibited an opposite relationship, underscoring the importance of these areas for habitat preservation and biodiversity protection, thus aligning with the principles of One Health. The validity of these findings was verified by comparing the results of the indicator system with the records reported in the Valencian Community in 2021, showing a strong positive correlation. Therefore, the indicator system is proposed as a tool for implementing the principles of the One Health approach when designing strategies for better public space planning.

Data availability statement

The original contributions presented in the study are included in the article/Supplementary material; further inquiries can be directed to the corresponding author.

Author contributions

DJ-E conceived the research, contributed to the literature review, analyzed the data, discussed the results, and wrote the manuscript. FM-V contributed to the literature review, produced the results, and wrote the manuscript. VM contributed to the literature review and produced the results. FC-R contributed to the literature review, wrote the manuscript, and reviewed the manuscript. LB contributed to the literature review and reviewed the manuscript. All authors contributed to the article and approved the submitted version.

Funding

This study was financed through the research projects ECOVAL (grant number CIGE/2021/079) and ECOHEALTH (grant number PII2022_04), funded by the Conselleria for Innovation, Universities, Science and Digital Society of the Generalitat Valenciana and the Valencian International University (VIU), respectively.

Conflict of interest

The authors declare that the research was conducted in the absence of any commercial or financial relationships that could be construed as a potential conflict of interest.

Publisher's note

All claims expressed in this article are solely those of the authors and do not necessarily represent those of their affiliated organizations, or those of the publisher, the editors and the reviewers. Any product that may be evaluated in this article, or claim that may be made by its manufacturer, is not guaranteed or endorsed by the publisher.

Supplementary material

The Supplementary material for this article can be found online at: https://www.frontiersin.org/articles/10.3389/fpubh.2023.1215574/full#supplementary-material

References

1. Salyer SJ, Silver R, Simone K, Barton BC. Prioritizing Zoonoses for Global Health capacity building—themes from one health zoonotic disease workshops in 7 countries, 2014–2016. *Emerg Infect Dis*. (2017) 23:S55–64. doi: 10.3201/eid2313.170418

2. Iwu CD, Okoh AI. Preharvest transmission routes of fresh produce associated bacterial pathogens with outbreak potentials: a review. *IJERPH*. (2019) 16:4407. doi: 10.3390/ijerph16224407

3. Allen T, Murray KA, Zambrana-Torrelio C, Morse SS, Rondinini C, Di Marco M, et al. Global hotspots and correlates of emerging zoonotic diseases. *Nat Commun*. (2017) 8:1124. doi: 10.1038/s41467-017-00923-8

4. CDC One health basics. Centers for Disease Control and Prevention. (2022) Available at: https://www.cdc.gov/onehealth/basics/index.html (Accessed April 4, 2023)

5. Rüegg SR, Nielsen LR, Buttigieg SC, Santa M, Aragrande M, Canali M, et al. A systems approach to evaluate one health initiatives. *Front Vet Sci*. (2018) 5:23. doi: 10.3389/fvets.2018.00023

6. Zinsstag J, Schelling E, Waltner-Toews D, Tanner M. From "one medicine" to "one health" and systemic approaches to health and well-being. *Prev Vet Med*. (2011) 101:148–56. doi: 10.1016/j.prevetmed.2010.07.003

7. Destoumieux-Garzón D, Mavingui P, Boetsch G, Boissier J, Darriet F, Duboz P, et al. The one health concept: 10 years old and a long road ahead. *Front Vet Sci*. (2018) 5:14. doi: 10.3389/fvets.2018.00014

8. Feng J, Guo Z, Ai L, Liu J, Zhang X, Cao C, et al. Establishment of an indicator framework for global one health intrinsic drivers index based on the grounded theory and fuzzy analytical hierarchy-entropy weight method. *Infect Dis Poverty*. (2022) 11:121. doi: 10.1186/s40249-022-01042-3

9. Zhang X-X, Liu J-S, Han L-F, Xia S, Li S-Z, Li OY, et al. Towards a global one health index: a potential assessment tool for one health performance. *Infect Dis Poverty*. (2022) 11:57. doi: 10.1186/s40249-022-00979-9

10. Zhao H-Q, Fei S-W, Yin J-X, Li Q, Jiang T-G, Guo Z-Y, et al. Assessment of performance for a key indicator of one health: evidence based on one health index for zoonoses in sub-Saharan Africa. *Infect Dis Poverty*. (2022) 11:109. doi: 10.1186/s40249-022-01020-9

11. Barton BC. Introduction One Health: over a decade of progress on the road to sustainability: -EN- -FR-Introduction. Une seule santé: plus d'une décennie d'avancées vers la durabilité-ES-Introducción. Una sola salud: más de un decenio de avances en la senda de la sostenibilidad. *Rev Sci Tech OIE*. (2019) 38:21–50. doi: 10.20506/rst.38.1.2939

12. Li P, Wu J, Shukla S. Achieving the one health goal: highlighting groundwater quality and public health. *WaterSA*. (2022) 14:3540. doi: 10.3390/w14213540

13. Ung L, Stothard JR, Phalkey R, Azman AS, Chodosh J, Hanage WP, et al. Towards global control of parasitic diseases in the Covid-19 era: one health and the future of multisectoral global health governance. *Adv Parasitol Elsevier*. (2021):1–26. doi: 10.1016/bs.apar.2021.08.007

14. Wilcox BA, Aguirre AA, De Paula N, Siriaroonrat B, Echaubard P. Operationalizing one health employing social-ecological systems theory: lessons from the greater Mekong sub-region. *Front Public Health*. (2019) 7:85. doi: 10.3389/fpubh.2019.00085

15. Moore SM, ten Bosch QA, Siraj AS, Soda KJ, España G, Campo A, et al. Local and regional dynamics of chikungunya virus transmission in Colombia: the role of mismatched spatial heterogeneity. *BMC Med*. (2018) 16:152. doi: 10.1186/s12916-018-1127-2

16. Sattenspiel L, Lloyd A. *The Geographic Spread of Infectious Diseases: Models and Applications*. Princeton, New Jersey, U.S.: Princeton University Press (2009). 304 p.

17. The Lancet. Zoonoses: beyond the human–animal–environment interface. *Lancet*. (2020) 396:1. doi: 10.1016/S0140-6736(20)31486-0

18. Liu Q, Xu W, Lu S, Jiang J, Zhou J, Shao Z, et al. Landscape of emerging and re-emerging infectious diseases in China: impact of ecology, climate, and behavior. *Front Med*. (2018) 12:3–22. doi: 10.1007/s11684-017-0605-9

19. Alirol E, Getaz L, Stoll B, Chappuis F, Loutan L. Urbanisation and infectious diseases in a globalised world. *Lancet Infect Dis*. (2011) 11:131–41. doi: 10.1016/S1473-3099(10)70223-1

20. Chowell G, Rothenberg R. Spatial infectious disease epidemiology: on the cusp. *BMC Med*. (2018) 16:192. doi: 10.1186/s12916-018-1184-6

21. Tasker A, Braam D. Positioning zoonotic disease research in forced migration: a systematic literature review of theoretical frameworks and approaches. *PLoS One*. (2021) 16:e0254746. doi: 10.1371/journal.pone.0254746

22. Eubank S, Guclu H, Anil Kumar VS, Marathe MV, Srinivasan A, Toroczkai Z, et al. Modelling disease outbreaks in realistic urban social networks. *Nature*. (2004) 429:180–4. doi: 10.1038/nature02541

23. Heesterbeek H, Anderson RM, Andreasen V, Bansal S, De Angelis D, Dye C, et al. Modeling infectious disease dynamics in the complex landscape of global health. *Science*. (2015) 347:aaa4339. doi: 10.1126/science.aaa4339

24. Felappi JF, Sommer JH, Falkenberg T, Terlau W, Kötter T. Green infrastructure through the lens of "one health": a systematic review and integrative framework uncovering synergies and trade-offs between mental health and wildlife support in cities. *Sci Total Environ*. (2020) 748:141589. doi: 10.1016/j.scitotenv.2020.141589

25. Wilson R, Tiedt S, Murray K. Zoonotic infectious diseases as ecosystem disservices: a retrospective data review. *Lancet Planet Health*. (2021) 5:S23. doi: 10.1016/S2542-5196(21)00107-8

26. Petrovan SO, Aldridge DC, Bartlett H, Bladon AJ, Booth H, Broad S, et al. Post COVID-19: a solution scan of options for preventing future zoonotic epidemics. *Biol Rev*. (2021) 96:2694–715. doi: 10.1111/brv.12774

27. Zhou X-N, Tanner M. Science in one health: a new journal with a new approach. *Sci One Health*. (2022) 1:100001. doi: 10.1016/j.soh.2022.100001

28. Arino J, van den Driessche P. A multi-city epidemic model. *Math Popul Stud*. (2003) 10:175–93. doi: 10.1080/08898480306720

29. Arino J, Davis JR, Hartley D, Jordan R, Miller JM, van den Driessche P. A multi-species epidemic model with spatial dynamics. *Math Med Biol J IMA*. (2005) 22:129–42. doi: 10.1093/imammb/dqi003

30. Bashir RSE, Hassan OA. A one health perspective to identify environmental factors that affect Rift Valley fever transmission in Gezira state. *Central Sudan Trop Med Health*. (2019) 47:54. doi: 10.1186/s41182-019-0178-1

31. Bhattacharya D, Kshatri JS, Choudhary HR, Parai D, Shandilya J, Mansingh A, et al. One health approach for elimination of human anthrax in a tribal district of Odisha: study protocol. *PLoS One*. (2021) 16:e0251041. doi: 10.1371/journal.pone.0251041

32. Sharun K, Tiwari R, Natesan S, Dhama K. SARS-CoV-2 infection in farmed minks, associated zoonotic concerns, and importance of the one health approach during the ongoing COVID-19 pandemic. *Vet Q*. (2021) 41:50–60. doi: 10.1080/01652176.2020.1867776

33. Taetzsch SJ, Bertke AS, Gruszynski KR. Zoonotic disease transmission associated with feral cats in a metropolitan area: a geospatial analysis. *Zoonoses Public Health*. (2018) 65:412–9. doi: 10.1111/zph.12449

34. Dietrich D, Dekova R, Davy S, Fahrni G, Geissbühler A. Applications of space technologies to Global Health: scoping review. *J Med Internet Res*. (2018) 20:e230. doi: 10.2196/jmir.9458

35. Olugasa BO, Fasunla AJ. One health data audit: a spatio-temporal approach to cultivating sustainable multi-disciplinary collaboration and communication in zoonoses surveillance, control and stepwise elimination. *PAMJ One Health*. (2020) 1:5. doi: 10.11604/pamj-oh.2020.1.5.22350

36. Guptill SC, Moore CG. Investigating vector-borne and zoonotic diseases with remote sensing and GIS In: O Selinus, editor. *Essentials of Medical Geology*. Dordrecht, The Netherlands: Springer Netherlands (2013). 647–63.

37. Jahanfar A, Drake J, Sleep B, Margolis L. Evaluating the shading effect of photovoltaic panels on green roof discharge reduction and plant growth. *J Hydrol*. (2019) 568:919–28. doi: 10.1016/j.jhydrol.2018.11.019

38. Mollalo A, Khodabandehloo E. Zoonotic cutaneous leishmaniasis in northeastern Iran: a GIS-based spatio-temporal multi-criteria decision-making approach. *Epidemiol Infect*. (2016) 144:2217–29. doi: 10.1017/S0950268816000224

39. Souza IP de O, Uberti MS, Tassinari W de SGeoprocessing and spatial analysis for identifying leptospirosis risk areas: a systematic review. *Rev Inst Med trop S Paulo*. (2020) 62:e35. doi: 10.1590/s1678-9946202062035

40. de Moura RR, Chiba de Castro WA, Farinhas JH, Pettan-Brewer C, Kmetiuk LB, dos Santos AP, et al. One health index (OHI) applied to Curitiba, the ninth-largest metropolitan area of Brazil, with concomitant assessment of animal, environmental, and human health indicators. *One Health*. (2022) 14:100373. doi: 10.1016/j.onehlt.2022.100373

41. Errecaborde KM, Macy KW, Pekol A, Perez S, O'Brien MK, Allen I, et al. Factors that enable effective one health collaborations—a scoping review of the literature. *PLoS One*. (2019) 14:e0224660. doi: 10.1371/journal.pone.0224660

42. Vesterinen HM, Dutcher TV, Errecaborde KM, Mahero MW, Macy KW, Prasarnphanich O-O, et al. Strengthening multi-sectoral collaboration on critical health issues: one health systems mapping and analysis resource toolkit (OH-SMART) for operationalizing one health. *PLoS One*. (2019) 14:e0219197. doi: 10.1371/journal.pone.0219197

43. Henley P, Igihozo G, Wotton L. One health approaches require community engagement, education, and international collaborations—a lesson from Rwanda. *Nat Med*. (2021) 27:947–8. doi: 10.1038/s41591-021-01350-5

44. Liberati A, Altman DG, Tetzlaff J, Mulrow C, Gøtzsche PC, Ioannidis JPA, et al. The PRISMA statement for reporting systematic reviews and Meta-analyses of studies that evaluate health care interventions: explanation and elaboration. *PLoS Med*. (2009) 6:e1000100. doi: 10.1371/journal.pmed.1000100

45. Falagas ME, Pitsouni EI, Malietzis GA, Pappas G. Comparison of PubMed, Scopus, web of science, and Google scholar: strengths and weaknesses. *FASEB J*. (2008) 22:338–42. doi: 10.1096/fj.07-9492LSF

46. Evans BR, Leighton FA. A history of one health: -EN-A history of one health-FR-histoire du concept « Une seule santé » -ES-Historia de «Una sola salud». *Rev Sci Tech OIE*. (2014) 33:413–20. doi: 10.20506/rst.33.2.2298

47. Mackenzie JS, Jeggo M. The one health approach—why is it so important? *Trop Med*. (2019) 4:88. doi: 10.3390/tropicalmed4020088

48. Elnathan R. English is the language of science — but precision is tough as a non-native speaker. *Nature* (2021) doi: 10.1038/d41586-021-00899-y (Epub ahead of print).

49. Ma W, Du Y, Liu X, Shen Y. Literature review: multi-criteria decision-making method application for sustainable deep-sea mining transport plans. *Ecol Indic*. (2022) 140:109049. doi: 10.1016/j.ecolind.2022.109049

50. Jato-Espino D, Castillo-Lopez E, Rodriguez-Hernandez J, Canteras-Jordana JC. A review of application of multi-criteria decision making methods in construction. *Autom Constr*. (2014) 45:151–62. doi: 10.1016/j.autcon.2014.05.013

51. Zeleny M. *Multiple criteria decision making*. New York (U.S.): McGraw-Hill (1982). 563 p.

52. Zhu Y, Tian D, Yan F. Effectiveness of entropy weight method in decision-making. *Math Probl Eng*. (2020) 2020:1–5. doi: 10.1155/2020/3564835

53. Hwang C-L, Yoon K. *Multiple Attribute Decision Making*. Berlin, Heidelberg: Springer Berlin Heidelberg (1981).

54. Çelen A. Comparative analysis of normalization procedures in TOPSIS method: with an application to Turkish deposit banking market. *Informatica*. (2014) 25:185–208. doi: 10.15388/Informatica.2014.10

55. Kirch W. Pearson's correlation coefficient In: . *Encyclopedia of Public Health*. Dordrecht: Springer Netherlands (2008). 1090–1.

56. European Commission Green infrastructure (GI)—Enhancing Europe's natural capital. (2013). Available at: https://eur-lex.europa.eu/legal-content/EN/TXT/?uri=CELEX:52013DC0249 (Accessed September 29, 2022).

57. European Union Copernicus land monitoring service. CORINE Land Cover (2015). Available at: https://land.copernicus.eu/pan-european/corine-land-cover (Accessed September 2, 2022).

58. Generalitat Valenciana Plan de Acción Territorial Forestal de la Comunitat Valenciana–PATFOR. Medio Natural (2019) Available at: https://agroambient.gva.es/ca/web/medio-natural/patfor (Accessed March 3, 2023).

59. Zdruli P. Land resources of the Mediterranean: status, pressures, trends and impacts on future regional development. *Land Degrad Dev*. (2014) 25:373–84. doi: 10.1002/ldr.2150

60. Millán Muñoz M. Sequía en el Mediterréneo e inundaciones en el Reino Unido y Centroeuropa: cosas que los modelos climáticos globales no ven del ciclo hídrico en Europa, y por qué. Cuides Cuaderno Interdisciplinar de Desarrollo Sostenible. (2010) 7–100. Available at: https://dialnet.unirioja.es/servlet/articulo?codigo=3201315 (Accessed March 3, 2023).

61. EVR. Generalitat Valenciana. Propuesta de Estrategia Valenciana para la Recuperación, EVR: documento de trabajo. Acuerdos para la recuperación de la Comunidad Valenciana (2020) https://gvaoberta.gva.es/es/acords-per-a-la-recuperacio-de-la-comunitat-valenciana-alcem-nos (Accessed June 20, 2023).

62. INE. Distribución porcentual de los activos por sector económico y provincia. Instituto Nacional de Estadística (2022) https://www.ine.es/jaxiT3/Tabla.htm?t=3994&L=0 (Accessed June 20, 2023).

63. Aledo A, Climent-Gil E, Mañas-Navarro JJ. "Aportaciones teóricas, metodológicas y aplicadas de la sociología a la planificación del turismo.," Sociología del turismo. Madrid (Spain): Centro de Investigaciones Sociológicas (2019). 93–125. Available at: http://rua.ua.es/dspace/handle/10045/120010 (Accessed March 3, 2023)

64. Gann GD, McDonald T, Walder B, Aronson J, Nelson CR, Jonson J, et al. International principles and standards for the practice of ecological restoration. *Restor Ecol*. (2019) 27:S1–S46. doi: 10.1111/rec.13035

65. WWF. Recuperando paisajes: un nuevo camino para la restauración ecológica. World Wide Fund for Nature (2016) https://www.wwf.es/?38160/Espaa-va-camino-de-incumplir-las-metas-europeas-de-restauracin-ecolgica (Accessed March 3, 2023).

66. Mencía-Ares O, Argüello H, Puente H, Gómez-García M, Manzanilla EG, Álvarez-Ordóñez A, et al. Antimicrobial resistance in commensal Escherichia coli and Enterococcus spp. is influenced by production system, antimicrobial use, and biosecurity measures on Spanish pig farms. *Porc Health Manag*. (2021) 7:27. doi: 10.1186/s40813-021-00206-1

67. Stentiford GD, Bateman IJ, Hinchliffe SJ, Bass D, Hartnell R, Santos EM, et al. Sustainable aquaculture through the one health lens. *Nat Food*. (2020) 1:468–74. doi: 10.1038/s43016-020-0127-5

68. Zira S, Röös E, Ivarsson E, Friman J, Møller H, Samsonstuen S, et al. An assessment of scenarios for future pig production using a one health approach. *Livest Sci*. (2022) 260:104929. doi: 10.1016/j.livsci.2022.104929

69. Dias D, Fonseca C, Caetano T, Mendo S. Oh, deer! How worried should we be about the diversity and abundance of the faecal resistome of red deer? *Sci Total Environ*. (2022) 825:153831. doi: 10.1016/j.scitotenv.2022.153831

70. Lambraki IA, Majowicz SE, Parmley EJ, Wernli D, Léger A, Graells T, et al. Building social-ecological system resilience to tackle antimicrobial resistance across the one health spectrum: protocol for a mixed methods study. *JMIR Res Protoc*. (2021) 10:e24378. doi: 10.2196/24378

71. Zana B, Erdélyi K, Nagy A, Mezei E, Nagy O, Takács M, et al. Multi-approach investigation regarding the West Nile virus situation in Hungary, 2018. *Viruses*. (2020) 12:123. doi: 10.3390/v12010123

72. Dow CT, Alvarez BL. *Mycobacterium paratuberculosis* zoonosis is a one health emergency. *Ecosyst Health*. (2022) 19:164–74. doi: 10.1007/s10393-022-01602-x

73. Kamaruzzaman EA, Aziz SA, Bitrus AA, Zakaria Z, Hassan L. Occurrence and characteristics of extended-spectrum β-lactamase-producing *Escherichia coli* from dairy cattle, milk, and farm environments in peninsular Malaysia. *Pathogens*. (2020) 9:1–10. doi: 10.3390/pathogens9121007

74. Nel LH. Discrepancies in data reporting for rabies. *Africa Emerg Infect Dis*. (2013) 19:529–33. doi: 10.3201/eid1904.120185

75. Singh BB, Gajadhar AA. Role of India's wildlife in the emergence and re-emergence of zoonotic pathogens, risk factors and public health implications. *Acta Trop*. (2014) 138:67–77. doi: 10.1016/j.actatropica.2014.06.009

76. Mercato A, Cortimiglia C, Abualshaar A, Piazza A, Marchesini F, Milani G, et al. Wild boars as an Indicator of environmental spread of ESβL-producing *Escherichia coli*. *Front Microbiol*. (2022) 13:838383. doi: 10.3389/fmicb.2022.838383

77. Rostal MK, Olival KJ, Loh EH, Karesh WB. Wildlife: the need to better understand the linkages. *Curr Top Microbiol Immunol*. (2013) 365:101–25. doi: 10.1007/82-2012-271

78. Benitez ADN, Martins FDC, Mareze M, Santos NJR, Ferreira FP, Martins CM, et al. Spatial and simultaneous representative seroprevalence of anti-toxoplasma gondii antibodies in owners and their domiciled dogs in a major city of southern Brazil. *PLoS One*. (2017) 12:e0192570. doi: 10.1371/journal.pone.0180906

79. Muramoto J, Parr DM, Perez J, Wong DG. Integrated soil health Management for Plant Health and one Health: lessons from histories of soil-borne disease Management in California Strawberries and Arthropod Pest Management. *Front Sustain Food Syst*. (2022) 6:839648. doi: 10.3389/fsufs.2022.839648

80. Paris JMG, Falkenberg T, Nöthlings U, Heinzel C, Borgemeister C, Escobar N. Changing dietary patterns is necessary to improve the sustainability of Western diets from a one health perspective. *Sci Total Environ*. (2022) 811:151437. doi: 10.1016/j.scitotenv.2021.151437

81. McAlester J, Kanazawa Y. Situating zoonotic diseases in peacebuilding and development theories: prioritizing zoonoses in Jordan. *PLoS One*. (2022) 17:e0265508. doi: 10.1371/journal.pone.0265508

82. Murray AG, Ives SC, Smith RJ, Moriarty M. A preliminary assessment of indirect impacts on aquaculture species health and welfare in Scotland during COVID-19 lockdown. Veterinary and animal. *Science*. (2021) 11:100167. doi: 10.1016/j.vas.2021.100167

83. Iwu CD, Patrick SM. An insight into the implementation of the global action plan on antimicrobial resistance in the WHO African region: a roadmap for action. *Int J Antimicrob Agents*. (2021) 58:106411. doi: 10.1016/j.ijantimicag.2021.106411

84. Molia S, Saillard J, Dellagi K, Cliquet F, Bart J-M, Rotureau B, et al. Practices in research, surveillance and control of neglected tropical diseases by one health approaches: a survey targeting scientists from french-speaking countries. *PLoS Negl Trop Dis*. (2021) 15:e0009246. doi: 10.1371/journal.pntd.0009246

85. Scott LC, Wilson MJ, Esser SM, Lee NL, Wheeler ME, Aubee A, et al. Assessing visitor use impact on antibiotic resistant bacteria and antibiotic resistance genes in soil and water environments of Rocky Mountain National Park. *Sci Total Environ*. (2021) 785:147122. doi: 10.1016/j.scitotenv.2021.147122

86. Cardoso MD, Santos AFDM, Rodrigues MDS, Pribul BR, Grael AS, Pedroso VM, et al. Salmonella spp. profiles isolated from seabird samples from the Brazilian coast. *Prev Vet Med*. (2021) 193:105413. doi: 10.1016/j.prevetmed.2021.105413

87. Ewbank AC, Esperón F, Sacristán C, Sacristán I, Neves E, Costa-Silva S, et al. Occurrence and quantification of antimicrobial resistance genes in the gastrointestinal microbiome of two wild seabird species with contrasting behaviors. *Front Vet Sci*. (2021) 8:651781. doi: 10.3389/fvets.2021.651781

88. Ewbank AC, Esperón F, Sacristán C, Sacristán I, Krul R, Macedo Cavalcanti E, et al. Seabirds as anthropization indicators in two different tropical biotopes: a one health approach to the issue of antimicrobial resistance genes pollution in oceanic islands. *Sci Total Environ*. (2021) 754:142141. doi: 10.1016/j.scitotenv.2020.142141

89. Chen Q, Ma X, Rainey JJ, Li Y, Mu D, Tao X, et al. Findings from the initial stepwise approach to rabies elimination (SARE) assessment in China, 2019. *PLoS Negl Trop Dis*. (2021) 15:e0009274. doi: 10.1371/journal.pntd.0009274

90. Meyers AC, Auckland L, Meyers HF, Rodriguez CA, Kontowicz E, Petersen CA, et al. Epidemiology of vector-borne pathogens among U.S. government working dogs. *Vector-Borne Zoo Dis*. (2021) 21:358–68. doi: 10.1089/vbz.2020.2725

91. Alcoba G, Ochoa C, Martins SB, de Castañeda RR, Bolon I, Wanda F, et al. Novel transdisciplinary methodology for cross-sectional analysis of snakebite epidemiology at national scale. *PLoS Negl Trop Dis*. (2021) 15:1–19. doi: 10.1371/journal.pntd.0009023

92. Plaza-Rodríguez C, Alt K, Grobbel M, Hammerl JA, Irrgang A, Szabo I, et al. Wildlife as sentinels of antimicrobial resistance in Germany? *Front Vet Sci*. (2021) 7:627821. doi: 10.3389/fvets.2020.627821

93. Silva RBS, Franco-Silva LF, Lima DA, de Andrade Freitas ABA, Ramalho WM, de Melo MA. Spatial analysis of canine leishmaniasis in an area of transmission of the semi-arid region of the state of Paraíba. *Brazil Rev Brasil Parasitol Vet*. (2021) 30:1–10. doi: 10.1590/s1984-296120201089

94. Catapan DC, Borges TD, Müller MO, Pimpão CT. Public policies for population management of dogs and cats and social indicators of the Curitiba metropolitan region in Brazil. *Acta Vet Brasil*. (2019) 13:215–23. doi: 10.21708/avb.2019.13.4.8504

95. Harvey TV, Heukelbach J, Assunção MS, Fernandes TM, da Rocha CMBM, Carlos RSA. Seasonal variation and persistence of tungiasis infestation in dogs in an endemic community, Bahia state (Brazil): longitudinal study. *Parasitol Res*. (2019) 118:1711–8. doi: 10.1007/s00436-019-06314-w

96. Innes GK, Lambrou AS, Thumrin P, Thukngamdee Y, Tangwangvivat R, Doungngern P, et al. Enhancing global health security in Thailand: strengths and challenges of initiating a one health approach to avian influenza surveillance. *One Health*. (2022) 14:100397. doi: 10.1016/j.onehlt.2022.100397

97. Schaufler K, Nowak K, Düx A, Semmler T, Villa L, Kourouma L, et al. Clinically relevant ESBL-producing *K. pneumoniae* ST307 and *E. coli* ST38 in an urban west African rat population. *Front Microbiol*. (2018) 9:150. doi: 10.3389/fmicb.2018.00150

98. Alegría-Morán R, Pastenes Á, Cabrera G, Fredes F, Ramírez-Toloza G. Urban public squares as potential hotspots of dog-human contact: a spatial analysis of zoonotic parasites detection in gran Santiago, Chile. *Vet Parasitol Reg Stud Rep*. (2021) 24:100579. doi: 10.1016/j.vprsr.2021.100579

99. Martín-Díaz J, García-Aljaro C, Pascual-Benito M, Galofré B, Blanch AR, Lucena F. Microcosms for evaluating microbial indicator persistence and mobilization in fluvial sediments during rainfall events. *Water Res*. (2017) 123:623–31. doi: 10.1016/j.watres.2017.07.017

100. Orusa T, Orusa R, Viani A, Carella E, Mondino EB. Geomatics and EO data to support wildlife diseases assessment at landscape level: a pilot experience to map infectious keratoconjunctivitis in chamois and phenological trends in Aosta Valley (NW Italy). *Remote Sens*. (2020) 12:1–22. doi: 10.3390/rs12213542

101. Rostal MK, Ross N, Machalaba C, Cordel C, Paweska JT, Karesh WB. Benefits of a one health approach: an example using Rift Valley fever. *One Health*. (2018) 5:34–6. doi: 10.1016/j.onehlt.2018.01.001

102. Ladbury GAF, Van Leuken JPG, Swart A, Vellema P, Schimmer B, Ter Schegget R, et al. Integrating interdisciplinary methodologies for one health: goat farm re-implicated as the probable source of an urban Q fever outbreak, the Netherlands, 2009. *BMC Infect Dis*. (2015) 15:372. doi: 10.1186/s12879-015-1083-9

103. Howe AC, Soupir ML. Antimicrobial resistance in integrated agroecosystems: state of the science and future opportunities. *J Environ Qual*. (2021) 50:1255–65. doi: 10.1002/jeq2.20289

104. Nelson A, Manandhar S, Ruzante J, Gywali A, Dhakal B, Dulal S, et al. Antimicrobial drug resistant non-typhoidal *Salmonella enterica* in commercial poultry value chain in Chitwan, Nepal. *One Health Outlook*. (2020) 2:18. doi: 10.1186/s42522-020-00025-4

105. Pearce N, Douwes J. Research at the interface between human and veterinary health. *Prev Vet Med*. (2013) 111:187–93. doi: 10.1016/j.prevetmed.2013.05.010

106. Melo AM, Stevens DA, Tell LA, Veríssimo C, Sabino R, Xavier MO. Aspergillosis, avian species and the one health perspective: the possible importance of birds in azole resistance. *Microorganisms*. (2020) 8:1–22. doi: 10.3390/microorganisms8122037

107. Mahefarisoa KL, Simon Delso N, Zaninotto V, Colin ME, Bonmatin JM. The threat of veterinary medicinal products and biocides on pollinators: a one health perspective. *One Health*. (2021) 12:100237. doi: 10.1016/j.onehlt.2021.100237

108. Alba P, Leekitcharoenphon P, Franco A, Feltrin F, Ianzano A, Caprioli A, et al. Molecular epidemiology of mcr-encoded colistin resistance in Enterobacteriaceae from food-producing animals in Italy revealed through the EU harmonized antimicrobial resistance monitoring. *Front Microbiol*. (2018) 9:1217. doi: 10.3389/fmicb.2018.01217

109. Alders RG, Chadag MV, Debnath NC, Howden M, Meza F, Schipp MA, et al. Planetary boundaries and veterinary services. *OIE Rev Sci Tech*. (2021) 40:439–53. doi: 10.20506/rst.40.2.3236

110. Amato L, Dente MG, Calistri P, Declich SMedi Lab Secure WG. Integrated early warning surveillance: achilles' heel of one health? *Microorganisms*. (2020) 8:84. doi: 10.3390/microorganisms8010084

111. Anjum MF, Schmitt H, Börjesson S, Berendonk TU, Donner E, Stehling EG, et al. The potential of using *E. coli* as an indicator for the surveillance of antimicrobial resistance (AMR) in the environment. *Curr Opin Microbiol*. (2021) 64:152–8. doi: 10.1016/j.mib.2021.09.011

112. Badul S, Abia ALK, Amoako DG, Perrett K, Bester LA, Essack SY. From the farms to the dining table: the distribution and molecular characteristics of antibiotic-resistant enterococcus spp. in intensive pig farming in South Africa. *Microorganisms*. (2021) 9:882. doi: 10.3390/microorganisms9050882

113. Bastos V, Mota R, Guimarães M, Richard Y, Lima AL, Casseb A, et al. Challenges of rabies surveillance in the eastern Amazon: the need of a one health approach to predict rabies spillover. *Front Public Health*. (2021) 9:624574. doi: 10.3389/fpubh.2021.624574

114. Butcher A, Cañada JA, Sariola S. How to make noncoherent problems more productive: towards an AMR management plan for low resource livestock sectors. Humanities and social sciences. *Communications*. (2021) 8:287. doi: 10.1057/s41599-021-00965-w

115. Cardoen S, De Clercq K, Vanholme L, De Winter P, Thiry E, Van Huffel X. Preparedness activities and research needs in addressing emerging infectious animal and zoonotic diseases. *OIE Rev Sci Tech*. (2017) 36:557–68. doi: 10.20506/rst.36.2.2674

116. Carvelli A, Scaramozzino P, Iacoponi F, Condoleo R, Marta UD. Size, demography, ownership profiles, and identification rate of the owned dog population in Central Italy. *PLoS One*. (2020) 15:e0240551. doi: 10.1371/journal.pone.0240551

117. Cilia G, Fratini F, Turchi B, Ebani VV, Turini L, Bilei S, et al. Presence and characterization of zoonotic bacterial pathogens in wild boar hunting dogs (*Canis lupus familiaris*) in tuscany (Italy). *Animals*. (2021) 11:1139. doi: 10.3390/ani11041139

118. Compri M, Mader R, Mazzolini E, De-Angelis G, Mutters NT, Rajendran NB, et al. White paper: bridging the gap between surveillance data and antimicrobial stewardship in the animal sector—practical guidance from the JPIAMR ARCH and COMBACTE-MAGNET EPI-net networks. *J Antimicrob Chemother*. (2020) 75:II52–II66. doi: 10.1093/jac/dkaa429

119. Cuong NV, Ly NPC, Van NTB, Phu DH, Kiet BT, Hien VB, et al. Feasibility study of a field survey to measure antimicrobial usage in humans and animals in the Mekong

Delta region of Vietnam. *JAC Antimicrob Resist*. (2021) 3:dlab107. doi: 10.1093/jacamr/dlab107

120. Denis-Robichaud J, Aenishaenslin C, Richard L, Desmarchelier M, Carabin H. Association between pet ownership and mental health and well-being of Canadians assessed in a cross-sectional study during the COVID-19 pandemic. *Int J Environ Res Public Health*. (2022) 19:2215. doi: 10.3390/ijerph19042215

121. Duffy SC, Srinivasan S, Schilling MA, Stuber T, Danchuk SN, Michael JS, et al. Reconsidering *Mycobacterium bovis* as a proxy for zoonotic tuberculosis: a molecular epidemiological surveillance study. *Lancet Microb*. (2020) 1:e66–73. doi: 10.1016/S2666-5247(20)30038-0

122. Eddy C, Sase E. Part 1: the zika virus threat and prevention challenges: an all-hazards and one health approach to pandemic and global epidemic prevention and mitigation. *J Environ Health*. (2021) 84:8–18.

123. Elton L, Haider N, Kock R, Thomason MJ, Tembo J, Arruda LB, et al. Zoonotic disease preparedness in sub-Saharan African countries. *One Health Outlook*. (2021) 3:5. doi: 10.1186/s42522-021-00037-8

124. Fusi F, Lorenzi V, Franceschini G, Compiani R, Harper V, Ginestreti J, et al. Animal welfare and biosecurity assessment: a comparison between Italian and Irish beef cattle rearing systems. *Anim Prod Sci*. (2020) 61:55–63. doi: 10.1071/AN19611

125. Gomes S, Fernandes C, Monteiro S, Cabecinha E, Teixeira A, Varandas S, et al. The role of aquatic ecosystems (river Tua, Portugal) as reservoirs of multidrug-resistant Aeromonas spp. water (Switzerland). *WaterSA*. (2021) 13:698. doi: 10.3390/w13050698

126. Gostin LO, Katz R. The international health regulations: the governing framework for Global Health security. *Milbank Q*. (2016) 94:264–313. doi: 10.1111/1468-0009.12186

127. Guo B, Huang J, Porterfield SL. Food security and health in transition to adulthood for individuals with disabilities. *Disabil Health J*. (2020) 13:100937. doi: 10.1016/j.dhjo.2020.100937

128. Häsler B, Hiby E, Gilbert W, Obeyesekere N, Bennani H, Rushton J. A one health framework for the evaluation of rabies control programmes: a case study from Colombo City, Sri Lanka. *PLoS Negl Trop Dis*. (2014) 8:e03270. doi: 10.1371/journal.pntd.0003270

129. Hosseini Jebeli SS, Rezapour A, Hajebi A, Moradi-Lakeh M, Damari B. Scaling-up a new socio-mental health service model in Iran to reduce burden of neuropsychiatric disorders: an economic evaluation study. *Int J Ment Heal Syst*. (2021) 15:47. doi: 10.1186/s13033-021-00468-w

130. Houe H, Nielsen SS, Nielsen LR, Ethelberg S, Mølbak K. Opportunities for improved disease surveillance and control by use of integrated data on animal and human health. *Front Vet Sci*. (2019) 6:301. doi: 10.3389/fvets.2019.00301

131. Huntington B, Bernardo TM, Bondad-Reantaso M, Bruce M, Devleesschauwer B, Gilbert W, et al. Global burden of animal diseases: a novel approach to understanding and managing disease in livestock and aquaculture. *OIE Rev Sci Tech*. (2021) 40:567–84. doi: 10.20506/rst.40.2.3246

132. Imanishi M, Rotstein DS, Reimschuessel R, Schwensohn CA, Woody DH, Davis SW, et al. Public veterinary medicine: public health outbreak of *salmonella enterica* serotype Infantis infection in humans linked to dry dog food in the United States and Canada, 2012. *J Am Vet Med Assoc*. (2014) 244:545–53. doi: 10.2460/javma.244.5.545

133. Jans C, Sarno E, Collineau L, Meile L, Stärk KDC, Stephan R. Consumer exposure to antimicrobial resistant bacteria from food at Swiss retail level. *Front Microbiol*. (2018) 9:362. doi: 10.3389/fmicb.2018.00362

134. Krecek RC, Rabinowitz PM, Conrad PA. Demystifying and demonstrating the value of a one health approach to parasitological challenges. *Vet Parasitol*. (2020) 287:109202. doi: 10.1016/j.vetpar.2020.109202

135. Léchenne M, Traore A, Hattendorf J, Kallo V, Oussiguere A, Tetchi M, et al. Increasing rabies data availability: the example of a one health research project in Chad, Côte d'Ivoire and Mali. *Acta Trop*. (2021) 215:105808. doi: 10.1016/j.actatropica.2020.105808

136. Machalaba C, Smith KM, Awada L, Berry K, Berthe F, Bouley TA, et al. One health economics to confront disease threats. *Trans R Soc Trop Med Hyg*. (2017) 111:235–7. doi: 10.1093/trstmh/trx039

137. Mantovani A. Human and veterinary medicine: the priority for public health synergies. *Vet Ital*. (2008) 44:577–82.

138. Mantovani A, Aquilina G, Cubadda F, Marcon F. Risk-benefit assessment of feed additives in the one health perspective. *Front Nutr*. (2022) 9:843124. doi: 10.3389/fnut.2022.843124

139. Mason C, Weber J. What predictors are associated with the social inclusion of people with disabilities? A comparison of community-based rehabilitation participants to the general population in Vietnam. *Disabil Rehabil*. (2021) 43:815–22. doi: 10.1080/09638288.2019.1643413

140. McIntyre KM, Setzkorn C, Hepworth PJ, Morand S, Morse AP, Baylis M. A quantitative prioritisation of human and domestic animal pathogens in Europe. *PLoS One*. (2014) 9:e0103529. doi: 10.1371/journal.pone.0103529

141. Mirzaei H, Damari B. Establishing calendar for health observatories studies: Islamic Republic of Iran's experience. *Iran Red Crescent Med J*. (2020) 22:e100363. doi: 10.32592/ircmj.Crossmark

142. Mo SS, Urdahl AM, Madslien K, Sunde M, Nesse LL, Slettemeås JS, et al. What does the fox say? Monitoring antimicrobial resistance in the environment using wild red foxes as an indicator. *PLoS One*. (2018) 13:e198019. doi: 10.1371/journal.pone.0198019

143. Moran D. A framework for improved one health governance and policy making for antimicrobial use. BMJ. *Glob Health*. (2019) 4:e001807. doi: 10.1136/bmjgh-2019-001807

144. Nguyen NT, Liu M, Katayama H, Takemura T, Kasuga I. Association of the colistin resistance gene mcr-1 with faecal pollution in water environments in Hanoi. *Vietnam Lett Appl Microbiol*. (2021) 72:275–82. doi: 10.1111/lam.13421

145. Nieto-Claudin A, Deem SL, Rodríguez C, Cano S, Moity N, Cabrera F, et al. Antimicrobial resistance in Galapagos tortoises as an indicator of the growing human footprint. *Environ Pollut*. (2021) 284:117453. doi: 10.1016/j.envpol.2021.117453

146. Nwafor CD, Ilori E, Olayinka A, Ochu C, Olorundare R, Edeh E, et al. The one health approach to incident management of the 2019 Lassa fever outbreak response in Nigeria. *One Health*. (2021) 13:100346. doi: 10.1016/j.onehlt.2021.100346

147. Ortmeyer HK, Katzel LI. Effects of proximity between companion dogs and their caregivers on heart rate variability measures in older adults: a pilot study. *Int J Environ Res Public Health*. (2020) 17:2674. doi: 10.3390/ijerph17082674

148. Purseid BV, Darshan N, Kasabi GS, Gerard F, Samrat A, George C, et al. Predicting disease risk areas through co-production of spatial models: the example of kyasanur forest disease in india's forest landscapes. *PLoS Negl Trop Dis*. (2020) 14:1–20. doi: 10.1371/journal.pntd.0008179

149. Ramsamy Y, Mlisana KP, Amoako DG, Abia ALK, Allam M, Ismail A, et al. Comparative pathogenomics of *aeromonas veronii* from pigs in South Africa: dominance of the novel st 657 clone. *Microorganisms*. (2020) 8:1–16. doi: 10.3390/microorganisms8122008

150. Rebelo A, Mourão J, Freitas AR, Duarte B, Silveira E, Sanchez-Valenzuela A, et al. Diversity of metal and antibiotic resistance genes in Enterococcus spp. from the last century reflects multiple pollution and genetic exchange among phyla from overlapping ecosystems. *Sci Total Environ*. (2021) 787:147548. doi: 10.1016/j.scitotenv.2021.147548

151. Rocha ADDL, Ferrari RG, Pereira WE, Lima LAD, Givisiez PEN, Moreno-Switt AI, et al. Revisiting the biological behavior of *Salmonella enterica* in hydric resources: a Meta-analysis study addressing the critical role of environmental water on food safety and public health. *Front Microbiol*. (2022) 13:802625. doi: 10.3389/fmicb.2022.802625

152. Rousham E, Unicomb L, Wood P, Smith M, Asaduzzaman M, Islam MA. Spatial and temporal variation in the community prevalence of antibiotic resistance in Bangladesh: an integrated surveillance study protocol. *BMJ Open*. (2018) 8:e023158. doi: 10.1136/bmjopen-2018-023158

153. Rudy JE, Khan Y, Bower JK, Patel S, Foraker RE. Cardiovascular health trends in electronic health record data (2012–2015): a cross-sectional analysis of the guideline advantage™. *eGEMs*. (2019) 7:30. doi: 10.5334/egems.268

154. Scoppetta F, Chiovoloni M, Spernanzoni G, Filippini G, Capuccella M. Pharmaco-epidemiological evaluation of veterinary antimicrobial prescriptions for cattle, swine, small ruminants, poultry, rainbow trout, and food-producing horses in Umbria in 2014. *Vet Ital*. (2018) 54:305–15. doi: 10.12834/VetIt.1174.6524.2

155. Sinclair JR. Importance of a one health approach in advancing global health security and the sustainable development goals. *Rev Sci Tech*. (2019) 38:145–54. doi: 10.20506/rst.38.1.2949

156. Smoglica C, Vergara A, Angelucci S, Festino AR, Antonucci A, Marsilio F, et al. Evidence of linezolid resistance and virulence factors in Enterococcus spp. *Antibiotics*. (2022) 11:223. doi: 10.3390/antibiotics11020223

157. Sweileh WM. Global research activity on antimicrobial resistance in food-producing animals. *Arch Public Health*. (2021) 79:49. doi: 10.1186/s13690-021-00572-w

158. Taruscio D, Bermejo-Sánchez E, Salerno P, Mantovani A. Primary prevention as an essential factor ensuring sustainability of health systems: the example of congenital anomalies. *Ann Istitut Super Sanita*. (2019) 55:258–64. doi: 10.4415/ANN_19_03_11

159. Tekola B, Myers L, Lubroth J, Plee L, Calistri P, Pinto J. International health threats and global early warning and response mechanisms. *OIE Rev Sci Tech*. (2017) 36:657–70. doi: 10.20506/rst.36.2.2683

160. Valadez-Noriega M, Estévez-Moreno LX, Rayas-Amor AA, Rubio-Lozano MS, Galindo F, Miranda-de la Lama GC. Livestock hauliers' attitudes, knowledge and current practices towards animal welfare, occupational wellbeing and transport risk factors: a Mexican survey. *Prev Vet Med*. (2018) 160:76–84. doi: 10.1016/j.prevetmed.2018.09.023

161. Zrnčić S. European union's action plan on antimicrobial resistance and implications for trading partners with example of national action plan for Croatia. *Asian Fish Sci*. (2020) 33:75–82. doi: 10.33997/j.afs.2020.33.S1.011

162. Arora NK. Agricultural sustainability and food security. *Environ Sustain*. (2018) 1:217–9. doi: 10.1007/s42398-018-00032-2

163. Silva RBS, Franco-Silva LF, Lima DA . Spatial analysis of canine leishmaniasis in an area of transmission of the semi-arid region of the state of Paraíba. *Brazil Rev Bras Parasitol Vet*. (2021) 30:e018620. doi: 10.1590/s1984-296120201089,Freitas ABA de A, Ramalho WM, Melo MA de

164. Plowright RK, Parrish CR, McCallum H, Hudson PJ, Ko AI, Graham AL, et al. Pathways to zoonotic spillover. *Nat Rev Microbiol*. (2017) 15:502–10. doi: 10.1038/nrmicro.2017.45

165. Kamaruzzaman EA, Abdul Aziz S, Bitrus AA, Zakaria Z, Hassan L. Occurrence and characteristics of extended-Spectrum β-lactamase-producing *Escherichia coli* from dairy cattle, milk, and farm environments in peninsular Malaysia. *Pathogens*. (2020) 9:1007. doi: 10.3390/pathogens9121007

166. Saurabh Sonwani SS, Vandana Maurya VM. Impact of air pollution on the environment and economy In: P Saxena and V Naik, editors. *Air Pollution: Sources, Impacts and Controls*. UK: CAB International (2019). 113–34.

167. Keesing F, Ostfeld RS. Impacts of biodiversity and biodiversity loss on zoonotic diseases. *Proc Natl Acad Sci U S A*. (2021) 118:e2023540118. doi: 10.1073/pnas.2023540118

168. Githeko AK, Lindsay SW, Confalonieri UE, Patz JA. Climate change and vector-borne diseases: a regional analysis. *Bull World Health Organ*. (2000) 78:1136–47.

169. Naicker PR. The impact of climate change and other factors on zoonotic diseases. *Arch Clin Microbiol*. (2011) 2:4. doi: 10.3823/226

170. Brownstein JS, Holford TR, Fish D. Effect of climate change on Lyme disease risk in North America. *Ecosyst Health*. (2005) 2:38–46. doi: 10.1007/s10393-004-0139-x

171. Evander M, Ahlm C. Milder winters in northern Scandinavia may contribute to larger outbreaks of haemorrhagic fever virus. *Glob Health Action*. (2009) 2:2020. doi: 10.3402/gha.v2i0.2020

172. Cecchi G, Munafò M, Baiocco F, Andreani P, Mancini L. Estimating river pollution from diffuse sources in the Viterbo province using the potential non-point pollution index. *Ann Istitut Super Sanita*. (2007) 43:295–301.

173. Meentemeyer RK, Haas SE, Václavík T. Landscape epidemiology of emerging infectious diseases in natural and human-altered ecosystems. *Annu Rev Phytopathol*. (2012) 50:379–402. doi: 10.1146/annurev-phyto-081211-172938

174. Lin C-H, Wen T-H. How spatial epidemiology helps understand infectious human disease transmission. *Trop Med*. (2022) 7:164. doi: 10.3390/tropicalmed7080164

175. Neiderud C-J. How urbanization affects the epidemiology of emerging infectious diseases. *Infect Ecol Epidemiol*. (2015) 5:27060. doi: 10.3402/iee.v5.27060

176. Yu D, Li X, Yu J, Shi X, Liu P, Tian P. Whether urbanization has intensified the spread of infectious diseases—renewed question by the COVID-19 pandemic. *Front Public Health*. (2021) 9:699710. doi: 10.3389/fpubh.2021.699710

177. Ahmed S, Dávila JD, Allen A, Haklay M, Tacoli C, Fèvre EM. Does urbanization make emergence of zoonosis more likely? Evidence, myths and gaps. *Environ Urban*. (2019) 31:443–60. doi: 10.1177/0956247819866124

178. Coutts C, Hahn M. Green infrastructure, ecosystem services, and human health. *IJERPH*. (2015) 12:9768–98. doi: 10.3390/ijerph120809768

179. Chandrasegaran K, Lahondère C, Escobar LE, Vinauger C. Linking mosquito ecology, traits, behavior, and disease transmission. *Trends Parasitol*. (2020) 36:393–403. doi: 10.1016/j.pt.2020.02.001

180. Pfäffle M, Littwin N, Muders SV, Petney TN. The ecology of tick-borne diseases. *Int J Parasitol*. (2013) 43:1059–77. doi: 10.1016/j.ijpara.2013.06.009

frontiers | Frontiers in Public Health

TYPE Original Research
PUBLISHED 06 July 2023
DOI 10.3389/fpubh.2023.1168613

OPEN ACCESS

EDITED BY
Xinjian Zhang,
Centers for Disease Control and Prevention (CDC), United States

REVIEWED BY
Yassmin Moatasim,
National Research Centre, Egypt
Amal Anis Mahdi Eid,
Zagazig University, Egypt

*CORRESPONDENCE
Ariful Islam
✉ arif@ecohealthalliance.org

RECEIVED 17 February 2023
ACCEPTED 30 May 2023
PUBLISHED 06 July 2023

CITATION
Islam A, Hossain ME, Amin E, Islam S, Islam M, Sayeed MA, Hasan MM, Miah M, Hassan MM, Rahman MZ and Shirin T (2023) Epidemiology and phylodynamics of multiple clades of H5N1 circulating in domestic duck farms in different production systems in Bangladesh.
Front. Public Health 11:1168613.
doi: 10.3389/fpubh.2023.1168613

Epidemiology and phylodynamics of multiple clades of H5N1 circulating in domestic duck farms in different production systems in Bangladesh

Ariful Islam[1,2]*, Mohammad Enayet Hossain[3], Emama Amin[4], Shariful Islam[4], Monjurul Islam[4], Md Abu Sayeed[4], Md Mehedi Hasan[4], Mojnu Miah[3], Mohammad Mahmudul Hassan[5], Mohammed Ziaur Rahman[3] and Tahmina Shirin[4]

[1]EcoHealth Alliance, New York, NY, United States, [2]Centre for Integrative Ecology, School of Life and Environmental Sciences, Deakin University, Geelong, VIC, Australia, [3]One Health Laboratory, International Centre for Diarrheal Diseases Research, Bangladesh (icddr,b), Dhaka, Bangladesh, [4]Institute of Epidemiology, Disease Control and Research (IEDCR), Dhaka, Bangladesh, [5]Queensland Alliance for One Health Sciences, School of Veterinary Science, University of Queensland, Brisbane, QLD, Australia

Waterfowl are considered to be natural reservoirs of the avian influenza virus (AIV). However, the dynamics of transmission and evolutionary patterns of AIV and its subtypes within duck farms in Bangladesh remain poorly documented. Hence, a cross-sectional study was conducted in nine districts of Bangladesh between 2019 and 2021, to determine the prevalence of AIV and its subtypes H5 and H9, as well as to identify risk factors and the phylodynamics of H5N1 clades circulating in domestic duck farms. The oropharyngeal and cloacal swab samples were tested for the AIV Matrix gene (M-gene) followed by H5, H7, and H9 subtypes using rRT-PCR. The exploratory analysis was performed to estimate AIV and its subtype prevalence in different production systems, and multivariable logistic regression model was used to identify the risk factors that influence AIV infection in ducks. Bayesian phylogenetic analysis was conducted to generate a maximum clade credibility (MCC) tree and the maximum likelihood method to determine the phylogenetic relationships of the H5N1 viruses isolated from ducks. AIV was detected in 40% (95% CI: 33.0–48.1) of the duck farms. The prevalence of AIV was highest in nomadic ducks (39.8%; 95% CI: 32.9–47.1), followed by commercial ducks (24.6%; 95% CI: 14.5–37.3) and backyard ducks (14.4%; 95% CI: 10.5–19.2). The H5 prevalence was also highest in nomadic ducks (19.4%; 95% CI: 14.0–25.7). The multivariable logistic regression model revealed that ducks from nomadic farms (AOR: 2.4; 95% CI: 1.45–3.93), juvenile (AOR: 2.2; 95% CI: 1.37–3.61), and sick ducks (AOR: 11.59; 95% CI: 4.82–32.44) had a higher risk of AIV. Similarly, the likelihood of H5 detection was higher in sick ducks (AOR: 40.8; 95% CI: 16.3–115.3). Bayesian phylogenetic analysis revealed that H5N1 viruses in ducks belong to two distinct clades, 2.3.2.1a, and 2.3.4.4b. The clade 2.3.2.1a (reassorted) has been evolving silently since 2015 and forming at least nine subgroups based on >90% posterior probability. Notably, clade 2.3.4.4b was introduced in ducks in Bangladesh by the end of the year 2020, which was genetically similar to viruses detected in wild birds in Japan, China, and Africa, indicating migration-associated transmission of an emerging panzootic clade. We recommend continuing AIV

surveillance in the duck production system and preventing the intermingling of domestic ducks with migratory waterfowl in wetlands.

KEYWORDS

avian influenza, HPAI H5N1, waterfowl, risk factors, phylogeny, 2.3.2.1a, 2.3.4.4b, zoonotic

1. Introduction

The avian influenza virus (AIV) has garnered increased attention recently because of its impact on productivity, commerce, and human health. The highly pathogenic avian influenza (HPAI) H5N1 virus has been linked to poultry epidemics and occasional human infections worldwide (1). In Bangladesh, the epidemic of H5N1 in poultry was reported for the first time in 2007. Since then, the disease has spread throughout the country, with 585 H5N1 outbreaks reported until the end of 2020 (2–4). In contrast, the first human case of H5N1 was detected through exposure to slaughtered poultry in Bangladesh on May 22, 2008 (5). AIV is now considered to be endemic and some recent research has identified a high percentage of AIV in birds from farms and live bird markets (LBM) including peri-urban and rural settings (6–9). Waterfowl from the order of Anseriformes (including ducks, geese, and swans), are distributed worldwide due to aquatic habitats and are considered one of the major natural reservoirs for AIV (10, 11). Other than domestic duck species, migratory waterfowl stopover for a few days to several weeks to rest at foraging areas (wetlands and lakes) along their migratory routes (10, 12). The AIV can spread to and from domestic duck populations due to the length of stay and wetland of both domestic and migratory duck populations, and the asymptomatic nature of infected individuals increases the likelihood that the virus will spread to other species (13). When an infected duck defecates in a specific wetland or waterbody, the AIV enters the environment and infects other ducks easily while they access the same areas. Although AIV has been replicated in the respiratory tract, we cannot overlook the fecal shedding of the AIV (14). Consequently, wetlands and water bodies can become contaminated with AIV through the defecation of infected birds, therefore, transmission of the virus is more likely when a significant number of birds roost on a small wetland (15). This evidence can be corroborated by another study in which the authors recovered the virus from the lake surface, where many different duck species graze (16). So, the high AIV titer in feces, the stability of the virus in the water, and the higher number of positive cloacal than tracheal samples suggest the virus persists in duck populations through fecal-oral transmission (17). Therefore, the present study is conducted to estimate the prevalence and risk factors of AIV in domestic ducks under different rearing systems and landscapes.

Bangladesh is an agriculture-based country where the total livestock population comprises around 311.8 million chickens and 63.85 million ducks throughout the country (18), which are housed in over 53 thousand commercial broiler farms, 18 thousand commercial layer farms, and 6.5 thousand commercial duck farms, whereas in rural settings on an average, each household rears 6.8 chickens and ducks in backyard systems for their consumption or even commercial activity (19, 20). Furthermore, Bangladesh is also known as a riverine country due to its numerous transboundary rivers, suitable habitats, and wetlands that attract millions of migratory birds of 244 species each winter (October to March) and allow them to intermingle with resident aquatic wild birds and domestic ducks (21, 22). Ducks are typically raised for household and commercial production in Bangladesh using nomadic or semi-scavenging systems. Consequently, domestic ducks have frequent access to wetlands and interact closely with various migratory bird species, which may facilitate the evolution and emergence of novel strains of AIV and eventually lead to widespread outbreaks of the virus. The reservoir duck species are able to shed and transmit the virus from the respiratory and intestinal tracts, showing few or no symptoms of the disease. Therefore, understanding the epidemiology of the origin and circulation pattern of H5N1 in the duck population in Bangladesh is deemed a priority.

The AIV RNA prevalence in domestic ducks in parts of Bangladesh has been previously documented as 0.9–89% (23–25), whereas the dominant AIV subtypes were H5 and H9 in ducks (26). Furthermore, since the first detection of HPAI H5N1 viruses, various clades, including 2.2.2, 2.3.2, 2.3.4.2 (27, 28), 2.3.2.1a (29, 30), and 2.3.4.4 (31) clade of H5N6, have been identified in Bangladesh. Besides, the novel reassortant H5N1 clade 2.3.2.1a has already been isolated from the LBMs in Bangladesh, having a close relatedness to the virus isolated from birds sampled in one of the four regions of this country (32). Furthermore, during the last 3 years, clade 2.3.4.4b of the H5N1 virus has recently spread to domestic poultry and wild birds widely in Europe, Africa, Asia, and America, leading to the loss of over 33 million domestic birds (33). On the other hand, northwest Spain encountered an outbreak of 2.3.4.4b H5N1 in Minks (34). Also, this clade of H5N1 was also detected in mammals like harbor porpoises in Sweden (35) and dolphins, Sea lions, Sanderlings, Pelicans, and Cormorants in Peru (36). There have been 893 sporadic human A(H5N1) cases reported from 21 countries since 1997, and eight of those cases have been caused by clade 2.3.4.4b since 2022, which raises the possibility of a pandemic (37, 38). Both nomadic and backyard ducks are reared in a free scavenging system in Bangladesh, sharing open wetlands with large numbers of migratory waterfowl, and other wild birds and transmission of HPAI H5N1 may occur easily where the migratory birds are considered one of the potential routes for introducing new clades of HPAI H5N1 in Bangladesh (39). The surveillance of AIV in ducks from different production systems and patterns of AIV and subtype circulation within these systems are not well documented. Molecular characterization and evolutionary dynamics of HPAI H5N1 in the duck population are crucial. Therefore, we conducted this study to know the prevalence of AIV and their subtypes H5 and H9, risk factors, and phylodynamics of H5N1 clades circulating in domestic ducks in the different production systems in Bangladesh.

2. Methodology

2.1. Ethical approval

The study protocol was approved by the ethics committee of Chattogram Veterinary and Animal Science University (CVASU) bearing the number CVASU/Dir(R&E) EC/2019/126(1) and CVASU/Dir(R&E)EC/2020/191/7.

2.2. Study design and site selection

Bangladesh currently has three duck production systems: nomadic farms, backyard farms, and commercial farms. Nomadic duck farming is a traditional approach to duck production where the ducks are kept in a free-range habitat and are allowed to roam and feed in various regions (40). In the backyard farming system, household ducks are kept overnight near or within the farmer's house and travel only over a short distance for scavenging (27), and in the commercial farming system, ducks are kept in total confinement (41). Considering the duck farming patterns, we conducted a cross-sectional study and purposive sampling to find out AIV, H5, and H9 subtype prevalence as well as risk factors among ducks in different production systems from 2019 to 2021 in Bangladesh. The study sites were selected based on duck density, the presence of wetlands, and migrating waterfowl. Data on the distribution of migratory bird staging areas in Bangladesh was obtained from the literature (42, 43). Additionally, the duck density data were gathered from the Bangladesh agriculture census 2019 (44). Figure 1 depicts the nine selected districts of Bangladesh, namely Dhaka, Faridpur, Cumilla, Kushtia, Meherpur, Moulovibazar, Sylhet, Sirajganj, and Rajshahi, which represent the wide spectrum of duck-rearing practices across the country. The sampling of nomadic ducks from Sylhet and Moulovibazar represented the wetland habitats of Haor basin (45), while Kushtia, Meherpur, and Sirajganj were considered as Jamuna floodplains (46). In wetlands, domestic ducks and migratory birds share foraging habits and intermingle. Consequently, backyard ducks were also sampled in wetlands areas. In addition, backyard ducks were sampled from Dhaka, Cumilla, and Faridpur. The samples of commercial duck farms were collected from Cumilla, Dhaka, Kushtia, Meherpur, Rajshahi, and Sylhet (Figure 1).

2.3. Sample and data collection procedure

We sampled a total of 522 ducks from 171 farms, with 270 ducks coming from 127 backyard farms, 61 ducks from 11 commercial farms, and 191 from 33 nomadic farms. The samples were collected from both sick and healthy ducks, and common signs observed in sick ducks were torticollis, lack of coordination, leg paralysis, and sudden death, which have also been associated with H5N1 symptoms in previous studies (24, 47). Pooled oropharyngeal with cloacal swabs were collected from each duck by an experienced field veterinarian while causing the birds as little distress as possible. The biological specimens were collected by wearing appropriate personal protective equipment like coveralls, gloves, and other safety equipment. Immediately after sampling, the swabs sticks were placed into a 1.8 ml cryovial containing 1 mL viral transport medium (VTM). Each vial was marked using a unique identification number and placed in the portable dry shipper before transport to the laboratory. In the lab, all the samples were stored at −80°C freezer until further laboratory evaluation. A pre-tested questionnaire and face-to-face interview were used to collect all biosecurity-related data, that could potentially be a risk factor.

2.4. Virological testing

The viral RNA was extracted from the pooled swab samples (oropharyngeal and cloacal) using a KingFisher Flex 96-well robot (Thermo Scientific, Waltham, MA) and the MagMAX 96 AI/ND Viral RNA Isolation Kit (Ambion, Inc. Austin, TX) in accordance with the manufacturer's instructions. Real-time reverse transcriptase PCR (rRT-PCR) was used in conjunction with reference primers and probes to detect the presence of the AIV (InfluA) Matrix (M) gene in viral RNA, as described by the CDC and Spackman (48, 49). Then, InfluA (M-gene) positive samples were examined with specific subtypes primers of H5, H7, and H9 as previously described (49, 50). The samples were considered as AIV positive for the M-gene if the cycle threshold (Ct) was less than 40 and as H5, H7, and H9 positive if $Ct < 37$ (51). Samples that tested positive for the M gene but negative for H5, H7, and H9 were classified as A/untyped.

2.5. H5N1 sequencing

The viral RNA was extracted using QIAamp viral RNA minikit (Qiagen). The influenza segments were amplified following the protocol described by Zhou et al. (52). After amplification, PCR amplicons were visualized by agarose gel electrophoresis, followed by purification in an AMPure XP Bead. Subsequent nanopore sequencing libraries were prepared using Ligation Sequencing Kit (SQK-LSK109) and the Native barcoding approach. In 2019, the Sanger sequencing was deployed to amplify and subjected to partial sequencing of HA and NA genes of the 2 H5N1 virus described by Hoffmann (53). In 2021, the final library was quantified in the Qubit 1× dsDNA High Sensitivity Assay Kit (Invitrogen) with a Qubit 4 fluorometer (Invitrogen) and loaded onto the FLO-MIN106D flow cell on an Oxford Nanopore MinION MK 1C platform. Raw fast5 reads were base called by real-time base-calling with Guppy 4.3.4, released with MinKNOW software with the fast base-calling mode, and subsequent analyses were performed in the appropriate bioinformatics tools. The HA and NA segments of H5N1 sequences were submitted to GenBank under the accession numbers from OQ430759 to OQ430762 and OQ423229 to OQ423237.

2.6. Statistical analysis

The frequency, percentage, and univariate value of p were computed at the socio-demographic level of the duck farmer, along with duck-rearing practices in different production systems and landscapes. A descriptive analysis was computed to determine the prevalence of AIV, H5, and H9 according to the different factors at the individual bird and flock levels. The cross-tabulation and chi-square tests were performed to identify the risk factors between AIV and H5N1 with different bird-level risk factors. Furthermore, the risk factors that were determined as significant at univariate analysis were forwarded to multivariable logistic regression. The likelihood ratio (Wald test) with a value of p of ≤ 0.05 was used to identify the primary risk factor. The results were presented as Adjusted Odds Ratios (AOR),

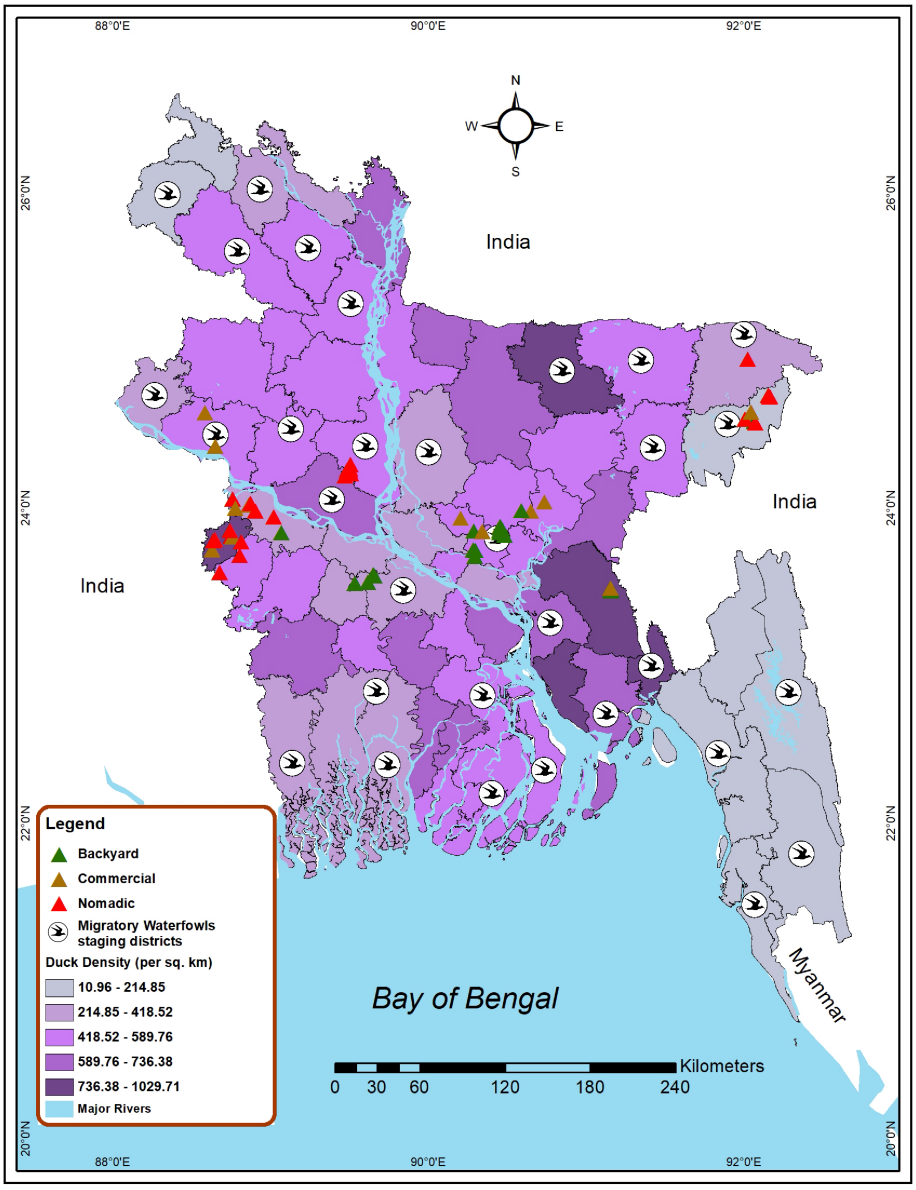

FIGURE 1
Map locating the site selected for investigating AIV risk analysis among duck farms in Bangladesh (2019–2021). Green triangles represent backyard duck farms, brown triangles represent commercial duck farms, and red triangles represent nomadic duck farms chosen for sampling in this study. Bird symbols denote districts that have migratory bird staging areas. The intensity of the color gradient shows the density of ducks in a district.

95% confidence intervals, and values of p. The data generated from this study were stored in MS Excel 2021 and checked the data integrity in MS Excel. We used RStudio version 4.1.2 for statistical analysis. We used "lme4" and "tidyverse" packages for the analysis in R software. The ArcGIS[1] software was used to create a duck density map and to visualize the spatial distribution of migratory waterfowl staging areas and duck farming sites of studied districts (Figure 1). The district-level administrative shape file was retrieved from freely available DIVA-GIS[2] (54).

2.7. Bayesian phylogenetic analysis of H5N1 viruses

To identify the clade diversity of H5N1 viruses circulating among ducks in Bangladesh, On January 1, 2023, all accessible HA gene sequences of A/H5N1 HPAIs found in Bangladesh from ducks with full-length HA sequences were retrieved from the GISAID Epiflu database (55). The HA sequences of H5N1 from 2007 to 2022, were retrieved from GISAID and NCBI and then the artifacts sequence were removed. A Maximum Clade Credibility (MCC) tree using the Bayesian Markov Chain Monte Carlo approach was generated using the temporal information of the sequence data to estimate the evolution of H5N1 viruses in

1 https://www.arcgis.com
2 https://www.diva-gis.org/gdata

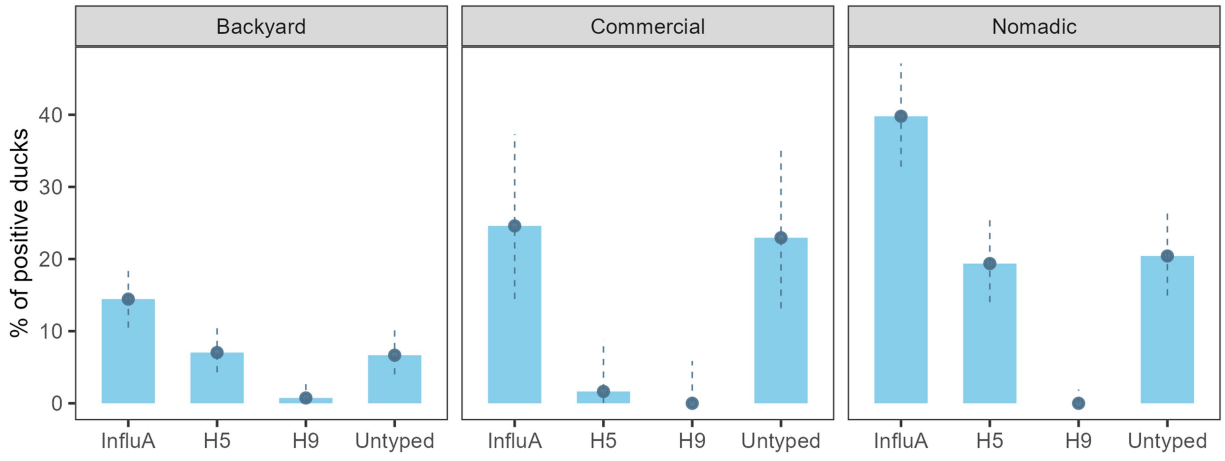

FIGURE 2
Bangladesh duck level InfluA (M gene), H5, H9, and A/Untyped prevalence with 95% confidence interval during 2019–2021.

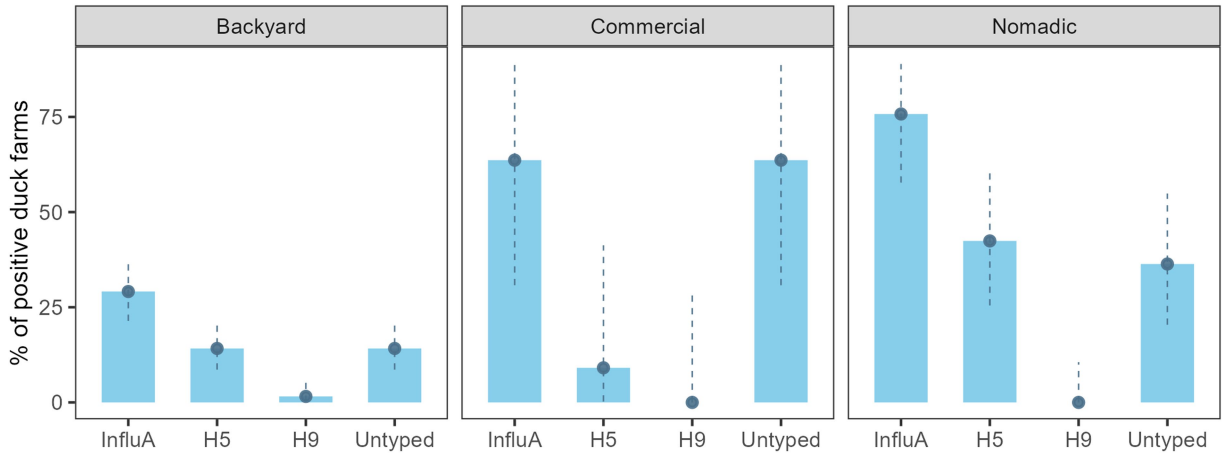

FIGURE 3
Duck farm level InfluA (M gene), H5, H9, and A/Untyed prevalence with 95% confidence interval in Bangladesh (2019–2021).

Bangladesh (BEAST 1.10.4) (56). The uncorrelated lognormal clock model with the Bayesian Skyline tree prior was used with 10 million generations (57). The gamma-distributed rate variation among sites with four rate categories (HKYþG) (58) was used. The sampling frequency was 1,000. We visualized the MCC trees in FigTree v1.4.4.[3] To identify the phylogenetic relationships of the seven H5N1 viruses sequenced in this study, the maximum likelihood method was used. For each gene segment of HA and NA, we used BLAST best matches to select the relevant sequences. TIM + F + G4 model for HA segments and K3Pu + F + G4 for NA segments was chosen by minimum BIC values using IQ-Tree (59). For each tree, we used 1,000 bootstrap replicates for generating the trees. The maximum likelihood tree was also visualized using Figtree v1.4.4.

3 http://tree.bio.ed.ac.uk/software/figtree/

3. Results

3.1. Prevalence of AIV, H5, H9, and A/Untyped in ducks and farming types

AIV prevalence for the overall sampled duck was 24.9% (130/522) (95% CI: 21.3–28.9) (Figure 2). Across the farming system, AIV prevalence was highest in the nomadic duck (76/191) (39.8%; 95% CI: 32.9–47.1) followed by commercial (15/61) (24.6%; 95% CI: 14.5–37.3) and backyard duck (39/270) (14.4%; 95% CI: 10.5–19.2). The H5 prevalence was prominent in nomadic ducks (37/191) (19.4%; 95% CI: 14.0–25.7). There was no H9 subtype found in commercial and nomadic ducks but in two backyard ducks (1.6, 95% CI: 0–8.8) (Figure 2). None of the sample was positive for H7.

On the other hand, AIV prevalence for the overall duck farm was 40.4% (69/171) (95% CI: 33.0–48.1%), backyard farm was 29.1% (37/127) (95% CI: 21.4–37.9), the commercial farm was 63.6% (7/11) (95% CI: 30.8–89.1), and the nomadic farm was 75.8% (25/33) (95% CI: 57.7–88.9) (Figure 3). The H5 subtype was higher (14/33) (42.4%;

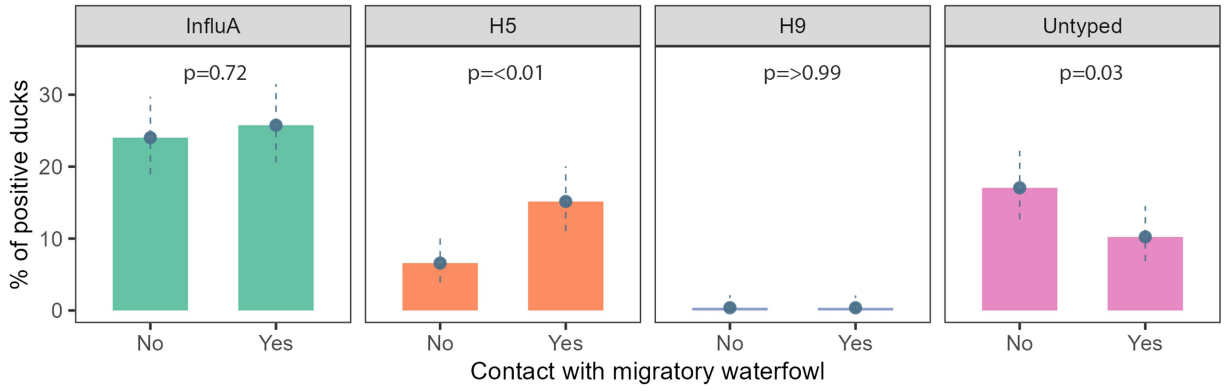

FIGURE 4
Prevalence of InfluA and its subtypes with migratory waterfowl contact in Bangladesh during 2019–2021.

TABLE 1 Cross table with chi-square analysis between AIV and bird-level factors of duck Bangladesh isolates (2019–2021).

	A positive (%)	95% CI	Value of *p*	H5 positive (%)	95% CI	Value of *p*
Farming system						
Backyard	39 (14.4)	10.5–19.2	<0.01	19 (7.0)	4.3–10.8	<0.01
Commercial	15 (24.6)	14.5–37.3		1 (1.6)	0–8.8	
Nomadic	76 (39.8)	32.8–47.1		37 (19.4)	14.0–25.7	
Age						
Adult	50 (16.1)	12.2–20.6	0.01	22 (7.1)	4.5–10.5	0.01
Juvenile	80 (37.9)	31.3–44.8		35 (16.6)	11.83–22.31	
Sex						
Female	115 (24.7)	20.8–28.9	0.86	52 (11.2)	8.5–14.4	0.78
Male	15 (26.8)	15.8–40.3		5 (8.9)	3.0–19.6	
Health condition						
Healthy	100 (20.6)	17.1–24.5	<0.01	28 (5.8)	3.9–8.2	<0.01
Sick	30 (83.3)	67.2–93.6		29 (80.6)	64.0–91.8	

Value of $p < 0.05$; statistically significant.

95% CI: 25.5–60.8) in the nomadic farming system. In backyard farming, the prevalence of H5 and A/Untyped subtypes on farms were similar (18/127) (14.2%; 95% CI: 8.6–21.5) (Figure 3).

3.2. Association of AIV and its subtypes with migratory waterfowl interface

We found evidence of an association between AIV subtypes and migratory waterfowl present in that area. A/H5 and A/Untyped were significantly associated with the presence of migratory waterfowl (Figure 4).

3.3. Risk factor for the circulation of AIV in ducks

We had four variables to check for association with AIV and H5. The farming system, age, and health condition were significantly associated with AIV and H5. Among the farming system, the nomadic system had a higher prevalence for AIV (39.8%; 95% CI: 32.8–47.1%) and H5 (19.4%; 95% CI: 32.8–47.1), whereas backyard and commercial were less positive. Juvenile age group birds were significantly more positive than adults, and sick birds were the most affected by AIV (83.3%; 95% CI: 67.2–93.7) and H5 (80.6%; 95% CI: 64.0–91.8) (Table 1). The sick ducks developed neurological signs including uncoordinated gait circling and torticollis at the terminal stage, digestive symptoms (whitish feces, fecal attached to the plumage and cloaca) and respiratory distress, dilated pupils and followed by death.

In the multivariable logistic regression model, we found three variables as significant risk factors for AIV and one risk factor for A/H5. The nomadic farming system had 2.39 times (95% CI: 1.45–3.93) higher odds of affecting AIV than backyard farming ($p = 0.01$). Compared to adults, juvenile ducks had 2.22 times (95% CI: 1.37–3.61) odds of having AIV ($p = 0.01$). The AIV detection in sick ducks (the ducks displayed dilated pupils and white feces remained on the plumage surrounding the cloaca and neurologic symptoms include an

10.3389/fpubh.2023.1168613

TABLE 2 Risk factors of AIV and A/H5 circulation in individual ducks from the different production systems in Bangladesh (2019–2021).

	A (M gene)		A/H5	
	AOR (95% CI)	Value of *p*	AOR (95% CI)	Value of *p*
Farming system				
Backyard	Reference		Reference	
Commercial	1.3 (0.6–2.7)	0.51	0.2 (0–1.1)	0.14
Nomadic	2.4 (1.5–3.9)	<0.01	1.3 (0.6–2.7)	0.56
Age				
Adult	Reference		Reference	
Juvenile	2.2 (1.4–3.6)	<0.01	1.7 (0.8–3.5)	0.18
Health condition				
Apparently healthy	Reference		Reference	
Sick	11.6 (4.8–32.4)	<0.01	46.5 (18.7–130.3)	<0.01

Value of $p < 0.05$; statistically significant.

uncoordinated gait, tremors, and torticollis) was 11.59 times (95% CI: 4.82–32.44) more likely ($p < 0.01$) than healthy birds (Table 2). We found health conditions to be a significant risk factor for H5. The odds of H5 detection in sick birds were 46.5 times (95% CI: 18.7–130.3) more likely than healthy ones ($p < 0.01$) (Table 2).

3.4. Bayesian phylogenetic analysis of the evolution of H5N1 clades in Bangladeshi ducks

The Bayesian phylogenetic tree (Figure 5) indicates that clade 2.3.2.1a has been circulating in ducks in Bangladesh since 2011. In 2015, the novel reassortant of the clade 2.3.2.1a H5N1 virus was discovered in ducks (Figure 5). The majority of H5N1 viruses detected in waterfowl are novel reassortant of clade 2.3.2.1a. Seven H5N1 sequences were identified as belonging to the emerging panzootic clade 2.3.4.4b (Figure 5). Sequences from this emerging clade clustered with white-tailed eagles from Japan (Hokkaido), geese from China (Hunan), and chickens and ducks from Africa (Nigeria and Benin). These sequences share a similarity of between 98.65 and 98.97% with H5N1 viruses of clade 2.3.4.4b from Japan and a similarity of 99.30% with viruses from China. This new clade may have been introduced to Bangladesh by the end of 2020 (Figure 5). Figure 6 shows clade 2.3.2.1a has been silently evolving among ducks, and based on posterior probability >90%, and that the clade has formed at least nine subgroups among ducks in Bangladesh. Currently, only subclade R9 of clade 2.3.2.1a is circulating in ducks in Bangladesh.

FIGURE 5
Bayesian phylogenetic tree of H5 HA viruses of diverse clades in Duck in Bangladesh. Taxon labels with blue color indicate the viruses found in ducks under this study, and taxon labels with green color indicate those reassorted H5N1 viruses detected as clade 2.3.4.4b.

3.5. Maximum likelihood phylogenetic analysis of HA and NA sequences of H5N1 viruses isolated in ducks in Bangladesh

Figures 7, 8 present the maximum likelihood phylogenetic trees of HA and NA gene segments of H5N1 viruses sequenced in this study. Five H5N1 viruses were detected in 2021 and the two viruses in 2019 belonged to the newly reassorted clade 2.3.2.1a. However, they clustered in different groups within this clade. The two virus sequences

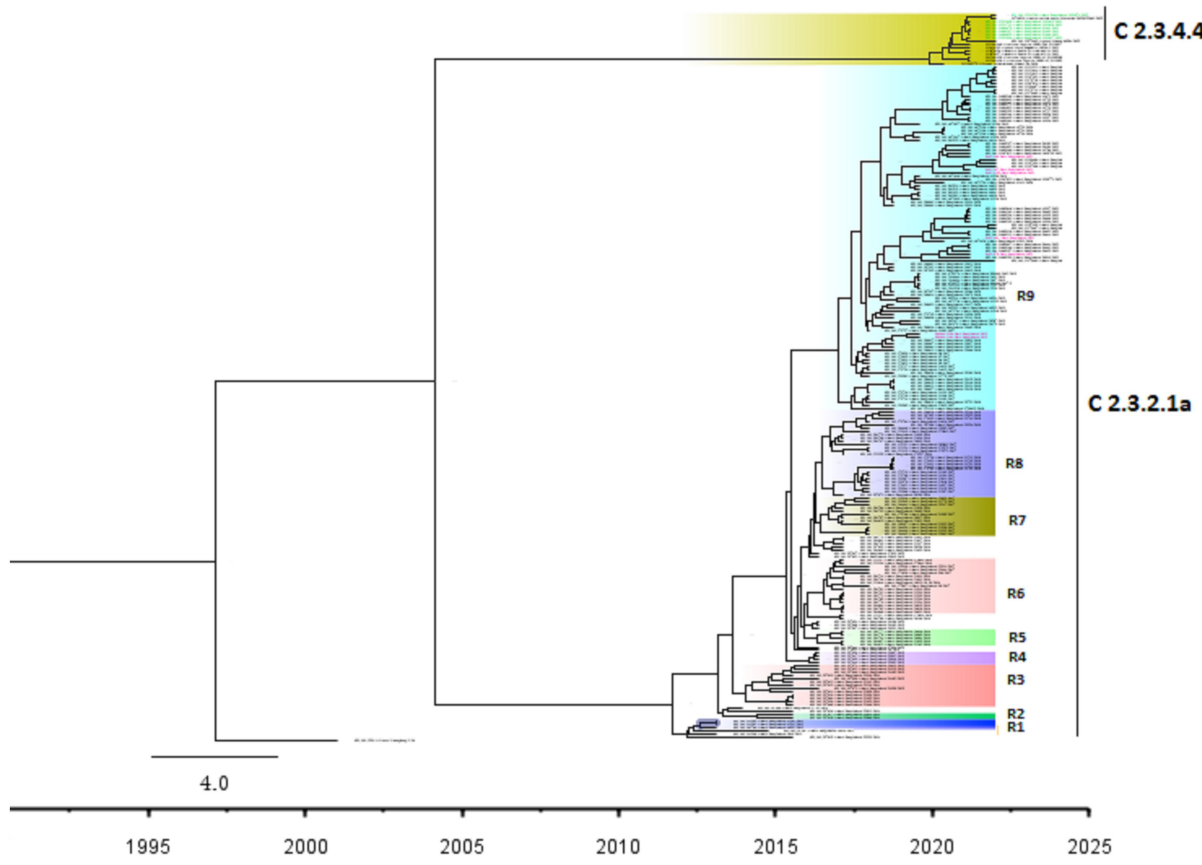

FIGURE 6
Bayesian phylogenetic tree of H5 HA viruses of diverse clades along with subgroups based on >90% posterior probability in Duck in Bangladesh. Taxon labels with red color indicate the viruses found in ducks under this study, and taxon labels with green color indicate those reassorted H5N1 viruses detected as clade 2.3.4.4b. Each colored box indicates a subgroup.

from 2019 have clustered together. The maximum likelihood tree of HA also shows that the viruses we detected in duck hosts are similar to those found in chickens. BAIV-570 and BAIV-404 have clustered within a group with virus sequences obtained from chicken (Bootstrap value>95%).

4. Discussion

4.1. Prevalence and risk factors of AIV and subtypes in the different duck production systems

The high prevalence of AIV with the H5N1 subtype in nomadic ducks compared to backyard and commercial ducks was consistent with the other study conducted by Khatun et al. (60), reported a higher prevalence of AIV in ducks reared in the hoar (wetland) region where the nomadic system is prevalent. This is because of the higher density of migratory birds in the hoar area, with a possible most increased interaction between the native duck and migratory bird species (61). Previous studies in Bangladesh detected AIV with H5N1 in both domestic and migratory ducks in wetland areas where domestic ducks and migratory birds shared the same feeding habitats in wetlands (62, 63).

Furthermore, the farm-level prevalence of AIV was also higher in nomadic ducks, supported by Hasan et al. (61) because the grazing land ecosystem is a critical factor for the circulation and spread of AIV. Concerning risk factors, there is a significant association among different farming systems, which is also supported by Henning et al. (64) reported that the birds that used to scavenge are most frequently affected. Juvenile ducks were mostly affected by both AIV M-gene and H5 subtype, which was supported by Strurm-Ramirez et al. (65). Our study revealed that the farming system significantly impacts the presence of AIV in ducks. The odds of AIV have been observed to be greater in ducks from nomadic farms than in backyard ducks. As low-lying areas with vast bodies of water are a favorable environment for raising nomadic ducks, and they have more interaction with migrating waterfowl than a backyard or commercial ducks, previous studies have shown that nomadic ducks are more susceptible to the AIV (66, 67). Our study also showed that juvenile ducks are more likely to be infected by AIV than adult ducks. A study in Canada also reported a higher detection rate of AIV in juvenile ducks than in adults (68). Adult birds presumably have acquired immunity or an enhanced immune response, but juvenile birds are immunologically more naive, rendering them more vulnerable to viral infection than adult birds (69).

Our study also showed that detecting AIV and A/H5 is higher in sick ducks than in apparently healthy ducks. Previous studies in Bangladesh and other countries have reported similar results for ducks

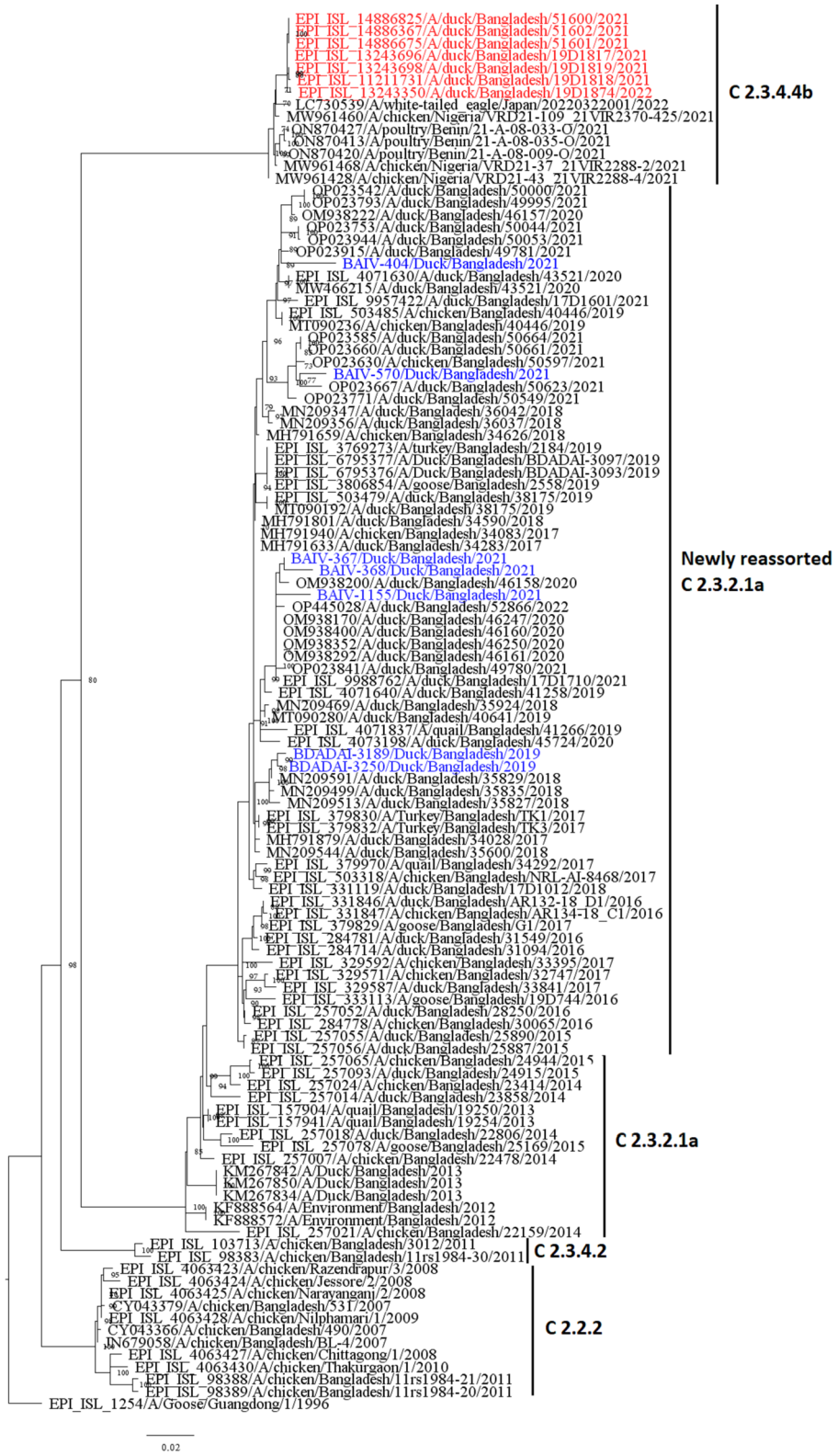

FIGURE 7
Maximum likelihood tree of HA sequences of H5N1 viruses in Bangladesh. Taxon labels with blue color indicate the viruses found in ducks under this study, and taxon labels with red color indicate those reassorted H5N1 viruses detected as clade 2.3.4.4b.

and poultry birds (2, 70–73). Even though ducks can secrete large quantities of a deadly virus without manifesting any outward signs of disease, H5N1 can cause the birds to have breathing difficulties such as gaping (mouth breathing), nasal snicking (coughing sound), sneezing, gurgling, or rattling. Since AIV causes bird sickness, the detection rate of AIV and H5 is higher in sick ducks (74–76).

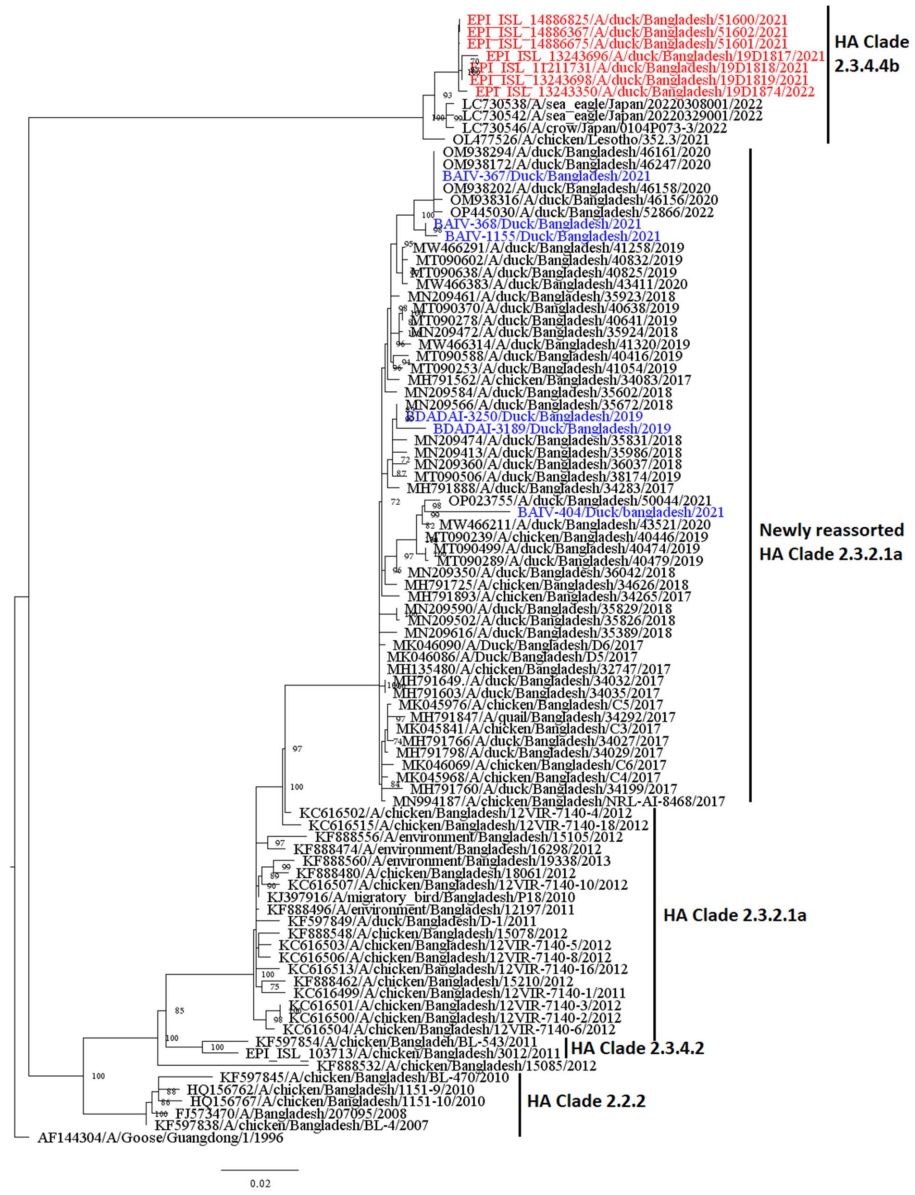

FIGURE 8
Maximum likelihood tree of 6 NA sequences of H5N1 viruses. Taxon labels with blue color indicate the viruses found in ducks under this study, and taxon labels with red color indicate those reassorted H5N1 viruses detected as HA clade 2.3.4.4b.

4.2. Phylodynamic of multiple clades of H5N1 viruses in duck farms

According to our study, multiple H5N1 virus clades are spreading in Bangladesh. Our study shows that two clades of H5N1 viruses are now circulating among ducks in Bangladesh. These two clades, 2.3.2.1a and 2.3.4.4b, of H5N1 viruses in ducks, have also been detected in nearby countries such as India and China (77, 78). Our study shows that clade 2.3.2.1a has been detected in ducks since 2011 and has become endemic in ducks in Bangladesh. Similar to our findings, other studies reported that this clade reassorted, resulting in a new subclade in 2015 (79). According to Barman et al. (32), this novel reassortant clade 2.3.2.1a virus emerged in Bangladesh via reassortment with LPAI viruses transmitted by migrating birds. Despite vaccination of commercial chicken farms in Bangladesh, Clade 2.3.2.1a HPAI has caused ongoing outbreaks in Bangladesh since 2011. Our study also shows that viruses of clade 2.3.2.1a have created at least nine subgroups within ducks based on >90% posterior probability. This suggests that the virus of this clade is silently evolving, and ducks may play an important role in the emergence of new clades in Bangladesh. Prior studies have also shown that clade 2.3.2.1a HPAIs are circulating in LBMs and domestic ducks in Bangladesh, where they play an important role in the maintenance and development of new reassortant viruses (25, 80).

The findings of the phylogenetic study also revealed that clade 2.3.4.4b was introduced to Bangladesh by the end of 2020. Cui et al. (33) also reported that one H5N1 virus from Bangladesh

clustered with Chinese viruses within the 2.3.4.4b clade. Since its emergence in the Netherlands in October 2020, H5N1 viruses with the clade 2.3.4.4b HA gene have spread to several countries in Europe, Africa, Asia, and North and South America (81, 82). On the other hand, in China, Between September 2021 and March 2022, H5N1 viruses bearing the HA clade 2.3.4.4b were discovered in wild birds and domestic poultry (33). Our study shows that seven viruses clustering within the 2.3.4.4b clade have similarities with viruses from Japan and China. So, it might be possible that migratory birds of the Central Asian flyway may influence the transmission of this novel clade in Bangladesh. Though the H5N1 viruses with clade 2.3.4.4b have only been detected in Ducks in Bangladesh, this clade has been detected in wild birds and domestic Anseriformes and Galliformes in other countries (83–85). On the other hand, this clade has also caused outbreaks in minks in Spain (86). More than 50 thousand mink were killed and their carcasses destroyed, and it was assumed that wild birds may have played a major role in the transmission of the virus (34). This virus has also been detected in harbor porpoises in Sweden (35) and dolphins, sea lions, sanderlings, pelicans, and cormorants in Peru (36), along with 8 human cases since 2022 (37). It is extremely alarming because the H5N1 virus is known to spread poorly among mammals; humans almost exclusively contract it from infected birds. However, it has since been established that the 2.3.4.4b outbreak in minks spread throughout a tightly-knit mammalian population (87). Given that the virus has already been introduced to Bangladesh, it is likely that this clade may also spread to chickens and other poultry through ducks and wild birds. As a result, there is a danger of transmission among humans as well as the possibility of a pandemic. We recommend carrying out a thorough risk analysis so that decision-makers may fully comprehend the risks connected to AIV and H5N1 outbreaks, the possible effects of the epidemic, and the steps that can be done to prevent or mitigate the disease's transmission.

5. Conclusion

This study demonstrates that H5N1 circulating in all three duck farming production systems and nomadic farms poses a higher risk of AIV infection than those from residential or commercial farms. Age and health of ducks influence the risk of AIV and H5N1 infection in populations of ducks. Clades 2.3.2.1a and 2.3.4.4b of H5N1 are circulating in Bangladeshi waterfowl. The duck farmer should receive appropriate training to enhance farm biosecurity practices in order to prevent the spread of AIV. Enhanced AIV surveillance is necessary for both domestic and migratory waterfowl, with a focus on Anseriformes production systems, to analyze the genetic diversity of H5N1 viruses and to determine the evolution of the virus at high-risk interfaces between domestic ducks and migratory birds.

Data availability statement

The datasets presented in this study can be found in online repositories. The names of the repository/repositories and accession number(s) can be found in the article/supplementary material.

Ethics statement

The studies involving human participants were reviewed and approved by the Ethics Committee (EC) (Protocol: CVASU/Dir(R&E) EC/2020/191/7) of the Chattogram Veterinary and Animal Sciences University. The participants provided their written informed consent to participate in this study. The animal study was reviewed and approved by the Chattogram Veterinary and Animal Sciences University-Animal Experimentation Ethics Committee (protocol: CVASU/Dir(R&E) EC/2020/191/7). Written informed consent was obtained from the owners for the participation of their animals in this study.

Author contributions

AI: conceptualization. AI, MdH, and SI: methodology. AI, MdH, SI, and MAS: field investigation. AI, MAS, and MI: validation. AI, EA, and MI: software and formal analysis. AI and EA: visualization and writing—original draft. AI, EA, MMH, and MI: data curation. MEH, MM, and MZR: laboratory analysis. AI, MAS, MI, and MMH: writing—review, and editing. TS and MZR: supervision. MMH, TS, and MZR: project administration and funding acquisition. All authors contributed to the article and approved the submitted version. All authors have read and approved the final version of the manuscript.

Funding

The sample collection was supported by the University Grant Commission (UGC) of Bangladesh through Chattogram Veterinary and Animal Sciences University (CVASU), grant number UGC/CVASU#06, and the United States Agency for International Development (USAID) Emerging Pandemic Threats PREDICT project (cooperative agreement number: AID-OAA-A-14-00102) through EcoHealth Alliance. We thank the governments of Bangladesh, Canada, Sweden, and the United Kingdom for providing core/unrestricted support to icddr, b. The team was partially supported by the Intramural Research Program of the National Institute of Allergy and Infectious Diseases (NIAID) National Institutes of Health (NIH) (U01AI153420).

Acknowledgments

We acknowledge the Institute of Epidemiology, Disease Control and Research (IEDCR) Bangladesh and EcoHealth Alliance, The Conservation, Food and Health Foundation(CFHF) and the Centre for Integrative Ecology at Deakin University, Australia, for their support in conducting this research. We acknowledge the use of sequences and metadata from the EpiFlu database of the Global Initiative on Sharing Avian Influenza Data (GISAID) and the animal surveillance database of the Influenza Research Database.

Conflict of interest

The authors declare that the research was conducted in the absence of any commercial or financial relationships that could be construed as a potential conflict of interest.

Publisher's note

References

1. Sun Y, Zhao X, Qian J, Jiang M, Jia M, Xu Y, et al. High activity levels of avian influenza upwards 2018–2022: a global epidemiological overview of fowl and human infections. *One Health*. (2023) 16:100511. doi: 10.1016/j.onehlt.2023.100511

2. Islam A, Amin E, Hasan R, Hassan MM, Miah M, Samad MA, et al. Patterns and risk factors of avian influenza a (H5) and a (H9) virus infection in pigeons and quail at live bird markets in Bangladesh, 2017–2021. *Front Veter Sci*. (2022) 9:9. doi: 10.3389/fvets.2022.1016970

3. FAO. EMPRES global animal disease information system (EMPRES-i). Available at: https://empres-i.apps.fao.org/ (accessed on April 20, 2023). (2023)

4. Islam A, Islam S, Amin E, Hasan R, Hassan MM, Miah M, et al. Annual trading patterns and risk factors of avian influenza a/H5 and a/H9 virus circulation in Turkey birds (*Meleagris gallopavo*) at live bird markets in Dhaka city, Bangladesh. *Front Veter Sci*. (2023) 9:684. doi: 10.3389/fvets.2022.1016970

5. IEDCR. First human infection with influenza a H5N1 confirmed in Bangladesh. Available at: https://www.iedcr.org/index.php?option=com_content&view=article&id=61&Itemid=115 (Accessed March 27, 2023) (2012)

6. Islam A, Islam S, Islam M, Hossain ME, Munro S, Samad MA, et al. Prevalence and risk factors for avian influenza virus (H5 and H9) contamination in peri-urban and rural live bird markets in Bangladesh. *Front Public Health*. (2023) 11:1349. doi: 10.3389/fpubh.2023.1148994

7. Rahman MA, Belgrad JP, Sayeed MA, Abdullah MS, Barua S, Chisty NN, et al. Prevalence and risk factors of avian influenza viruses among household ducks in Chattogram, Bangladesh. *Vet Res Commun*. (2022) 46:471–80. doi: 10.1007/s11259-021-09874-4

8. Chowdhury M, Islam S, Hossain ME, Rahman MZ, Zulkar Nine HSM, Sadik AS, et al. Detection of influenza a and adenovirus in captive wild birds in Bangladesh. *Int J Infect Dis*. (2020) 101:229. doi: 10.1016/j.ijid.2020.11.034

9. Islam A, Islam S, Rahman MK, Hossain ME, Samad MA, Rostral MK, et al. Circulation of avian influenza H5N1 and H9N2 virus in dhamrai and savar upazila, Bangladesh. *Int J Infect Diseases*. (2023) 130:S75. doi: 10.1016/j.ijid.2023.04.186

10. Olsen B, Munster VJ, Wallensten A, Waldenström J, Osterhaus ADME, Fouchier RAM. Global patterns of influenza a virus in wild birds. *Science*. (2006) 312:384–8. doi: 10.1126/science.1122438

11. Hassan MM, Hoque MA, Debnath NC, Yamage M, Klaassen M. Are poultry or wild birds the main reservoirs for avian influenza in Bangladesh? *EcoHealth*. (2017) 14:490–500. doi: 10.1007/s10393-017-1257-6

12. Torrontegi O, Alvarez V, Acevedo P, Gerrikagoitia X, Höfle U, Barral M. Long-term avian influenza virus epidemiology in a small Spanish wetland ecosystem is driven by the breeding Anseriformes community. *Vet Res*. (2019) 50:4. doi: 10.1186/s13567-019-0623-5

13. Mateus-Anzola J, Martínez-López B, Espinosa-García AC, Ojeda-Flores R. Global subtype diversity, spatial distribution patterns, and phylogenetic analysis of avian influenza virus in water. *Transbound Emerg Dis*. (2022) 69:e344–55. doi: 10.1111/tbed.14307

14. Zhang H, Xu B, Chen Q, Chen J, Chen Z. Characterization of an H10N8 influenza virus isolated from Dongting lake wetland. *Virol J*. (2011) 8:1–9. doi: 10.1186/1743-422X-8-42

15. Blagodatski A, Trutneva K, Glazova O, Mityaeva O, Shevkova L, Kegeles E, et al. Avian influenza in wild birds and poultry: dissemination pathways, monitoring methods, and virus ecology. *Pathogens*. (2021) 10:630. doi: 10.3390/pathogens10050630

16. Ahrens AK, Selinka HC, Wylezich C, Wonnemann H, Sindt O, Hellmer HH, et al. Investigating environmental matrices for use in avian influenza virus surveillance—surface water, sediments, and avian fecal samples. *Microbiol Spectrum*. (2023) 11:e02664–22. doi: 10.1128/spectrum.02664-22

17. Kim JK, Negovetich NJ, Forrest HL, Webster RG. Ducks: the "Trojan horses" of H5N1 influenza. *Influenza Other Respir Viruses*. (2009) 3:121–8. doi: 10.1111/j.1750-2659.2009.00084.x

18. DLS. Livestock economy at a glance. Available at: http://dls.portal.gov.bd/sites/default/files/files/dls.portal.gov.bd/page/ee5f4621_fa3a_40ac_8bd9_898fb8ee4700/2022-07-18-03-43-37d18965a6458cda3c542ab146480962.pdf (Accessed November 27, 2022). (2022)

19. Banglapedia. Livestock. Available at https://en.banglapedia.org/index.php/Livestock#:~:text=Livestock%20population%20in%20Bangladesh%20is,chicken%20and%2034.1%20million20ducks (Accessed November 27, 2022). (2021).

20. Karmoker Y. Self sufficiency in protein: poultry industry in Bangladesh. Available at: https://businessinspection.com.bd/poultry-industry-in-bangladesh/ (Accessed November 27, 2022).(2022).

21. Mahmud I., Bangladesh saw 100,000 more migratory birds in 2019. Prothom Alo. Available at: https://en.prothomalo.com/bangladesh/Bangladesh-saw-100-000-more-migratory-birds-in (Accessed November 27, 2022). (2019).

22. Hoque MA, Hassan MM, Haque E, Shaikat AH, Khan SA, Alim A, et al. A survey of gastro-intestinal parasitic infection in domestic and wild birds in Chittagong and greater Sylhet. *Bang Prevent Veter Med*. (2014) 117:305–12. doi: 10.1016/j.prevetmed.2014.07.012

23. Ansari WK, Parvej MS, el Zowalaty ME, Jackson S, Bustin SA, Ibrahim AK, et al. Surveillance, epidemiological, and virological detection of highly pathogenic H5N1 avian influenza viruses in duck and poultry from Bangladesh. *Vet Microbiol*. (2016) 193:49–59. doi: 10.1016/j.vetmic.2016.07.025

24. Haider N, Sturm-Ramirez K, Khan SU, Rahman MZ, Sarkar S, Poh MK, et al. Unusually high mortality in waterfowl caused by highly pathogenic avian influenza a (H5N1) in Bangladesh. *Transbound Emerg Dis*. (2017) 64:144–56. doi: 10.1111/tbed.12354

25. Khan SU, Gurley ES, Gerloff N, Rahman MZ, Simpson N, Rahman M, et al. Avian influenza surveillance in domestic waterfowl and environment of live bird markets in Bangladesh, 2007-2012. *Sci Rep*. (2018) 8:9396. doi: 10.1038/s41598-018-27515-w

26. Islam A, Qayum MO, Hossain ME, Islam S, Islam K, Alam HMS, et al. Epidemiological investigation of H9N2 virus circulation in backyard poultry farms and humans in a rural community. *BANG Int J Infect Diseases*. (2023) 130:S72. doi: 10.1016/j.ijid.2023.04.179

27. Dutta P, Islam A, Sayeed MA, Rahman MA, Abdullah MS, Saha O, et al. Epidemiology and molecular characterization of avian influenza virus in backyard poultry of Chattogram, Bangladesh. *Infect Genet Evol*. (2022) 105:105377. doi: 10.1016/j.meegid.2022.105377

28. Hoque MA, Tun HM, Hassan MM, Khan SA, Islam SKMA, Islam MN, et al. Molecular epidemiology of influenza a (H5N1) viruses, Bangladesh, 2007–2011. *Prev Vet Med*. (2013) 111:314–8. doi: 10.1016/j.prevetmed.2013.06.003

29. Islam A, Islam S, Samad MA, Hossain ME, Hassan MM, Alexandersen S, et al. Epidemiology and molecular characterization of multiple avian influenza A/H5 subtypes circulating in house crow (*Corvus splendens*) and poultry in Bangladesh. *Int J Infect Dis*. (2022) 116:S92–3. doi: 10.1016/j.ijid.2021.12.218

30. Islam A, Islam S, Hossain ME, Samad MA, Billah MM, Hassan MM, et al. One health investigation of house crow (*Corvus splendens*) mortality event linked to the potential circulation of H5N1 virus at live bird Markets in Northwestern Bangladesh. *Int J Infect Dis*. (2022) 116:S112. doi: 10.1016/j.ijid.2021.12.265

31. Islam A, Hossain ME, Islam S, Samad MA, Rahman MK, Chowdhury MGA, et al. Detection and genetic characterization of avian influenza a (H5N6) virus clade 2.3.4.4 in isolates from house crow and poultry in Bangladesh, 2017. *Int J Infect Dis*. (2020) 101:339–40. doi: 10.1016/j.ijid.2020.09.894

32. Barman S, Marinova-Petkova A, Hasan MK, Akhtar S, el-Shesheny R, Turner JCM, et al. Role of domestic ducks in the emergence of a new genotype of highly pathogenic H5N1 avian influenza a viruses in Bangladesh. *Emerg Microbes Infect*. (2017) 6:1–13. doi: 10.1038/emi.2017.60

33. Cui P, Shi J, Wang C, Zhang Y, Xing X, Kong H, et al. Global dissemination of H5N1 influenza viruses bearing the clade 2.3.4.4 b HA gene and biologic analysis of the ones detected in China. *Emerg Microbes Infect*. (2022) 11:1693–704. doi: 10.1080/22221751.2022.2088407

34. Agüero M, Monne I, Sánchez A, Zecchin B, Fusaro A, Ruano MJ, et al. Highly pathogenic avian influenza a (H5N1) virus infection in farmed minks, Spain, October 2022. *Eur Secur*. (2023) 28:2300001. doi: 10.2807/1560-7917.ES.2023.28.3.2300001

35. Thorsson E, Zohari S, Roos A, Banihashem F, Bröjer C, Neimanis A. Highly pathogenic avian influenza a (H5N1) virus in a harbor porpoise, Sweden. *Emerg Infect Dis*. (2023) 29:852–5. doi: 10.3201/eid2904.221426

36. Leguia M, Garcia-Glaessner A, Munoz-Saavedra B, Juarez D, Barrera P, Calvo-Mac C, et al. Highly pathogenic avian influenza a (H5N1) in marine mammals and seabirds in Peru. *bioRxiv*. (2023). doi: 10.1101/2023.03.03.531008

37. CDC, Technical report: highly pathogenic avian influenza A(H5N1) viruses. Available at: https://www.cdc.gov/flu/avianflu/spotlights/2022-2023/h5n1-technical-report.htm#infections-among-mammals (Accessed May 3, 2023). (2023).

38. WHO, Avian influenza weekly update number 891. Available at: https://www.who.int/docs/default-source/wpro---documents/emergency/surveillance/avian-influenza/ai_20230414.pdf?sfvrsn=5f006f99_113 (Accessed May 3, 2023). (2023).

39. Parvin R, Kamal AH, Haque ME, Chowdhury EH, Giasuddin M, Islam MR, et al. Genetic characterization of highly pathogenic H5N1 avian influenza virus from live migratory birds in Bangladesh. *Virus Genes*. (2014) 49:438–48. doi: 10.1007/s11262-014-1118-0

40. Henning J, Henning KA, Long NT, Ha NT, Vu LT, Meers J. Characteristics of two duck farming systems in the Mekong Delta of Viet Nam: stationary flocks and moving flocks, and their potential relevance to the spread of highly pathogenic avian influenza. *Trop Anim Health Prod*. (2013) 45:837–48. doi: 10.1007/s11250-012-0296-9

41. das SC, Chowdhury SD, Khatun MA, Nishibori M, Isobe N, Yoshimura Y. Poultry production profile and expected future projection in Bangladesh. *Worlds Poult Sci J*. (2008) 64:99–118. doi: 10.1017/S0043933907001754

42. Muzaffar SB, Takekawa JY, Prosser DJ, Douglas DC, Yan B, Xing Z. Ecological determinants of highly pathogenic avian influenza (H5N1) outbreaks in Bangladesh. *PLoS One*. (2012) 7:e33938. doi: 10.1371/journal.pone.0033938

43. Muzaffar SB, Takekawa JY, Prosser DJ, Douglas DC, Yan B, Xing Z, et al. Seasonal movements and migration of Pallas's gulls *Larus ichthyaetus* from Qinghai Lake. *China Forktail*. (2008) 2008:100–7.

44. Preliminary Report on Agriculture Census (2019). Bangladesh Bureau of Statistics: Bangladesh.

45. Khan KA, Saha S, Hossain M, Haque M, Haq M, Islam M. Epidemiological investigation of recurrent outbreaks of duck plague in selected Haor (wetland) areas of Bangladesh. *J Adv Veter Anim Res*. (2018) 5:131–9. doi: 10.5455/javar.2018.e256

46. Hossain M, Hoque M, Fournie G, Das G, Henning J, et al. *Management and health of stationary and nomadic ducks in the coastal and Haor areas of Bangladesh*. (2019)

47. Khan SU, Berman LS, Haider N, Gerloff N, Rahman MZ, Shu B, et al. Investigating a crow die-off in January–February 2011 during the introduction of a new clade of highly pathogenic avian influenza virus H5N1 into Bangladesh. *Arch Virol*. (2014) 159:509–18. doi: 10.1007/s00705-013-1842-0

48. Spackman E. Avian influenza virus detection and quantitation by real-time RT-PCR. *Anim Influenza Virus*. (2014):105–18. doi: 10.1007/978-1-4939-0758-8_10

49. CDC laboratory support for influenza surveillance (CLSIS). Centers for Disease Control and Prevention. Atlanta, GA, USA (2013).

50. Ali MZ, Hasan M, Giasuddin M. Potential risk factors of avian influenza virus infection in asymptomatic commercial chicken flocks in selected areas of Bangladesh during 2019. *J Adv Vet Ani Res*. (2021) 8:51–7. doi: 10.5455/javar.2021.h484

51. Kim Y, Biswas PK, Giasuddin M, Hasan M, Mahmud R, Chang YM, et al. Prevalence of avian influenza a (H5) and a (H9) viruses in live bird markets, Bangladesh. *Emerg Infect Dis*. (2018) 24:2309–16. doi: 10.3201/eid2412.180879

52. Zhou B, Donnelly ME, Scholes DT, St. George K, Hatta M, Kawaoka Y, et al. Single-reaction genomic amplification accelerates sequencing and vaccine production for classical and swine origin human influenza a viruses. *J Virol*. (2009) 83:10309–13. doi: 10.1128/JVI.01109-09

53. Hoffmann E, Stech J, Guan Y, Webster RG, Perez DR. Universal primer set for the full-length amplification of all influenza a viruses. *Arch Virol*. (2001) 146:2275–89. doi: 10.1007/s007050170002

54. Hijmans RJ, Guarino L, Bussink C, Mathur P, Cruz M, Barrentes I, et al. Diva-gis. (2004), Vsn.

55. Elbe S, Buckland-Merrett G. Data, disease and diplomacy: GISAID's innovative contribution to global health. *Global Chall*. (2017) 1:33–46. doi: 10.1002/gch2.1018

56. Drummond AJ, Rambaut A. BEAST: Bayesian evolutionary analysis by sampling trees. *BMC Evol Biol*. (2007) 7:214–8. doi: 10.1186/1471-2148-7-214

57. Baele G, Li WL, Drummond AJ, Suchard MA, Lemey P. Accurate model selection of relaxed molecular clocks in Bayesian phylogenetics. *Mol Biol Evol*. (2012) 30:239–43. doi: 10.1093/molbev/mss243

58. Hasegawa M, Kishino H, Yano T-A. Dating of the human-ape splitting by a molecular clock of mitochondrial DNA. *J Mol Evol*. (1985) 22:160–74. doi: 10.1007/BF02101694

59. Kalyaanamoorthy S, Minh BQ, Wong TKF, von Haeseler A, Jermiin LS. ModelFinder: fast model selection for accurate phylogenetic estimates. *Nat Methods*. (2017) 14:587–9. doi: 10.1038/nmeth.4285

60. Khatun A, Giasuddin M, Islam KM, Khanom S, Samad MA, Islam MR, et al. Surveillance of avian influenza virus type a in semi-scavenging ducks in Bangladesh. *BMC Vet Res*. (2013) 9:1–8. doi: 10.1186/1746-6148-9-196

61. Hassan MM, el Zowalaty ME, Islam A, Khan SA, Rahman MK, Järhult JD, et al. Prevalence and diversity of avian influenza virus hemagglutinin sero-subtypes in poultry and wild birds in Bangladesh. *Veter Sci*. (2020) 7:73. doi: 10.3390/vetsci7020073

62. Islam A, Hill N, Mikolon A, Sturm-Ramirez K, Rahman M, Paul S, et al. Avian influenza a viruses in wild birds and domestic ducks in Bangladesh, in options for the control of avian influenza VIII, Cape Town, South Africa (2013) 5–10:2013.

63. Islam A, Mikolon A, Khan M, Rahman A, Paul S, Islam A, et al. *A survey of avian influenza in wild birds and domestic ducks in Bangladesh, in international conference on emerging infectious diseases 2012*. (2012)

64. Henning KA, Henning J, Morton J, Long NT, Ha NT, Meers J. Farm-and flock-level risk factors associated with highly pathogenic avian influenza outbreaks on small holder duck and chicken farms in the Mekong Delta of Viet Nam. *Prev Vet Med*. (2009) 91:179–88. doi: 10.1016/j.prevetmed.2009.05.027

65. Sturm-Ramirez K, Hulse-Post DJ, Govorkova EA, Humberd J, Seiler P, Puthavathana P, et al. Are ducks contributing to the endemicity of highly pathogenic H5N1 influenza virus in Asia? *J Virol*. (2005) 79:11269–79. doi: 10.1128/JVI.79.17.11269-11279.2005

66. Sarkar S, Khan SU, Mikolon A, Rahman MZ, Abedin J, Zeidner N, et al. An epidemiological study of avian influenza a (H5) virus in nomadic ducks and their raising practices in northeastern Bangladesh, 2011-2012. *Influenza Other Respir Viruses*. (2017) 11:275–82. doi: 10.1111/irv.12438

67. Hidayat M, Dewi AM, Schoonman L, Wibawa H, Lubis EP, Lockhart C, et al. *Investigating the endemic presence and persistence of HPAI H5N1 virus on Java*. Indonesia: Authorea Preprints (2020).

68. Huang Y, Wille M, Dobbin A, Robertson GJ, Ryan P, Ojkic D, et al. A 4-year study of avian influenza virus prevalence and subtype diversity in ducks of Newfoundland. *Canada Canadian J Microbiol*. (2013) 59:701–8. doi: 10.1139/cjm-2013-0507

69. Wahlgren J. Influenza a viruses: an ecology review. *Infect Ecol Epidemiol*. (2011) 1:6004. doi: 10.3402/iee.v1i0.6004

70. Islam A, Islam S, Amin E, Shano S, Samad MA, Shirin T, et al. Assessment of poultry rearing practices and risk factors of H5N1 and H9N2 virus circulating among backyard chickens and ducks in rural communities. *PLoS One*. (2022) 17:e0275852. doi: 10.1371/journal.pone.0275852

71. Kayali G, Kandeil A, el-Shesheny R, Kayed AS, Gomaa MM, Maatouq AM, et al. Active surveillance for avian influenza virus, Egypt, 2010–2012. *Emerg Infect Dis*. (2014) 20:542–51. doi: 10.3201/eid2004.131295

72. Scheibner D, Ulrich R, Fatola OI, Graaf A, Gischke M, Salaheldin AH, et al. Variable impact of the hemagglutinin polybasic cleavage site on virulence and pathogenesis of avian influenza H7N7 virus in chickens, turkeys and ducks. *Sci Rep*. (2019) 9:1–13. doi: 10.1038/s41598-019-47938-3

73. Islam A, Islam S, Flora MS, Amin E, Woodard K, Webb A, et al. Epidemiology and molecular characterization of avian influenza a viruses H5N1 and H3N8 subtypes in poultry farms and live bird markets in Bangladesh. *Sci Rep*. (2023) 13:7912. doi: 10.1038/s41598-023-33814-8

74. Ligon BL. Avian influenza virus H5N1: a review of its history and information regarding its potential to cause the next pandemic In: . *Seminars in pediatric infectious diseases*, vol. *16*: Elsevier (2005). 326–35.

75. Cardona CJ, Xing Z, Sandrock CE, Davis CE. Avian influenza in birds and mammals. *Comp Immunol Microbiol Infect Dis*. (2009) 32:255–73. doi: 10.1016/j.cimid.2008.01.001

76. Young SG, Carrel M, Malanson G, Ali M, Kayali G. Predicting avian influenza co-infection with H5N1 and H9N2 in northern Egypt. *Int J Environ Res Public Health*. (2016) 13:886. doi: 10.3390/ijerph13090886

77. Li Y, Li X, Lv X, Xu Q, Zhao Z, Qin S, et al. Highly pathogenic avian influenza A (H5Nx) virus of Clade 2.3. 4.4 b emerging in Tibet, China, 10. *Microbiol Spectr*. (2022)10:e00643–22. doi: 10.1128/spectrum.00643-22

78. Nagarajan S, Tosh C, Smith DK, Peiris JSM, Murugkar HV, Sridevi R, et al. Avian influenza (H5N1) virus of clade 2.3. 2 in domestic poultry in India. *PLoS One*. (2012) 7:e31844. doi: 10.1371/journal.pone.0031844

79. Islam A, Klaassen M, Hossain ME, Samad MA, Hassan MM, Amin E, et al. Risk assessment, detection, and molecular characterization of H5N1 virus in a backyard chicken flock and a commercial FARM in Bangladesh. *Int J Infect Dis*. (2023) 130:S79–80. doi: 10.1016/j.ijid.2023.04.196

80. Biswas P, Giasuddin M, Nath BK, Islam MZ, Debnath NC, Yamage M. Biosecurity and circulation of influenza a (H5N1) virus in live-bird markets in Bangladesh, 2012. *Transbound Emerg Dis*. (2017) 64:883–91. doi: 10.1111/tbed.12454

81. Bevins SN, Shriner SA, Cumbee JC Jr, Dilione KE, Douglass KE, Ellis JW, et al. Intercontinental movement of highly pathogenic avian influenza a (H5N1) clade 2.3. 4.4 virus to the United States, 2021. *Emerg Infect Dis*. (2022) 28:1006–11. doi: 10.3201/eid2805.220318

82. European Food Safety Authority, European Centre for Disease Prevention, Control, European Union Reference Laboratory for Avian InfluenzaAdlhoch C, Fusaro A, Gonzales JL, Kuiken T, Marangon S, et al. Control, European Union reference Laboratory for Avian Influenza, et al., avian influenza overview December 2021–march 2022. *EFSA J*. (2022) 20:e07289. doi: 10.2903/j.efsa.2022.7289,

83. Mosaad Z, Elhusseiny MH, Zanaty A, Fathy MM, Hagag NM, Mady WH, et al. Emergence of highly pathogenic avian influenza a virus (H5N1) of clade 2.3. 4.4 b in Egypt, 2021–2022. *Pathogens*. (2023) 12:90. doi: 10.3390/pathogens12010090

84. Sanogo IN, Djegui F, Akpo Y, Gnanvi C, Dupré G, Rubrum A, et al. Highly pathogenic avian influenza a (H5N1) clade 2.3. 4.4 b virus in poultry, Benin, Emerging. *Infect Diseases*. (2021) 28:2534–7. doi: 10.3201/eid2812.221020

85. Ouoba LB, Habibata-Zerbo L, Zecchin B, Barbierato G, Hamidou-Ouandaogo S, Palumbo E, et al. Emergence of a reassortant 2.3. 4.4 b highly pathogenic H5N1 avian influenza virus containing H9N2 PA gene in Burkina Faso, West Africa, in 2021. *Viruses*. (2022) 14:1901

86. De Vries E, De Haan CA. Highly pathogenic influenza a (H5N1) viruses in farmed mink outbreak contain a disrupted second sialic acid binding site in neuraminidase, similar to human influenza a viruses. *Eur Secur*. (2023) 28:2300085. doi: 10.2807/1560-7917.ES.2023.28.7.2300085

87. Kupferschmidt K. Bird flu spread between mink is a 'warning bell'. *Science*. (2023) 379:316–7. doi: 10.1126/science.adg8342

frontiers | Frontiers in Public Health

TYPE Study Protocol
PUBLISHED 17 August 2023
DOI 10.3389/fpubh.2023.1236690

OPEN ACCESS

EDITED BY
Debdutta Bhattacharya,
Regional Medical Research Center (ICMR), India

REVIEWED BY
Martyn Regan,
The University of Manchester, United Kingdom
Tanveer Rehman,
Regional Medical Research Center (ICMR), India

*CORRESPONDENCE
Rizwan S. Abdulkader
✉ sarizwan1986@gmail.com

RECEIVED 08 June 2023
ACCEPTED 04 August 2023
PUBLISHED 17 August 2023

CITATION
Abdulkader RS, Potdar V, Mohd G, Chadwick J, Raju MK, Devika S, Bharadwaj SD, Aggarwal N, Vijay N, Sugumari C, Sundararajan T, Vasuki V, Bharathi Santhose N, Mohammed Razik CA, Madhavan V, Krupa NC, Prabakaran N, Murhekar MV and Gupta N (2023) Protocol for establishing a model for integrated influenza surveillance in Tamil Nadu, India.
Front. Public Health 11:1236690.
doi: 10.3389/fpubh.2023.1236690

Protocol for establishing a model for integrated influenza surveillance in Tamil Nadu, India

Rizwan S. Abdulkader[1]*, Varsha Potdar[2], Gulam Mohd[1], Joshua Chadwick[1], Mohan Kumar Raju[1], S. Devika[1], Sumit Dutt Bharadwaj[2], Neeraj Aggarwal[3], Neetu Vijay[3], C. Sugumari[4], T. Sundararajan[5], V. Vasuki[6], N. Bharathi Santhose[7], C. A. Mohammed Razik[1], Vinoth Madhavan[1], N. C. Krupa[1], Nandhini Prabakaran[1], Manoj V. Murhekar[1] and Nivedita Gupta[3]

[1]National Institute of Epidemiology, Chennai, India, [2]National Institute of Virology, Pune, India, [3]Indian Council of Medical Research, New Delhi, India, [4]Madurai Medical College, Madurai, India, [5]Government Mohan Kumaramangalam Medical College, Salem, India, [6]Tiruvarur Medical College Hospital, Tiruvarur, India, [7]Coimbatore Medical College and Hospital, Coimbatore, India

The potential for influenza viruses to cause public health emergencies is great. The World Health Organisation (WHO) in 2005 concluded that the world was unprepared to respond to an influenza pandemic. Available surveillance guidelines for pandemic influenza lack the specificity that would enable many countries to establish operational surveillance plans. A well-designed epidemiological and virological surveillance is required to strengthen a country's capacity for seasonal, novel, and pandemic influenza detection and prevention. Here, we describe the protocol to establish a novel mechanism for influenza and SARS-CoV-2 surveillance in the four identified districts of Tamil Nadu, India. This project will be carried out as an implementation research. Each district will identify one medical college and two primary health centres (PHCs) as sentinel sites for collecting severe acute respiratory infections (SARI) and influenza like illness (ILI) related information, respectively. For virological testing, 15 ILI and 10 SARI cases will be sampled and tested for influenza A, influenza B, and SARS-CoV-2 every week. Situation analysis using the WHO situation analysis tool will be done to identify the gaps and needs in the existing surveillance systems. Training for staff involved in disease surveillance will be given periodically. To enhance the reporting of ILI/SARI for sentinel surveillance, trained project staff will collect information from all ILI/SARI patients attending the sentinel sites using pre-tested tools. Using time, place, and person analysis, alerts for abnormal increases in cases will be generated and communicated to health authorities to initiate response activities. Advanced epidemiological analysis will be used to model influenza trends over time. Integrating virological and epidemiological surveillance data with advanced analysis and timely communication can enhance local preparedness for public health emergencies. Good quality surveillance data will facilitate an understanding outbreak severity and disease seasonality. Real-time data will help provide early warning signals for prevention and control of influenza and COVID-19 outbreaks. The implementation strategies found to be effective in this project can be scaled up to other parts of the country for replication and integration.

KEYWORDS

influenza, ILI, SARI, model, integrated surveillance, strengthening, capacity building, situation analysis

Introduction

Acute respiratory infections (ARI) are the most common infectious diseases worldwide and cause significant morbidity and mortality (1). Almost 4 million people die from ARIs every year, of which 98% are due to lower respiratory tract infections (LRI) (2). Influenza viruses cause a significant proportion of these infections (3–5). The economic loss due to respiratory infections caused by influenza viruses was estimated to be between US$71 and US$167 billion annually (6). The potential of influenza viruses to cause public health emergencies in society, evidenced by several incidents in the past, such as the Spanish flu of 1918, the Asian influenza of 1957, the Hong Kong influenza of 1968 and the H1N1 pandemic of 2009, cannot be overstated (7–10).

International committees convened by the World Health Organization (WHO) had found that the world was unprepared to respond to an influenza pandemic. The International Health Regulations 2005 require that each member state develop and maintain capabilities to detect, assess, and report disease events nationally and internationally to the WHO within 48 h of confirmation (11). However, reviews of national pandemic planning indicate that surveillance systems are often inadequate to support current preparedness strategies (12–16), especially in low-and middle-income countries (LMIC) like India and the available surveillance guidelines for pandemic influenza lack the specificity that would enable many countries to establish operational surveillance plans (17, 18). Also, the WHO has proposed a global influenza strategy 2019–2030, which focuses on improving global research and innovation to fill the gaps in our current knowledge about the transmission and host response of the influenza viruses, strengthen the influenza surveillance and pandemic preparedness and to expand the seasonal influenza prevention and control policies (19).

A routine sentinel surveillance system for influenza will gather data that can aid healthcare policy makers and providers in making decisions regarding program management and patient care (18). In India, influenza-like illness (ILI) and severe acute respiratory infection (SARI) surveillance are only partially implemented as part of the National Integrated Disease Surveillance Programme (IDSP). There are several pitfalls in the existing surveillance system. Lack of information sharing between surveillance reporting units and feedback from higher centres, combined with poor reporting quality and lack of epidemiological information crucial to identify and responding to outbreaks, result in poor disease surveillance and pandemic preparedness. Moreover, information on the current knowledge, practice and problems associated with the existing influenza surveillance system is scarce and it should be assessed to address problems and formulate solutions in order to get quality data for enhanced public health response (20, 21).

Recently, a strong need to include more epidemiological information to complement the virological data (18) for better understanding the influenza epidemiology and it severity has been emphasized globally (22–24). In the long run, establishment of a model for influenza and related infections surveillance will guide national approaches to optimal vaccination policies and appropriate allocation of healthcare resources (25). Previous studies have highlighted the need for a strong surveillance system to enhance and strengthen a country's capacity to detect and prevent seasonal, novel, and pandemic influenza (17).

There are several variations of influenza surveillance systems across the developed world. Most of these nations follow the WHO guidance for influenza surveillance (virological surveillance, primary care surveillance and hospital surveillance) (18). For example, the European influenza surveillance network (EISN) by European Centre for Disease Prevention and Control (ECDC) is responsible for the combined epidemiological and virological surveillance for influenza in European Union countries. Moreover these systems are complemented by initiatives like Influenzanet and EuroMOMO project for community surveillance and mortality surveillance, respectively (26, 27). The U.S. WHO Collaborating Laboratories System and National Respiratory and Enteric Virus Surveillance System (NREVSS) are responsible for the virological surveillance in US whereas the outpatient illness and hospital surveillance are monitored by the ILINet and FluSurv-NET, respectively (28). In developing countries, on the other hand, there are very few examples of such organized systems of surveillance for influenza (29–31).

Globally, the number of countries conducting routine influenza surveillance has increased over the last decade (32). Lessons from existing surveillance systems suggest that countries need to set up a robust surveillance system with components in both hospital and community settings and include epidemiologic and virologic aspects of data collection. Another important recommendation is to use data for action, especially as a tool for early detection and response to outbreaks (27, 28, 33, 34). However, it is also true that setting up developed countries' style systems can be very resource intensive and impractical for low-and middle-income countries like India. For example, countries like China and Malaysia have tried to set up surveillance systems but lack some components of influenza surveillance, such as sentinel surveillance in primary care, non-medically attended surveillance, mortality surveillance and integration with the routine health system (31).

Keeping these lessons in mind, we have incorporated some lessons from the ongoing global surveillance programs. In our proposed surveillance, we will be incorporating joint virologic and epidemiologic surveillance at primary care and sentinel hospital levels. This will also be integrated into the existing routine health systems to ensure sustainability. In order to ensure this integration, staff of the routine health care system will be regularly trained to carry out the surveillance activities and perform advanced data analysis for informing policy and action. Another important addition to the project is the mortality and disability surveillance which will be performed for both ILI and SARI cases. Since routine health systems are already burdened with several other priorities, we will integrate surveillance for influenza with other major pathogens such as SARS-CoV-2. Finally, we will be selecting sentinel sites which represent different climatic and geographical conditions.

Tamil Nadu is the 11th largest state situated in the southern part of India. The State is divided into 32 districts and estimated to have a population of over 7.21 crores which accounts for approximately 5.94% of India's total population (35). According to National Centre for Disease Control—India, Tamil Nadu state reported 2,827 cases and 25 deaths associated with influenza A (H1N1) compared to 13,202 cases and 410 deaths in the entire country during 2022 (36). However, these figures are likely to be gross underestimates of the actual burden since there is no on-going robust surveillance system for influenza in India. In order to address these circumstances, a well-designed epidemiological and virological surveillance is required to understand

local influenza epidemiology, detect and respond to outbreaks, establish disease burden, detect mutants and identify emerging new strains. In this paper, we present a study protocol for establishing a novel integrated influenza surveillance model in Tamil Nadu, India.

Study objectives

This project aims to develop a model of strengthened ILI/SARI surveillance for the country through the following objectives (Figure 1).

Objective 1: to establish influenza and SARS-CoV-2 surveillance in four identified districts of Tamil Nadu, India.

Objective 2: to strengthen the hospital-based epidemiological ILI/SARI surveillance in the identified districts of Tamil Nadu with the following sub-objectives

- Identify the gaps and strengthen the existing ILI/SARI surveillance.
- Develop the capacity of the surveillance system for undertaking advanced epidemiological analysis of surveillance data.

Materials and methods

This project will be carried out as implementation research in four selected districts of Tamil Nadu (Figure 2). One medical college hospital and two primary health care centres (PHCs) will be selected in each district to establish prospective sentinel surveillance, from which the SARI and ILI-related information will be collected, respectively. We chose primary care centres as sentinel sites for mild to moderate infections which will be captured under the influenza-like illness (ILI) definition and medical colleges as sentinel sites for severe infections which will fall under the severe acute respiratory infections (SARI) case definition. The number of districts and health care facilities selected for this study was based on available financial resources and the need for optimal geographical representation. The intended time period for completing this project will be 3 years.

Methods for objective 1

Study design

We will adopt a prospective sentinel surveillance approach.

Study setting

We will select one medical college hospital and two PHCs in each district to collect information related to SARI and ILI, respectively.

Study population

We will include all ILI/SARI patients of all age groups attending the selected healthcare facilities.

Study definitions

A case with an acute respiratory infection accompanied by a fever of ≥38°C and cough with onset within the last ten days will be considered as ILI. A case with an acute respiratory infection accompanied by a fever of ≥38°C, and cough with onset within the last ten days requiring hospitalization will be considered SARI.

Samples size

All patients attending the identified healthcare facilities will be included for epidemiological surveillance. The number of nasopharyngeal samples to be tested was determined based on several factors, including the available testing budget, the capacity of the laboratory, manpower available and the population size under surveillance. We have decided to collect 10 SARI and 15 ILI samples

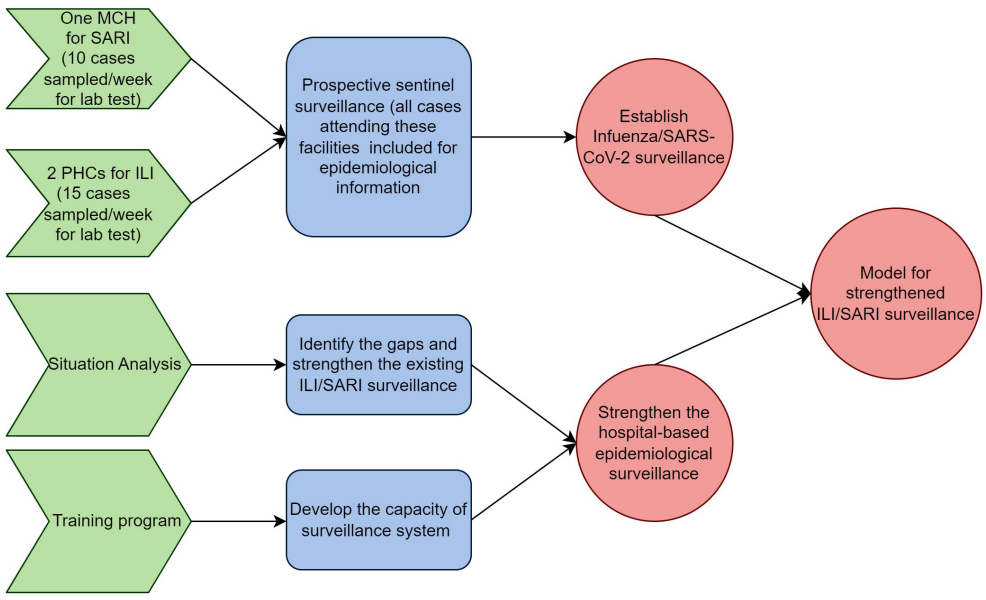

FIGURE 1
Schematic representation of objectives and activities of the model for integrated influenza surveillance in Tamil Nadu, India (MIST) project.

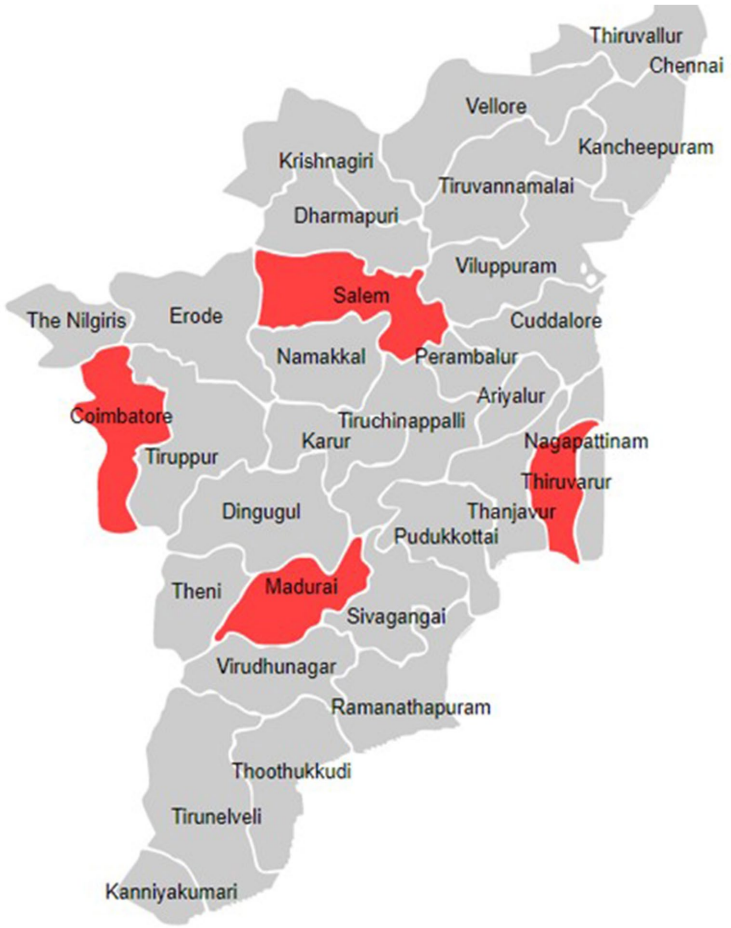

FIGURE 2
Location of the districts included in the model for integrated influenza surveillance in Tamil Nadu, India (MIST) project.

per site per week. This will lead to a collection of 1,300 samples per year for three years (total of 5,200 samples). This sample size was considered appropriate to determine the current strains of viruses circulating in the community in a given week. The total budget available for testing samples will be equally allocated to the four project sites. The primary purpose of virological testing was to inform the public health decision makers of the nature of the outbreak, if any, and the emergence of any novel or unknown strains and not as a part of clinical diagnostic requirement.

Study tool

A pre-tested and structured case reporting form (CRF) will be utilized to collect information from ILI and SARI cases. The CRF will collect personal characteristics, comorbidity status, current illness, factors contributing to the illness, clinical features, treatment given, and outcomes (Supplementary material).

Laboratory procedures for virological testing

Clinical specimens, including nasal, throat, and combined nasal/throat swabs, will be collected and preserved in 2–3 mL of viral transport medium (VTM), stored at 4°C, and transported to the laboratory within 4 h. Real-time polymerase chain reaction (RT-PCR) method will be used for molecular analysis of the samples (SARS-CoV-2 and influenza) using a multiplex assay kit containing three primer/probe sets (influenza A, influenza B, SARS-CoV-2) targeting the RNA of influenza A, influenza B, and SARS-CoV-2. The primers/probes will detect influenza A viruses from a conserved region of the matrix (M1) gene and influenza B virus from the non-structural gene (NS2). The influenza A positive samples will further be subtyped for A (H3N2) and A (H1N1)pdm09, and influenza B positive samples for Yamagata and Victoria (B/Y, B/V). Positive clinical specimens will be shipped to the referral lab earmarked by the sentinel lab for isolation and genetic characterization for SARS-CoV-2 and influenza novel variants. All laboratory procedures will be performed following standard operating procedures (Figure 3).

Data collection and analysis plan

Trained project staff will collect samples for testing and epidemiological information. Separate CRFs (Annexure 1) will be used for ILI and SARI-related data collection which includes demographic, clinical, hospitalization, management & outcome details. The collected data will be entered into the REDCap platform and analysed weekly for quality and completeness. District and pathogen-wise data analyses will be carried out

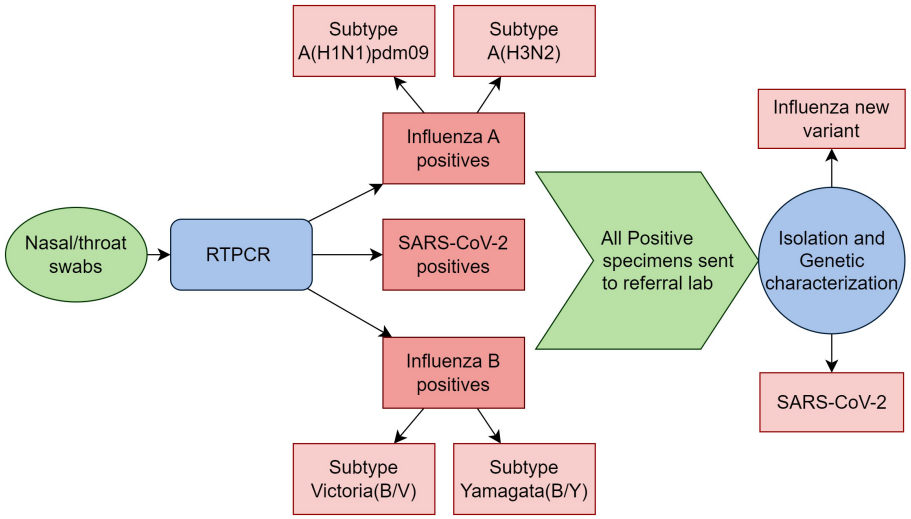

FIGURE 3
Schematic representation of laboratory procedures in the model for integrated influenza surveillance in Tamil Nadu, India (MIST) project.

weekly and reported to the appropriate authorities. A real-time dashboard will be developed, maintained, and shared with the authorities for displaying the total number of SARI/ILI cases enrolled and trends in test positivity for influenza viruses A & B and SARS-CoV-2 by week, age group and district. Analysed data will be expressed as frequency/proportion in the case of categorical variables and as the mean and standard deviation in the case of continuous variables.

Quality assurance

The project site laboratories will undergo periodic inspections to ensure testing quality. An external quality assurance system will be established through the laboratory at the National Institute of Virology, Pune. A periodic check for the quality of the data entered will be carried out, and daily and weekly review meetings will be conducted for the project staff to ensure proper data collection and reporting.

Methods for objective 2

Objective 2.1. Situation analysis of surveillance systems

The surveillance for ILI and SARI is a critical component of the public health response to these diseases. However, implementing ILI/SARI surveillance has many challenges, such as inadequate resources, lack of standardization, and insufficient manpower and training. To identify these gaps and challenges, we will conduct a situation analysis of the ILI/SARI surveillance system in the study districts.

Study design

We will adopt a mixed-methods approach.

Study setting

We will conduct the study in the selected health facilities of the study districts.

Study population

All personnel involved in ILI/SARI surveillance in the selected facilities will be included in the study.

Sampling and sample size

One medical college each from the government and private sectors, one district hospital, two sub-district hospitals, a sample of PHCs, two private hospitals and one microbiology laboratory (one each from the government and private sectors) will be selected by convenience. In addition to these, we will interview the personnel of the district and state surveillance units.

Study tools

We will use interview guides for carrying out in-depth interviews with study participants and observation check-lists for health facilities based on the components of the WHO situation analysis tool (37) (Supplementary material).

Data collection and analysis plan

We will describe the current status of the surveillance system in terms of the availability of human resources and facilities, data collection process, analysis of samples, reporting methods and the training requirements from the facility checklist and in-depth interviews. We will interview the nodal person involved in the ILI/SARI surveillance at different levels, collect information regarding their views and challenges on ILI/SARI surveillance, and obtain their recommendations to improve it. Quantitative variables will be expressed in mean and SD and frequencies and percentages. Qualitative data will be transcribed into English, and a thematic analysis will be carried out.

Strategies for strengthening the surveillance system

Based on the situation analysis, we will identify the existing gaps in the surveillance system. We will advocate for strengthening identified laboratories by optimizing logistics supply, training testing

staff regularly, and implementing an enhanced data management system. These measures will be implemented in the identified laboratories within the project districts, bolstering their overall capacity.

We will develop and share with the district health authorities the surveillance manuals, standard operating procedures (SOPs) for data collection, sample collection, sample transport, data collection tools, and data analysis format. Nodal persons will be identified in the concerned departments to ensure sustained collaboration and undertake required initiatives whenever required. SOPs will also be developed for information exchange and regular meetings of stakeholders to ensure sustained collaboration between the concerned departments. Periodic reports will be sent to district and state officials to coordinate response activities to ensure the effectiveness of the ILI/SARI surveillance.

Objective 2.2. Develop the capacity of the surveillance system for analysis of surveillance data

To enhance the effectiveness of the ILI/SARI surveillance system, we need to develop the capacity within the system for routine analysis of surveillance data. To achieve this, we will train the district and state-level staff involved in ILI/SARI surveillance for epidemiological data collection, collation, analysis, and reporting. We will utilise the situation analysis results to develop training sessions targeting the knowledge gap within the disease surveillance system. These training sessions will be designed to address and bridge any existing gaps in their understanding and expertise. The training program will be conducted in batches of 20 members at state headquarters until all personnel are trained.

By providing this training, we aim to empower the staff to efficiently and effectively analyse surveillance data, enabling the concerned authorities to make data-driven decisions and take proactive measures to control the spread of infectious diseases.

Ethics statement

The study protocol has been approved by the Institutional Human Ethics Committee (IHEC) of all the participating sites. The study participants will be given details of the study objectives and data collection methods. Age-appropriate written informed consent will be obtained. Complete confidentiality and anonymity of the identifiers and information collected will be maintained. Personal identifiers will be available only in the data collection proforma and not used during the analysis or publication/dissemination. Biological samples such as nasal/nasopharyngeal swabs will be collected and tested as per standard laboratory procedures. During follow-up, if any participant requires medical attention, they will be referred to the appropriate hospital for further management.

Discussion

Implementing an integrated approach for collecting virological and epidemiological surveillance data, combined with the potential of advanced analysis, could strengthen the country's efforts for preparedness during public health emergencies (28, 38, 39). Good quality historical surveillance data can be used to understand better and answer critical questions such as the severity and seasonality of outbreaks and help compare trends between various regions of the country and even between different countries (40).

India has faced several epidemics and pandemics in the past (7). However, because of the lack of communication and coordination in surveillance, it is practically impossible to predict and prepare for any pandemic occurring in the future. Laboratory detection for the viruses is the only way to confirm the diagnosis of a particular respiratory viral infection, as all respiratory viral infections have overlapping symptoms (41). This project will use the existing Virus Research Diagnostic Laboratory (VRDL) network labs attached to the study site for the lab confirmation of influenza and SARS-CoV-2. This will strengthen the existing surveillance and help administer timely antiviral treatment to patients to reduce the duration of symptoms and prevent transmission to others (3). Also, epidemiological data collection of ILI/SARI cases will help provide specific disease transmission and impact indicators. This surveillance model and its outputs will provide the health system with valuable tools for conducting advanced analysis of surveillance data and detect warning signals of potential outbreaks in a timely manner. These capabilities greatly enhance the development of prevention and control policies, including the implementation of effective vaccination strategies and specific non-pharmacological interventions such as mask mandates, quarantine and isolation measures. By leveraging the insights derived from this model, the health system will be empowered to make more informed decisions and optimize their approaches for mitigating the spread of influenza and other respiratory viruses.

The strategies adopted in this project have several strengths. First, we base our interventions on the situation analysis of the existing ILI/SARI surveillance system to identify the needs and gaps. Based on these findings we will develop "plug-ins" in the existing surveillance system to further strengthen it. Second, real-time data analysis and presenting it in the form of an easily accessible dashboard will help provide early warning signals and guide strategies for prevention and control. Lastly, we will train the staff involved in disease surveillance with standard definitions for ILI/SARI for correctly identifying and reporting ILI/SARI cases from the community as part of situation analysis and training.

There are a few limitations in this implementation project. We intend to test only for influenza A, influenza B and SARS-CoV-2. Other dominant respiratory viruses like respiratory syncytial virus (RSV) which may cause severe disease among high-risk groups (HRGs) are not included in the testing algorithm (42, 43). Since the surveillance method used here is of the sentinel type, we will miss cases occurring outside the catchment areas of the sentinel sites (44).

Ethics statement

The studies involving humans were approved by Institutional Human Ethics Committee, ICMR—National Institute of Epidemiology. The studies were conducted in accordance with the local legislation and institutional requirements. Written informed

consent for participation in this study was provided by the participants' legal guardians/next of kin.

Author contributions

RA, VP, NG, GM, JC, MR, SD, MM, SB, NA, and NV were responsible for conceptualization, design, and development of the methodology. RA, CM, and VM drafted the initial manuscript. VP, NG, GM, JC, MR, SD, MM, SB, NA, NV, CS, TS, VV, NB, NK, and NP provided the critical comments to the manuscript. All authors contributed to the article and approved the submitted version.

Funding

This work was funded and supported by the Indian Council Medical Research (Project grant ID-R.15013/10/2021-HR-VRDL). The funding body had no role in the design of the study and collection, analysis, and interpretation of data and in writing the manuscript.

Conflict of interest

The authors declare that the research was conducted in the absence of any commercial or financial relationships that could be construed as a potential conflict of interest.

Publisher's note

All claims expressed in this article are solely those of the authors and do not necessarily represent those of their affiliated organizations, or those of the publisher, the editors and the reviewers. Any product that may be evaluated in this article, or claim that may be made by its manufacturer, is not guaranteed or endorsed by the publisher.

Supplementary material

The Supplementary material for this article can be found online at: https://www.frontiersin.org/articles/10.3389/fpubh.2023.1236690/full#supplementary-material

References

1. Stockwell MS, Reed C, Vargas CY, Wang L, Alba LR, Jia H, et al. Five-year community surveillance study for acute respiratory infections using text messaging: findings from the MoSAIC study. *Clin Infect Dis*. (2022) 75:987–95. doi: 10.1093/cid/ciac027

2. World Health Organization. *Infection prevention and control of epidemic-and pandemic-prone acute respiratory infections in health care. Introduction and scope of the guidelines*. Geneva: World Health Organization (2014) Available at: https://www.ncbi.nlm.nih.gov/books/NBK214360/.

3. Buchan SA, Hottes TS, Rosella LC, Crowcroft NS, Tran D, Kwong JC. Contribution of influenza viruses to medically attended acute respiratory illnesses in children in high-income countries: a meta-analysis. *Influenza Other Respir Viruses*. (2016) 10:444–54. doi: 10.1111/irv.12400

4. Walker GJ, Stelzer-Braid S, Shorter C, Honeywill C, Wynn M, Willenborg C, et al. Viruses associated with acute respiratory infection in a community-based cohort of healthy New Zealand children. *J Med Virol*. (2022) 94:454–60. doi: 10.1002/jmv.25493

5. Taylor S, Lopez P, Weckx L, Borja-Tabora C, Ulloa-Gutierrez R, Lazcano-Ponce E, et al. Respiratory viruses and influenza-like illness: epidemiology and outcomes in children aged 6 months to 10 years in a multi-country population sample. *J Infect*. (2017) 74:29–41. doi: 10.1016/j.jinf.2016.09.003

6. Forum of International RespiratorySocieties. *The global impact of respiratory disease. 2nd* ed. Sheffield: European Respiratory Society, on behalf of the Forum of International Respiratory Societies (2017).

7. Swetha G, Eashwar VMA, Gopalakrishnan S. Epidemics and pandemics in India throughout history: a review article. *Indian J Public Health Res Dev*. (2019) 10:1570. doi: 10.5958/0976-5506.2019.02328.3

8. Johnson NPAS, Mueller J. Updating the accounts: global mortality of the 1918–1920 "Spanish" influenza pandemic. *Bull Hist Med*. (2002) 76:105–15. doi: 10.1353/bhm.2002.0022

9. Chandra S, Kassens-Noor E. The evolution of pandemic influenza: evidence from India, 1918–1919. *BMC Infect Dis*. (2014) 14:510. doi: 10.1186/1471-2334-14-510

10. Kilbourne ED. Influenza pandemics of the 20th century. *Emerg Infect Dis*. (2006) 12:9–14. doi: 10.3201/eid1201.051254

11. World Health Organisation. *International Health Regulations (2005). 3rd* ed WHO Publications (2023) Available at: https://www.who.int/publications-detail-redirect/9789241580496.

12. Ortu G, Mounier-Jack S, Coker R. Pandemic influenza preparedness in Africa is a profound challenge for an already distressed region: analysis of national preparedness plans. *Health Policy Plan*. (2008) 23:161–9. doi: 10.1093/heapol/czn004

13. Oshitani H, Kamigaki T, Suzuki A. Major issues and challenges of influenza pandemic preparedness in developing countries. *Emerg Infect Dis*. (2008) 14:875–80. doi: 10.3201/eid1406.070839

14. Breiman RF, Nasidi A, Katz MA, Njenga MK, Vertefeuille J. Preparedness for highly pathogenic avian influenza pandemic in Africa. *Emerg Infect Dis*. (2007) 13:1453–8. doi: 10.3201/eid1310.070400

15. Mounier-Jack S, Jas R, Coker R. Progress and shortcomings in European national strategic plans for pandemic influenza. *Bull World Health Organ*. (2007) 85:923–9. doi: 10.2471/BLT.06.039834

16. Coker R, Mounier-Jack S. Pandemic influenza preparedness in the Asia-Pacific region. *Lancet*. (2006) 368:886–9. doi: 10.1016/S0140-6736(06)69209-X

17. Ortiz JR, Sotomayor V, Uez OC, Oliva O, Bettels D, McCarron M, et al. Strategy to enhance influenza surveillance worldwide 1. *Emerg Infect Dis*. (2009) 15:1271–8. doi: 10.3201/eid1508.081422

18. World Health Organization. Global epidemiological surveillance standards for influenza. *WHO Technical Document*; (2013). Available at: https://apps.who.int/iris/handle/10665/311268. (Accessed February 11, 2023)

19. World Health Organization. Global influenza strategy 2019–2030. (2023). *WHO guidelines*. Available at: https://www.who.int/publications-detail-redirect/9789241515320. (Accessed March 7, 2023)

20. Rajan D. "Situation Analysis of the Health Sector." (World Health Organization, Geneva, 2016: Strategizing National Health in the 21st Century: A Handbook, First ed.) (2016).

21. Lm F, Fields R, Pk M, Posner S, Le M. *Situation analysis of infectious disease surveillance in two districts in Tanzania 2002*. Washington, U.S: Seattle (2003).

22. Capitani E, Montomoli E, Camarri A, Bova G, Capecchi PL, Mercone A, et al. Epidemiological and virological surveillance of severe acute respiratory infections in the 2019/2020 season in Siena, Tuscany, Italy. *J Prev Med Hyg*. (2021) 31:E782–8. doi: 10.1093/eurpub/ckab165.641

23. Salute M della. *Monitoraggio delle forme gravi e complicate* (2003). Available at: https://www.salute.gov.it/portale/influenza/dettaglioContenutiInfluenza.jsp?lingua=italiano&id=4246&area=influenza&menu=vuoto. (Accessed July 9, 2023)

24. Macias AE, McElhaney JE, Chaves SS, Nealon J, Nunes MC, Samson SI, et al. The disease burden of influenza beyond respiratory illness. *Vaccine*. (2021) 39:A6–A14. doi: 10.1016/j.vaccine.2020.09.048

25. Fleming DM, van der Velden J, Paget WJ. The evolution of influenza surveillance in Europe and prospects for the next 10 years. *Vaccine*. (2003) 21:1749–53. doi: 10.1016/S0264-410X(03)00066-5

26. Guerrisi C, Turbelin C, Blanchon T, Hanslik T, Bonmarin I, Levy-Bruhl D, et al. Participatory syndromic surveillance of influenza in Europe. *J Infect Dis*. (2016) 214:S386–92. doi: 10.1093/infdis/jiw280

27. de Fougerolles TR, Damm O, Ansaldi F, Chironna M, Crépey P, de Lusignan S, et al. National influenza surveillance systems in five European countries: a qualitative comparative framework based on WHO guidance. *BMC Public Health*. (2022) 22:1151. doi: 10.1186/s12889-022-13433-0

28. Centers for Disease Control and Prevention. U.S. influenza surveillance: purpose and methods|CDC. *CDC flu weekly*. (2022). Available at: https://www.cdc.gov/flu/weekly/overview.htm. (Accessed March 9, 2023)

29. Yang P, Duan W, Lv M, Shi W, Peng X, Wang X, et al. Review of an influenza surveillance system, Beijing, People's republic of China. *Emerg Infect Dis*. (2009) 15:1603–8. doi: 10.3201/eid1510.081040

30. *Home-influenza surveillance dashboard-School of Public Health, The University of Hong Kong*. (2023). Available at: https://dashboard.sph.hku.hk/index.php/en/. (Accessed July 13, 2023)

31. El Guerche-Séblain C, Rigoine De Fougerolles T, Sampson K, Jennings L, Van Buynder P, Shu Y, et al. Comparison of influenza surveillance systems in Australia, China, Malaysia and expert recommendations for influenza control. *BMC Public Health*. (2021) 21:1750. doi: 10.1186/s12889-021-11765-x

32. Polansky LS, Outin-Blenman S, Moen AC. Improved global capacity for influenza surveillance. *Emerg Infect Dis*. (2016) 22:993–1001. doi: 10.3201/eid2206.151521

33. Brammer L, Budd A, Cox N. Seasonal and pandemic influenza surveillance considerations for constructing multicomponent systems. *Influenza Other Respir Viruses*. (2009) 3:51–8. doi: 10.1111/j.1750-2659.2009.00077.x

34. Marbus SD, van der Hoek W, van Dissel JT, van Gageldonk-Lafeber AB. Experience of establishing severe acute respiratory surveillance in the Netherlands: evaluation and challenges. *Public Health Pract*. (2020) 1:100014. doi: 10.1016/j.puhip.2020.100014

35. NHSRC. *Health dossier 2021: reflections on key health indicators—Tamil Nadu* (2021). 24 p Available at: https://nhsrcindia.org/sites/default/files/practice_image/HealthDossier2021/Tamil%20Nadu.pdf.

36. NCDC. *State/UT—wise, year-wise number of cases and deaths from 2016–2021* Ministry of Health and Family Welfare (2023). 1 p Available at: https://ncdc.gov.in/showfile.php?lid=280.

37. World Health Organisation. *Ear and hearing care: situation analysis tool*. Geneva: World Health Organization (2015).

38. Chu HY, Boeckh M, Englund JA, Famulare M, Lutz B, Nickerson DA, et al. The Seattle flu study: a multiarm community-based prospective study protocol for assessing influenza prevalence, transmission and genomic epidemiology. *BMJ Open*. (2020) 10:e037295. doi: 10.1136/bmjopen-2020-037295

39. Global Influenza Surveillance and Response System (GISRS). *WHO initiatives*. (2023). Available at https://www.who.int/initiatives/global-influenza-surveillance-and-response-system. (Accessed February 8, 2023)

40. Influenza surveillance outputs. *WHO global influenza programme*. (2023). Available at: https://www.who.int/teams/global-influenza-programme/surveillance-and-monitoring/influenza-surveillance-outputs. (Accessed March 10, 2023)

41. Waghmode R, Jadhav S, Nema V. The burden of respiratory viruses and their prevalence in different geographical regions of India: 1970–2020. *Front Microbiol*. (2021) 12:12. doi: 10.3389/fmicb.2021.723850

42. Zhang Y, Zhao J, Zou X, Fan Y, Xiong Z, Li B, et al. Severity of influenza virus and respiratory syncytial virus coinfections in hospitalized adult patients. *J Clin Virol*. (2020) 133:104685. doi: 10.1016/j.jcv.2020.104685

43. Welliver TP, Reed JL, Welliver RCS. Respiratory syncytial virus and influenza virus infections: observations from tissues of fatal infant cases. *Pediatr Infect Dis J*. (2008) 27:S92–6. doi: 10.1097/INF.0b013e318168b706

44. Gilbert R, Cliffe SJ. Public health surveillance In: K Regmi and I Gee, editors. *Public health intelligence: issues of measure and method*. Cham: Springer (2016). 91–110.

frontiers | Frontiers in Public Health

TYPE Original Research
PUBLISHED 30 August 2023
DOI 10.3389/fpubh.2023.1193839

OPEN ACCESS

EDITED BY
Zhimin Tao,
Jiangsu University, China

REVIEWED BY
Shymaa Mamdouh,
Mansoura University, Egypt
Abhishek Mishra,
Lala Lajpat Rai Memorial Medical College, India

*CORRESPONDENCE
Jia Lu
✉ cpulj@126.com
Ye Yao
✉ yyao@fudan.edu.cn

†These authors have contributed equally to this work

RECEIVED 10 May 2023
ACCEPTED 18 August 2023
PUBLISHED 30 August 2023

CITATION
Zhang Z, Shi L, Liu N, Jia B, Mei K, Zhang L, Zhang X, Lu Y, Lu J and Yao Y (2023) Coverage and impact of influenza vaccination among children in Minhang District, China, 2013–2020.
Front. Public Health 11:1193839.
doi: 10.3389/fpubh.2023.1193839

Coverage and impact of influenza vaccination among children in Minhang District, China, 2013–2020

Zhaowen Zhang[1†], Liming Shi[2,3†], Nian Liu[1], Biyun Jia[1], Kewen Mei[1], Liping Zhang[1], XuanZhao Zhang[1], Yihan Lu[2,3], Jia Lu[1*] and Ye Yao[2,3*]

[1]Minhang Center for Disease Control and Prevention, Shanghai, China, [2]School of Public Health, Fudan University, Shanghai, China, [3]Key Laboratory of Public Health Safety of Ministry of Education, Fudan University, Shanghai, China

Background: Young children have a great disease burden and are particularly vulnerable to influenza. This study aimed to assess the direct effect of influenza vaccination among children and to evaluate the indirect benefit of immunizing children.

Methods: The influenza vaccination records for all children born during 2013–2019 in Minhang District and surveillance data for reported influenza cases were obtained from the Minhang CDC. 17,905 children were recorded in the vaccination system and included in this study. Descriptive epidemiology methods were used for data analysis, including an ecological approach to estimate the number of influenza cases averted by vaccination and linear regression to estimate the reduction in influenza cases in the general population per thousand additional childhood vaccination doses.

Results: During the study period, the annual vaccination coverage rate ranged from 10.40% in 2013–2014 to 27.62% in 2015–2016. The estimated number of influenza cases averted by vaccination ranged from a low of 0.28 (range: 0.23–0.34) during 2013–2014 (PF: 6.15%, range: 5.11–7.38%) to a high of 15.34 (range: 12.38–18.51) during 2017–2018 (PF: 16.54%, range: 13.79–19.30%). When increasing vaccination coverage rate by 10% in each town/street, a ratio of 7.27–10.69% cases could be further averted on the basis of observed cases. In four selected periods, the number of influenza cases in the general population was most significantly correlated with the cumulative childhood vaccination doses in the prior 2–5 months, and the reduction in influenza cases ranged from 0.73 to 3.18 cases per thousand additional childhood vaccination doses.

Conclusion: Influenza vaccination among children is estimated to have direct effects in terms of averted cases and might provide an underlying indirect benefit to the general population. Vaccination coverage in high-coverage areas should be further expanded to avert more influenza cases.

KEYWORDS

influenza, vaccination, children, averted cases, burden, China

1. Introduction

Seasonal influenza is an infectious respiratory disease caused by influenza viruses and poses substantial morbidity and mortality annually (1). Young children have a great disease burden and are particularly vulnerable to influenza. It was estimated that 109.5 million influenza virus infections occurred worldwide in 2018 among children under 5 years of age (2). The highest influenza notification rates in Australia were observed among children aged 0–4 years (111 cases per 100,000 population compared with a total rate of 60 cases per 100,000 population) (3). The attack rate was highest among children aged 0–4 years (31.9%) for the 2015–2016 season in Beijing, China (4). Children have been identified as the main spreaders in influenza transmission. It was estimated that 40–48% of the secondary cases exposed to a child sick with influenza in the household are attributable to transmission from the child (5). In influenza B outbreaks, children aged 0–4 years had the highest estimated relative risk (6). Thus, relieving the disease burden among children will decrease the opportunity for influenza transmission to others.

Influenza vaccination is considered the most effective means of preventing influenza and can significantly reduce the risk of influenza and serious complications among vaccinated people (7, 8). An estimated 4.4 million illnesses and 58,000 hospitalizations were prevented due to influenza vaccination during the US 2018–2019 influenza season (9). Vaccinating children can protect them directly and is presumed to interrupt influenza transmission in the general population, which indirectly protects susceptible contacts (10). A cluster randomized controlled trial revealed that immunizing children aged 36 months to 15 years with inactivated influenza vaccine produced a protective effectiveness of 61% against confirmed influenza illness among unimmunized residents of communities (11). The Chinese Center for Disease Prevention and Control (Chinese CDC) has recommended annual seasonal influenza vaccines to be administered to children aged 6–59 months (12). However, because influenza vaccines are not included in the National Immunization Program (NIP) in most areas of China, vaccination coverage among children is relatively low (13). Influenza vaccination coverage among children aged under 5 years was estimated to range from 12 to 32% in China during 2009–2012 (14, 15).

Different models have been used to evaluate the impact of influenza vaccination on averted influenza-associated events (16–22). Averted events were defined as the difference between observed events and projected events in the absence of vaccination (23). Backer et al. developed a stochastic transmission model to estimate an average of 13% infections, 24% hospitalizations, and 35% deaths averted in the Netherlands (24). Zhang et al. used a dynamic transmission model to assess the impact of vaccinating school-going children in Beijing, China for the 2013–2016 seasons (19). Although these methods can take some factors into account, such as indirect effects, loss of immunity, and influenza activity variations between seasons, a series of parameters need to be estimated, and heavy computations are needed. Kostova et al. originally proposed a method to estimate the direct effect of influenza vaccination in terms of averted events in the US 2005–2011 seasons (21), and this method was then used and developed by some other researchers (18, 22, 25, 26). This method estimates the averted influenza cases and prevented fraction using three parameters: number of observed cases, vaccination coverage, and vaccine effectiveness. These measures to evaluate vaccine impact are easy to understand and interpret.

The objective of this study was to assess the direct effects of influenza vaccination among children by estimating the number of averted cases and prevented fractions, and to estimate the indirect effects by quantifying the relationship between cumulative vaccination doses among children and influenza cases in the general population.

2. Methods

2.1. Study design and population

In this study, based on multiyear vaccination records and surveillance data, we give observational evidences on direct and indirect effects of immunizing children. Children living in Minhang District, including permanent and nonpermanent residents, are registered on the National Immunization Program (NIP) system. The vaccination records of these children include demographic information such as age and sex and vaccination information such as vaccine type and vaccination time.

2.2. Data sources

2.2.1. Vaccination data

We extracted the influenza vaccination records from July 2013 to June 2020 from the Minhang Center for Disease Prevention and Control (Minhang CDC) NIP system. One record was excluded due to a date of birth outside of the study period and 9 records were removed for their inaccurate vaccination dates. Finally, a total of 170,915 children who were born between January 2013 and December 2019 were enrolled in this study. Depending on the time pattern, we defined one vaccination year as being from July 1st to June 30th the next year. Thus, there were 7 vaccination years in this study from 2013–2014 to 2019–2020.

2.2.2. Surveillance data

We obtained the surveillance data of confirmed influenza cases during 2016/01–2020/01 from the Minhang CDC Notifiable Infectious Diseases Reporting Information System, with missing data from April to November 2018. This dataset included age, sex, residential address, time of influenza onset, time of diagnosis, and flu types.

2.2.3. Influenza incidence data

The monthly statistics of influenza in Shanghai during 2013–2018 were downloaded from the China CDC's public health science data center (27). Influenza incidence by age group was used to estimate the number of observed influenza cases among children due to a lack of surveillance data before 2016 and missing data in 2018.

2.2.4. Vaccination coverage

According to the China Technical Guidelines for Influenza Vaccines (12), children aged over 6 months can receive influenza vaccines. Yearly vaccination coverage (VC) was calculated using the vaccination data from the Minhang CDC by dividing the number of actually vaccinated children by the total population of children who met the vaccination criteria during the same period.

2.2.5. Vaccine effectiveness

Influenza vaccine effectiveness (VE) varies widely in different seasons and influenza types and subtypes (28–30). Therefore, in this study, VE was assumed to be at a moderate level of 60%. We also performed a sensitivity analysis by adjusting the VE in an interval of +/− 10%. The results of the sensitivity analyses were presented as ranges of the estimated averted influenza cases to indicate uncertainties.

2.3. Averted influenza cases estimation method

To assess the impact of influenza vaccination on children, we estimated the number of averted influenza cases in two steps. First, the number of influenza cases among children during 2013–2018 was estimated by multiplying the monthly influenza incidence in each age group by the number of children who met the criteria for vaccination in that month. Yearly influenza cases were calculated by adding the monthly estimations together (details available in the supplementary file). The averted influenza cases were the difference between the expected influenza cases if there were no vaccinations given (N) and the observed burden with vaccination (n). The number of averted influenza cases (NAC) was then estimated using the following formula (22, 25):

$$NAC = N - n = \frac{n \cdot (VE \cdot VC)}{1 - (VE \cdot VC)}$$

where n is the observed influenza cases, and VC and VE represent vaccination coverage and vaccine effectiveness, respectively.

The number of averted cases depends not only on VC and VE during that season but also on the influenza epidemic intensity, i.e., seasons with high epidemic intensity will result in a higher number of averted cases (21). Therefore, we estimated the prevented fraction (PF) as:

$$PF = \frac{NAC}{(NAC + n)}$$

a relative term measuring the impact of vaccination (22).

2.4. Statistical analysis

A chi-square test was performed to compare different features between vaccinated and unvaccinated groups. Pearson's correlation analysis was performed between cumulative vaccination doses and influenza cases. Statistical analyses were performed in R language (version 4.1.3, R Core Team, Vienna, Austria).

2.5. Ethics statement

The study was reviewed and approved by the Institutional Review Board of the Minhang Center for Disease Control and Prevention. The number of the ethical letter regarding this study is EC-P-2020-010. Informed consent was waived for this study because it involved the use of surveillance data and no potentially identifiable human data were presented.

3. Results

During the study period, 170,915 children who resided in Minhang and were born between January 2013 and December 2019 were registered in the NIP system. Of these, 78,027 (45.65%) received at least one dose of influenza vaccine during the study period. The vaccination coverage rate among children with permanent residency was significantly higher than that among children with nonpermanent residency (47.45% vs. 43.85%, $p < 0.001$) (Supplementary Table S1). From 2013–2014 to 2015–2016, the annual influenza vaccination coverage rate increased nearly 3-fold from 10.40 to 27.62% (Table 1). The coverage rate rebounded to 27.57% after a slight fluctuation in 2016–2017. However, a sharp decline occurred in the following years, and vaccination coverage fell to 14.16% in 2018–2019 and 18.13% in 2019–2020. From the perspective of monthly trends, the peak vaccination period was from September to February the next year, with a minor period in August and March (Supplementary Figure S1). There were rare vaccinations in other months, except in 2019–2020. The vaccination coverage in each town was computed according to the children's residential addresses on the records. During the study period, the lowest vaccination coverage rate was 6.11% on Pujin Street in 2016–2017, and the highest was 44.26% on Jiangchuan Street in 2017–2018 (Table 2). The mean coverage rates in each town over the study period ranged from 10.39 to 33.46%. The mean coverage rate in Minhang District during the study period was 21.93%, and the coverage rates of seven towns/streets were below the mean (Table 2). The coverage rates in Qibao Town, Meilong Town, Pujin Street, and Zhuanqiao Town were always below the average in each vaccination year, and the coverage rates in Meilong Town, Pujiang Town, and Pujin Street were 6 times below the lower quantile. In contrast, the coverage rates in Jiangchuan Street, Maqiao Town, and Xinhong Street were always higher than the yearly average.

Due to insufficient surveillance data compared to vaccination data, the number of influenza cases among registered children between 2013–2014 and 2017–2018 was estimated using incidence data and vaccination data (Supplementary Table S2). As newborn children continued to join the study cohort, the population of children and estimated number of influenza cases both increased substantially, from 24,652 and 4.27 in 2013–2014 to 126,054 and 77.41 in 2017–2018, respectively (Table 1 and Supplementary Table S2). Influenza vaccination prevented an average of 5.52 (range: 4.46–6.65) cases per year during the 5 years (Table 3). The largest number of averted cases occurred during 2017–2018, when 15.34 (range: 12.38–18.51) influenza cases were prevented by vaccination, corresponding to a prevented fraction of 16.54% (range: 13.79%-19.30). The year with the lowest number of averted events was 2013–2014, when 0.28 (0.23–0.34) cases were averted, with a prevented fraction of 6.15% (5.10–7.4%). The largest prevented fraction was 16.58% (range: 13.82–1.32%) in 2015–2016 when the vaccination coverage rate was the highest. Sensitivity analysis was also performed to test the influence of vaccination coverage on averted cases and prevented fractions (Supplementary Table S3). When vaccination coverage increased by

10.3389/fpubh.2023.1193839

TABLE 1 Yearly vaccination coverage rates in Minhang District from 2013–2014 to 2019–2020.

Year	Number of vaccinated children	Number of vaccination doses	The population of children in the same period	Vaccination coverage rates
2013–2014	2,563	4,670	24,652	10.40%
2014–2015	11,690	21,932	50,961	22.94%
2015–2016	19,984	37,156	72,356	27.62%
2016–2017	24,267	36,733	100,427	24.16%
2017–2018	34,757	54,208	126,054	27.57%
2018–2019	21,111	30,912	149,098	14.16%
2019–2020	30,991	40,930	170,915	18.13%

One vaccination year is defined as July 1st to June 30th in the following year. The study period was divided into 7 consecutive vaccination years from 2013–2014 to 2019–2020. Children aged 6 months and older could meet the criteria for receiving the influenza vaccine, and all children who met the criteria composed the population of children in the same period. Vaccination coverage was calculated by the number of vaccinated children divided by the population of children in the same period in each vaccination year.

TABLE 2 Annual and mean vaccination coverage rates in each town/street in Minhang District from 2013–2014 to 2019–2020.

Town/Street	2013–2014 (%)	2014–2015 (%)	2015–2016 (%)	2016–2017 (%)	2017–2018 (%)	2018–2019 (%)	2019–2020 (%)	Mean coverage rate
Huacao Town	10.53†	22.96	37.87	33.02	44.22	18.87	25.99	27.64
Qibao Town	6.29††	20.68	23.33	18.85	27.65	10.67	14.71	17.45
Hongqiao Town	14.18	22.35	30.17	27.39	27.40	18.94	22.78	23.32
Xinzhuang Town	9.33	28.16	35.24	35.84	37.50	19.24	21.48	26.68
Meilong Town	9.11	15.95	19.58	16.34	19.04	8.33	11.14	14.21
Zhuanqiao Town	7.11	19.24	25.96	21.21	24.05	11.83	19.31	18.39
Maqiao Town	20.15	35.26	42.32	35.43	39.48	22.13	19.77	30.65
Wujing Town	14.79	32.08	29.09	23.15	20.11	13.39	14.22	20.98
Pujiang Town	11.71	14.20	9.28	7.62	16.13	5.89	7.89	10.39
Xinhong Street	19.89	34.85	40.70	41.59	40.33	21.85	33.87	33.30
Gumei Street	6.67	18.90	31.16	23.79	16.61	11.76	14.54	17.63
Pujin Street	6.12	16.95	8.03	6.11	12.64	10.88	16.46	11.03
Jiangchuan Street	14.67	35.53	42.94	39.89	44.26	23.89	33.01	33.46

Vaccination coverage rates from 2013–2014 to 2019–2020 in each town/street were calculated according to children's residential addresses. The mean coverage rate is the average coverage rate of that town/street from 2013–2014 to 2019–2020. †Gray shading indicates that the vaccination coverage rate is below the mean in that column. ††Underscoring indicates that the vaccination coverage rate is below the lower quartile in that column.

TABLE 3 Predicted impact of vaccination among children from 2013–2014 to 2017–2018.

	2013–2014	2014–2015	2015–2016	2016–2017	2017–2018
Vaccination coverage	10.40%	22.94%	27.62%	24.16%	27.57%
Estimated number of observed influenza cases	4.27	10.13	26.51	29.99	77.41
Estimated number of averted influenza cases (+/− 10%VE) †	0.28 (0.23–0.34)	1.62 (1.31–1.94)	5.27 (4.25–6.35)	5.08 (4.12–6.10)	15.34 (12.38–18.51)
Prevented fraction (+/−10%VE)††	6.15% (5.11–7.38%)	13.79% (11.45–16.07%)	16.58% (13.82–19.32%)	14.49% (12.08–16.90%)	16.54% (13.79–19.30%)

The number of averted influenza cases among children was estimated using three parameters: number of observed influenza cases, vaccination coverage, and vaccine effectiveness. The number of observed cases was estimated using incidence data in Shanghai and the number of children in vaccination records. Vaccine effectiveness was assumed to be 60%. The results of sensitivity analyses with an interval of +/− 10% VE were presented as ranges of uncertainties. †Number of averted influenza cases (NAC), computed as $NAC = \frac{n \cdot VC \cdot VE}{1 - VC \cdot VE}$, where n: observed influenza cases, VC, vaccination coverage; VE, vaccine effectiveness. ††Prevented fraction (PF), calculated as $PF = \frac{NAC}{n + NAC}$, where NAC, number of averted influenza cases, n, observed influenza cases.

10%, the mean averted cases per year increased from 5.52 (range: 4.46–6.65) to 8.22 (range: 6.54–10.05), with an average improvement of 6% in the prevented fraction.

The impact of improving vaccination coverage in each town/street was also estimated by the ratio of the difference in the number of averted cases when increasing the vaccination coverage rate by 10% to

observed cases (Table 4). The ratio was significantly positively correlated with the original vaccination coverage rate ($r = 0.99$, $p < 0.001$). The mean ratio in each area ranged from 7.27% on Pujin Street to 10.69% on Jiangchuan Street. Using a regression model, an original vaccination coverage rate of 31.53% was predicted to obtain a ratio of 10% when coverage was increased.

Confirmed influenza cases in the general population in Minhang District from January 2016 to January 2020 with missing data from April to November 2018 are presented in Figure 1. The peak of influenza mainly arose in the winter months, with an exception in the summer of 2017. To quantify the relationship between the decrease in influenza cases in all age groups and the cumulative vaccination doses in prior or identical months, four time periods when the case counts declined were selected: January–June 2016, December 2016–June 2017, January–March 2018, and February–June 2019. The most correlated results between the number of influenza cases in the selected periods and the cumulative vaccination volume in that vaccination year were summarized (Table 5). The number of influenza cases from January to June 2016 was most strongly correlated with cumulative vaccination doses 5 months before, with a correlation coefficient of −0.99. There was a time lag of 3 months between cases in both of the periods, December 2016 to June 2017 and February to June 2019, and the most correlated cumulative vaccination doses, of which correlation coefficients were − 0.98 and − 0.94, respectively. The number of cases from January to March 2018 was completely negatively correlated with cumulative vaccinations 2 months before. Regressions on the influenza cases and cumulative vaccination doses in most correlated months were conducted to estimate the reduction in influenza cases per thousand additional vaccinations (Table 5). An estimated reduction of 3.18 cases occurred from December 2016 to June 2017 with 1,000 additional vaccinations from September 2016 to March 2017, which was the greatest reduction estimated. The smallest reduction was 0.73 cases from January to June 2016, with 1,000 additional vaccinations from August 2015 to January 2016. The estimated case reductions climbed upward in the first 2 years and then fell to a moderate level in the following 2 years, which equaled 1.55 and 1.69 per 1,000 additional vaccinations, respectively.

4. Discussion

The aim of this study was to explore whether influenza vaccination among children could provide direct effects in themselves and indirect effects in the general population by using surveillance data of the vaccination records for children born between 2013 and 2019, and of the reported influenza cases between 2016 and 2020.

There were several findings arising from the present study. First, the influenza vaccination rate was suboptimal among children in Minhang considering the goal of 75% coverage proposed by the WHO recommendation (31). Second, the vaccination program could provide direct protections to children as an average fraction of 13.15% of potential influenza cases was estimated to be averted. Third, the indirect effects provided by inoculating children were observed as a strong negative correlation between the cumulative number of influenza vaccinations and the number of cases with time lags. Finally, improving the vaccination coverage rates in higher coverage areas were estimated to be associated with more averted cases.

In this study, the annual influenza vaccination coverage among children in the vaccination records ranged from 10.40 to 27.62%, with a mean coverage of 20.71%. This vaccination coverage of influenza in Minhang was lower than that reported in other studies. A study revealed that the coverage was 59.15% among children at high risk of influenza in the United States (32), and similarly, a coverage of 58.28% was documented in the United Kingdom according to WHO Data Portal (33). In China, a meta-analysis found that the pooled influenza vaccination coverage was 28.4% for children aged 6 months to 5 years (13). There may be several reasons that contributed to the low coverage rate. First, the supply of influenza vaccines available to young children in the study period was insufficient. Second, the vaccination procedure is cumbersome. Regardless of the history of influenza vaccination, children need to be vaccinated before the influenza

TABLE 4 The ratio of the difference in NAC to observed cases with a 10% increase in vaccination coverage.

Town/Street	2013–2014 (%)	2014–2015 (%)	2015–2016 (%)	2016–2017 (%)	2017–2018 (%)
Huacao Town	7.32	8.68	10.90	10.09	12.11
Qibao Town	6.91	8.40	8.72	8.18	9.29
Hongqiao Town	7.70	8.6	9.65	9.26	9.26
Xinzhuang Town	7.19	9.36	10.44	10.54	10.83
Meilong Town	7.16	7.86	8.26	7.90	8.20
Zhuanqiao Town	7.00	8.22	9.06	8.46	8.81
Maqiao Town	8.32	10.44	11.72	10.47	11.18
Wujing Town	7.75	9.94	9.49	8.70	8.33
Pujiang Town	7.42	7.67	7.19	7.03	7.88
Xinhong Street	8.28	10.38	11.41	11.58	11.34
Gumei Street	6.95	8.18	9.80	8.78	7.93
Pujin Street	6.90	7.97	7.07	6.89	7.51
Jiangchuan Street	7.72	10.49	11.85	11.26	12.11

NAC represents the number of averted cases, computed as $\mathrm{NAC} = \frac{n \cdot VC \cdot VE}{1 - VC \cdot VE}$. The difference in NAC was calculated using the formula when increasing the VC by 10%. The observed cases were distributed according to the proportion of qualified children in each town/street. The ratio was calculated as the difference in NAC divided by the observed cases.

10.3389/fpubh.2023.1193839

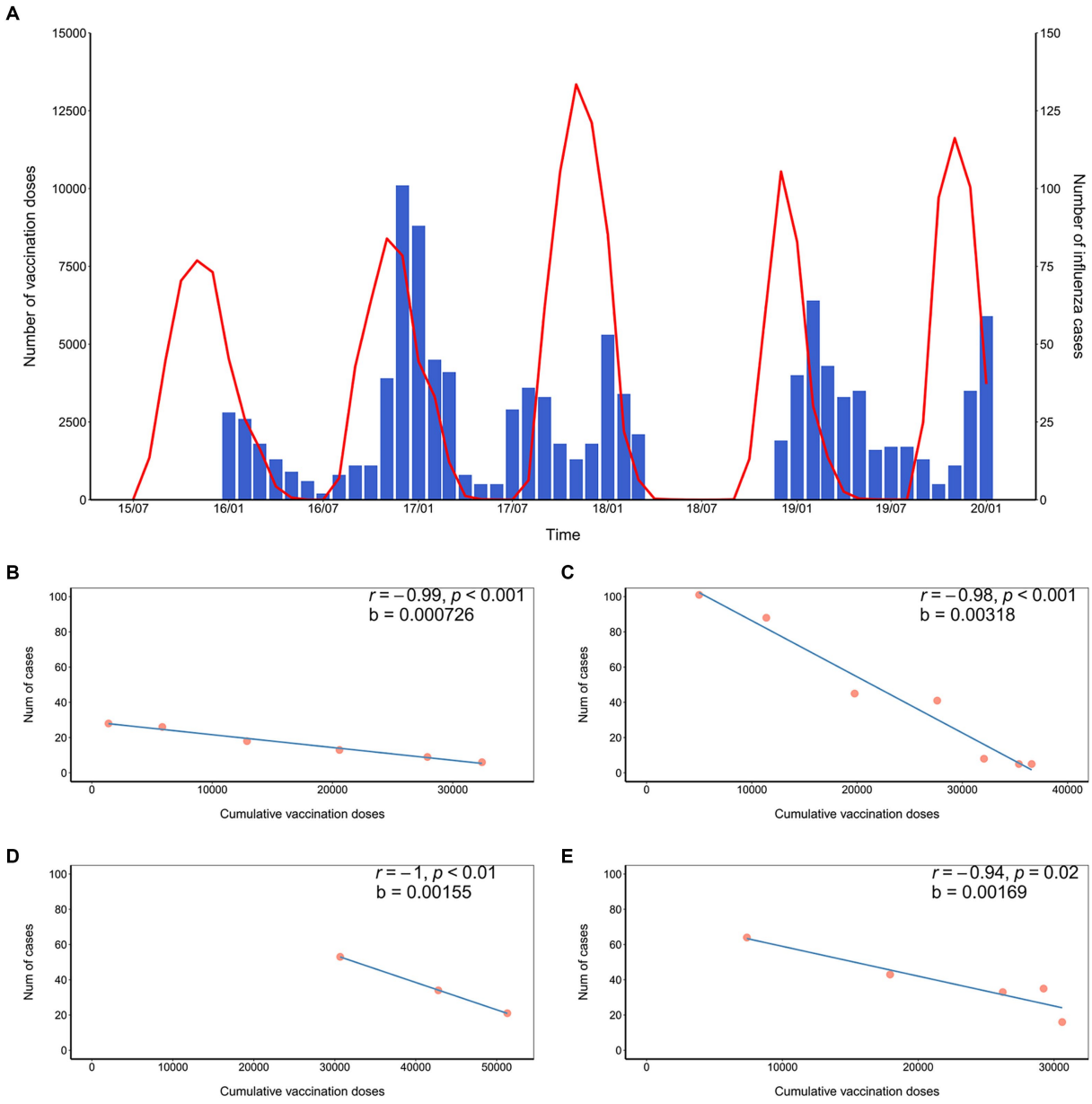

FIGURE 1
Monthly vaccination doses and influenza cases from July 2015 to January 2020 and the fitted regression line. **(A)** Monthly number of vaccination doses and influenza cases from July 2015 to January 2020. The left *y*-axis represents the number of vaccination doses per month. The right y-axis represents the number of reported influenza cases per month. The vaccination doses among children are shown by a red line. The number of notified influenza cases is shown by a blue bar, with data unavailable before January 2016 and data missing from April to November 2018; **(B)** Influenza cases from January to June 2016 fitted with cumulative vaccination doses from August 2015 to January 2016; **(C)** Influenza cases from December 2016 to June 2017 fitted with cumulative vaccination doses from September 2016 to March 2017; **(D)** Influenza cases from January to March 2018 fitted with cumulative vaccination doses from November 2017 to January 2018; **(E)** Influenza cases from February to June 2019 fitted with cumulative vaccination doses from December 2018 to March 2019.

season each year. Otherwise, children aged 6 months to 3 years need to receive two doses of influenza vaccine with an interval of more than 4 weeks (34). In addition, parents tend to regard influenza vaccines as being of little importance and refuse to pay out-of-pocket (35), as they are not included in the national immunization program in China. Consequently, parents do not prioritize immunizing their children with influenza vaccines in the absence of an influenza epidemic.

Despite the comparatively low vaccination coverage, this study identified the direct protective effects of inoculating children by an average estimation of 13.51% of averted cases. The impact of influenza vaccination programs varied across the influenza seasons, ranging from 6.15 to 16.58%. This result is higher compared to a study conducted in Suzhou, China, that reported an average prevented fraction of 7% over five seasons (17). The difference may attribute to higher vaccination coverage rate of 21% in this study than 9% in the latter. Similarly, a research reported an average prevented fraction of 53% when coverage rate reaching 46% (19). However, the number of averted cases was estimated to be low, even close to zero in 2013–2014.

10.3389/fpubh.2023.1193839

TABLE 5 Relationship between cumulative vaccination doses and influenza cases.

Surveillance periods	Vaccination periods	$r^{\dagger}$	p value	$b^{\dagger\dagger}$
16/01–16/06	15/08–16/01	−0.99	< 0.001	-7.26×10^{-4}
16/12–17/06	16/09–17/03	−0.98	< 0.001	-3.18×10^{-3}
18/01–18/03	17/11–18/01	−1.00	0.01	-1.55×10^{-3}
19/02–19/06	18/11–19/03	−0.94	0.02	-1.69×10^{-3}

Four surveillance periods in which the number of influenza cases decreased were selected. Correlation analyses were conducted between the number of influenza cases in surveillance periods and the number of cumulative vaccination doses in prior or identical months in the same vaccination year. Only the most correlated results for each period are listed here. Then, the reduction in influenza cases per additional vaccination dose was estimated by the regression coefficient between the number of influenza cases and cumulative vaccination doses. $^{\dagger}r$, Pearson's correlation coefficient. $^{\dagger\dagger}b$, regression coefficient, represents the estimated reduction in influenza cases per additional vaccination dose.

This reflected the low number of influenza cases that year and that few cases can be prevented when the underlying incidence is low (21). Since the number of influenza cases were based on the statistics of influenza incidence from the China CDC, it may underestimate the real burden. As the sample submitted for confirmed diagnosis and influenza subtyping is usually a nasopharyngeal swab or serum specimen, and collecting these samples is an invasive, sometimes painful experience, children and even parents are reluctant to cooperate. In addition, infected children with mild symptoms generally choose to receive treatment in clinics or community health centers that are not included in the infectious disease reporting system. Therefore, reported childhood cases are inpatients with serious symptoms to a large extent. As a result, the estimations in this study can be regarded as the number of severe cases.

Due to the lack of reliable evidence of VE in Shanghai and the wide variations in VE, simulated vaccine effectiveness was used in this study. A meta-analysis study reported pooled vaccine effectiveness against types of influenza ranging from 43 to 69% in pediatric age groups (28). To assess the benefit of vaccination, the influenza vaccine was assumed to have a moderate effectiveness of 60% in our study, and the results of the sensitivity analyses of VE were presented as ranges of estimates to indicate uncertainties. Compared to the upper limit of the uncertainty range, the increment in vaccination impact estimates was larger when improving VC by 10%. As VE varies across seasons, populations, age groups, and products (36), it is more beneficial to focus on measures aiming to improve vaccination coverage.

This study also measured the influence of increasing the vaccination coverage rate in each town/street by the ratio of the difference in NAC to observed influenza cases. The ratio represented what fraction of cases could be further averted on the basis of observed cases when increasing the vaccination coverage rate by 10%. The observed cases were proportional to the number of children who met the criteria for vaccination in each area. The results indicated that a larger proportion of influenza cases can be averted in areas of higher coverage than in lower coverage areas when increasing the coverage rate. Thus, areas with high vaccination coverage should further increase the rates to avoid more influenza cases and even establish herd immunity. In this simulation, Jiangchuan, Maqiao and Xinhong received more benefits than other areas from the increase in coverage. We also calculated a threshold of 31.53% of the original vaccination coverage to achieve a 10% ratio.

This study quantified the relationship between influenza cases in the general population and cumulative vaccination doses among children from two aspects. First, a strong negative correlation was observed, which implied underlying indirect protection provided by vaccinating children. This is consistent with previous studies, in which statistically significant indirect protection by inoculating children was found ranging from 24 to 61% (11, 37, 38). The time lag between cumulative vaccination doses and influenza cases ranged from 2 to 5 months, with a median of 3 months. The two periods with complete surveillance data were found in a three-month gap, while the remaining periods with incomplete surveillance data had a time lag of two and 5 months. Incomplete data may have contributed to the variations in time lags. Second, we estimated the reduction in influenza cases in the general population per thousand additional vaccinations among children. The estimated reduction increased from 0.73 cases to 3.18 cases in the first two periods and then fell to a moderate level of 1.55 and 1.69 cases. The mismatch between the vaccine strain and circulating viruses may have resulted in the small estimated reduction in influenza cases from January to June 2016 (39, 40).

This study described the trend in influenza vaccination coverage among children from a spatiotemporal perspective for 7 consecutive years in Minhang District. The method to estimate averted cases used in this study has been widely used to evaluate the impact of influenza vaccination (18, 21, 22, 25). However, this is the first study to apply this method to estimate the impact of influenza vaccination among children in China. Compared to other estimation models, this method involved fewer intensive computations and easily interpretable results. The relationship between influenza cases and cumulative vaccination doses was quantified to explore the underlying benefit provided by the vaccination of children.

There were some limitations in this study. First, we could not stratify children's age to calculate age-specific influenza vaccination coverage rates. As newborn infants were enrolled in this cohort successively, the coverage rate was computed by the number of vaccinated children divided by the total number of children who were eligible for vaccination in one vaccination year. Second, the number of influenza cases among children from 2013 to 2018 was estimated using influenza incidence data in Shanghai multiplied by the number of children in vaccination records rather than the surveillance data. The difference in influenza incidence among children between Shanghai and Minhang may have introduced an underestimation or overestimation in later estimations. Third, the method used did not consider the indirect effects of the vaccination program and thus presented a more conservative estimate of the impact. Moreover, the annual averted cases could only be estimated within limited age groups, as we used the vaccination data of a birth cohort. Finally,

we did not have VE data specifically for Minhang District for the study period, and the simulated level may not reflect the real effectiveness of the influenza vaccine.

The current study suggests that influenza vaccinations among children could offer both direct and indirect protections, which emphasize the importance of increasing influenza vaccination coverage to reduce influenza morbidity. These results provide easily interpretable evidence for childhood vaccination to public health recommendations and can be particularly useful in countries including China currently developing influenza vaccination policies.

5. Conclusion

In summary, the current study identified the distribution of influenza vaccination coverage in Minhang District on a spatiotemporal scale. Vaccination coverage in high-coverage areas should be further expanded to avert more influenza cases and even to establish herd immunity. In low-coverage areas, a threshold of 31.53% was estimated to maximize the benefit of vaccinations. Vaccinations among children averted an average of 13.51% of influenza cases per year. The results of quantifying the relationship between cumulative vaccination doses and influenza cases indicated that the influenza vaccine program among children was strongly correlated with influenza activities and might provide underlying indirect protection to the general population.

Data availability statement

The data analyzed in this study is subject to the following licenses/restrictions: the dataset is part of Minhang CDC Notifiable Communicable Disease Reporting System and the National Immunization Program System, it's not public available according to the legislations. Requests to access these datasets should be directed to yyao@fudan.edu.cn.

Ethics statement

The studies involving humans were approved by the Institutional Review Board of the Minhang Center for Disease Control and Prevention. The studies were conducted in accordance with the local legislation and institutional requirements. The ethics committee/institutional review board waived the requirement of written informed consent for participation from the participants or the participants' legal guardians/next of kin because this study involved the use of surveillance data and no potentially identifiable human data were presented.

Author contributions

YY and YL contributed to the conception and design of the study. NL, BJ, and KM organized the database. LS performed the statistical analysis and wrote the first draft of the manuscript. ZZ, LZ, and XZ contributed to the discussion and revision of the manuscript. JL provided the financial support for the manuscript. All authors contributed to manuscript revision, read, and approved the submitted version.

Funding

This study was supported by the Talent Program by Minhang District Health Commission (2020FM29), Minhang Public Health Brand Department (MGWKS01), the Shanghai Municipal Health Commission Clinical Research Program (20214Y0020), the General Program of Natural Science Foundation of Shanghai Municipality (22ZR1414600), and the Young Health Talents Program of Shanghai Municipality (2022YQ076).

Conflict of interest

The authors declare that the research was conducted in the absence of any commercial or financial relationships that could be construed as a potential conflict of interest.

Publisher's note

All claims expressed in this article are solely those of the authors and do not necessarily represent those of their affiliated organizations, or those of the publisher, the editors and the reviewers. Any product that may be evaluated in this article, or claim that may be made by its manufacturer, is not guaranteed or endorsed by the publisher.

Supplementary material

The Supplementary material for this article can be found online at: https://www.frontiersin.org/articles/10.3389/fpubh.2023.1193839/full#supplementary-material

References

1. Iuliano AD, Roguski KM, Chang HH, Muscatello DJ, Palekar R, Tempia S, et al. Estimates of global seasonal influenza-associated respiratory mortality: a modelling study. *Lancet*. (2018) 391:1285–300. doi: 10.1016/S0140-6736(17)33293-2

2. Wang X, Li Y, O'Brien KL, Madhi SA, Widdowson M-A, Byass P, et al. Global burden of respiratory infections associated with seasonal influenza in children under 5 years in 2018: a systematic review and modelling study. *Lancet Glob Health*. (2020) 8:e497–510. doi: 10.1016/S2214-109X(19)30545-5

3. The Department of Health and Aged Care. Annual report of the National Influenza Surveillance Scheme (2018) 2010 Available at: https://www1.health.gov.au/internet/main/publishing.nsf/Content/cdi4104-f

4. Wu S, Van Asten L, Wang L, Mcdonald SA, Pan Y, Duan W, et al. Estimated incidence and number of outpatient visits for seasonal influenza in 2015–2016 in Beijing. *China Epidemiol Infect*. (2017) 145:3334–44. doi: 10.1017/S0950268817002369

5. Viboud C, Boëlle P-Y, Cauchemez S, Lavenu A, Valleron A-J, Flahault A, et al. Risk factors of influenza transmission in households. *Int Congr Ser*. (2004) 1263:291–4. doi: 10.1016/j.ics.2004.01.013

6. Worby CJ, Chaves SS, Wallinga J, Lipsitch M, Finelli L, Goldstein E. On the relative role of different age groups in influenza epidemics. *Epidemics*. (2015) 13:10–6. doi: 10.1016/j.epidem.2015.04.003

7. Jackson ML, Phillips CH, Benoit J, Jackson LA, Gaglani M, Murthy K, et al. Burden of medically attended influenza infection and cases averted by vaccination – United States, 2013/14 through 2015/16 influenza seasons. *Vaccine*. (2018) 36:467–72. doi: 10.1016/j.vaccine.2017.12.014

8. World Health Organization. Vaccines against influenza: WHO position paper - May 2022. (2022) 97:185–208. Available at: https://www.who.int/publications/i/item/who-wer9719

9. Chung JR, Rolfes MA, Flannery B, Prasad P, O'Halloran A, Garg S, et al. Effects of influenza vaccination in the United States during the 2018–2019 influenza season. *Clin Infect Dis*. (2020) 71:e368–76. doi: 10.1093/cid/ciz1244

10. Yin JK, Heywood AE, Georgousakis M, King C, Chiu C, Isaacs D, et al. Systematic review and meta-analysis of indirect protection afforded by vaccinating children against seasonal influenza: implications for policy. *Clin Infect Dis*. (2017) 65:719–28. doi: 10.1093/cid/cix420

11. Loeb M, Russell ML, Moss L, Fonseca K, Fox J, Earn DJD, et al. Effect of influenza vaccination of children on infection rates in Hutterite communities: a randomized trial. *JAMA*. (2010) 303:943–50. doi: 10.1001/jama.2010.250

12. Feng L, Yang P, Zhang T, Yang J, Fu C, Qin Y, et al. Technical guidelines for the application of seasonal influenza vaccine in China (2014–2015). *Hum Vaccin Immunother*. (2015) 11:2077–101. doi: 10.1080/21645515.2015.1027470

13. Wang Q, Yue N, Zheng M, Wang D, Duan C, Yu X, et al. Influenza vaccination coverage of population and the factors influencing influenza vaccination in mainland China: a meta-analysis. *Vaccine*. (2018) 36:7262–9. doi: 10.1016/j.vaccine.2018.10.045

14. Zhou L, Su Q, Xu Z, Feng A, Jin H, Wang S, et al. Seasonal influenza vaccination coverage rate of target groups in selected cities and provinces in China by season (2009/10 to 2011/12). *PLoS One*. (2013) 8:e73724. doi: 10.1371/journal.pone.0073724

15. Lau JTF, Ng CSM, Wu AMS, Ma YL, Lau MMC. Low coverage of influenza vaccination among Chinese children aged 12-23 months: prevalence and associated factors. *PLoS One*. (2018) 13:e0205561. doi: 10.1371/journal.pone.0205561

16. Arinaminpathy N, Kim IK, Gargiullo P, Haber M, Foppa IM, Gambhir M, et al. Estimating direct and indirect protective effect of influenza vaccination in the United States. *Am J Epidemiol*. (2017) 186:92–100. doi: 10.1093/aje/kwx037

17. Zhang W, Gao J, Chen L, Tian J, Biggerstaff M, Zhou S, et al. Estimated influenza illnesses and hospitalizations averted by influenza vaccination among children aged 6–59 months in Suzhou, China, 2011/12 to 2015/16 influenza seasons. *Vaccine*. (2020) 38:8200–5. doi: 10.1016/j.vaccine.2020.10.069

18. Foppa IM, Cheng P-Y, Reynolds SB, Shay DK, Carias C, Bresee JS, et al. Deaths averted by influenza vaccination in the U.S. during the seasons 2005/06 through 2013/14. *Vaccine*. (2015) 33:3003–9. doi: 10.1016/j.vaccine.2015.02.042

19. Zhang Y, Cao Z, Costantino V, Muscatello DJ, Chughtai AA, Yang P, et al. Influenza illness averted by influenza vaccination among school year children in Beijing, 2013-2016. *Influenza Other Respir Viruses*. (2018) 12:687–94. doi: 10.1111/irv.12585

20. Tokars JI, Rolfes MA, Foppa IM, Reed C. An evaluation and update of methods for estimating the number of influenza cases averted by vaccination in the United States. *Vaccine*. (2018) 36:7331–7. doi: 10.1016/j.vaccine.2018.10.026

21. Kostova D, Reed C, Finelli L, Cheng P-Y, Gargiullo PM, Shay DK, et al. Influenza illness and hospitalizations averted by influenza vaccination in the United States, 2005–2011. *PLoS One*. (2013) 8:e66312. doi: 10.1371/journal.pone.0066312

22. Machado A, Kislaya I, Larrauri A, Matias Dias C, Nunes B. Impact of national influenza vaccination strategy in severe influenza outcomes among the high-risk Portuguese population. *BMC Public Health*. (2019) 19:1690. doi: 10.1186/s12889-019-7958-8

23. Reed C, Kim IK, Singleton JA, Chaves SS, Flannery B, Finelli L, et al. Estimated influenza illnesses and hospitalizations averted by vaccination — United States, 2013–14 influenza season (2014) 63:4. Available at: https://www.who.int/publications/i/item/who-wer9719

24. Backer JA, Wallinga J, Meijer A, Donker GA, van der Hoek W, van Boven M. The impact of influenza vaccination on infection, hospitalisation and mortality in the Netherlands between 2003 and 2015. *Epidemics*. (2019) 26:77–85. doi: 10.1016/j.epidem.2018.10.001

25. Machado A, Mazagatos C, Dijkstra F, Kislaya I, Gherasim A, McDonald SA, et al. Impact of influenza vaccination programmes among the elderly population on primary care, Portugal, Spain and the Netherlands: 2015/16 to 2017/18 influenza seasons. *Euro Surveill*. (2019) 24. doi: 10.2807/1560-7917.ES.2019.24.45.1900268

26. Sacco C, Mateo-Urdiales A, Petrone D, Spuri M, Fabiani M, Vescio MF, et al. Estimating averted COVID-19 cases, hospitalisations, intensive care unit admissions and deaths by COVID-19 vaccination, Italy, January−September 2021. *Euro Surveil*. (2021) 26. doi: 10.2807/1560-7917.ES.2021.26.47.2101001

27. Center of Public Health Science Data. Statistics of influenza cases by age group in Shanghai during 2013–2018. (2021) Available at: https://www.phsciencedata.cn/Share/index.jsp (Accessed February 10, 2023).

28. Belongia EA, Simpson MD, King JP, Sundaram ME, Kelley NS, Osterholm MT, et al. Variable influenza vaccine effectiveness by subtype: a systematic review and meta-analysis of test-negative design studies. *Lancet Infect Dis*. (2016) 16:942–51. doi: 10.1016/S1473-3099(16)00129-8

29. Colucci ME, Affanni P, Cantarelli A, Caruso L, Bracchi MT, Capobianco E, et al. Influenza vaccine effectiveness in children: a retrospective study on eight post-pandemic seasons with trivalent inactivated vaccine. *Acta Bio Medica Atenei Parmensis*. (2020) 91:63–70. doi: 10.23750/abm.v91i3-S.9424

30. Yang X, Zhao H, Li Z, Zhu A, Ren M, Geng M, et al. Influenza vaccine effectiveness in mainland China: a systematic review and Meta-analysis. *Vaccine*. (2021) 9:79. doi: 10.3390/vaccines9020079

31. Jorgensen P, Mereckiene J, Cotter S, Johansen K, Tsolova S, Brown C. How close are countries of the WHO European region to achieving the goal of vaccinating 75% of key risk groups against influenza? Results from national surveys on seasonal influenza vaccination programmes, 2008/2009 to 2014/2015. *Vaccine*. (2018) 36:442–52. doi: 10.1016/j.vaccine.2017.12.019

32. Tian C, Wang H, Wang W, Luo X. Infuenza vaccination coverage among US children from 2004/2005 to 2015/2016 (2018) 41:e62–9. doi: 10.1093/pubmed/fdy081,

33. World Health Organization. Influenza vaccination coverage. (2021) Available at: https://immunizationdata.who.int/pages/coverage/flu.html (Accessed July 15, 2023).

34. National Immunization Advisory Committee Technical Working Group. Technical guidelines for seasonal influenza vaccination in China, 2019–2020. *Chin J Prevent Med*. (2020) 54:21–36. doi: 10.3760/cma.j.issn.0253-9624.2020.01.007

35. Wei Z, Sun X, Yang Y, Zhan S, Fu C. Seasonal influenza vaccine hesitancy profiles and determinants among Chinese children's guardians and the elderly. *Expert Rev Vaccines*. (2021) 20:601–10. doi: 10.1080/14760584.2021.1908134

36. McLean HQ, Belongia EA. Influenza vaccine effectiveness: new insights and challenges. *Cold Spring Harb Perspect Med*. (2021) 11:a038315. doi: 10.1101/cshperspect.a038315

37. Esposito S, Marchisio P, Cavagna R, Gironi S, Bosis S, Lambertini L, et al. Effectiveness of influenza vaccination of children with recurrent respiratory tract infections in reducing respiratory-related morbidity within the households. *Vaccine*. (2003) 21:3162–8. doi: 10.1016/S0264-410X(03)00253-6

38. Hurwitz ES. Effectiveness of influenza vaccination of day care children in reducing influenza-related morbidity among household contacts. *JAMA*. (2000) 284:1677–82. doi: 10.1001/jama.284.13.1677

39. Lei H, Yang L, Wang G, Zhang C, Xin Y, Sun Q, et al. Transmission patterns of seasonal influenza in China between 2010 and 2018. *Viruses*. (2022) 14:2063. doi: 10.3390/v14092063

40. World Health Organization. Recommended composition of influenza virus vaccines for use in the 2015–2016 northern hemisphere influenza season. (2015). Available at: https://www.who.int/publications/m/item/recommended-composition-of-influenza-virus-vaccines-for-use-in-the-2015-2016-northern-hemisphere-influenza-season

frontiers | Frontiers in Public Health

TYPE Original Research
PUBLISHED 08 January 2024
DOI 10.3389/fpubh.2023.1307425

OPEN ACCESS

EDITED BY
Jian Wu,
Suzhou Municipal Hospital, China

REVIEWED BY
Seba Contreras,
Max Planck Society, Germany
Adriano La Vecchia,
University of Milano-Bicocca, Italy

*CORRESPONDENCE
Aida Perramon-Malavez
✉ aida.perramon@upc.edu

RECEIVED 04 October 2023
ACCEPTED 19 December 2023
PUBLISHED 08 January 2024

CITATION
Perramon-Malavez A, Bravo M, López de Rioja V, Català M, Alonso S, Álvarez-Lacalle E, López D, Soriano-Arandes A and Prats C (2024) A semi-empirical risk panel to monitor epidemics: multi-faceted tool to assist healthcare and public health professionals.
Front. Public Health 11:1307425.
doi: 10.3389/fpubh.2023.1307425

A semi-empirical risk panel to monitor epidemics: multi-faceted tool to assist healthcare and public health professionals

Aida Perramon-Malavez[1]*, Mario Bravo[1], Víctor López de Rioja[1], Martí Català[2], Sergio Alonso[1], Enrique Álvarez-Lacalle[1], Daniel López[1], Antoni Soriano-Arandes[3,4] and Clara Prats[1]

[1]Department of Physics, Computational Biology and Complex Systems (BIOCOM-SC) group, Barcelona School of Agri-Food and Biosystems Engineering, Universitat Politècnica de Catalunya, Castelldefels, Spain, [2]Health Data Sciences, NDORMS, University of Oxford, Oxford, United Kingdom, [3]Paediatric Infectious Diseases and Immunodeficiencies Unit, Children's Hospital, Vall d'Hebron Barcelona Hospital Campus, Barcelona, Catalonia, Spain, [4]Infection and Immunity in Paediatric Patients, Vall d'Hebron Research Institute, Barcelona, Catalonia, Spain

Introduction: Bronchiolitis, mostly caused by Respiratory Syncytial Virus (RSV), and influenza among other respiratory infections, lead to seasonal saturation at healthcare centers in temperate areas. There is no gold standard to characterize the stages of epidemics, nor the risk of respiratory infections growing. We aimed to define a set of indicators to assess the risk level of respiratory viral epidemics, based on both incidence and their short-term dynamics, and considering epidemical thresholds.

Methods: We used publicly available data on daily cases of influenza for the whole population and bronchiolitis in children <2 years from the Information System for Infection Surveillance in Catalonia (SIVIC). We included a Moving Epidemic Method (MEM) variation to define epidemic threshold and levels. We pre-processed the data with two different *nowcasting* approaches and performed a 7-day moving average. Weekly incidences (cases per 10^5 population) were computed and the 5-day growth rate was defined to create the effective potential growth (EPG) indicator. We performed a correlation analysis to define the forecasting ability of this index.

Results: Our adaptation of the MEM method allowed us to define epidemic weekly incidence levels and epidemic thresholds for bronchiolitis and influenza. EPG was able to anticipate daily 7-day cumulative incidence by 4–5 (bronchiolitis) or 6–7 (influenza) days.

Discussion: We developed a semi-empirical risk panel incorporating the EPG index, which effectively anticipates surpassing epidemic thresholds for bronchiolitis and influenza. This panel could serve as a robust surveillance tool, applicable to respiratory infectious diseases characterized by seasonal epidemics, easy to handle for individuals lacking a mathematical background.

KEYWORDS

respiratory infections, epidemic, levels, threshold, effective potential growth, epidemic indicators, bronchiolitis, influenza

1 Introduction

Lower respiratory tract infections (LRTIs) are a significant global health burden, causing substantial morbidity and mortality worldwide. According to the Global Burden of Disease (GBD) Study 2019, LRTIs were responsible for approximately 2.5 million deaths and around 500 million infections globally in 2019 (1–3). LRTIs affect individuals of all ages but disproportionately impact children under 5 years of age and older adults. In the former age group, acute LRTIs are a leading cause of morbidity and mortality, with Respiratory Syncytial Virus (RSV) and Influenza Viruses (IVs) being the two most common causes (4).

The RSV causes approximately 70% of bronchiolitis, a seasonal LRTI that is particularly critical in children under 2 years, with 3.5 million hospitalizations and almost 1% of deaths among admitted children, mostly infants <6 months (4). Bronchiolitis is mostly contagious 5 days after infection, and it is associated with respiratory distress, wheezing, apnea, fever, and nasal flaring, although these symptoms are correlated with the severity of the disease and age (5). Similarly, seasonal influenza, caused by IVs, is responsible for a significant burden of LRTIs in children under 5 years, with an estimated 120,000 deaths annually (6). Nonetheless, adults, particularly those with underlying medical conditions, adults over 60 years of age, and pregnant women (7) are the most affected. The World Health Organization (WHO) describes influenza's clinical manifestations as fever, dry cough, headache, muscle and joint pain, severe malaise, sore throat, and a runny nose (7). Although seemingly mild, according to the Centers for Disease Control and Prevention (CDC), IVs are responsible for an estimated 9–45 million cases, 140,000–810,000 hospitalizations, and 12,000–61,000 deaths annually in the United States (8–10). Moreover, influenza has a shorter incubation period and is mostly contagious between 48 h and 6 days from infection (11).

In Catalonia, a region with about 7.6 million population in Spain, bronchiolitis and influenza are also significant health concerns for patients and healthcare providers (12). Between 10,000 and 15,000 children under two years get infected with RSV seasonally (13), similar to the values that the peak number of total weekly infections of influenza reaches (14). Given the high incidence and substantial morbidity and mortality associated with bronchiolitis and influenza, conducting effective surveillance of these viral infections is crucial. Surveillance can inform public health interventions and guide the allocation of resources to reduce the burden of these infections, including vaccination campaigns, infection control measures, and appropriate clinical management of patients. Besides, it can guide and comfort healthcare providers during the epidemics.

Epidemic indicators are used to guide surveillance in public health domains, some of them are computed empirically and others are estimated from model parameters, such as the well-known reproduction number (R) (15). Due to the nature of this work, mostly empirical indicators will be described, such as incidence, one of the most commonly used. Incidence measures the disease occurrence in a population, and it is often expressed as the number of cases per 100,000 population over a specific period. The CDC also uses cumulative hospitalization incidence and admissions, in addition to deaths, infection fatality ratio and pediatric deaths, to monitor influenza (16–18). Other organizations such as the European Centre for Disease Prevention and Control (ECDC) monitor laboratory data to detect variants of the viruses circulating or compute the percentage of positive tests for respiratory viral infections (RVIs). In addition, they use sentinel groups to estimate the epidemic incidence levels that a disease achieves, in different countries (19). Another useful measure is the growth rate of the epidemic, which is defined as the relative change in cumulated infections from 1 week to the next. Similarly, the empirical reproduction number is used to estimate and monitor the average number of infections that a single individual triggers. Usually computed from mathematical mechanistic models, the empirical reproduction number is a good measure of the stage of an epidemic, and several studies have been made to improve the calculation of this indicator while reducing complexity avoiding complicated models (20–22). This range of indicators helps us to identify potential outbreaks and track the progression of the disease over time, as was evident during the COVID-19 pandemic (23).

In the present study, we aim to define a set of semi-empirical indicators to assess the risk level of seasonal respiratory epidemics, based on both incidence and their dynamics, and considering epidemical thresholds. We base this risk evaluation system on our previously developed method for monitoring COVID-19 (23, 24). By limiting the use of models, we intend to provide a precise surveillance and short-term forecasting tool for healthcare or public health professionals without an expertise in mathematical epidemiological modeling, not to design immediate control plans, but to assist decisions on the relocation of health resources or simply to provide direct knowledge of the current and short-term expected burden.

2 Materials and methods

2.1 Data collection

We used publicly available data on daily clinical diagnoses of influenza for the whole Catalan population and bronchiolitis in children less than 2 years old, from 1st September 2014 to 31st March 2023. We obtained the data from the Information System for Infection Surveillance in Catalonia (SIVIC) (25) of the Health Department of Catalonia, a database that contains information on clinical diagnoses in Primary Healthcare, usually mostly without microbiological confirmation. However, previous studies showed that clinical diagnoses data are a good proxy of the epidemiological dynamics of respiratory diseases like influenza, because their results have been representative of laboratory confirmed diagnoses and sentinel systems but entail a shorter delay, as demonstrated by Aguilar Martín et al. (26). We used data from children <2 years for assessing bronchiolitis because this is the main age group affected by this disease. Otherwise, influenza is not only focused on a determined age group and can have an impact among the general population.

2.2 Data pre-processing

In this study, we divided the data pre-processing into three different stages: two of *nowcasting* and one of smoothing (Supplementary material). The first *nowcasting* approach is to account for the delayed notification or report in medical databases, while the second one is to consider the differences in data reporting (i.e., influenza cases) depending on whether the day of the week is a

working day or a holiday. Finally, to the pre-processed data we performed a smoothing 7-day moving average. To facilitate understanding of the two *nowcasting* methods, we provide a more extensive explanation in the following subsections. The aim of this extensive pre-processing is to extract the global dynamics of the diseases by clearing out all the noise present within them. Notwithstanding that, the rest of the study could be implemented simply smoothing the data. Note that all processes and analyses were done using Python and the codes for this paper are available in https://github.com/BIOCOM-SC/cloud-of-codes.

2.2.1 *Nowcasting* delayed reporting or notifications

There is a well-described problem when working with medical diagnostic databases, data are constantly being updated and the true number of infections for a certain day can only be verified after some period of time. However, the general agreement is to use these data after 1 month since being reported, once it has consolidated (27). In this regard, we had been downloading the SIVIC database each week since the beginning of 2021. We performed a week-to-week comparison of the daily reports in the different databases and ascertained that while records were generally coherent after 30 days from their entry, the most recent registers were still being updated. With a retrospective analysis, we intended to define the percentage of data completion for the last 30 entries in the database, and use them to weight the data into a more accurate approximation of the real number of cases.

Since the reporting methods in Catalan healthcare changed substantially during the pandemic, we focused our process only in the datasets downloaded in mid-October, November and December 2022. These datasets were considered consolidated, being more than three months old by the end of the study period. Additionally, their reporting pattern was closer to the ongoing and pre-pandemic ones than that of 2021. We decided to take records after 30 days from entry as ground truths (consolidated data) and iteratively compute the percentage of completion of each day from October to December 2022, ending up with thirty 30-last days iterations. Thereafter, we averaged the results to obtain the mean percentage of completion per each of the days, which we named *reporting weights*:

$$\omega_j = \frac{C_i}{C_{i+30}}, for\ i = 1,\ldots,30\ days, for\ j = \text{day}\ 1,\ldots,day\ 30 \quad (1)$$

$$reporting\ \ weights = \overline{\omega_r} = \frac{\sum_{j=1}^{30}\omega_j}{N_{repetitions}}, for\ j = day\ 1,\ldots,day\ 30 \quad (2)$$

In Eq. 1, ω_j states for the normalized percentage of completion, C_i is the number of cases reported in a day and C_{i+30} the number of cases reported for the same day but 30 days later. The *reporting weights* in Eq. (2) ($\overline{\omega_r}$) are constructed as the average ω_j for all iterations performed. In our case, $N_{repetitions} = 30$ since we started computing ω_j from 20/10/2022 to 20/11/2022 and ended at the iteration from 20/11/2022 to 20/12/2022.

Finally, we estimated the daily cases for the last month since the day the data is downloaded from SIVIC as:

$$C_i^{(i)} = \frac{C_i}{\overline{\omega_r}}, for\ i = 1,\ldots,30 \quad (3)$$

In Eq. (3), $C_i^{(i)}$ states for the estimated diagnoses in the 30 days previous to the last update of the database. Former works share this approximation (24, 28, 29).

To end the pre-processing and smooth the data of bronchiolitis infections, we apply to $C_i^{(i)}$ a cumulative 7-day moving average filter, while the influenza series undergo the weekly pattern correction detailed in the next subsection.

2.2.2 *Nowcasting* weekly patterns

SIVIC data followed a weekly pattern, Mondays having approximately double the cases of weekends or holidays (Supplementary material). However, bronchiolitis cases usually follow a highly stochastic nature thus their pattern of report is not stable nor avoidable. Hence, this approach can only be applied when an evident pattern is present like in the influenza diagnoses.

The main process comprises labeling every day in the study period as Monday (1), Tuesday (2), Wednesday (2), Thursday (2), Friday (2), Saturday (3), Sunday (3) or Holiday (3) as stated by the working calendar in Catalonia for each year. Therefore, we created three groups of days, the regular working days from Tuesday to Friday, the weekends and festivities when the healthcare centers only attend emergencies, and Mondays when all non-urgent cases occurring in weekends are finally attended. In addition, days after a festivity are labeled as Mondays (1) to capture the same effect as described.

Afterwards, we took daily windows of 7-days from the start to the end of the study period and computed the weights per type of day as the difference between the raw number of diagnoses reported in SIVIC and the daily filtered number of diagnoses with a 7-day moving average (MM7), that is:

$$\delta_j = \frac{C(j)}{CMM7(j)}, for\ j = 1,2,3 \quad (4)$$

In Eq. (4), δ_j are the weights computed for Mondays (j = 1), regular workdays (j = 2) and weekends and festivities (j = 3) in a certain 7-days window. C states for the raw daily reports in SIVIC and CMM7 for the 7-day moving mean of C. The j index indicates that to compute a certain weight, we only consider the cases of its kind. We saved all the iterative computations per type of day and graphically observed a time-varying pattern in which stochasticity was reduced when epidemic peaks were reached. Therefore, we took the weights per kind of day as the median among the intervals in which the values were more stable, which were detected with a signal processing algorithm detecting local maxima, as displayed as an example in Figure 1. We decided to take the median value instead of the average to account for instability.

However, we wanted to account for the stochasticity present in the data. Hence, instead of using a constant weight value we used a random Gaussian distribution in which the aforementioned computed weights are the mean of the distribution, but its standard deviation is inversely proportional to the recorded number of diagnoses, ensuring that negative weights are avoided. Consequently, the more daily cases, i.e., the closer to the epidemic peak, the more the final weight

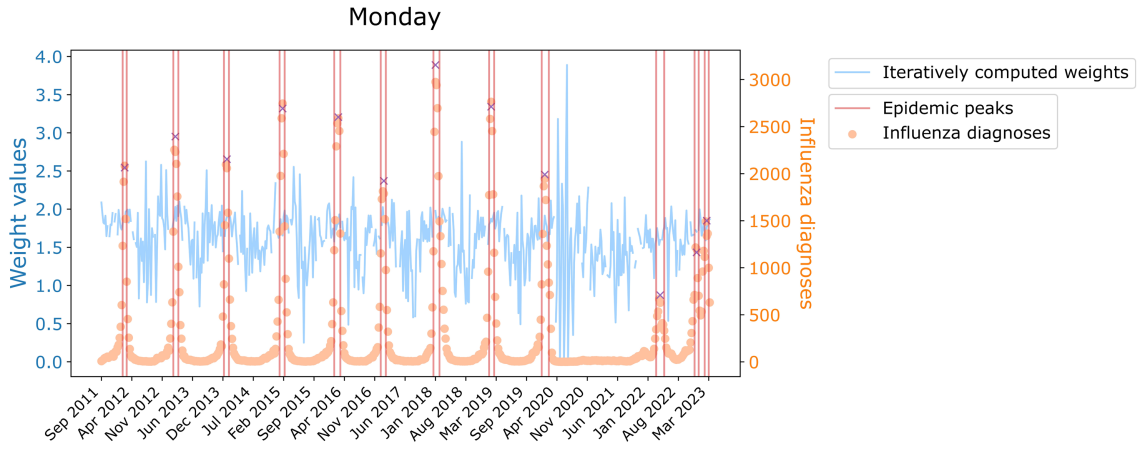

FIGURE 1
Value of the weight of Monday for its iterative calculations historically (blue, left axis). In orange and referred to the right axis, the time series of influenza diagnoses. Delimited in red, are the zones where the median weight value has been computed. Red crosses indicate the peaks detected.

resembles the average. Besides, we only apply this modification when CMM7 are over 100 influenza infections, when fluctuations are low enough to have a signal-to-noise ratio large enough to make the computation of weights reliable.

Finally, we applied the weekly reporting pattern to the daily estimated diagnoses $C_i^{(i)}$ that we already computed in order to obtain more balanced data:

$$D = \frac{C_i^{(i)}}{\delta_j}, for\ i = days\ in\ the\ study\ period\ and\ j = 1,2,3 \quad (5)$$

In Eq. (5), D represents the final weighted diagnoses. We based this approach on the work of Català et al. (18, 23) and Villanueva et al. (30). Further information can be found in the Supplementary material. To end the pre-processing and smooth the data of influenza infections, we apply to D a cumulative 7-day moving average filter.

2.3 Epidemic levels

To define epidemic levels, we employed a novel approach based on the Moving Epidemic Method (MEM) which is used in European institutions such as the ECDC (31, 32). But first, we needed to compute the weekly incidence for each disease and set an epidemic threshold from which to compute these stages.

From the pre-processed dataset, we measured the weekly incidence of bronchiolitis and influenza computing the number of daily diagnoses per 10^5 population (<2 years and all Catalonia respectively) and resampling them to weekly frequency. To determine the start of the epidemic, we used the first derivative of daily diagnoses. The first derivative represents the rate of change of the number of reported cases with respect to time. By looking at a certain value of the derivative, we can identify the day when the number of reported cases started to increase rapidly. We set this value to a three-fold increase in the number of reported cases over a single day. We then looked for the number of cases reported that day from 2014 to 2019 and averaged them. The exclusion of pandemic years is deliberate to avoid skewing the result. Once we found the epidemic threshold, we selected the epidemy as the first and last days when we are over this boundary.

With the epidemy delimited, we computed an average epidemy among the pre-pandemic ones and calculated the 25th, 50th, 75th and 95th percentiles of cases. The number of cases up to the threshold represent the basal level of the epidemy, from the threshold to the 25th percentile correspond to a very low level of the epidemy, from the 25th to the 50th percentile indicates a low level, from 50th to 75th signifies a medium level, from 75th to 95th represents a high level and above the 95th constitutes very high epidemic levels. Since with this method we obtain epidemic thresholds for weekly incidence, we divide the values obtained by 7 to also have the daily incidence levels. This whole process has been coded in R and is available in (33).

2.4 Epidemic indicators

In the present work, we used four different epidemic indicators: the daily incidence of disease, the weekly growth rate, the semi-empirical reproduction number and the Effective Potential Growth (EPG) (24). All of them are computed from the pre-processed datasets.

2.4.1 Daily incidence

To calculate the daily incidence of bronchiolitis and influenza, we took the daily number of diagnoses weighted and filtered with a cumulative 7-day moving average and computed cases per 100,000 population as:

$$I_i^{influenza} = 10^5 . \frac{D_i}{P_i}, for \cdot i = days \text{ in } the\ study\ period \quad (6)$$

$$I_i^{bronchiolitis} = 10^5 \cdot \frac{C_i^{(i)}}{P_i}, \cdot for \cdot i = days\ in\ the\ study\ period \quad (7)$$

In Eq. (6), $I_i^{influenza}$ states for the daily incidence of the disease, D_i represents the pre-processed number of infections in a day and P_i the

general number of inhabitants of Catalonia. Regarding Eq. (7), $I_i^{bronchiolitis}$ represents the daily incidence of bronchiolitis, $C_i^{(i)}$ the pre-processed number of infections in a day and P_i the number of infants <2 years in Catalonia. The population has been considered constant intra-yearly but variable inter-annually.

2.4.2 Weekly growth rate

To assess the weekly growth rate, we first define the weekly incidence as previously explained, resampling daily incidence to weekly frequency. With this, we define the weekly growth rate as the percentage of more (or less) cases reported in a week compared to the previous week:

$$\mu_j = \frac{\varphi_j}{\varphi_{j-1}}, \text{for } j = \text{all weeks in the study period} \quad (8)$$

In Eq. (8), φ_j stands for the weekly growth rate, obtained from φ_j that represents the weekly incidence of disease in a certain week. The higher the weekly growth rate, the faster the disease is spreading.

2.4.3 Effective reproduction number

The effective reproduction number (R) is an estimation of the average number of infections produced by a single infected individual over their infectious period. It is computed taking into account the generation time, which is defined as the average interval between the infection of an individual and the infection of its secondary cases. It usually corresponds to the infectious period. For influenza, the generation time is between $\gamma = 2$ and $\gamma = 6$ days. For bronchiolitis, the generation time is in the order of $\gamma = 5$ days. This index is usually computed through the equations of mathematical mechanistic models such as the Susceptible-Infected-Recovered (SIR) model (34). However, it has undergone several redefinitions to enable alternative (rough) estimations without detailed knowledge of specific disease characteristics or the need to solve complex equations (20–22). When the effective reproduction number has temporal resolution, it can be used to predict disease dynamics and evolution. An $R > 1$ means the number of new infections is increasing while $R < 1$ indicates that the new infections have decreased over the generation time.

In this work, we define a semi-empirical reproduction number (ρ_γ), as the ratio of new cases with respect to cases γ days ago, with γ the most contagious period of the disease that also corresponds to the time between cases, and filtered with a 3-day moving mean:

$$\rho_\gamma^i = \frac{D_{i-1} + D_i + D_{i+1}}{D_{i-\gamma-1} + D_{i-\gamma} + D_{i-\gamma+1}}, \text{for } i = 1, \ldots, N \text{ days} \quad (9)$$

In Eq. (9) the semi-empirical reproduction number is presented, with N the number of days of the study period, D the filtered and pre-processed diagnoses either of bronchiolitis (Eq. (3)) or of influenza (Eq. (5)), and $\gamma = 5$ both for bronchiolitis and influenza. We decided to use $\gamma = 5$ for influenza after analyzing the robustness of the results obtained for $\gamma = 2$ to $\gamma = 6$ days, which is the interval that literature proposes as time between infections. Since the resulting ρ_γ, especially for bronchiolitis, were strongly fluctuating, we decided to apply a 7-day moving mean filter to smooth the effects of the stochasticity of certain diagnostic reports.

From all possible estimations of the reproduction number, we decided to use the semi-empirical ρ_γ, from now on ρ_5, (Eq. (9) due to its simplicity. Our aim is not to find the most accurate reproduction number, but an estimate that allows us to make a good monitoring of the dynamics of the epidemic. We intend for professionals without mathematical background to understand epidemic dynamics and indicators, hence so we applied the Occam's Razor Principle.

2.4.4 Effective potential growth

The Effective Potential Growth (EPG) is based on the one defined for COVID-19 (24). EPG is an epidemic index that combines the incidence level and the incidence trend into a single parameter, and it has shown to be a useful risk indicator for the monitoring of COVID-19. In this work, we defined it as the product of the daily 7-day cumulated incidence of infections (A_7) by the corrected semi-empirical reproduction number (ρ_γ). Since the time $t = 7$ for A_7 and the generation interval are different, the reproduction number has to be corrected as:

$$\rho_{\gamma_c} = \left(\rho_\gamma\right)^{\frac{t}{\gamma}} \quad (10)$$

$$EPG = A_7 \cdot \rho_{\gamma_c} \quad (11)$$

We defined in Eq. (10) the corrected semi-empirical reproduction number, with $t = 7$ and $\gamma = 5$ in our particular case. In Eq. (11) we presented the EPG index as the product of A_7 and the ρ_{γ_c}, from now on ρ'_5, afore introduced. The semi-empirical reproduction number is an estimation of how many new infections generates one infected individual. EPG amplifies or narrows the weekly incidence according to whether there has been an increase ($\rho'_5 > 1 \Rightarrow EPG > A_7$) or decrease ($\rho'_5 < 1 \Rightarrow EPG < A_7$) in cases over the last γ days. In this way, the rate of growth is considered when looking at the weekly incidence of infections and we can anticipate a threshold crossing of the epidemic. Hence, the EPG can be interpreted as a *forecaster* of trend changes, the anticipation of which needs to be determined. However, EPG is not a predictor of incidences, but of the dynamic changes in the evolution of an epidemic, anticipating the level of risk to which we are going to be exposed.

The EPG has an advantage over using ρ_5 or A_7 alone in that it is more easily interpretable for healthcare or public health professionals. It presents, in incidence terms, the effects of the reproduction number on the evolution of the epidemic. In addition, it can be combined with risk levels to provide a short-term snapshot.

2.5 Measure of anticipation

The objective of creating a monitoring and risk panel for RVIs is not only to assess the current epidemiological situation but to be able to forecast how the course of events will unfold. Subsequently, we performed a Pearson correlation analysis for EPG to determine its suitability and anticipation to the surpassing of epidemic levels. For that, we analyzed how influenza and bronchiolitis incidences correlate and what lag they have with their EPG sequences globally, for their whole series, but also for each of their seasons separately. In Figure 2, you can see a representation of this process, and further visualizations

can be found in the Supplementary material. Keeping EPG intact (dark purple line), we move forward or backwards A_7 (light brown lines) and compute the Pearson correlation among both signals. That way, the anticipation of EPG to A_7 can be computed, since that number of days will correspond to the strongest correlation coefficient.

We also looked at how many days EPG advances the different epidemic levels, computing the difference in days when a certain threshold is reached.

3 Results

3.1 Epidemic levels and threshold

After performing the extensive pre-processing, we obtain smooth visualizations of daily number of diagnoses of bronchiolitis and influenza throughout the study period. With them, we have been able to compute daily and weekly incidence of disease, allowing us to define epidemic stages. The resulting computations of daily and weekly epidemic incidence threshold and levels for influenza and bronchiolitis are collected in Table 1. Furthermore, weekly thresholds are represented in Figures 3, 4, for influenza and bronchiolitis respectively, together with their weekly incidences.

These results suggest that when we have a weekly incidence of 9/27 or a daily incidence of 1/4 for influenza/bronchiolitis, we can consider the epidemic wave to have started and we will remain at very low numbers of infections until we cross the low epidemic thresholds, after which we should already observe effects at the level of occupancy in health care facilities.

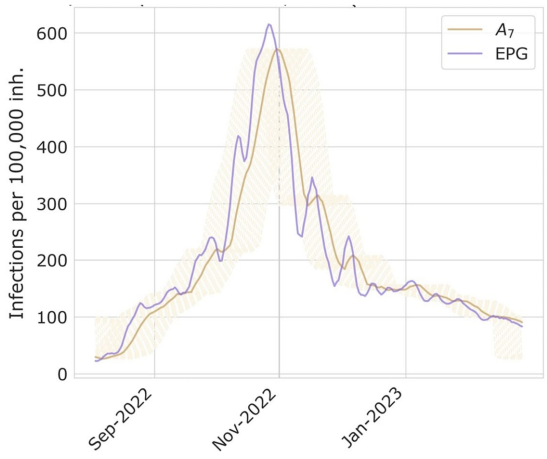

FIGURE 2
Examples of A_7 and EPG computed for season 2022–2023 of bronchiolitis, and the process on how to compute the days of delay between both time series peaks.

We can notice from Figures 3, 4 the disappearance of influenza when the COVID-19 pandemic spread in March 2020, until mid-2022 when a small epidemic occurred. Meanwhile, diagnoses of bronchiolitis were reported in winter 2020 and two consecutive relatively small epidemics in 2021, both during summer and winter, surpassing the epidemic thresholds defined but not reaching very high levels.

Nonetheless, as Figure 4 shows, the latter epidemic of bronchiolitis has been the historically greatest appearing 1 month earlier. As concerning influenza, in Figure 3 we can ascertain that we are still moving toward a new "normal" seasonality. The latter epidemic wave of influenza was advanced also 1 month from previous seasons, and actually consisted of two different outbreaks, the first one mainly corresponding to influenza A and the subsequent to mainly influenza B viruses (35).

On another note, these visualizations allow us to contrast the nature of both diseases. Bronchiolitis is of a highly stochastic nature, partially because it affects a smaller population (only children) and because the disease can be caused by several viral agents creating plateaus before and after the epidemic peak, which is mostly caused by RSV. On the other hand, influenza presents a smoother signal, both because the number of daily diagnoses is higher and because in Catalonia only two different strains of influenza viruses, A and B, are widespread (32).

Comparing Figures 3, 4, the distance between the low and medium epidemic thresholds is narrower for bronchiolitis than for influenza, as an effect of that previously described *plateau* present in the bronchiolitis infections data. This indicates that for bronchiolitis, the epidemic thresholds defined might only be useful from the medium threshold, when the clear epidemic wave started before the pandemic. Besides, we still have to be cautious with the levels calculated since there are still many unknowns about how future epidemics of influenza and bronchiolitis will unfold in Catalonia after COVID-19.

3.2 Effective potential growth

With a correlation coefficient higher than 0.98, we found that the EPG anticipates weekly influenza incidence by 6 to 7 days and bronchiolitis by 4 to 5 days. In Figure 5 we provide the results of the correlation analyses for both diseases.

TABLE 1 Epidemic threshold and levels of daily and weekly incidence for influenza and bronchiolitis diseases.

Level	Daily		Weekly	
	Influenza (diagnoses/10^5)	Bronchiolitis (diagnoses/10^5)	Influenza (diagnoses/10^5)	Bronchiolitis (diagnoses/10^5)
Threshold	1	4	9	27
Low	3	13	21	89
Medium	8	20	53	141
High	20	36	138	250
Very high	31	65	214	453

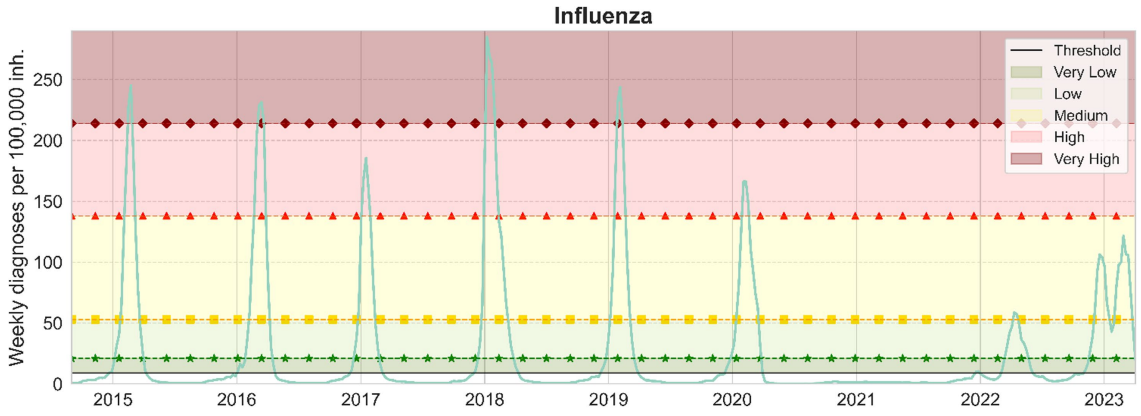

FIGURE 3
Weekly influenza cases per 100,000 inhabitants in Catalonia. From bottom to top, the epidemic threshold (black), the low (green, stars), medium (yellow, squares), high (red, triangles) and very high (maroon, diamonds) epidemic levels are also displayed.

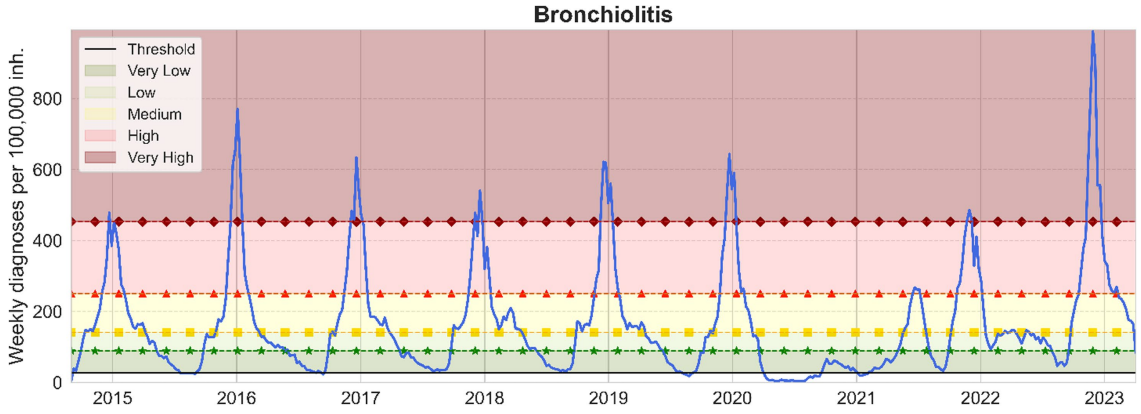

FIGURE 4
Weekly bronchiolitis cases per 100,000 inhabitants <2 years in Catalonia. From bottom to top, the epidemic threshold (black), the low (green, stars), medium (yellow, squares), high (red, triangles) and very high (maroon, diamonds) epidemic levels are also displayed.

It is noteworthy that the EPG effectively predicted the incidence of bronchiolitis and influenza almost a week in advance, maintaining strong correlation coefficients even during and after the pandemic. During the first epidemic following the SARS-CoV-2 outbreak, it experienced only a slight decrease in predictive ability, losing 1–2 days of anticipation. However, the 2020–2021 epidemic period should be excluded from the analysis due to the negligible incidence of influenza and the low occurrence of bronchiolitis cases.

We also looked at how many days EPG anticipates the different epidemic levels, and the results are collected in Table 2.

Notice that not all columns in Table 2 are filled. That is because not all epidemic seasons reach all the different thresholds, some of them only achieve medium levels of incidence. In addition, the robustness of EPG in influenza anticipation is palpable when compared to the results for bronchiolitis, a consequence of the nature of the data used, with much less daily diagnoses than influenza. Hence the bronchiolitis reports present and therefore can cause artifacts leading to less robust results, presented as >10 days. For the same reason, for bronchiolitis, only EPG anticipating high and very high risks should be considered, since lower incidences still present reporting variability that adds noise to the metric. Medium risk is also faithfully anticipated, but one should be cautious as to read the results because artifacts appear in some seasons as a result of the plateaus occupying these incidence ranges, plateaus caused by the many viruses that can produce bronchiolitis before the RSV predominates.

For further insight into the results, we present the historical diagnoses, incidences, ρ_5 and EPG measurements in Figures 6, 7 for influenza and bronchiolitis, respectively.

Once again, the stochastic nature of epidemic medical records is ascertained, in particular when looking at the estimated reproduction numbers ρ_5. In addition, we see how before an epidemic peak there is a raise of ρ_5 up to 3, which means that a large number of contagions are taking place.

The similarity between the incidence of diagnoses and the EPG for both diseases can be corroborated, as well as the slight advancement of EPG, and how it reaches incidences higher than the equivalent weekly diagnoses, due to prompt growths in infections. This way, it indicates the risk of growth of an epidemic.

10.3389/fpubh.2023.1307425

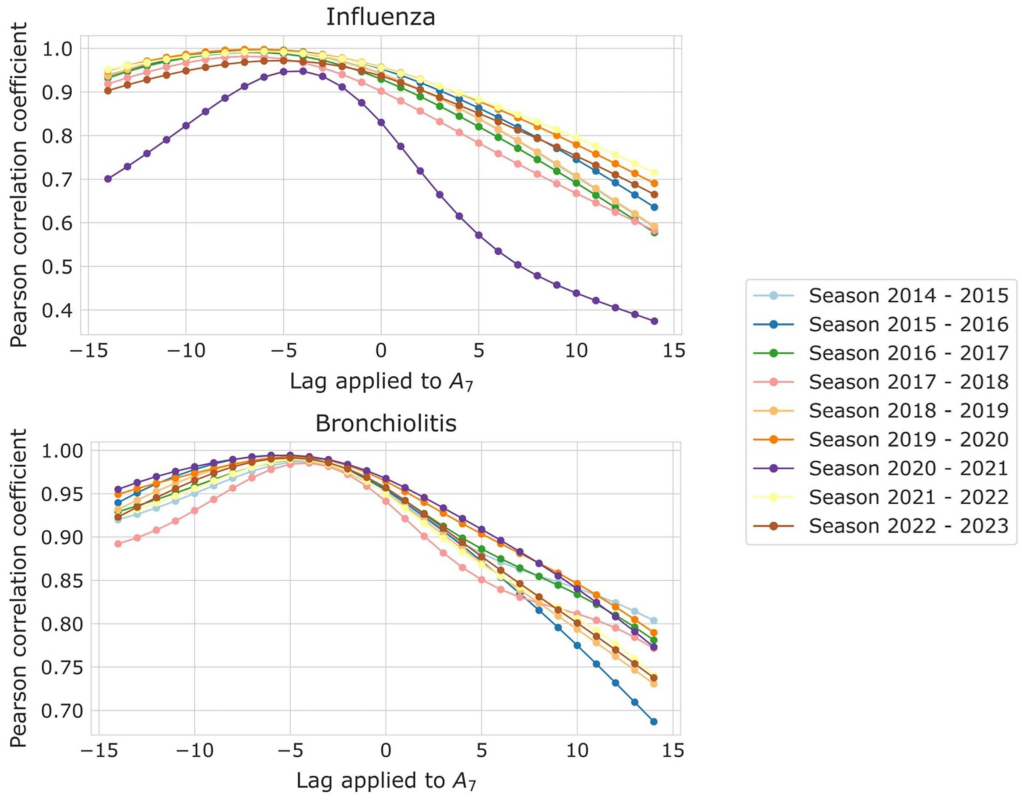

FIGURE 5
Pearson correlation coefficient among A_7 and EPG, for the different lags applied to A_7, for (top) influenza and (bottom) bronchiolitis, and the different epidemic seasons, each corresponding to a different color.

TABLE 2 **Number of days in which EPG advances the reaching of the different epidemic thresholds with respect to A_7.**

Bronchiolitis				
Season	Threshold			
	Low	Medium	High	Very high
2014–2015	>10	9	6	6
2015–2016	7	>10	7	10
2016–2017	7	>10	7	9
2017–2018	5	9	6	8
2018–2019	6	9	>10	6
2019–2020	>10	>10	7	>10
2020–2021	9	-	-	-
2021–2022	0	5	>10	>12
2022–2023	0	6	>10	4

Influenza				
Season	Threshold			
	Low	Medium	High	Very high
2014–2015	8	3	8	8
2015–2016	>10	>10	10	7
2016–2017	7	6	7	–
2017–2018	5	5	6	8
2018–2019	>10	8	6	9
2019–2020	>10	6	7	–
2020–2021	–	–	–	–
2021–2022	9	5	–	–
2022–2023	0	>10	–	–

For (top) bronchiolitis and (bottom) influenza diseases.

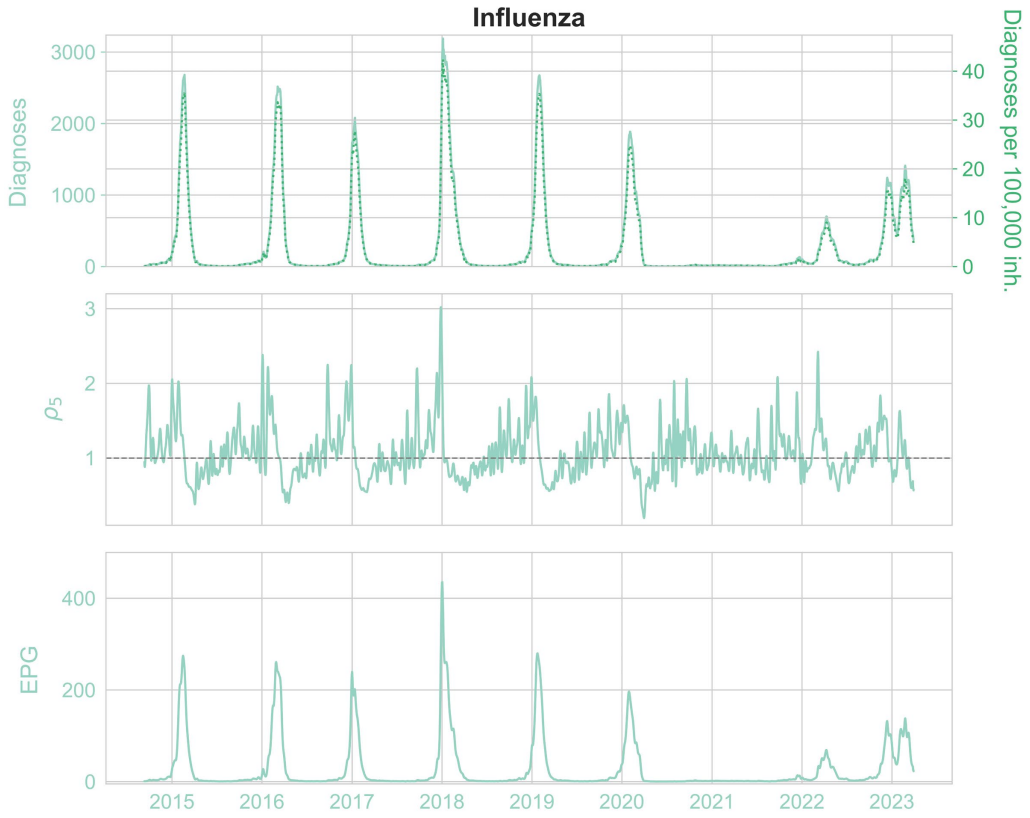

FIGURE 6
From top to bottom, the daily diagnoses (left) and daily diagnoses per 100,000 population (right, pointed), ρ_5 rate and EPG (weekly) infections per 100,000 population, for influenza.

3.3 Risk diagrams

To assist the visualization of EPG to better interpret it, we plotted the so-called risk diagrams (24) in which we have ρ'_5 in front of A_7 and a shaded background in a color scale representing the different epidemiological levels defined: dark green for very low or basal level, light green for low, yellow for medium, red for high and maroon for very high weekly incidence levels. To enhance readability and assist all readers, we have incorporated distinct symbols in our presentation. We differentiate between very low and low levels by "*," low and medium levels by a square, medium and high levels by triangles and high and very high levels by diamonds. The growth/decrease threshold ($\rho'_5 = 1$) is shown as a dotted line. Each dot in the plot depicts an EPG value for the corresponding A_7 and ρ_5 in a certain day, and the dashed line joins two consecutive days. The more separated the points, the greater the increase or decrease in incidence (horizontal direction) or growth rate (vertical direction). The day the epidemic threshold is crossed initially is drawn as a blue dot and the final day of the epidemy, when we cross that value again, is in red. The x-axes are limited to only show A_7 incidences above the weekly epidemic threshold. An example of risk diagram can be found in Figure 8 but the complete set of risk diagrams for all epidemic seasons during the period of study can be found in the Supplementary material.

The risk diagrams allow us to anticipate the evolution of an epidemic in a very straightforward way. If we have an influenza incidence of 50 cases per 10^5 inhabitants but we are above the dotted line that separates growth from decrease, we expect that the number of active cases will continue to increase, following the pattern of the last 5 years. On the other hand, if the same incidence is located below the dotted line, it will not. Then, the color scale helps us to define where we are in the epidemic, whether we are at low (dark and light green), medium (yellow) or high (bright and dark red) incidence values.

3.4 Surveillance table

To enhance and simplify surveillance of respiratory diseases in Catalonia, and facilitate the visualization of the epidemiological indicators, we have developed an automatized control panel, as depicted in Figure 9, that displays the weekly incidence rates for the previous and current weeks, the growth rates for the previous and current weeks, and the EPG. These data are updated daily and the weekly incidence rates and growth rates are calculated by grouping the reported diagnoses over the last 7 days. In Figure 9 we represented the panel at 5th December 2022, when the epidemic of bronchiolitis started vanishing and the influenza wave started to increase.

The last three columns present a color scale such that *Current week growth rate (%)* is green if it is lower than the previous week one, orange if it is the same and red if it is higher; *Semi-empirical reproduction number* ρ_5 is green when below 1, orange if equal to 1, and red if greater than 1; and *EPG (diagnoses per 100,000 population)*

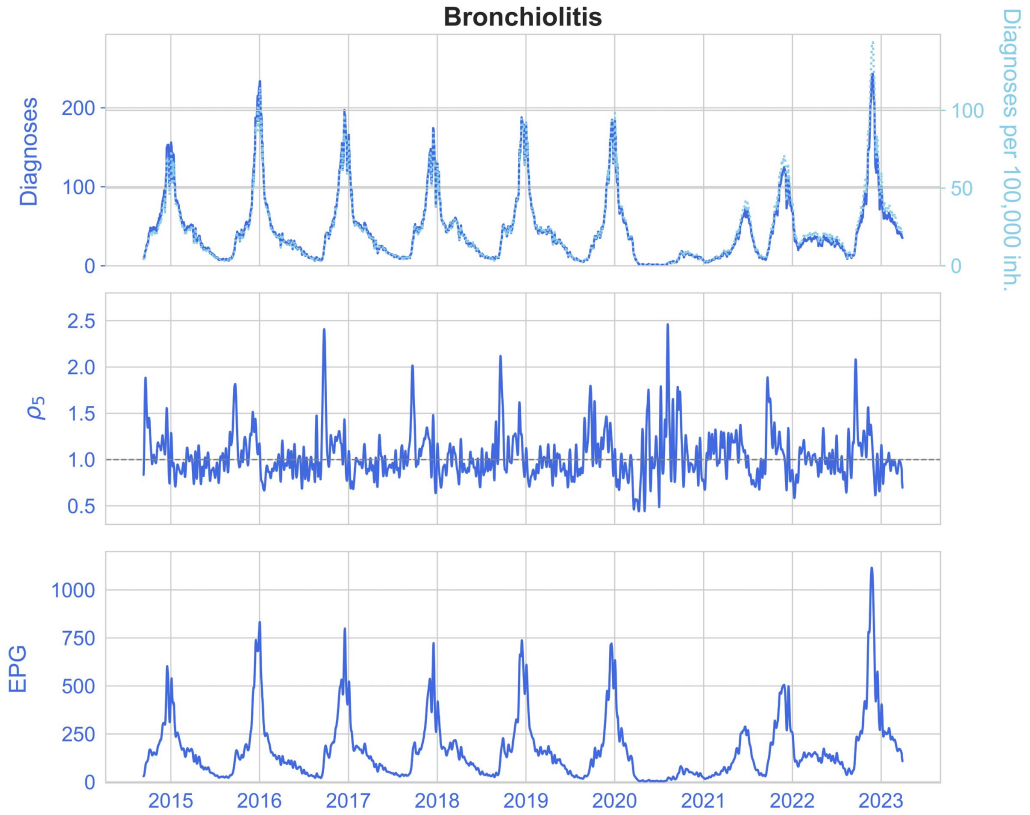

FIGURE 7
From top to bottom, the daily diagnoses (left) and daily diagnoses per 100,000 population (right, pointed), ρ_5 rate and EPG (weekly) infections per 100,000 population, for bronchiolitis.

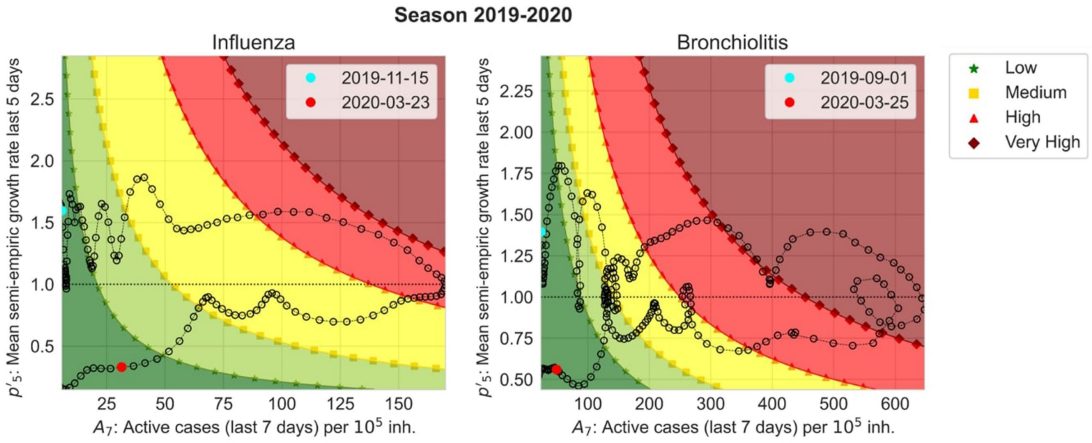

FIGURE 8
Risk diagrams for season 2019–2020 for influenza (left) and bronchiolitis (right). They show ρ'_5 with respect to A_7 starting from the cyan point and finishing at the red point. The background colors correspond to EPG values classified by the epidemic levels. Very low (dark green) and low (light green) levels are separated by "*", low and medium (yellow) levels by a square, medium and high (red) levels by triangles and high and very high (maroon) levels by diamonds.

is white if the epidemic threshold is not surpassed, dark green if we are in very low level, green for low level, yellow for medium level, orange for high level and maroon for very high level. In Figure 9, we observe that we are in a period where the bronchiolitis epidemic is over and we are slowly decreasing incidence, although maintained in high incidences, while at the height of the flu epidemic, with a high number of infections and moving toward greater incidences.

Risk Panel for Seasonal Epidemics

	Previous week incidence (diagnoses per 100,000 population)	Current week incidence (diagnoses per 100,000 population)	Previous week growth rate (%)	Current week growth rate (%)	Semi-empirical reproduction number ρ_5	EPG (diagnoses per 100,000 population)
Bronchiolitis	899.00	899.00	23.00	-9.00	0.80	683.00
Influenza	61.00	61.00	41.00	56.00	1.35	92.00

FIGURE 9
Capture of the risk panel for seasonal epidemics in Catalonia, as of 5th of December 2022.

4 Discussion

We redefine an epidemic indicator named Effective Potential Growth (EPG) that potentially anticipates changes in weekly epidemic incidence by 4 to 5 days for bronchiolitis and 6 to 7 days for influenza disease. This index, together with a semi-empirical reproduction number, the weekly changes in incidences and growth rates, are the core of the epidemic surveillance panel we developed based on previous work that showed how this approach could work for COVID-19 monitoring (23).

Since the SARS-CoV-2 pandemic, the need for epidemiological surveillance of infectious diseases, especially respiratory diseases, became evident, as airborne transmission is highly effective (36). Several countries already have established publicly available epidemic surveillance systems and outbreak risk indicators, such as the USA (37), UK (38), Canada (39), Australia (40), and even Spain, in particular Catalonia (25). Nonetheless, we have not found any that anticipate the evolution of an epidemic wave targeting a general public without a strong mathematical background. Mathematical modeling of infectious diseases is highly dependent on the quality of the epidemiological data available, and requires expertise to produce and understand the models' results and parameters. Even though being the most accurate way of forecasting infectious diseases, models can be counter intuitive for medical practitioners or policy makers, who may require of previous formation in the topic. That is why EPG can be a support index for very short-term forecasting, since it shows in advance when the different epidemic thresholds will be achieved and can anticipate by almost a week the epidemic peak. This information is given in incidence terms, which is a common measure of the state of a disease in both public health policy and in medical settings. In addition, we introduce the visualization of EPG in a risk diagram, which can give an illustration of the state of the epidemic in a very straightforward manner. Besides, this epidemiological indicator could be introduced in mathematical models to enhance their prediction capability.

We have also shown that, with a proper pre-processing of the data, and taking into account the weekly differences in reporting, the epidemic waves of influenza and bronchiolitis have had clearly defined thresholds in the last decade, at least in the Catalan healthcare system. These thresholds are particularly robust to different analyses that deal with data reporting fluctuations and, even in the case of bronchiolitis data, where more artifacts are present, they provide an accurate picture of its short-term evolution. Indeed, when the number of weekly cases reaches a certain threshold with a certain weekly growth, a large wave of cases appears in subsequent weeks systematically. For future surveillance, this can be a crucial input to warn the health care system a few weeks in advance of the increase in workload.

Certainly, our proposed scheme has some limitations and the EPG indicator is more robust for influenza than for bronchiolitis, in particular until the medium level threshold. That is due to the stochastic nature of bronchiolitis data, as stated before, and because of the *plateau* present in its epidemic waves. Nonetheless, in most cases we are able to anticipate the change in epidemic threshold by approximately a week in advance. Another limitation is the simplicity of the calculation of the effective reproduction number, which might not be accurately describing the epidemic dynamics. However, is within the error that we accept in exchange for simplicity of interpretation, and we observe that it performs adequately. We could also use it in an anticipatory way, but this is not the objective of this work, since its output is more complex to interpret than that of the incidence, which is why we rely on the EPG.

In addition, currently, hospitalizations are not publicly available, which restricts us to using only primary healthcare data. With hospital admissions, further information could be introduced in our risk panel, such as the severity of the infections by a certain disease, including the ratio of people admitted to the hospital versus clinical diagnoses in primary healthcare, or the percentage of Intensive Care Units (ICUs) occupied. From these data, other risk indicators could be designed, such as an ICU-increase associated risk indicator. Besides, data on mortality could also be a good indicator of the sternness of the disease, but these data are not provided in a daily manner in our region. Additionally, preprocessing medical records is a hard task and there is not a standardized way to do so, yet. The bronchiolitis diagnoses' stochasticity limits both our preprocessing and predictions abilities with the disease.

Nevertheless, the availability of centralized databases with primary care clinical diagnoses has been enhanced by the pandemic, thus providing a rapid way to monitor the evolution of an epidemic. The panel of semi-empirical indicators that we have presented can be easily incorporated to such databases due to their empirical nature, thus becoming a simple and useful tool to help on the management and surveillance of such epidemic episodes. Our proposed preprocessing methodology allowed us to work with smoother and more reliable data and the defined monitoring panel is the only one to our knowledge using mostly empirical data to construct forecasting indicators, with concept and visualization easy to understand for healthcare practitioners and the general public.

Data availability statement

The original contributions presented in the study are included in the article/Supplementary material, further inquiries can be directed to the corresponding author.

Author contributions

AP-M: Conceptualization, Data curation, Formal analysis, Investigation, Methodology, Software, Validation, Visualization, Writing – original draft. MB: Methodology, Software, Validation, Writing – review & editing. VL: Formal analysis, Investigation, Methodology, Supervision, Validation, Writing – review & editing. MC: Conceptualization, Methodology, Supervision, Validation, Writing – review & editing. SA: Conceptualization, Formal analysis, Funding acquisition, Methodology, Supervision, Validation, Writing – review & editing. EÁ-L: Conceptualization, Formal analysis, Methodology, Supervision, Validation, Writing – review & editing. DL: Conceptualization, Methodology, Supervision, Validation, Writing – review & editing. AS-A: Conceptualization, Formal analysis, Funding acquisition, Investigation, Project administration, Resources, Supervision, Validation, Writing – original draft, Writing – review & editing. CP: Conceptualization, Formal analysis, Funding acquisition, Investigation, Methodology, Project administration, Resources, Supervision, Validation, Writing – original draft, Writing – review & editing.

Funding

The author(s) declare financial support was received for the research, authorship, and/or publication of this article. Grant number 202134-30-31, funded by "La Fundació La Marató de TV3." Grant PDI2022-139215NB-I00 funded by MCIN/AEI/10.13039/501100011033 and by "ERDF A way of making Europe."

Conflict of interest

The authors declare that the research was conducted in the absence of any commercial or financial relationships that could be construed as a potential conflict of interest.

The author(s) declared that they were an editorial board member of Frontiers, at the time of submission. This had no impact on the peer review process and the final decision.

Publisher's note

Supplementary material

The Supplementary material for this article can be found online at: https://www.frontiersin.org/articles/10.3389/fpubh.2023.1307425/full#supplementary-material

References

1. Institute for Health Metrics and Evaluation (IHME). *GBD Compare Data Visualization*. Seattle, WA: IHME, University of Washington. (2020). Available at: http://vizhub.healthdata.org/gbd-compare (Accessed May 02, 2023).

2. Globally F, Bill F. Age-sex differences in the global burden of lower respiratory infections and risk factors, 1990-2019: results from the global burden of disease study 2019. *Lancet Infect Dis*. (2022) 22:1626–47. doi: 10.1016/S1473-3099(22)00510-2

3. GBD 2019 Diseases and Injuries Collaborators. Global burden of 369 diseases and injuries in 204 countries and territories, 1990–2019: a systematic analysis for the global burden of disease study 2019. *Lancet*. (2020) 396:1204–22. doi: 10.1016/S0140-6736(20)30925-9

4. Li Y, Wang X, Blau DM, Caballero MT, Feikin DR, Gill CJ, et al. Global, regional, and national disease burden estimates of acute lower respiratory infections due to respiratory syncytial virus in children younger than 5 years in 2019: a systematic analysis. *Lancet*. (2022) 399:2047–64. doi: 10.1016/S0140-6736(22)00478-0

5. Piedimonte G, Perez MK. Respiratory syncytial virus infection and bronchiolitis. *Pediatr Rev*. (2014) 35:519–30. doi: 10.1542/PIR.35-12-519

6. Wang X, Li Y, O'Brien KL, Madhi SA, Widdowson MA, Byass P, et al. Global burden of respiratory infections associated with seasonal influenza in children under 5 years in 2018: a systematic review and modelling study. *Lancet Glob Heal*. (2020) 8:e497–510. doi: 10.1016/S2214-109X(19)30545-5

7. World Health Organization, "*Influenza (Seasonal)*." (2023). Available at: https://www.who.int/news-room/fact-sheets/detail/influenza- (Accessed May 02, 2023).

8. Lafond KE, Porter RM, Whaley MJ, Suizan Z, Ran Z, Aleem MA, et al. Global burden of influenza-associated lower respiratory tract infections and hospitalizations among adults: a systematic review and meta-analysis. *PLoS Med*. (2021) 18:e1003550. doi: 10.1371/JOURNAL.PMED.1003550

9. Molinari NAM, Ortega-Sanchez IR, Messonnier ML, Thompson WW, Wortley PM, Weintraub E, et al. The annual impact of seasonal influenza in the US: measuring disease burden and costs. *Vaccine*. (2007) 25:5086–96. doi: 10.1016/j.vaccine.2007.03.046

10. Centers for Disease Control and Prevention, "*Disease burden of flu*." (2023). Available at: https://www.cdc.gov/flu/about/burden/index.html (Accessed May 02, 2023).

11. Harding N, Spinney R, Prokopenko M. Phase transitions in spatial connectivity during influenza pandemics. *Entropy 2020*. (2020) 22:133. doi: 10.3390/E22020133

12. Soler-Font M, Aznar-Lou I, Basile L, Soldevila N, Godoy P, Martínez A, et al. Costs and factors associated with hospitalizations due to severe influenza in Catalonia (2017–2020). *Int J Environ Res Public Health*. (2022) 19:14793. doi: 10.3390/IJERPH192214793

13. Coma E, Vila J, Méndez-Boo L, Antón A, Mora N, Fina F, et al. Respiratory syncytial virus infections in young children presenting to primary Care in Catalonia during the COVID-19 pandemic. *J Pediatric Infect Dis Soc*. (2021) 11:69–72. doi: 10.1093/JPIDS/PIAB121

14. Coma Redon E, Mora N, Prats-Uribe A, Fina Avilés F, Prieto-Alhambra D, Medina M. Excess cases of influenza and the coronavirus epidemic in Catalonia: a time-series analysis of primary-care electronic medical records covering over 6 million people. *BMJ Open*. (2020) 10:e039369. doi: 10.1136/BMJOPEN-2020-039369

15. Biggerstaff M, Cauchemez S, Reed C, Gambhir M, Finelli L. Estimates of the reproduction number for seasonal, pandemic, and zoonotic influenza: a systematic review of the literature. *BMC Infect Dis*. (2014) 14:1–20. doi: 10.1186/1471-2334-14-480/FIGURES/5

16. CDC, "*Weekly U.S. influenza surveillance report*." (2023). Available at: https://www.cdc.gov/flu/weekly/index.htm#ILINet (Accessed May 02, 2023).

17. CDC, "*COVID-19 pandemic planning scenarios*." (2023). Available at: https://www.cdc.gov/coronavirus/2019-ncov/hcp/planning-scenarios.html (Accessed May 02, 2023).

18. Català M, Alonso S, Álvarez E, López D, Marchena M, Conesa D, et al. *"Análisis de los retrasos en la actualización de las series históricas de casos en España". Research report. Computational Biology and Complex Systems, Universitat Politècnica de Catalunya*. (2020). Available at: https://biocomsc.upc.edu/en/covid-19/delays_spain_30062020.pdf (Accessed December 24, 2023).

19. European Centre for Disease Prevention and Control, "*Flu news Europe: Weekly influenza updates*." (2023). Available at: https://www.ecdc.europa.eu/en/seasonal-influenza/surveillance-and-disease-data/flu-news-europe (Accessed May 02, 2023).

20. Wallinga J, Teunis P. Different epidemic curves for severe acute respiratory syndrome reveal similar impacts of control measures. *Am J Epidemiol*. (2004) 160:509–16. doi: 10.1093/AJE/KWH255

21. Jorge DCP, Oliveira JF, Miranda JGV, Andrade RFS, Pinho STR. Estimating the effective reproduction number for heterogeneous models using incidence data. *R Soc Open Sci*. (2022) 9:220005. doi: 10.1098/RSOS.220005

22. Cori A, Ferguson NM, Fraser C, Cauchemez S. A new framework and software to estimate time-varying reproduction numbers during epidemics. *Am J Epidemiol*. (2013) 178:1505–12. doi: 10.1093/aje/kwt133

23. Català M, Cardona PJ, Prats C, Alonso S, Álvarez E, Marchena M, et al. On the weekend effect on confirmed cases and the resulting oscillations in the empiric reproduction number (Part II). In: *Analysis and prediction of COVID-19 for EU-EFTA-UK and other countries. Daily report. Computational Biology and Complex Systems, Universitat Politècnica de Catalunya*. (2020), p. 10–14.

24. Catala M, Coma E, Alonso S, Álvarez-Lacalle E, Cordomi S, López D, et al. Risk diagrams based on primary care electronic medical records and linked real-time PCR data to monitor local COVID-19 outbreaks during the summer 2020: a prospective study including 7,671,862 people in Catalonia. *Front Public Heal*. (2021) 9:890. doi: 10.3389/fpubh.2021.693956

25. Health Department of the Catalan Government. Sistema d'Informació per a la Vigilància d'Infeccions a Catalunya - SIVIC. (2021). Available at: https://sivic.salut.gencat.cat/ (Accessed February 16, 2023).

26. Aguilar Martín C, Dalmau Llorca MR, Castro Blanco E, Carrasco-Querol N, Hernández Rojas Z, Forcadell Drago E, et al. Concordance between the clinical diagnosis of influenza in primary care and epidemiological surveillance systems (PREVIGrip study). *Int J Environ Res Public Health*. (2022) 19:1263. doi: 10.3390/IJERPH19031263

27. Rosenfeld R, Tibshirani RJ. Epidemic tracking and forecasting: lessons learned from a tumultuous year. *Proc Natl Acad Sci U S A*. (2021) 118:1–6. doi: 10.1073/pnas.2111456118

28. Altmejd A, Rocklöv J, Wallin J. Nowcasting COVID-19 statistics reported with delay: a case-study of Sweden and the UK. *Int J Environ Res Public Health*. (2023) 20:3040. doi: 10.3390/ijerph20043040

29. Català M, Alonso S, Alvarez-Lacalle E, López D, Cardona PJ, Prats C. Empirical model for short-time prediction of COVID-19 spreading. *PLoS Comput Biol*. (2020) 16:e1008431. doi: 10.1371/JOURNAL.PCBI.1008431

30. Villanueva I, Conesa D, Català M, Cano CL, Perramon A, Molinuevo D, et al. Country-report pattern corrections of new cases allow accurate two-week predictions of Covid19 evolution with the Gompertz model. *ResearchSquare*. (2022). doi: 10.21203/rs.3.rs-1581688/v1

31. Vega T, Lozano JE, Meerhoff T, Snacken R, Beauté J, Jorgensen P, et al. Influenza surveillance in Europe: comparing intensity levels calculated using the moving epidemic method. *Influenza Other Respir Viruses*. (2015) 9:234–46. doi: 10.1111/IRV.12330

32. Vega T, Lozano JE, Meerhoff T, Snacken R, Mott J, Ortiz de Lejarazu R, et al. Influenza surveillance in Europe: establishing epidemic thresholds by the moving epidemic method. *Influenza Other Respir Viruses*. (2013) 7:546–58. doi: 10.1111/j.1750-2659.2012.00422.x

33. Perramon-Malavez A. Cloud of codes of the BIOCOM-SC group. (2023). Available at: https://github.com/BIOCOM-SC/cloud-of-codes/tree/main/Aida_Perramon-Malavez (Accessed December 24, 2023).

34. Kretzschmar M, Wallinga J. *Mathematical models in infectious disease epidemiology*. London: CRC Press (2009).

35. Carlos III Health Institute. "*Vigilancia centinela de Infección Respiratoria Aguda en Atención Primaria (IRAs) y en Hospitales (IRAG) Gripe, COVID-19 y otros virus respiratorios", Red Nacional de Vigilancia Epidemiológica and Instituto de Salud Carlos III*. (2023). Available at: https://www.isciii.es/QueHacemos/Servicios/VigilanciaSaludPublicaRENAVE/EnfermedadesTransmisibles/Paginas/Gripe.aspx (Accessed December 24, 2023).

36. Wang CC, Prather KA, Sznitman J, Jimenez JL, Lakdawala SS, Tufekci Z, et al. Airborne transmission of respiratory viruses. *Science*. (2021) 373:eabd9149. doi: 10.1126/science.abd9149

37. CDC, "*National Respiratory and enteric virus surveillance system*." (2023). Available at: https://www.cdc.gov/surveillance/nrevss/index.html (Accessed May 08, 2023).

38. GOV.UK, "*Weekly national flu reports*." (2023). Available at: https://www.gov.uk/government/collections/weekly-national-flu-reports (Accessed May 08, 2023).

39. Government of Canada. *Flu (influenza): FluWatch surveillance - Canada.ca*. (2023). Available at: https://www.canada.ca/en/public-health/services/diseases/flu-influenza/influenza-surveillance.html (Accessed May 08, 2023).

40. Australian Government Department of Health and Aged Care, "*National Notifiable Diseases Surveillance System (NNDSS)*." (2023). Available at: https://www.health.gov.au/our-work/nndss (Accessed May 08, 2023).

frontiers | Frontiers in Public Health

TYPE Original Research
PUBLISHED 17 May 2024
DOI 10.3389/fpubh.2024.1386495

OPEN ACCESS

EDITED BY
Mahmoud Kandeel,
King Faisal University, Saudi Arabia

REVIEWED BY
Amir Elalouf,
Bar-Ilan University, Israel
Fengshi Jing,
City University of Macau, Macao SAR, China

*CORRESPONDENCE
Sunmi Lee
✉ sunmilee@khu.ac.kr

†These authors have contributed equally to this work and share first authorship

RECEIVED 15 February 2024
ACCEPTED 06 May 2024
PUBLISHED 17 May 2024

CITATION
Kim E, Kim Y, Jin H, Lee Y, Lee H and Lee S (2024) The effectiveness of intervention measures on MERS-CoV transmission by using the contact networks reconstructed from link prediction data.
Front. Public Health 12:1386495.
doi: 10.3389/fpubh.2024.1386495

The effectiveness of intervention measures on MERS-CoV transmission by using the contact networks reconstructed from link prediction data

Eunmi Kim[1†], Yunhwan Kim[2†], Hyeonseong Jin[3], Yeonju Lee[4], Hyosun Lee[5] and Sunmi Lee[5*]

[1]Institute of Mathematical Sciences, Ewha Womans University, Seoul, Republic of Korea, [2]College of General Education, Kookmin University, Seoul, Republic of Korea, [3]Department of Mathematics, Jeju National University, Jeju, Republic of Korea, [4]Division of Applied Mathematical Sciences, Korea University—Sejong, Sejong, Republic of Korea, [5]Applied Mathematics, Kyung Hee University, Yongin, Republic of Korea

Introduction: Mitigating the spread of infectious diseases is of paramount concern for societal safety, necessitating the development of effective intervention measures. Epidemic simulation is widely used to evaluate the efficacy of such measures, but realistic simulation environments are crucial for meaningful insights. Despite the common use of contact-tracing data to construct realistic networks, they have inherent limitations. This study explores reconstructing simulation networks using link prediction methods as an alternative approach.

Methods: The primary objective of this study is to assess the effectiveness of intervention measures on the reconstructed network, focusing on the 2015 MERS-CoV outbreak in South Korea. Contact-tracing data were acquired, and simulation networks were reconstructed using the graph autoencoder (GAE)-based link prediction method. A scale-free (SF) network was employed for comparison purposes. Epidemic simulations were conducted to evaluate three intervention strategies: Mass Quarantine (MQ), Isolation, and Isolation combined with Acquaintance Quarantine (AQ + Isolation).

Results: Simulation results showed that AQ + Isolation was the most effective intervention on the GAE network, resulting in consistent epidemic curves due to high clustering coefficients. Conversely, MQ and AQ + Isolation were highly effective on the SF network, attributed to its low clustering coefficient and intervention sensitivity. Isolation alone exhibited reduced effectiveness. These findings emphasize the significant impact of network structure on intervention outcomes and suggest a potential overestimation of effectiveness in SF networks. Additionally, they highlight the complementary use of link prediction methods.

Discussion: This innovative methodology provides inspiration for enhancing simulation environments in future endeavors. It also offers valuable insights for informing public health decision-making processes, emphasizing the importance of realistic simulation environments and the potential of link prediction methods.

KEYWORDS

MERS-CoV, link prediction, network-based models, interventions, graph autoencoder (GAE)

1 Introduction

The spread of infectious diseases is an issue of paramount societal significance. As evidenced by the profound impact of the recent COVID-19 pandemic, the failure to effectively prevent or mitigate disease transmission can result in substantial social and economic costs. Therefore, it is imperative for the safety of society to uncover the fundamental mechanisms underlying infectious diseases and devise preventive measures accordingly. Collaborative efforts across various academic disciplines have been directed toward this goal. Insights from fields such as medicine, pharmacy, biology, engineering and sciences, and even social sciences play a crucial role in enhancing our understanding of disease transmission dynamics. Of particular importance is understanding how individuals engage in physical interactions, as disease transmission is intricately linked to the types and patterns of human contacts. Consequently, there have been concerted efforts to quantitatively describe and analyze human contacts within the context of disease transmission. One of the representatives has been network models (1, 2). Infected cases and their contacts were represented as nodes and links, respectively, on a network, and the network was analyzed to obtain insights into the transmission process (3, 4). In addition, a network can offer an environment for epidemic simulations, allowing for the acquisition of new knowledge not possible with compartmental model simulations (5). Contact-tracing data can be conducive to generating environments for epidemic simulations. The transmission dynamics of a network highly depends on the network structure, and networks generated based on real human behaviors can provide opportunities to build more realistic models of transmission dynamics in the literature (6–9) than the theoretical models of networks such as random (10, 11), small-world (12, 13), and scale-free (SF) (14, 15) networks.

However, using empirical contact-tracing data for epidemic simulation has limitations (16, 17). One theoretical limitation arises from the fact that individuals have numerous social relationships, but only a portion of these relationships result in actual contacts in practice. In other words, the contacts that individuals make represent only a subset of the many possibilities within their social connections. When conducting simulations, we essentially explore artificial scenarios where social relationships could have played out differently from the real world. Therefore, the network environments used in simulations should reflect the range of possibilities within these relationships, rather than replicating a single, actual realization. Conducting simulations on a contact-tracing network may involve exploring artificial scenarios based on a specific realization, which can pose logical challenges. Another limitation is of an empirical nature. Real-world data, including contact-tracing data, are inherently affected by noise. Contact information can be collected through various means, such as self-reports, cell phone location tracking, or third-party observations. However, noise originating from human errors or technical inaccuracies can result in missing nodes or links within contact-tracing networks. This missing or inaccurate data can affect the reliability and accuracy of simulations that rely on such data. Therefore, using empirical contact-tracing data for epidemic simulations has limitations related to both theoretical considerations, where simulations explore artificial scenarios based on partial realizations, and empirical issues, including noise and missing data inherent in real-world contact-tracing information. Researchers and modelers need to be aware of these limitations and consider them when using such data for epidemiological simulations.

The aforementioned limitations can be complemented by network reconstruction (18). Network reconstruction entails generating a network from another network that has missing or spurious links in its observed status (19). It can be considered as correcting errors in network data because the observed network topology is compared with the theoretical models of network evolution (20). Among many, link prediction (LP) is a promising network reconstruction technique (21–23). LP entails estimating the probability of connecting two nodes that are currently not connected based on the linkage patterns and node features. Several techniques, including matrix factorization, the stochastic block model (24), DeepWalk (25), node2vec (26), and LINE (27), have been used for LP. Recently, advanced techniques in graph neural networks (GNNs) have been actively employed for LP, and the prediction accuracy has been significantly improved in various domains. Since the notion of GNN was initially devised (28), various learning models in the graph domain have been developed (29–31). Convolutional neural networks in the computer vision domain have been redefined for graph data and developed in parallel as convolutional GNNs (ConvGNNs) (29, 30). Recent studies have increased the capabilities and expressive power of ConvGNNs in various practical applications, such as antibacterial discovery (31), fake news detection (32), traffic prediction (33), and recommendation systems (34).

Based on the above considerations, in this study, we reconstruct networks from real-world contact-tracing data and perform epidemic simulations on them. In particular, we examine how the network structure impacts the transmission dynamics and the effectiveness of intervention strategies. As a case study, we consider the Middle East Respiratory Syndrome Coronavirus (MERS-CoV) transmission in South Korea, 2015. Most existing studies on MERS-CoV focused on its epidemic characteristics and demonstrated its super-spreading events (35–37). Some other studies analyzed the contact-tracing data, but their networks were confined only to confirmed cases (38, 39), single hospitals (40), or regions without large-scale outbreaks (41). Thus, their contact networks were of limited use for epidemic simulations. Another study extracted the parameter of an SF network from MERS-CoV contact-tracing data and generated a simulation environment with it, but the contact network itself was not used for simulation (42). In this study, we construct simulation environments using reconstructed networks and examine the dynamics of the epidemic within these environments. Simulation involves utilizing a network generated through graph autoencoder-based link prediction (GAE network), and a scale-free (SF) network is employed for comparative analysis. Then, we conduct epidemic simulations to assess three intervention strategies: Mass Quarantine (MQ), Isolation, and Isolation combined with Acquaintance Quarantine (AQ + Isolation).

The remainder of this article is organized as follows. Section 2 introduces the empirical contact network of the 2015 MERS-CoV transmission in South Korea and demonstrates the network reconstruction for simulation environments. Section 3 presents the simulation procedure, and Section 4 describes the simulation

results. The implications, and limitations of this study are discussed in Section 5. Finally, the conclusions are given in Section 6.

2 Materials and methods

2.1 Reconstructing the empirical contact network by link prediction

2.1.1 Empirical contact network

The data for the 2015 MERS-CoV outbreak was obtained from the websites of the Korea Centers for Disease Control and Prevention (KCDC) and the Ministry of Health and Welfare of South Korea (43). These data included information on confirmed cases and their contacts. A network was created from this information, which consisted of 33,093 nodes and 33,090 links, with 186 confirmed cases represented as red nodes and the individuals who had close or casual contact with them represented as blue nodes. Figure 1 shows this contact network.

2.1.2 Link prediction using graph autoencoder

The generated contact network lacks some links between nodes due to some missing information in the data. Thus, the contact network was reconstructed by LP using a graph autoencoder. The graph autoencoder is a neural network model for learning interpretable latent representations of graph-structured data based on an autoencoder (44). In the graph autoencoder framework for LP, the encoder employs a graph convolutional network (GCN) incorporating node features for the latent embedding of each node. Then, the decoder computes the distance between two nodes in the given node embeddings, from which the occurrence of an edge between the two nodes is predicted (see Figure 2 for the model architecture).

Formally, for a graph $G = (V, E)$ defined by a set of node V and a set of edges E between nodes, the encoder maps nodes $v \in V$ with node features $x_v \in \mathbb{R}^n$ to latent embedding vectors $z_v \in \mathbb{R}^d$ with Equation (1):

$$\begin{aligned} ENC : V \times \mathbb{R}^n &\to \mathbb{R}^d \\ (v, x_v) &\mapsto z_v. \end{aligned} \tag{1}$$

Employing the decoder for a pair of node embeddings (z_u, z_v) will estimate a graph-structured similarity score $S[u, v]$ between nodes u and v. The objective of the encoder and decoder is to minimize the reconstruction loss such that Equation (2),

$$DEC(ENC(u), ENC(v)) = DEC(z_u, z_v) \approx S[u, v]. \tag{2}$$

For LP, the similarity score between nodes can be considered as representing whether nodes are neighbors or not; this means that node embeddings z_u and z_v are close in the embedding space if they are linked. The links in the contact network stand for the contact from confirmed cases to other individuals, and individuals in the same cluster may have more contacts with each other than with those in other clusters (the visualization of the contact network in Figure 1 shows the cluster structure). Thus, the cluster, as well as infection status, was used as node features to predict links between nodes using a graph autoencoder. A label propagation algorithm (45) was used for cluster analysis on the contact network, and 61 clusters were detected.

Our GCN model for the encoder has two graph convolution layers with a 256-dim hidden layer and 128-dim latent embedding space. A simple inner product was used for the decoder, which could provide a score as the probability of internode link occurrence, and the sigmoid function was used as the activation function. The model was trained for 500 iterations using an Adam optimizer with a learning rate of 0.005. The reconstructed networks were obtained from the ensemble of 10 trained models. Next, two types of networks were generated. First, a pair of nodes whose similarity score was >0.995 was connected by links; we name this network GAE. Second, as an extended version, a pair of nodes whose similarity score was >0.95 (lower than that of GAE) was connected by links; we name this network GAE_ex as we extend GAE. A similarity score of 0.95 was selected to attain a 99.99% accuracy in recovering existing links. Reducing the similarity score further did not lead to a significant improvement in accuracy. A score of 0.995 was employed for 0.95 networks when they were deemed excessively large (almost twice larger in edges). Increasing the similarity score results in the prediction of additional links. When viewed as a generative model for situations where the original contact network is unavailable, it becomes essential to generate a network of an appropriate scale for practical use.

We validate the accuracy of our graph encoder model in generating results that closely match the actual contact network. It is worth noting that GAE_ex, generated by our graph encoder model, reconstructs the contact network with an accuracy of 99.99% (missing only three edges out of the existing 33,090 edges) and generates 211,778 new possible edges. Similarly, GAE reconstructs the contact network with an accuracy of 98.92% (missing 359 edges out of the existing 33,090 edges) and generates 111,536 new possible edges. Subsequently, both GAE_ex and GAE are finalized by adding missing edges, likely aiming to enhance the completeness of the reconstructed networks. Both GAE_ex and GAE demonstrate effectiveness in reconstructing the contact network, with GAE_ex achieving slightly higher accuracy in capturing existing edges, while GAE generates fewer new possible edges. Therefore, we have selected these two networks for our simulation network.

2.1.3 Properties of reconstructed networks

In this section, we analyzed the characteristics of the networks reconstructed using the graph autoencoder before running the simulations. We opted for the scale-free network for comparative purposes. By conducting simulations on both types of networks, we aimed to illustrate the differences in disease spread within the reconstructed networks compared to the well-understood scale-free network. We chose the scale-free network because it has been more commonly employed in the literature than other models, such as the random-network model, making it more suitable for meaningful comparisons. First, we fitted the degree distribution of the GAE network to the power-law distribution, and found that the scale parameter was 2.19. We then used this parameter to

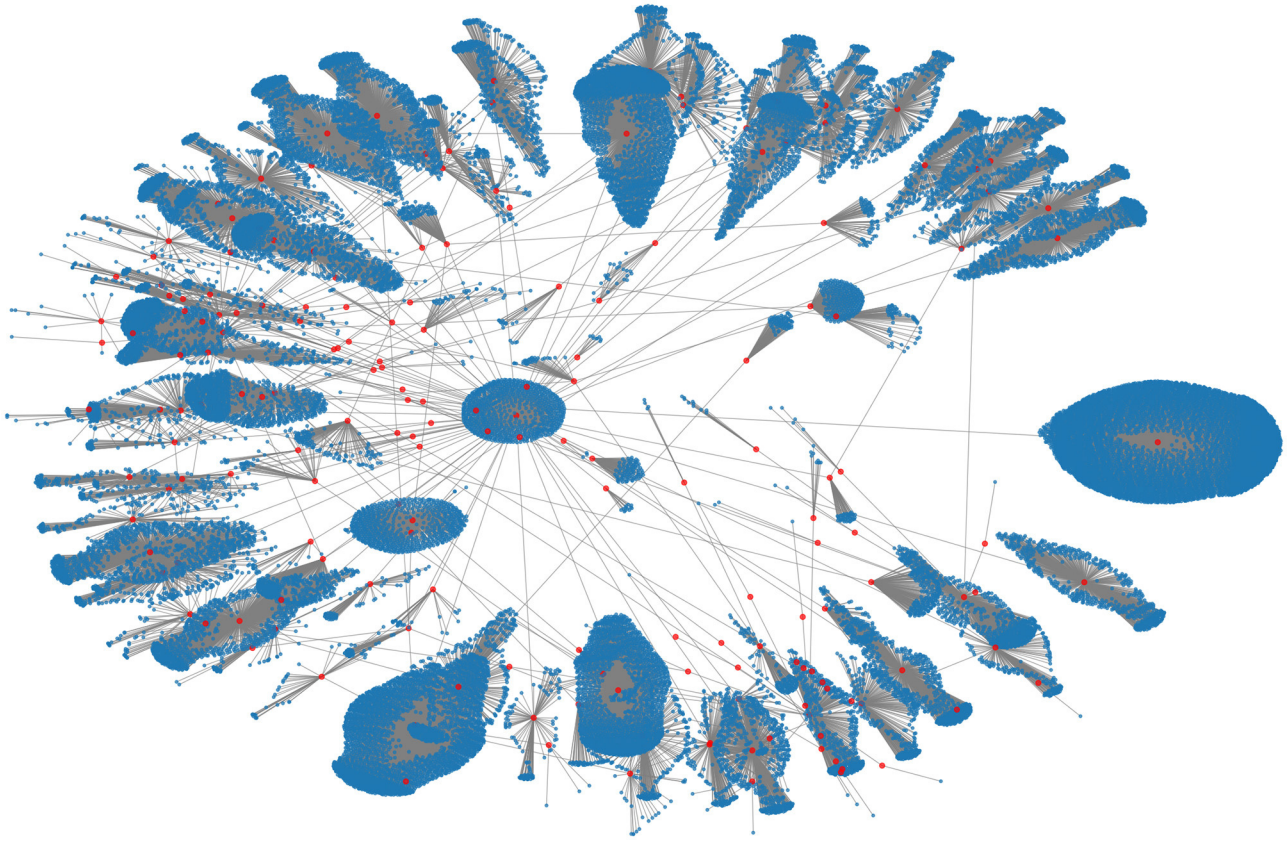

FIGURE 1
The empirical contact network of the 2015 MERS-CoV transmission in South Korea. The red and blue nodes denote 186 confirmed cases and their contact nodes (a total of 33,093), respectively.

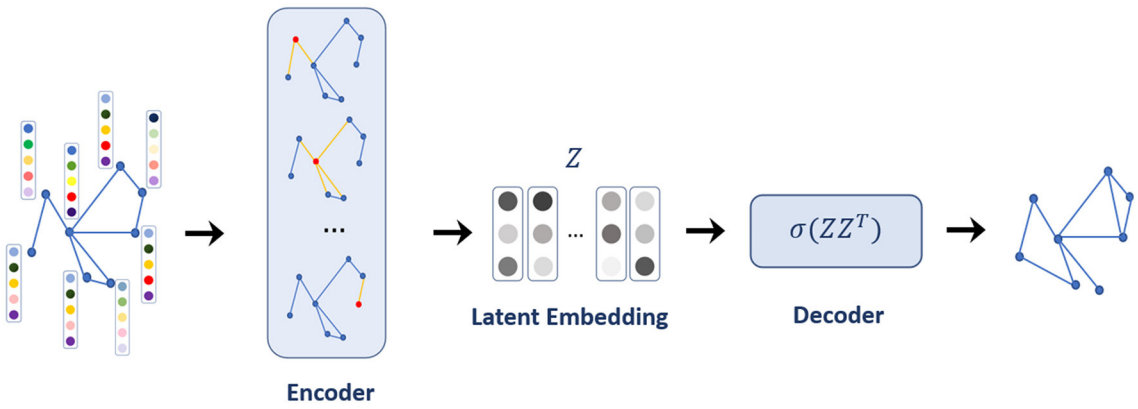

FIGURE 2
The model architecture of a graph autoencoder.

generate a scale-free network using the configuration model (46). The main properties of the scale-free, GAE, and GAE_ex networks are outlined in Tables 1, 2 and Figures 3, 4.

We compare the properties of networks generated using a graph autoencoder (GAE), an extended version of the GAE (GAE_ex), and a scale-free (SF) model. The average degree of GAE_ex is found to be significantly greater than that of GAE and SF in Table 1. All three networks have similar degree distributions, with few nodes having much greater degrees than others as shown in Figure 3A. GAE and GAE_ex have higher average clustering coefficients than SF, indicating that the reconstructed networks have a highly clustered structure similar to those found in real-world social networks (47). Additionally, while SF had multiple disconnected components (a total of 44 connected components),

TABLE 1 Basic characteristics of two reconstructed contact networks and scale-free (SF) network.

	Nodes	Edges	Avg. degree	Connected components	Avg. shortest path length	Avg. clustering coefficient
SF	31,091	132,372	8.5151	44	3.3481	0.1037
GAE	33,093	144,626	8.7406	1	3.4727	0.4825
GAE_ex	33,093	244,868	14.7988	1	3.3386	0.7275

TABLE 2 Comparison of centrality indexes among two reconstructed contact networks and scale-free (SF) network.

	Degree centrality		Closeness centrality		Betweenness centrality		Eigenvector centrality	
	Avg.	Cent(%)	Avg.	Cent(%)	Avg.	Cent(%)	Avg.	Cent(%)
SF	0.000274	17.6450	0.301515	42.8943	0.000075	4.91e-8	0.002145	46.0836
GAE	0.000264	25.4405	0.291004	37.7405	0.000075	6.87e-8	0.002006	29.8501
GAE_ex	0.000447	25.4282	0.301885	37.0357	0.000071	3.01e-8	0.002044	22.4648

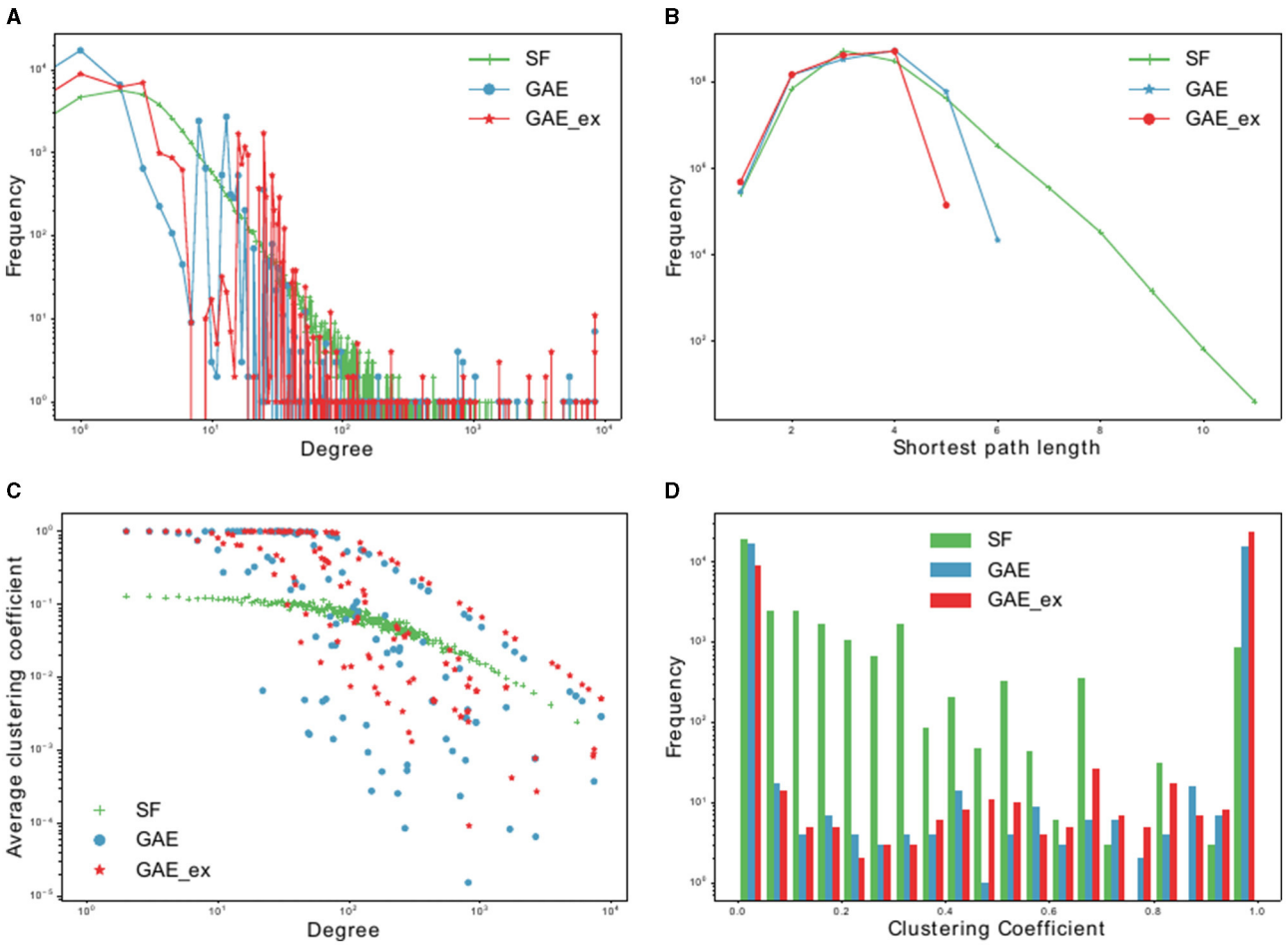

FIGURE 3
Basic characteristics of two reconstructed contact networks and scale-free (SF) network. **(A)** Degree distributions, **(B)** distribution of shortest path lengths, **(C)** clustering coefficient distributions per degree, and **(D)** clustering coefficient distributions.

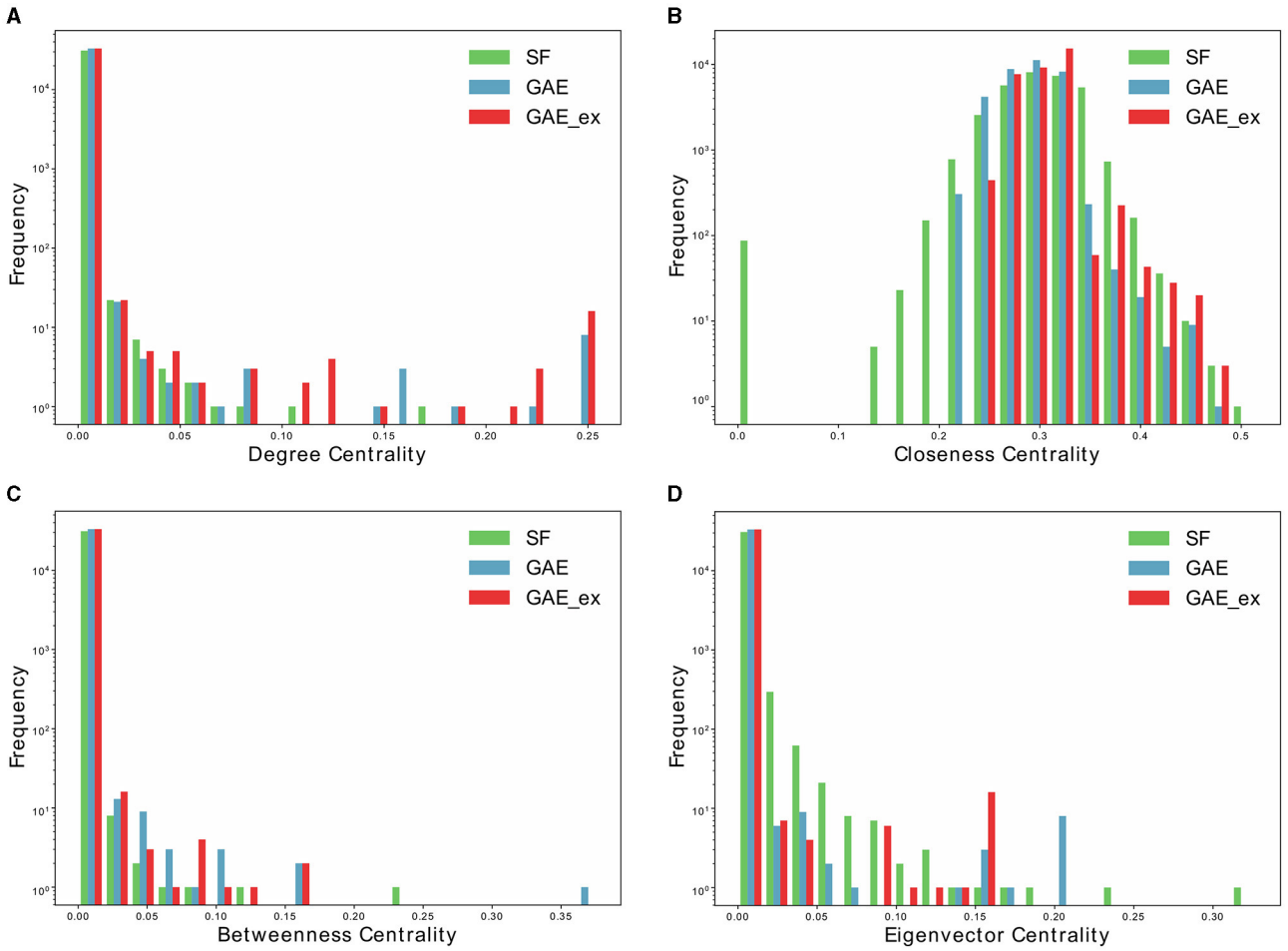

FIGURE 4
Distributions of centrality indexes of two reconstructed contact networks and scale-free (SF) network. **(A)** Degree centrality distribution, **(B)** closeness centrality distribution, **(C)** betweenness centrality distribution, and **(D)** Eigenvector centrality distribution.

GAE and GAE_ex were fully connected. The average shortest path length for all three networks is short (see Figure 3B and Table 1), making them small-world networks. However, SF is found to have a larger diameter than GAE and GAE_ex, indicating that some pairs of nodes in SF are connected by larger hops. The reconstructed networks, GAE and GAE_ex, exhibit greater variation in the average clustering coefficients per degree when compared to the SF network (as shown in Figures 3C, D). This suggests that the connections among the neighbors of nodes with similar degrees are more varied in GAE and GAE_ex than in SF. Additionally, even though the average degrees of GAE and SF are similar, their distributions of average clustering coefficients differ.

Furthermore, Table 2 and Figure 4 present average centrality and centralization index using four different centrality measures in the three networks. Average centrality reflects the characteristics of each node in the network, while the centralization index assesses the distribution of centrality. A higher centralization index suggests a more centralized network, while a lower index indicates a more evenly distributed centrality (see distributions of centrality in Figure 4). Specifically, the average degree centrality for GAE_ex is 0.00044, which is twice as high as that of the GAE and SF networks presented in Table 2. This indicates that, on average, nodes in the GAE_ex network have approximately twice as many connections compared to nodes in the GAE and SF networks. For the other three centrality measures, there are no significant differences between the SF and GAE networks. Closeness centrality, which measures how well-connected a node is to all other nodes, shows similar low values in both networks. Eigenvector centrality, indicating the level of influence of nodes within their respective networks, is similar for nodes in both networks, and it suggests a relatively low level of influence on average. Betweenness centrality, which assesses the role of nodes as intermediaries or bridges between others, also shows similar low values for nodes in both the SF and GAE networks, indicating a limited intermediary role on average. In summary, the analysis of these centrality measures suggests that while the average degree centrality differs significantly between GAE_ex and the other networks, the other three centrality measures (closeness, eigenvector, and betweenness centrality) do not reveal significant distinctions between the SF and GAE networks. This implies that, in terms of these specific centrality metrics, the networks share

similarities in how nodes are connected and their roles within the network.

2.2 Simulation model

We employed agent-based simulations on the generated networks as reported in Kim et al. (42). The simulations were based on the SEIR model, where each agent (node) was assigned one of four epidemiological statuses: susceptible (S), exposed (E), infected (I), and recovered (R). The simulation assumed that when a susceptible agent comes into contact with an exposed or infected agent, it has a probability of becoming infected with a transmission rate of β with below Equation (3):

$$\beta = 1 - (1 - \beta_0)^n \tag{3}$$

In the simulations, an infection was generated when a susceptible individual came into contact with an exposed or infected individual, with a transmission probability determined by the transmission rate constant, β given above. The transmission rate was modeled as a function of the number of neighbors in the network and a baseline transmission constant, β_0. The simulations also accounted for the incubation and infectious periods, which were modeled as gamma probability density functions with means of $1/\kappa$ and $1/\gamma$ days and standard deviations of σ_κ and σ_γ days, respectively. The parameters used in the model were estimated from confirmed cases data from the Korean Centers for Disease Control and Prevention (KCDC) (43) and are listed in Table 3.

At the initialization phase of each simulation run, all agents, except an index case (the first infected agent), are set to be S status, and the predetermined index case is set to be I status. The index case is selected among the agents (nodes) with a sufficient number of links; an outbreak does not occur when the index agent is too far from the hub (when a node with a small degree is selected as the index case). Based on the preliminary experiments, the threshold of degree for selecting an index case was set to 100. The number of agents with more than 100○ was 232 (out of 31,901) in SF, 80 (out of 33,093) in GAE, and 109 (out of 33,093) in GAE_ex; the index case for each simulation run is randomly chosen among them.

The intervention strategies in our research were developed based on an extensive review of existing literature on mathematical models of disease transmission (48–51). Previous studies have incorporated a variety of intervention measures into their models, with a specific focus on social distancing as a key strategy. Social distancing aims to reduce the chances of contact between individuals and has been a major topic of research in disease modeling (52, 53). In our study, we initially emphasized the "Mass Quarantine" strategy, which involves quarantining a certain percentage of the population (53). This strategy serves as an abstraction of real-world measures that restrict social activities, such as store closures and changes in public transportation operations. We selected a parameter of 10% for this strategy, guided by prior research (54).

We also introduced an "Isolation" strategy, which isolates individuals who have tested positive for the infection. This approach is conceptually similar to targeted social distancing, as it specifically targets infected individuals (52). While it may seem unrealistic to isolate all infected individuals, it was observed during the 2015 MERS-CoV outbreak and the early stages of the COVID-19 pandemic in South Korea, where infected individuals voluntarily isolated at home or were hospitalized under government guidance. Implicitly, the first two strategies were included for the purpose of comparison to assess the effectiveness of our third strategy: "Isolation and Acquaintance Quarantine (AQ + Isolation)." This approach involves quarantining individuals who have had close and effective contact with infectious individuals. We selected a parameter of 50% for this strategy, informed by previous research findings.

These intervention strategies are central to our study, allowing us to evaluate and compare their effectiveness in controlling disease spread. Specifically, the following three intervention strategies were investigated in terms of their effectiveness. Mass Quarantine (MQ): quarantining 10% of randomly chosen agents from S and E statuses; Isolation: isolating all agents from I status; and Isolation combined with Acquaintance Quarantine (AQ + Isolation): isolating all confirmed cases (individuals from I status) and quarantining 50% of randomly chosen agents from all agents who had effective contact with infected individuals. The intervention began on day 10 in each simulation run. Owing to the stochastic nature of agent-based models, all simulations were run 1,000 times, and their epidemic outputs were obtained.

TABLE 3 Model parameters and their values.

Parameter	Description	Value	References
S	Susceptible individual	–	–
E	Exposed individual	–	–
I	Infected individual	–	–
R	Recovered individual	–	–
N	Total population size	31,091	–
T	Total simulation time	100 day	–
β_0	Background transmission constant	0.002	Estimated
n	A number of infected neighbors	–	–
β	Transmission rate	$\beta = 1 - (1 - \beta_0)^n$	(42)
$1/\kappa$	Mean incubation period	8.7	(42)
σ_κ	Standard deviation of the incubation period	16	(42)
$1/\gamma$	Mean infectious period	21	(42)
σ_γ	Standard deviation of the infectious period	76	(42)

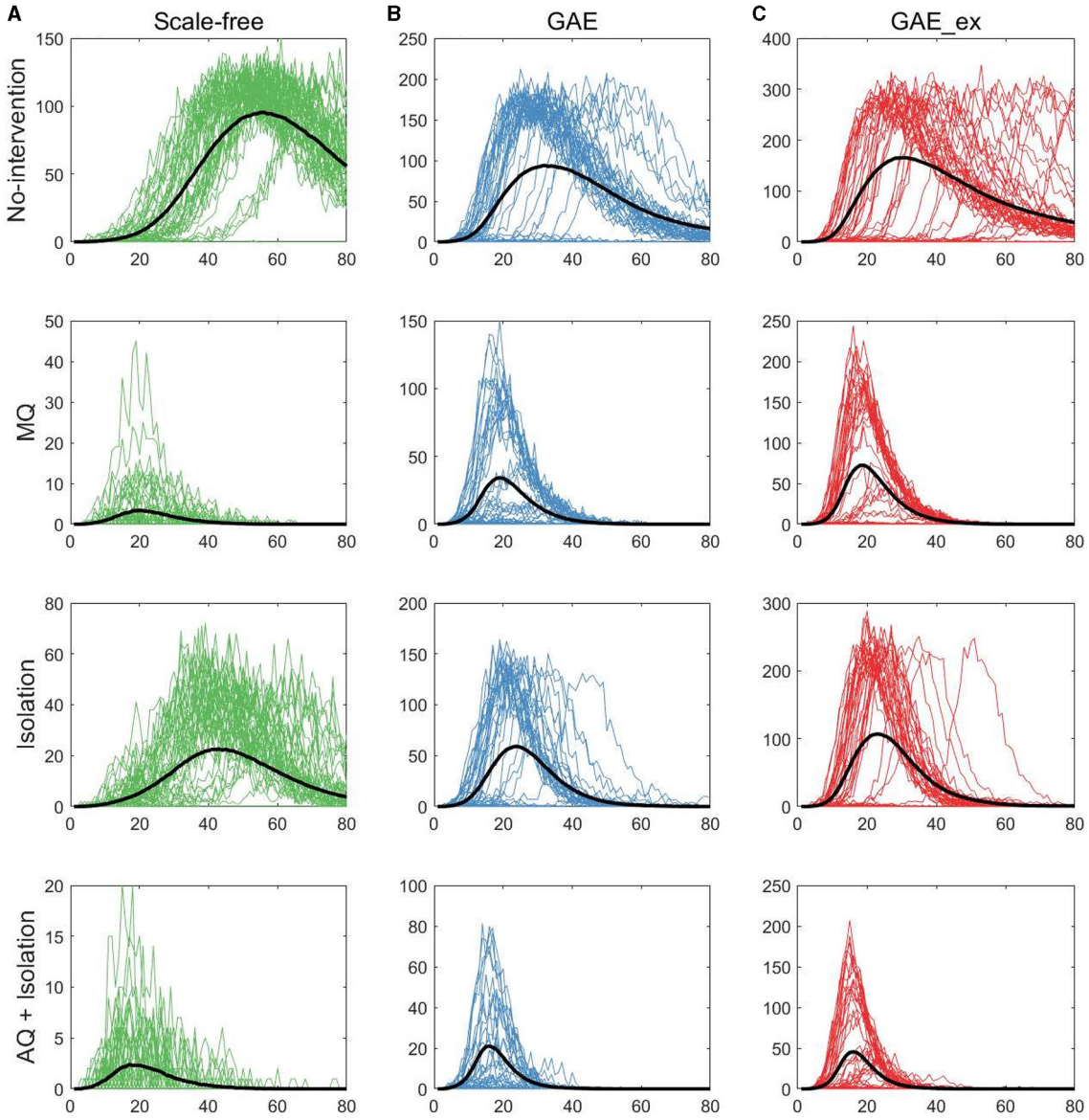

FIGURE 5
Daily incidences on three contact networks: **(A)** scale-free (SF), **(B)** GAE, and **(C)** GAE_ex [for each plot, 50 realizations of incidence are displayed with the mean (black curve). Each row shows the results for four distinct intervention strategies; top rows with a much larger peak size are the results with no intervention].

3 Results

3.1 The impacts of intervention strategies and different network structure

In this section, we investigate the impact of different network structures and intervention strategies on epidemic outputs. First, we present epidemic curves of MERS-CoV transmission dynamics: daily incidence in Figure 5 and cumulative incidence in Figure 6. The columns of the figures show the dynamics of three network structures: (a) SF (green), (b) GAE (blue), and (c) GAE_ex (red). Meanwhile, the rows show the dynamics for four intervention scenarios: No intervention, MQ, Isolation, and AQ + Isolation. Owing to the stochastic nature of our agent-based epidemic model, each result displays 50 realizations with the mean (black curve).

The first row of Figure 5 shows the impact of different network structures in the absence of interventions; it indicates that the outbreak gets worse in the order of SF, GAE, and GAE_ex, the peak size gets larger in that order (around 100, 200, and 300, respectively), and the peak time occurs earlier in GAE and GAE_ex (around day 30) than in SF (around day 60), attributable to the shortest path length (see Figure 3B). In addition, larger variances in the epidemic curve are observed in GAE (blue) and GAE_ex (red) than in SF (green), attributable to the larger variance in degree distributions and their clustering coefficients (Figures 3A, C).

Next, the impact of the three intervention strategies is shown from the second to the last rows in Figure 5, which indicates that

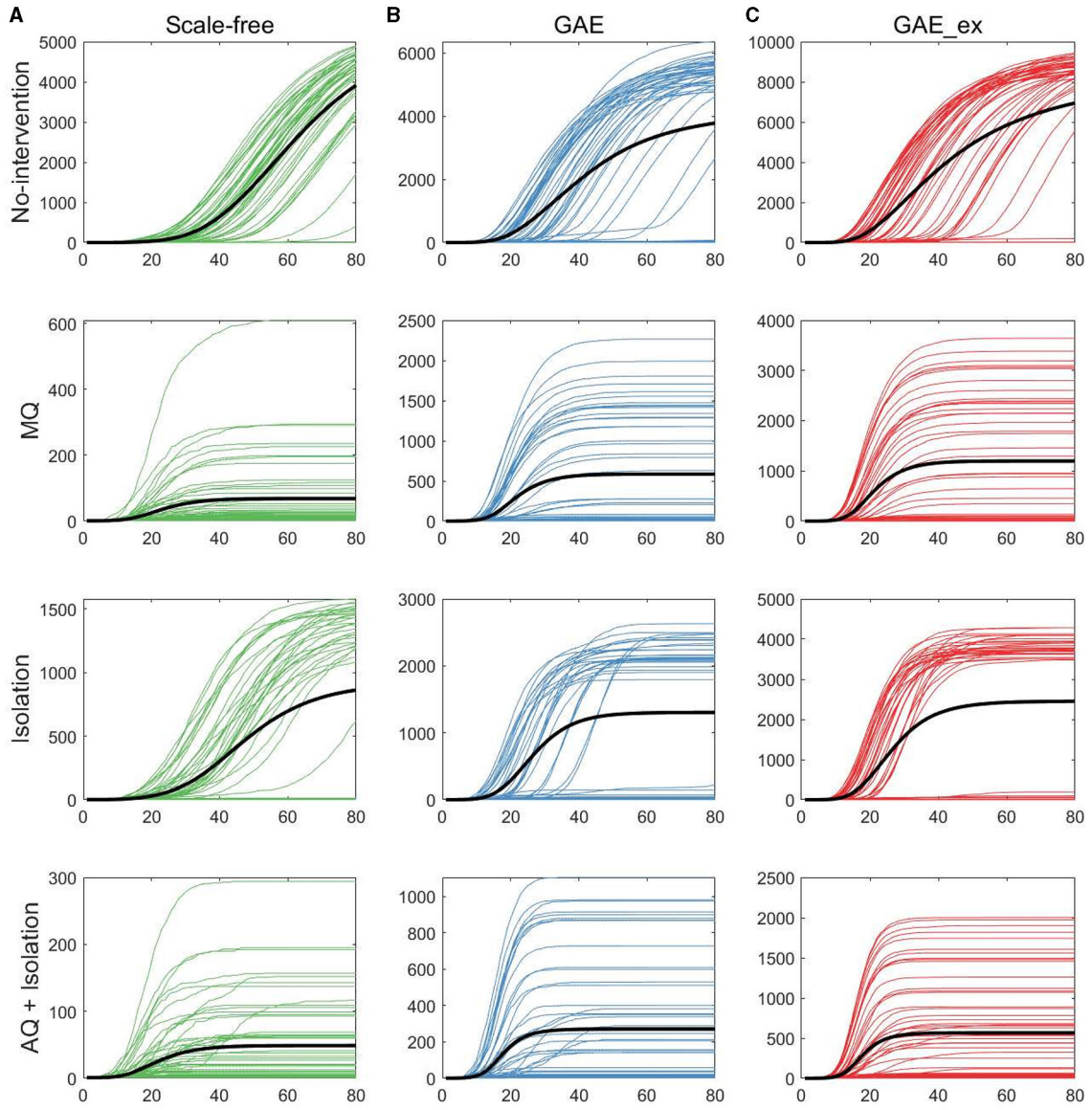

FIGURE 6
Cumulative incidences on three contact networks: **(A)** scale-free (SF), **(B)** GAE, and **(C)** GAE_ex [for each plot, 50 realizations of incidence are displayed with the mean (black curve). Each row shows the results for four distinct intervention strategies; top rows with a much larger peak size are the results with no intervention].

the daily incidence gets larger in the order of SF, GAE, and GAE_ex for all intervention strategies. In addition, from the second row, MQ reduced incidence in SF much more dramatically than in GAE and GAE_ex, attributable to the average and variance of clustering coefficients being much smaller in SF than in GAE and GAE_ex [recall that the average clustering coefficient is 0.1037, 0.4825, and 0.7275 for SF, GAE, and GAE_ex, respectively (Table 1), and see variances in Figure 3C]. Further, these results suggest that the most effective intervention is AQ + Isolation in all three network structures (see the bottom panels), with the earliest peak time and smallest peak size in all three networks. Besides, for AQ + Isolation, the most dramatic reduction of incidence was observed in SF than in GAE and GAE_ex. Isolation is the least effective in all network structures because only infected individuals are isolated without any contact-tracing and quarantine. The effectiveness of the three interventions is further described in Figure 7.

The results in Figure 6 show that, as in daily incidence in Figure 5, the variances of the cumulative incidences were larger in GAE and GAE_ex than in SF regardless of the intervention strategy; the 50 realization curves are less centered around the black mean curve in GAE and GAE_ex than in SF. Notably, for Isolation, the 50 realization curves generated bimodal results in GAE and GAE_ex: the black mean curves are placed between high and low cumulative incidences. These detailed epidemic outputs are further explored in the next subsection.

Finally, the incidence dynamics are compared with actual MERS-CoV incidence data and the number of quarantined individuals in the simulations. Figure 7 shows the averaged

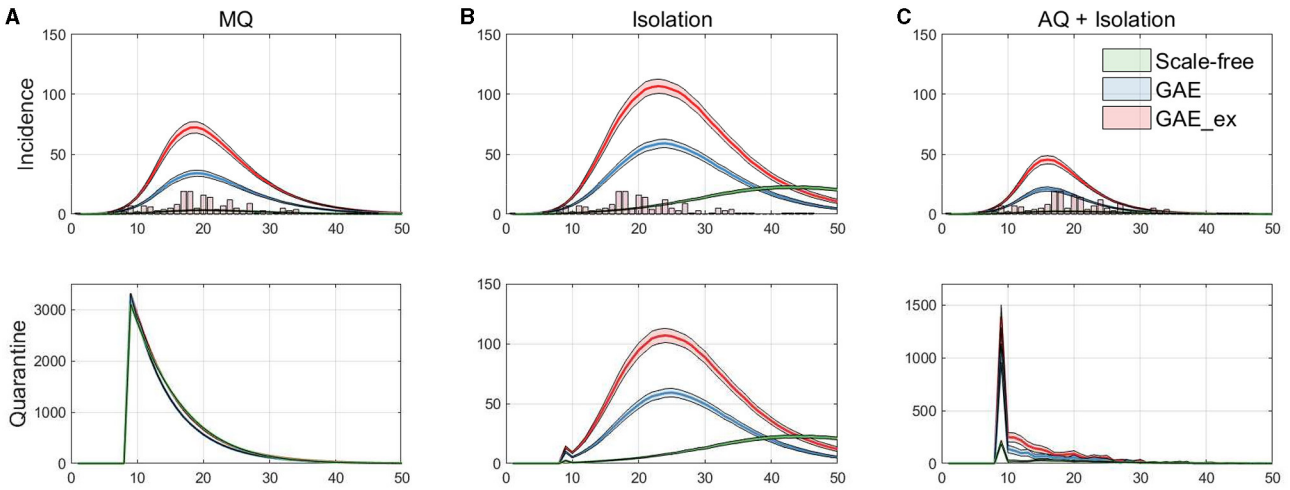

FIGURE 7
Daily incidences displayed with MERS-CoV data in vertical bar (top row), and the corresponding daily quarantined individuals (bottom row). **(A)** Mass Quarantine (MQ), **(B)** Isolation, and **(C)** Acquaintance Quarantine (AQ) + Isolation.

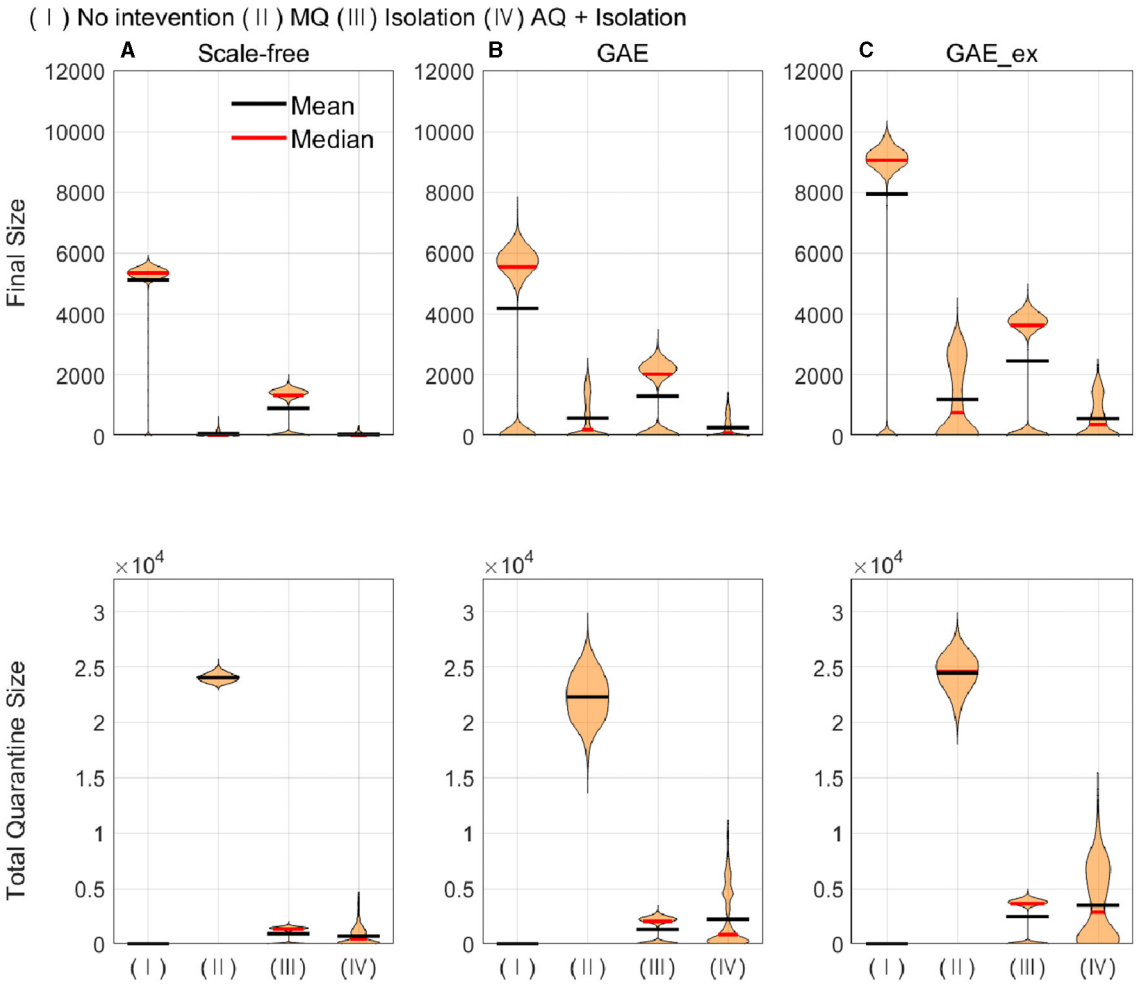

FIGURE 8
Cumulative infected (top row) and quarantined individuals (bottom row) under different intervention scenarios and on different networks (for each intervention, the result of 1,000 runs is shown). **(A)** SF, **(B)** GAE, and **(C)** GAE_ex.

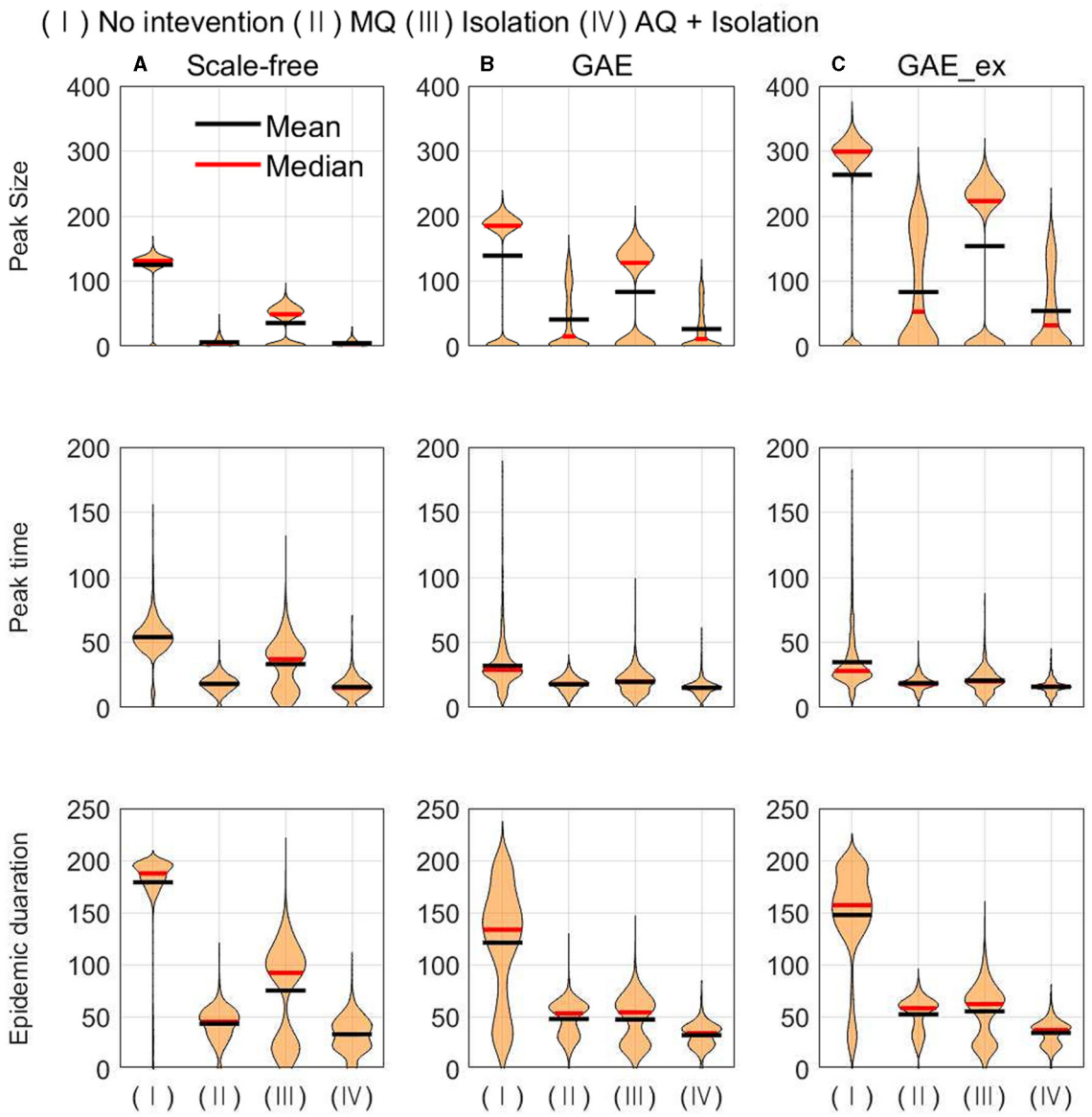

FIGURE 9
Peak size (top row), peak time (middle row), and epidemic duration (bottom row) under different intervention scenarios and on different networks (for each intervention, the result of 1,000 runs is shown). **(A)** SF, **(B)** GAE, and **(C)** GAE_ex.

dynamics (mean of 1,000 realizations) of incidences on the three networks with actual MERS-CoV incidence data (histogram) at the top panels and the number of quarantined individuals at the bottom panels. Each column in the figure shows the results for the MQ, Isolation, and AQ + Isolation intervention strategies. The results in the figure suggest that MQ requires the maximum level of quarantine at the beginning for all three networks. In addition, although a similar number of individuals are quarantined under all networks, MQ is the most effective strategy for SF than GAE and GAE_ex (see green curves). Obviously, AQ + Isolation is the most effective intervention strategy for incidence reduction in all three networks (see the epidemic curves in the top panel). This strategy combines contact-tracing with quarantine; thus, much fewer people than in the MQ intervention are quarantined but much fewer people are infected.

3.2 The impacts of three network on various epidemic outputs

In this subsection, the mean, median, and distributions of 1,000 simulation runs are summarized in terms of five epidemic outputs. The final size (cumulative incidence) and the total number of quarantined individuals for each network structure for different intervention strategies are presented in Figure 8. In addition, the peak size, peak time, and epidemic duration are summarized in Figure 9.

Figure 8 shows that the final size gets larger in the order of SF, GAE, and GAE_ex. Notably, the variances are smaller in SF than in GAE and GAE_ex. In addition, there are weak bi-modes in GAE and GAE_ex. For instance, for No intervention, SF shows mean and median of around 5,000, respectively, with a very small variance.

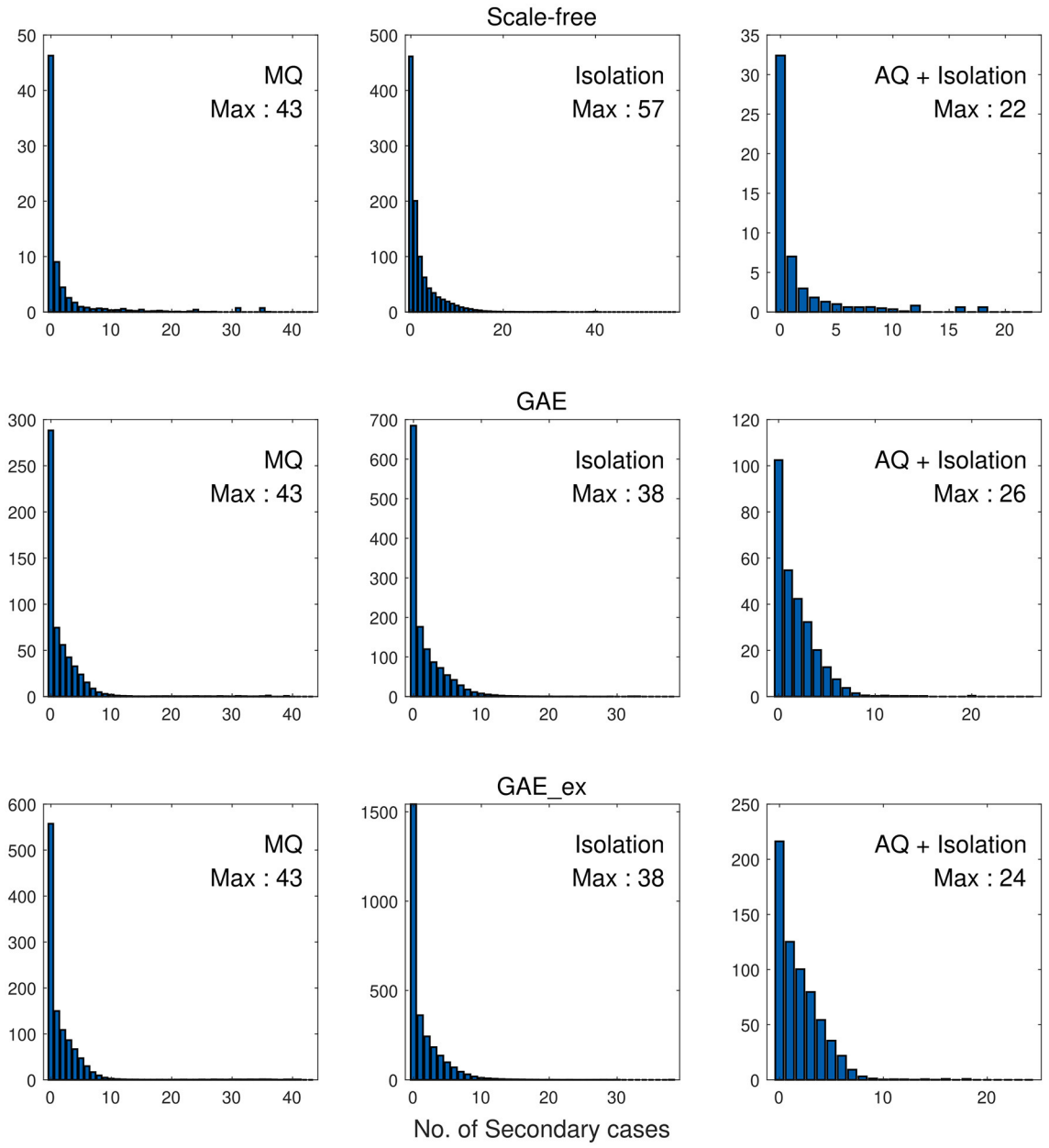

FIGURE 10
Distributions of secondary cases under different intervention scenarios and on different networks.

Meanwhile, GAE shows median and mean around 6,000 and 4,000, respectively (most of the results are around 6,000 and some are around 100), and GAE_ex shows median and mean around 9,000 and 8,000, respectively (most of the results are around 9,000 and some are around 100). The impacts of the three intervention strategies are distinct on the final size distributions. Again, there is a very small variance in SF and weak bi-modes in GAE and GAE_ex, which can be explained by the distributions of index cases and clustering coefficients (Figure 3D).

Comparing the effectiveness of MQ and AQ + Isolation, both intervention strategies dramatically reduced the final size in SF (the first panel at the top row of Figure 8). However, the total quarantine size significantly differed; MQ quarantined around 25,000 individuals, whereas AQ + Isolation quarantined only 2,000 individuals (the first panel at the bottom row of Figure 8). Thus, AQ + Isolation can be a more effective strategy than MQ in SF. This is also the case in GAE and GAE_ex because similar patterns are observed. Although the means of cumulative quarantined individuals are similar in all three networks, the overall effectiveness of SF and GAE are quite different.

In Figure 9, the impacts of intervention strategies on different networks are compared in terms of the peak size, peak time, and epidemic duration. The results in the first row show that the peak size is the largest under No intervention and the second largest for Isolation in all networks. AQ + Isolation shows the smallest peak size in all networks. Peak size manifested a small variance

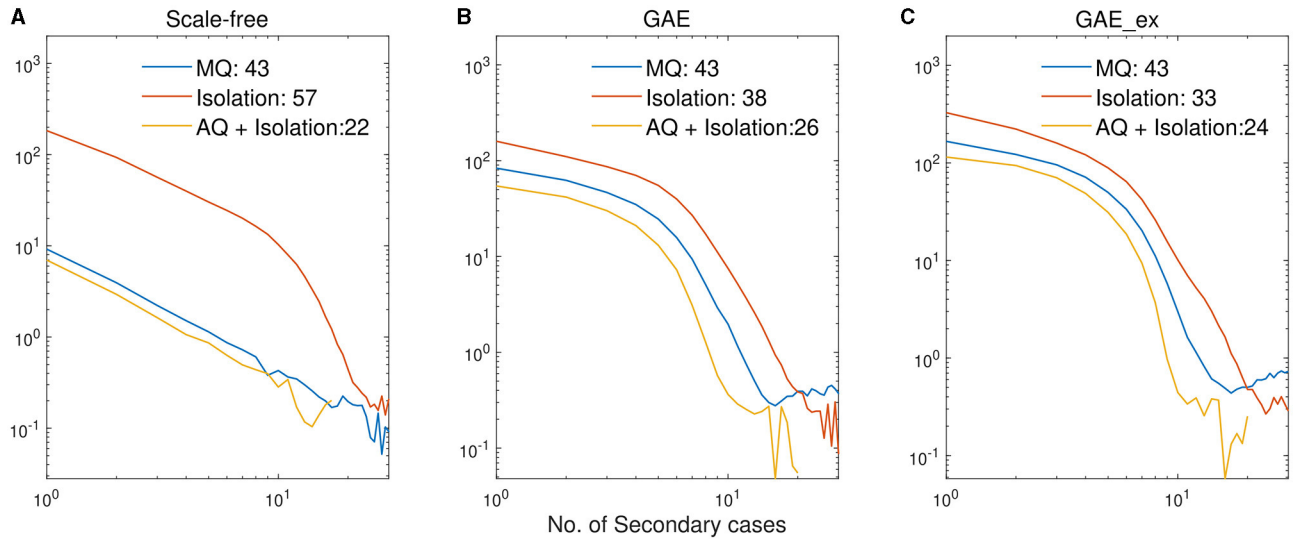

FIGURE 11
Log-log plots of distributions of secondary cases in Figure 10. **(A)** SF, **(B)** GAE, and **(C)** GAE_ex.

in SF and weak bi-modes in GAE and GAE_ex, as the final size did in Figure 8; the mean and median are almost the same in SF, whereas they are quite different in GAE and GAE_ex. The results in the second row show that the mean and median of peak time distributions for all intervention strategies are very similar in GAE and GAE_ex. In addition, the mean, and median of SF are in the order of No intervention, Isolation, MQ, and AQ + Isolation, attributable to the shortest path (Figure 3B). The results in the third row suggest that the impacts of interventions are very different among networks. Under No intervention, outbreaks lasted about 180 days in SF with a very small variance. However, outbreaks lasted about 150 days in GAE and GAE_ex with very large variances. Notably, epidemic duration is longer for Isolation than for the other two intervention strategies in SF.

Finally, we investigate the impacts of the three intervention strategies on the distributions of secondary cases in each network structure. The mean distribution of 1,000 simulation runs is presented in Figure 10. An outbreak can be considered a super-spreading event when its distribution of secondary cases exhibits a large degree of heterogeneity. Each panel illustrates the type of intervention strategy and the maximum number of secondary cases by a single infected individual (denoted by Max). In fact, during the MERS-CoV outbreak in South Korea in 2015, a single patient infected 79 other individuals, referred to as a super-spreader (42). The results in Figure 10 suggest that Isolation is the least effective strategy to prevent super-spreading events on all networks. For instance, Max = 57 in SF, which is worse than Max = 38 in GAE and GAE_ex. AQ + Isolation showed the lowest level of heterogeneity in the secondary cases, with Max of 22, 26, and 24 in SF, GAE, and GAE_ex, respectively. Furthermore, Figure 11 provides a log–log representation of Figure 10, allowing for a comparison of the secondary cases for three interventions across various network configurations. This analysis verifies that Isolation alone (depicted by the red curves) consistently yields the highest values, signifying its limited effectiveness, while AQ + Isolation (indicated by the yellow curves) consistently exhibits the lowest values, highlighting its superior effectiveness across all network structures.

4 Discussions

We have employed an innovative graph autoencoder technique to recreate the contact network using real-world contact-tracing data. This marks the first utilization of such an approach for reconstructing networks based on contact-tracing data derived from the 2015 MERS-CoV outbreak in South Korea. We conducted a comparative analysis between the reconstructed networks and a scale-free network (SF) concerning the effectiveness of various intervention strategies. Furthermore, we explored the influence of network structure on epidemic outcomes, including peak size, final size, incidence, and cumulative incidence. The study's findings revealed that the severity of outbreaks followed the order of SF, GAE, and GAE_ex. Moreover, GAE and GAE_ex exhibited higher variances in both incidence and cumulative incidence compared to SF.

We also evaluated the impact of different intervention strategies, such as mass quarantine (MQ) and acquaintance quarantine (AQ) + isolation, on epidemic outputs in simulations on different networks. First, the results showed that MQ was found to be an equally effective strategy as AQ + isolation in the SF network. However, the study found that although the average shortest paths were similar in the three networks, the SF network was less influenced by hub nodes and had a wider distribution of shortest paths. We found that the effectiveness of MQ and AQ+Isolation in the SF network was excessively good, which is attributed to the low clustering coefficient of SF. The low clustering coefficient means that the SF network is less dense, which makes it more sensitive to interventions like MQ and AQ+Isolation.

Moreover, isolation was the least effective strategy in SF. This is due to the shortest path length and isolation of confirmed cases only

which do not take pre-symptomatic cases into account. The Scale-free network is a type of network structure that is often used to model the spread of infectious diseases with a long tail distribution. This means that a small number of individuals (referred to as "super-spreaders") are responsible for a large proportion of transmission. However, it has been found that this structure can lead to over estimations of the impact of interventions, as they may not be able to effectively target the super-spreaders.

It is important to note that the peak time of the outbreaks in the GAE and GAE_ex networks did not differ significantly when comparing the results of no intervention to those of the various intervention strategies. This is because the high clustering coefficients in GAE and GAE_ex lead to similar peak times. This is because nodes with low clustering coefficients do not typically experience outbreaks, while outbreaks are likely to occur in nodes with high clustering coefficients. Thus, outbreaks in GAE and GAE_ex spread uniformly throughout the network, which is different from the SF network, where the clustering coefficients and shortest path lengths are different. This trend is due to the unique characteristics of the GAE and GAE_ex networks, which are more similar to the contact networks found in hospital settings, specifically, emergency rooms in South Korea, and have higher clustering coefficients which implies higher density in most emergency rooms of hospitals in South Korea (55).

This study has several limitations worth noting. Firstly, it does not comprehensively explore the influence of index cases on the outbreak of the epidemic. In our simulations, index cases were randomly chosen from nodes with a sufficient number of connections. However, selecting super-spreaders identified in the contact-tracing data as index cases might produce different outcomes. Additionally, we refrained from conducting comparisons with other reconstruction methods. Analyzing our graph auto encoder approach alongside alternative link prediction models like Exponential Random Graph Model (ERGM) (56) and Bayesian statistical models (57) might have provided valuable insights into the effectiveness of our model. Furthermore, our study highlights a high clustering coefficient in the reconstructed network due to the concentrated distribution of emergency rooms in South Korea. This observation may not be applicable to other regions. Additionally, since our study utilized contact-tracing data from the 2015 MERS-CoV outbreak in South Korea, the generalizability of our findings is limited. Utilizing contact-tracing data from other outbreaks could lead to more universally applicable results. Moreover, future research could explore the impact of population mobility, as it is widely recognized that mobility plays a significant role in disease transmission (58). Incorporating mobility into simulation models could offer valuable insights.

5 Conclusions

We employed an innovative graph autoencoder technique to reconstruct the contact network using real-world contact-tracing data. This marks the first instance of utilizing such an approach to reconstruct networks based on contact-tracing data from the 2015 MERS-CoV outbreak in South Korea, which were subsequently employed in epidemic simulations. Our investigation focused on five key epidemic outcomes, conducting a comparative analysis of various network structures and intervention strategies. Our findings underscore the significant impact of network structures on epidemic outcomes, emphasizing the variable effectiveness of intervention strategies across different contexts. These findings carry significant implications for tailoring precise intervention measures in response to disease outbreaks.

Our results reveal substantial differences in the impacts of various network structures on epidemic outputs: outbreaks were more extensive in the scale-free network, a widely used theoretical model for epidemic simulation, compared to the reconstructed network generated by the link prediction method. Consequently, the effectiveness of intervention strategies can vary depending on the network structure: intervention measures on the reconstructed network were found to be less effective than those on the scale-free network. These results suggest a potential overestimation of intervention impact in scale-free networks, while our reconstructed network offers a more realistic assessment of intervention effectiveness. In this study, we opted for a scale-free network structure due to its suitability for meaningful comparisons compared to other models such as random networks. However, it is crucial to acknowledge the limitations associated with scale-free networks, as discussed earlier. Thus, to account for potential biases in our analysis, we emphasize the importance of recognizing the increased risk of overestimation when utilizing scale-free networks, as their structure may influence intervention outcomes. Therefore, the consideration of networks constructed through alternative methods, such as small-world networks or spatial networks, may introduce variability in the results (1, 14).

The utilization of networks reconstructed through link prediction methods proves to be a valuable asset for conducting epidemic simulations. In the specific context of the 2015 MERS-CoV outbreak in South Korea, this study leveraged this approach to reconstruct the contact-tracing network, aiming to evaluate the effectiveness of intervention strategies. We anticipate that this innovative methodology will inspire future endeavors aimed at enhancing simulation environments, providing valuable insights to guide the decisions of public health authorities. Moreover, it has the potential to stimulate further research to enhance the realism of simulation environments through data-driven network reconstruction methods.

Data availability statement

The datasets presented in this article are not readily available because, this data was provided by the Korean Disease Control and Prevention Agency and is not publicly available. Therefore, this data should not be disclosed for purposes other than research. Requests to access the datasets should be directed to: https://www.kdca.go.kr/.

Author contributions

EK: Conceptualization, Data curation, Formal analysis, Funding acquisition, Investigation, Methodology, Project administration, Resources, Software, Supervision, Validation, Visualization, Writing—original draft, Writing—review &

editing. YK: Conceptualization, Data curation, Formal analysis, Funding acquisition, Investigation, Methodology, Project administration, Resources, Software, Supervision, Validation, Visualization, Writing—original draft, Writing—review & editing. HJ: Conceptualization, Data curation, Formal analysis, Funding acquisition, Investigation, Methodology, Project administration, Resources, Software, Supervision, Validation, Visualization, Writing—original draft, Writing—review & editing. YL: Conceptualization, Data curation, Formal analysis, Funding acquisition, Investigation, Methodology, Project administration, Resources, Software, Supervision, Validation, Visualization, Writing—original draft, Writing—review & editing. HL: Writing—original draft, Writing—review & editing. SL: Conceptualization, Data curation, Formal analysis, Funding acquisition, Investigation, Methodology, Project administration, Resources, Software, Supervision, Validation, Visualization, Writing—original draft, Writing—review & editing.

Funding

The author(s) declare that financial support was received for the research, authorship, and/or publication of this article. This work was supported by the National Research Foundation of Korea (NRF) grant funded by the Korea Government (MSIT; Nos. 2022R1A5A1033624 and 2021R1A2B5B0100261113), Basic Science Research Program through the NRF funded by the Ministry of Education (No. 2019R1A6A1A11051177). This work was also supported by the Basic Science Research Program through the National Research Foundation of Korea (NRF) funded by the Ministry of Education of the Government of the Republic of Korea (2021R1A2C1008360).

Conflict of interest

The authors declare that the research was conducted in the absence of any commercial or financial relationships that could be construed as a potential conflict of interest.

Publisher's note

All claims expressed in this article are solely those of the authors and do not necessarily represent those of their affiliated organizations, or those of the publisher, the editors and the reviewers. Any product that may be evaluated in this article, or claim that may be made by its manufacturer, is not guaranteed or endorsed by the publisher.

References

1. Keeling MJ, Eames KT. Networks and epidemic models. *J Royal Soc Interf.* (2005) 2:295–307. doi: 10.1098/rsif.2005.0051

2. Britton T. Epidemic models on social networks—with inference. *Stat Neerland.* (2020) 74:222–41. doi: 10.1111/stan.12203

3. Yang Z, Song J, Gao S, Wang H, Du Y, Lin Q. Contact network analysis of COVID-19 in tourist areas—based on 333 confirmed cases in China. *PLoS ONE* (2021) 16:e0261335. doi: 10.1371/journal.pone.0261335

4. Salathé M, Kazandjieva M, Lee JW, Levis P, Feldman MW, Jones JH. A high-resolution human contact network for infectious disease transmission. *Proc Natl Acad Sci USA.* (2010) 107:22020–5. doi: 10.1073/pnas.1009094108

5. Danon L, Ford AP, House T, Jewell CP, Keeling MJ, Roberts GO, et al. Networks and the epidemiology of infectious disease. *Interdiscipl Perspect Infect Dis.* (2011) 2011:284909. doi: 10.1155/2011/284909

6. Shao Q, Jia M. Influences on influenza transmission within terminal based on hierarchical structure of personal contact network. *BMC Publ Health.* (2015) 15:1–11. doi: 10.1186/s12889-015-1536-5

7. Machens A, Gesualdo F, Rizzo C, Tozzi AE, Barrat A, Cattuto C. An infectious disease model on empirical networks of human contact: bridging the gap between dynamic network data and contact matrices. *BMC Infect Dis.* (2013) 13:1–15. doi: 10.1186/1471-2334-13-185

8. Perisic A, Bauch CT. Social contact networks and disease eradicability under voluntary vaccination. *PLoS Comput Biol.* (2009) 5:e1000280. doi: 10.1371/journal.pcbi.1000280

9. Klinkenberg D, Fraser C, Heesterbeek H. The effectiveness of contact tracing in emerging epidemics. *PLoS ONE.* (2006) 1:e12. doi: 10.1371/journal.pone.0000012

10. Bartlett J, Plank MJ. Epidemic dynamics on random and scale-free networks. *ANZIAM J.* (2012) 54:3–22. doi: 10.1017/S1446181112000302

11. Shang Y. SEIR epidemic dynamics in random networks. *Int Scholar Res Not.* (2013) 2013:345618. doi: 10.5402/2013/345618

12. Masuda N, Konno N, Aihara K. Transmission of severe acute respiratory syndrome in dynamical small-world networks. *Phys Rev E.* (2004) 69:e031917. doi: 10.1103/PhysRevE.69.031917

13. Liu M, Li D, Qin P, Liu C, Wang H, Wang F. Epidemics in interconnected small-world networks. *PLoS ONE.* (2015) 10:e0120701. doi: 10.1371/journal.pone.0120701

14. Pastor-Satorras R, Vespignani A. Epidemic spreading in scale-free networks. *Phys Rev Lett.* (2001) 86:3200. doi: 10.1103/PhysRevLett.86.3200

15. Small M, Tse CK. Small world and scale free model of transmission of SARS. *Int J Bifurcat Chaos.* (2005) 15:1745–55. doi: 10.1142/S0218127405012776

16. Eames K, Bansal S, Frost S, Riley S. Six challenges in measuring contact networks for use in modelling. *Epidemics.* (2015) 10:72–7. doi: 10.1016/j.epidem.2014.08.006

17. VanderWaal K, Enns EA, Picasso C, Packer C, Craft ME. Evaluating empirical contact networks as potential transmission pathways for infectious diseases. *J Royal Soc Interf.* (2016) 13:20160166. doi: 10.1098/rsif.2016.0166

18. Cimini G, Mastrandrea R, Squartini T. *Reconstructing Networks.* Cambridge: Cambridge University Press (2021).

19. Guimerà R, Sales-Pardo M. Missing and spurious interactions and the reconstruction of complex networks. *Proc Natl Acad Sci USA.* (2009) 106:22073–8. doi: 10.1073/pnas.0908366106

20. Li RD, Guo Q, Ma HT, Liu JG. Network reconstruction of social networks based on the public information. *Chaos.* (2021) 31:e033123. doi: 10.1063/5.0038816

21. Kumar A, Singh SS, Singh K, Biswas B. Link prediction techniques, applications, and performance: a survey. *Phys A.* (2020) 553:124289. doi: 10.1016/j.physa.2020.124289

22. Mutlu EC, Oghaz T, Rajabi A, Garibay I. Review on learning and extracting graph features for link prediction. *Machine Learn Knowl Extr.* (2020) 2:672–704. doi: 10.3390/make2040036

23. Lü L, Zhou T. Link prediction in complex networks: a survey. *Phys A.* (2011) 390:1150–70. doi: 10.1016/j.physa.2010.11.027

24. Airoldi EM, Blei D, Fienberg S, Xing E. Mixed membership stochastic blockmodels. *Adv Neural Inform Process Syst.* (2008) 21. Available online at: http://jmlr.csail.mit.edu/papers/v9/airoldi08a (accessed May 11, 2024).

25. Perozzi B, Al-Rfou R, Skiena S. Deepwalk: online learning of social representations. In: *Proceedings of the 20th ACM SIGKDD International Conference on Knowledge Discovery and Data Mining.* Association for Computing Machinery (2014). p. 701–10. doi: 10.1145/2623330.2623732

26. Grover A, Leskovec J. node2vec: scalable feature learning for networks. In: *Proceedings of the 22nd ACM SIGKDD International Conference on Knowledge Discovery and Data Mining.* Association for Computing Machinery (2016). p. 855–64. doi: 10.1145/2939672.2939754

27. Tang J, Qu M, Wang M, Zhang M, Yan J, Mei Q. Line: large-scale information network embedding. In: *Proceedings of the 24th International Conference on World WideWeb*. International World Wide Web Conferences Steering Committee (2015). p. 1067–77. doi: 10.1145/2736277.2741093

28. Gori M, Monfardini G, Scarselli F. A new model for learning in graph domains. In: *Proceedings. 2005 IEEE International Joint Conference on Neural Networks, Vol. 2*. IEEE (2005). p. 729–34. doi: 10.1109/IJCNN.2005.1555942

29. Bruna J, ZarembaW, SzlamA, LeCun Y. Spectral networks and locally connected networks on graphs. *arXiv [preprint]*. (2013). Available online at: https://arxiv.org/abs/1312.6203 (accessed May 11, 2024).

30. Henaff M, Bruna J, LeCun Y. Deep convolutional networks on graph-structured data. In: *2nd International Conference on Learning Representations, ICLR 2014, Banff, AB, Canada, April 14-16, 2014, Conference Track Proceedings*. Banff, AB (2014).

31. Stokes JM, Yang K, Swanson K, Jin W, Cubillos-Ruiz A, Donghia NM, et al. A deep learning approach to antibiotic discovery. *Cell*. (2020) 180:688–702. doi: 10.1016/j.cell.2020.01.021

32. Monti F, Frasca F, Eynard D, Mannion D, Bronstein MM. Fake news detection on social media using geometric deep learning. *arXiv [preprint]*. (2019). Available online at: https://arxiv.org/abs/1902.06673 (accessed May 11, 2024).

33. Lange O, Perez L. *Traffic Prediction With Advanced Graph Neural Networks*. DeepMind Research Blog Post (2020). Available online at: https://deepmindcom/blog/article/traffic-prediction-with-advanced-graph-neural-networks (accessed May 11, 2024).

34. Eksombatchai C, Jindal P, Liu JZ, Liu Y, Sharma R, Sugnet C, et al. Pixie: a system for recommending 3+ billion items to 200+ million users in real-time. In: *Proceedings of the 2018 World Wide Web Conference*. International World Wide Web Conferences Steering Committee (2018). p. 1775–84. doi: 10.1145/3178876.3186183

35. Chun BC. Understanding and modeling the super-spreading events of the Middle East respiratory syndrome outbreak in Korea. *Infect Chemother*. (2016) 48:147–9. doi: 10.3947/ic.2016.48.2.147

36. Hui DS. Super-spreading events of MERS-CoV infection. *Lancet*. (2016) 388:942–3. doi: 10.1016/S0140-6736(16)30828-5

37. Kucharski A, Althaus CL. The role of superspreading in Middle East respiratory syndrome coronavirus (MERS-CoV) transmission. *Eurosurveillance*. (2015) 20:21167. doi: 10.2807/1560-7917.ES2015.20.25.21167

38. Ki M. 2015 MERS outbreak in Korea: hospital-to-hospital transmission. *Epidemiol Health*. (2015) 37:e2015033. doi: 10.4178/epih/e2015033

39. Nishiura H, Endo A, Saitoh M, Kinoshita R, Ueno R, Nakaoka S, et al. Identifying determinants of heterogeneous transmission dynamics of the Middle East respiratory syndrome (MERS) outbreak in the Republic of Korea, 2015: a retrospective epidemiological analysis. *Br Med J Open*. (2016) 6:e009936. doi: 10.1136/bmjopen-2015-009936

40. Cho SY, Kang JM, Ha YE, Park GE, Lee JY, Ko JH, et al. MERS-CoV outbreak following a single patient exposure in an emergency room in South Korea: an epidemiological outbreak study. *Lancet*. (2016) 388:994–1001. doi: 10.1016/S0140-6736(16)30623-7

41. Kang M, Song T, Zhong H, Hou J, Wang J, Li J, et al. Contact tracing for imported case of Middle East respiratory syndrome, China, 2015. *Emerg Infect Dis*. (2016) 22:1644. doi: 10.3201/eid2209.152116

42. Kim Y, Ryu H, Lee S. Effectiveness of intervention strategies on MERS-CoV transmission dynamics in South Korea, 2015: simulations on the network based on the real-world contact data. *Int J Environ Res Publ Health*. (2021) 18:3530. doi: 10.3390/ijerph18073530

43. Kim S, Yang T, Jeong Y, Park J, Lee K, Kim K, et al. Middle East respiratory syndrome coronavirus outbreak in the Republic of Korea, 2015. *Osong Publ Health Res Perspect*. (2016) 6:269–78. doi: 10.1016/j.phrp.2015.08.006

44. Kipf TN, Welling M. Variational graph auto-encoders. In: *Paper at Bayesian Deep Learning (NIPS Workshops 2016) Dec 10, 2016*. Barcelona, Spain (2016).

45. Cordasco G, Gargano L. Community detection via semi-synchronous label propagation algorithms. In: *2010 IEEE International Workshop on: Business Applications of Social Network Analysis (BASNA)*. Bangalore: IEEE (2010). p. 1–8.

46. Barabási AL, Bonabeau E. Scale-free networks. *Sci Am*. (2003) 288:60–9. doi: 10.1038/scientificamerican0503-60

47. Newman M, Takei H, Klokkevold P, Carranza F. *Newman and Carranza's Clinical Periodontology*. Elsevier Health Sciences (2018).

48. Germann TC, Kadau K, Longini Jr IM, Macken CA. Mitigation strategies for pandemic influenza in the United States. *Proc Natl Acad Sci USA*. (2006) 103:5935–40. doi: 10.1073/pnas.0601266103

49. Perlroth DJ, Glass RJ, Davey VJ, Cannon D, Garber AM, Owens DK. Health outcomes and costs of community mitigation strategies for an influenza pandemic in the United States. *Clin Infect Dis*. (2010) 50:165–74. doi: 10.1086/649867

50. DS B. Individual-based computational modeling of smallpox epidemic control strategies. *Soc Acad Emerg Med*. (2006) 13:114–9. Available online at: https://cir.nii.ac.jp/crid/1573387450792859520 (accessed May 11, 2024).

51. Glass RJ, Beyeler WE, Min HSJ, Davey VJ, Glass LM. *Effective Robust Design of Community Mitigation for Pandemic Influenza: Effective Robust Design of Community Mitigation for Pandemic Influenza: A Networked Agent-based Modeling Study*. Albuquerque, NM: Sandia National Lab (SNL-NM) (2008).

52. Glass RJ, Glass LM, Beyeler WE, Min HJ. Targeted social distancing designs for pandemic influenza. *Emerg Infect Dis*. (2006) 12:1671. doi: 10.3201/eid1211.060255

53. Halloran ME, Ferguson NM, Eubank S, Longini Jr IM, Cummings DA, Lewis B, et al. Modeling targeted layered containment of an influenza pandemic in the United States. *Proc Natl Acad Sci USA*. (2008) 105:4639–44. doi: 10.1073/pnas.0706849105

54. Kelso JK, Halder N, Postma MJ, Milne GJ. Economic analysis of pandemic influenza mitigation strategies for five pandemic severity categories. *BMC Public Health*. (2013) 13:1–17. doi: 10.1186/1471-2458-13-211

55. Choe S, Kim HS, Lee S. Exploration of superspreading events in 2015 MERS-CoV outbreak in Korea by branching process models. *Int J Environ Res Publ Health*. (2020) 17:6137. doi: 10.3390/ijerph17176137

56. Jing F, Zhang Q, Tang W, Wang JZ, Lau JTf, Li X. Reconstructing the social network of HIV key populations from locally observed information. *AIDS Care*. (2023) 35:1243–50. doi: 10.1080/09540121.2021.1883514

57. Peixoto TP. Network reconstruction and community detection from dynamics. *Phys Rev Lett*. (2019) 123:128301. doi: 10.1103/PhysRevLett.123.128301

58. Jing F, Ye Y, Zhou Y, Zhou H, Xu Z, Lu Y, et al. Modelling the geographical spread of HIV among MSM in Guangdong, China: a metapopulation model considering the impact of pre-exposure prophylaxis. *Philos Trans Royal Soc A*. (2022) 380:20210126. doi: 10.1098/rsta.2021.0126

frontiers | Frontiers in Public Health

TYPE Original Research
PUBLISHED 24 December 2024
DOI 10.3389/fpubh.2024.1440673

OPEN ACCESS

EDITED BY
José Tuells,
University of Alicante, Spain

REVIEWED BY
Maria Francesca Piazza,
University of Genoa, Italy
Raul Moragues,
University of Alicante, Spain

*CORRESPONDENCE
Sherrie Xie
✉ sherrie.xie@pennmedicine.upenn.edu

RECEIVED 29 May 2024
ACCEPTED 09 December 2024
PUBLISHED 24 December 2024

CITATION
Xie S, Rieders M, Changolkar S, Bhattacharya BB, Diaz EW, Levy MZ and Castillo-Neyra R (2024) Enhancing mass vaccination programs with queueing theory and spatial optimization.
Front. Public Health 12:1440673.
doi: 10.3389/fpubh.2024.1440673

Enhancing mass vaccination programs with queueing theory and spatial optimization

Sherrie Xie[1]*, Maria Rieders[2], Srisa Changolkar[2], Bhaswar B. Bhattacharya[3], Elvis W. Diaz[4], Michael Z. Levy[1,4] and Ricardo Castillo-Neyra[1,4]

[1]Department of Biostatistics, Epidemiology, and Informatics, University of Pennsylvania, Philadelphia, PA, United States, [2]Department of Operations, Information, and Decisions, The Wharton School, University of Pennsylvania, Philadelphia, PA, United States, [3]Department of Statistics and Data Science, The Wharton School, University of Pennsylvania, Philadelphia, PA, United States, [4]Zoonotic Disease Research Lab, School of Public Health and Administration, Universidad Peruana Cayetano Heredia, Lima, Peru

Background: Mass vaccination is a cornerstone of public health emergency preparedness and response. However, injudicious placement of vaccination sites can lead to the formation of long waiting lines or *queues*, which discourages individuals from waiting to be vaccinated and may thus jeopardize the achievement of public health targets. Queueing theory offers a framework for modeling queue formation at vaccination sites and its effect on vaccine uptake.

Methods: We developed an algorithm that integrates queueing theory within a spatial optimization framework to optimize the placement of mass vaccination sites. The algorithm was built and tested using data from a mass dog rabies vaccination campaign in Arequipa, Peru. We compared expected vaccination coverage and losses from queueing (i.e., attrition) for sites optimized with our queue-conscious algorithm to those used in a previous vaccination campaign, as well as to sites obtained from a queue-naïve version of the same algorithm.

Results: Sites placed by the queue-conscious algorithm resulted in 9–32% less attrition and 11–12% higher vaccination coverage compared to previously used sites and 9–19% less attrition and 1–2% higher vaccination coverage compared to sites placed by the queue-naïve algorithm. Compared to the queue-naïve algorithm, the queue-conscious algorithm placed more sites in densely populated areas to offset high arrival volumes, thereby reducing losses due to excessive queueing. These results were not sensitive to misspecification of queueing parameters or relaxation of the constant arrival rate assumption.

Conclusion: One should consider losses from queueing to optimally place mass vaccination sites, even when empirically derived queueing parameters are not available. Due to the negative impacts of excessive wait times on participant satisfaction, reducing queueing attrition is also expected to yield downstream benefits and improve vaccination coverage in subsequent mass vaccination campaigns.

KEYWORDS

mass vaccination, One Health, queueing theory, rabies, spatial optimization, zoonosis, emergency preparedness, facility location

1 Introduction

The expeditious and equitable distribution of vaccinations and other health services is a cornerstone of public health emergency preparedness. *Queues*, or waiting lines, result from scarce or misallocated resources and volatility in traffic and service patterns; they can hinder the delivery of critical services and thereby jeopardize the achievement of public health targets. Not only can long queues deter people from waiting to receive essential health services, they can erode individuals' trust in health systems in certain contexts (1, 2) and can thus discourage participation in future programs. Long wait times was a major structural barrier to testing for COVID-19 during the early phase of the pandemic (3), and poor planning in some jurisdictions resulted in people waiting hours at some mass COVID-19 vaccination sites (4–6). Moreover, excessive queueing during pandemic emergencies also poses health risks, as long wait times may increase exposure to infectious pathogens (7), underscoring the need for safe and efficiently managed healthcare settings (8, 9).

Queueing theory is a branch of applied mathematics that offers a valuable framework for studying the behaviors and effects of waiting lines or queues (10). In brief, queueing models aim to capture how a customer population moves through a queueing system via a series of processes dictated by probabilistic rates: arriving at a service site, receiving service, waiting in a queue if the server is busy, or leaving the queue before service is rendered when waiting times exceed a customer's willingness to wait. Queueing theory is foundational to operations research and has been applied to many facets of healthcare operations, including the triage process in emergency care departments (11), staffing needs in operating rooms (12), hospital bed management (13, 14), and outpatient scheduling (15). Additionally, it has been applied to COVID-19 vaccine distribution and capacity planning (7, 16–20), as well as the containment of disease outbreaks, bioterrorist attacks, and other public health emergencies (21–24).

Mass dog vaccination campaigns (MDVCs) are held annually in Arequipa, Peru to address the re-emergence of dog rabies in the region (25); they have important parallels with early pandemic vaccination and testing programs in that success depends, in part, on strategically placing and optimally allocating resources across a discrete number of fixed-location facility sites (26). While the World Health Organization (WHO) and Pan American Health Organization (PAHO) recommend a minimum vaccination coverage of 70–80% sustained over multiple years to achieve control and eventual elimination of rabies, the MDVCs in Arequipa, which have relied on convenient or *ad hoc* placement of fixed-location vaccination sites, have continually fallen short of this goal (27, 28).

We have previously developed a data-driven strategy to optimize the placement of fixed-location MDVC sites and found that spatially optimized vaccination sites improves both overall vaccination coverage and spatial evenness of coverage (28). However, optimization that addresses spatial accessibility without considering queueing is likely to result in an uneven volume of arrivals across facility sites, which may result in long waiting lines (28). Here, we incorporate queueing theory into our existing spatial optimization framework to improve dog rabies vaccine uptake by accounting for both the spatial accessibility of MDVC sites and losses resulting from dog owners who refuse to wait for service in the face of excessive queue lengths (i.e., *queueing attrition*). We compare the performance of our queue-conscious algorithm to the queue-naïve algorithm in terms of expected vaccination coverage and queueing attrition and evaluate the sensitivity of our results to misspecification of queueing parameters and the assumption of a constant arrival rate within our queueing model.

2 Materials and methods

2.1 A queueing model for MDVCs

We modeled queueing, vaccination, and attrition at each MDVC vaccination site according to an M/M/1 system with first-in-first-out (FIFO) service (Figure 1). The M/M/1 system is a widely used queueing model for single server systems and assumes that customer arrivals occur according to a Poisson process, and job service times are independent and identically distributed (iid) exponential random variables that are independent of the arrival process and queue length. Applied to MDVCs, the M/M/1 queueing model assumes that dogs arrive with their owners to a vaccination site according to a Poisson process with arrival rate λ, meaning that the interarrival times are iid and follow an exponential distribution with parameter λ. The service times (i.e., the time it takes for a dog to get vaccinated) are iid exponential with parameter μ, such that the average service time is equal to $1/\mu$. The system is assumed to be FIFO, meaning that dogs are vaccinated in the order that their owners join the queue. Only one dog can get vaccinated at a time, as there is only one vaccinator per site, and dogs are assumed to leave the system as soon as they get vaccinated.

The service rate μ was assumed to equal 30 h^{-1} in accordance with the empirical observation that it takes 2 min on average to vaccinate a dog. The arrival rates were assumed to vary across MDVC sites and were determined as follows. First, the MDVC participation probability function described above was applied to all households falling within an MDVC site's *catchment* (i.e., all houses closest to the given MDVC site in terms of travel distance) to determine the probability that each household would participate in the MDVC if the house were inhabited and owned dogs. To obtain the total number of dogs arriving at MDVC site s, these participation probabilities were summed and scaled by the habitability rate, household-dog-ownership rate, and average number of dogs per dog-owning household (57, 40%, and 1.86, respectively); these estimates were derived from household surveys administered following previous MDVCs, and the survey methodology has been described previously (25). The total number of arrivals was then divided by the total operation time for the MDVC site to obtain λ_s, the arrival rate for site s.

A dog enters the queueing system at site s after it arrives at the site and its owner elects to join the vaccination queue. However, some owners may decline to join the queue if they judge the queue to be too long. This first form of attrition is known as *balking* and was modeled by modifying the arrival rate λ_s so that it decreases by a discouragement factor $e^{-\alpha n/\mu} < 1$ (10). The *modified arrival rate* $\lambda_{s,n}$ captures the rate that owners join the queue after accounting for those that balk and is given by:

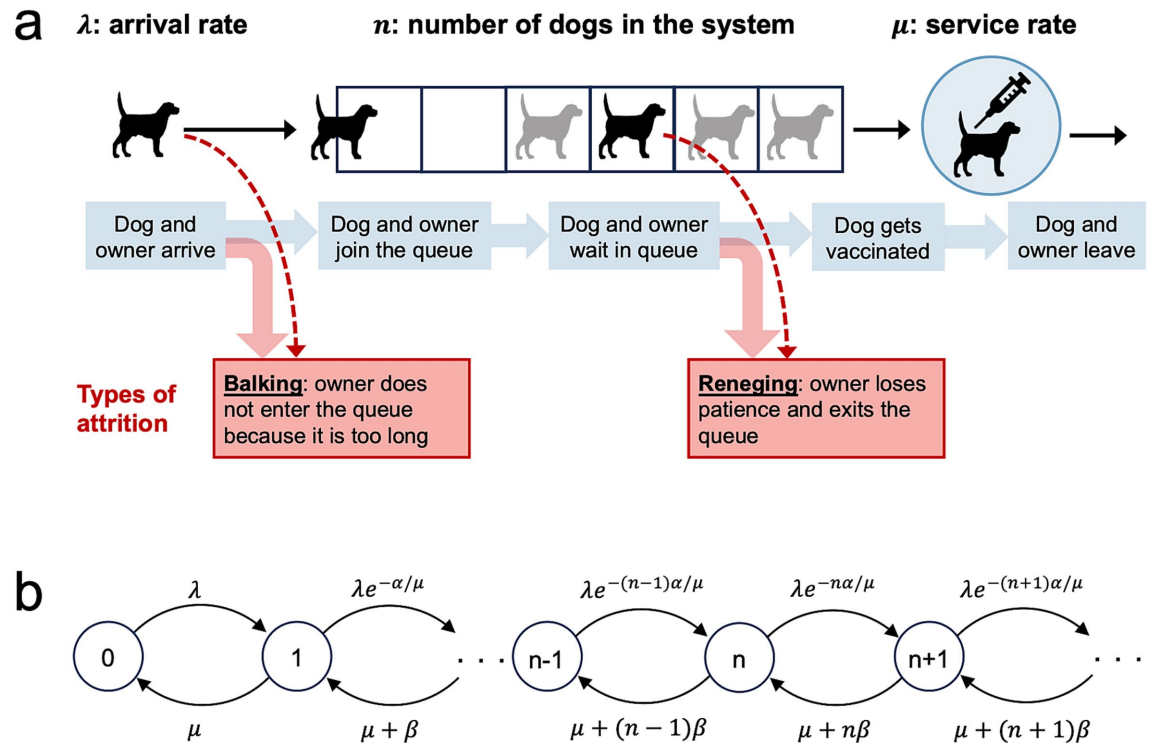

FIGURE 1
An M/M/1 first-in-first-out queueing model for an MDVC vaccination site. **(A)** Illustrates the processes captured by the queueing model, with the forms of queuing attrition highlighted by the red boxes. **(B)** Shows the transition-state diagram for the queueing model, where states, depicted by circles, are defined by the number of dogs in the system, and transitions between states, depicted with curved arrows, are labeled by their corresponding transition rates.

$$\lambda_{s,n} = e^{-\alpha n/\mu} \cdot \lambda_s \tag{1}$$

Where n is the number of dogs that are currently in the system (waiting in queue or being vaccinated), μ is equal to the service rate, and α is a parameter that scales with balking propensity (10).

The other form of attrition, known as *reneging*, occurs when an owner who has already joined the queue loses patience and exits the queue before their dogs are vaccinated. We modeled reneging by modifying the service rate μ to capture all those leaving the system - both those leaving after vaccination and those who renege. This *exit rate* μ_n is equal to:

$$\mu_n = \mu + (n-1)\cdot\beta \tag{2}$$

Where the second term captures the rate that each of the present $n-1$ dogs in queue are reneging, and β scales with reneging propensity (29). Note that in Equations 1, 2, above, the rates of attrition (both balking and reneging) increase with the queue length $n-1$, as expected.

In order to calculate the expected number of dogs vaccinated during an MDVC, we need to find a closed-form expression for the vaccination rate at a given vaccination site that accounts for losses due to attrition. The derivation of these closed-form equations can be found in Supplementary Text A, and are based on the stationary distribution of the queueing model, i.e., on $p_{s,n}$, the probability of finding n dogs in the queueing system at MDVC site s with arrival rate λ_s:

$$p_{s,n} = \frac{e^{\frac{-\alpha n(n-1)}{2\mu}} \lambda_s^n \Gamma\left(\frac{\mu}{\beta}\right)}{\beta^n \Gamma\left(n + \frac{\mu}{\beta}\right)} p_{s,0} \tag{3}$$

where $\Gamma(z)$ denotes the gamma function, i.e., $\Gamma(n) = (n-1)!$ for any integer $n > 0$ and $\Gamma(z) = \int t^{z-1} e^{-t} dt$ interpolates the factorial function to non-integer values, and $p_{s,0}$ is a normalizing constant given by:

$$p_{s,0} = \left[1 + \sum_{n=1}^{\infty} \frac{\lambda_s^n e^{\frac{-\alpha n(n-1)}{2\mu}} \Gamma\left(\frac{\mu}{\beta}\right)}{\beta^n \Gamma\left(n + \frac{\mu}{\beta}\right)}\right]^{-1} \tag{4}$$

The expected rate that dogs are vaccinated at site s is then equal to:

$$v_s = \sum_{n=0}^{\infty} p_{s,n} \lambda_{s,n} - \sum_{n=1}^{\infty} p_{s,n} (n-1)\beta \tag{5}$$

where the first term is equal to the rate that dog owners join the queue after accounting for balking, and the second term is equal to the

rate that dog owners renege and thus leave the queue before their dogs are vaccinated. The expected number of dogs vaccinated during an MDVC is thus equal to:

$$V = \sum_{s \in S} v_s t \tag{6}$$

Where S is the set of all selected vaccination sites and t is equal to the total operation time, which is assumed to be the same for all MDVC sites.

In addition to the closed-form equations for the expected behavior of the MDVC queueing system, which were derived assuming the system had reached steady state (Equations 3–6), we also conducted stochastic simulations to study the behavior of the system in the absence of such assumptions. Simulations were conducted for low- and high-attrition parameter regimes (low: $\alpha = 0.01$ and $\beta = 0.02$; high: $\alpha = 0.1$ and $\beta = 0.1$) and for a range of arrival rates (0.5–37.5 dogs/h in increments of 0.5 dogs/h). Low- and high-attrition parameter regimes were chosen to represent the high and low range of feasible values based on our observations of balking and reneging at MDVC sites. An MDVC site operates for four weekend days (over two weekends) for about 4 h per day ($t = 16$ total hours). To mimic these conditions, a single simulation consisted of four independent four-hour-long trials (days), each initialized with no dogs in the queue at time zero; the number of dogs vaccinated each day was summed across the 4 days to obtain the total dogs vaccinated at an MDVC site. The simulation was run for 1,000 iterations per set of parameter values, and the simulation results were compared to the expected number of dogs vaccinated as determined via the closed-form equations to see how well the two approximated each other.

2.2 Optimizing the location of vaccination sites

We optimized the placement of MDVC sites for the Alto Selva Alegre district of Arequipa; no more than 20 sites can operate in this region during a campaign due to resource constraints, and 70 locations have been approved by the Ministry of Health for use as feasible MDVC sites (Figure 2) (28). We determined the optimal placement of $k = 20$ sites among these 70 candidate sites by maximizing the expected number of households participating in the MDVC (and hence the total dogs vaccinated). To determine the number of participating households, we first used a fixed-effects Poisson distance-decay function that links a household's travel distance to their nearest vaccination site and their probability of participating in an MDVC (henceforth referred to as the "MDVC participation probability function"); this function was fit previously using survey data (28). We assumed that participating households travel to their closest MDVC site, and we used the MDVC participation probability function to estimate the number of households that are expected to arrive at each site. We divided the number of arrivals by the total operation time for an MDVC site (i.e., 16 h) to calculate the arrival rate λ_s at each site s. Then, for queue-conscious optimization, we estimated the number of dogs vaccinated at each site using Equation 5, which accounts for attrition resulting from queue formation due to high arrival rates. *Queue-naïve* optimization, in contrast, assumes that all arriving dogs get vaccinated and thus does not account for queueing-related losses. The objective function (total vaccinated dogs) was then calculated by summing the number of dogs vaccinated at each site.

We performed queue-conscious and queue-naïve optimization by implementing a hybrid recursive interchange-genetic algorithm (Supplementary Text B and Supplementary Figures S1, S2). The recursive interchange portion of our algorithm is similar to Teitz and Bart's (30) solution to the p-median problem that solves the facility location problem by minimizing the average distance traveled by all households to their nearest site, but instead of minimizing average travel distance, our algorithm aims to maximize the expected number of households participating in the MDVC, which allowed our *queue-conscious* optimization algorithm to simultaneously account for travel distance and queue-length-dependent attrition rates.

The general steps of the recursive interchange algorithm are as follows:

1. Select a random subset of 20 vaccination sites and use the MDVC participation probability function to determine the expected arrival rate λ at each site.
2. Calculate the expected number of dogs vaccinated at each site and sum across all sites to calculate the total number of dogs vaccinated.
3. Exchange one selected site with all non-selected candidate locations and keep the one that maximizes the number of dogs vaccinated.
4. Repeat step 3 with remaining sites to obtain a locally optimized set of sites.
5. Perform steps 1–4 over 1,000 iterations, initializing each iteration with a different random subset of sites.

An animation showing a single iteration of the recursive interchange algorithm can be viewed in the Supplementary materials. The recursive interchange algorithm was repeated over 1,000 iterations to increase performance, as the algorithm does not guarantee a globally optimal solution. Performance was further enhanced by combining the recursive interchange algorithm with a genetic algorithm that "mates" parental sets output by the recursive interchange algorithm, mimicking natural selection by introducing crossover and mutation and ultimately producing new starting sets on which to repeat the recursive interchange algorithm. The cycling between the recursive interchange and genetic algorithms was repeated until the expected number of dogs vaccinated did not increase over two subsequent rounds of optimization (stopping condition). A full description of the hybrid algorithm can be found in the Supplementary Text B.

MDVC sites were optimized under three scenarios: no attrition ($\alpha = \beta = 0$), low attrition ($\alpha = 0.01$, $\beta = 0.02$), and high attrition ($\alpha = 0.1$, $\beta = 0.1$). Note the no-attrition scenario is the least realistic, as some degree of balking and reneging is expected to occur in the real world. The low- and high-attrition *queue-conscious* solutions were compared to the *queue-naïve* solution obtained under the assumption of no attrition (i.e., all dogs that arrive get vaccinated) to determine how the incorporation of queueing behaviors impacted the amount of dogs lost to attrition and the total vaccination coverage, which was calculated as the proportion of dog-owning households that are expected to participate in the MDVC. Additionally, the

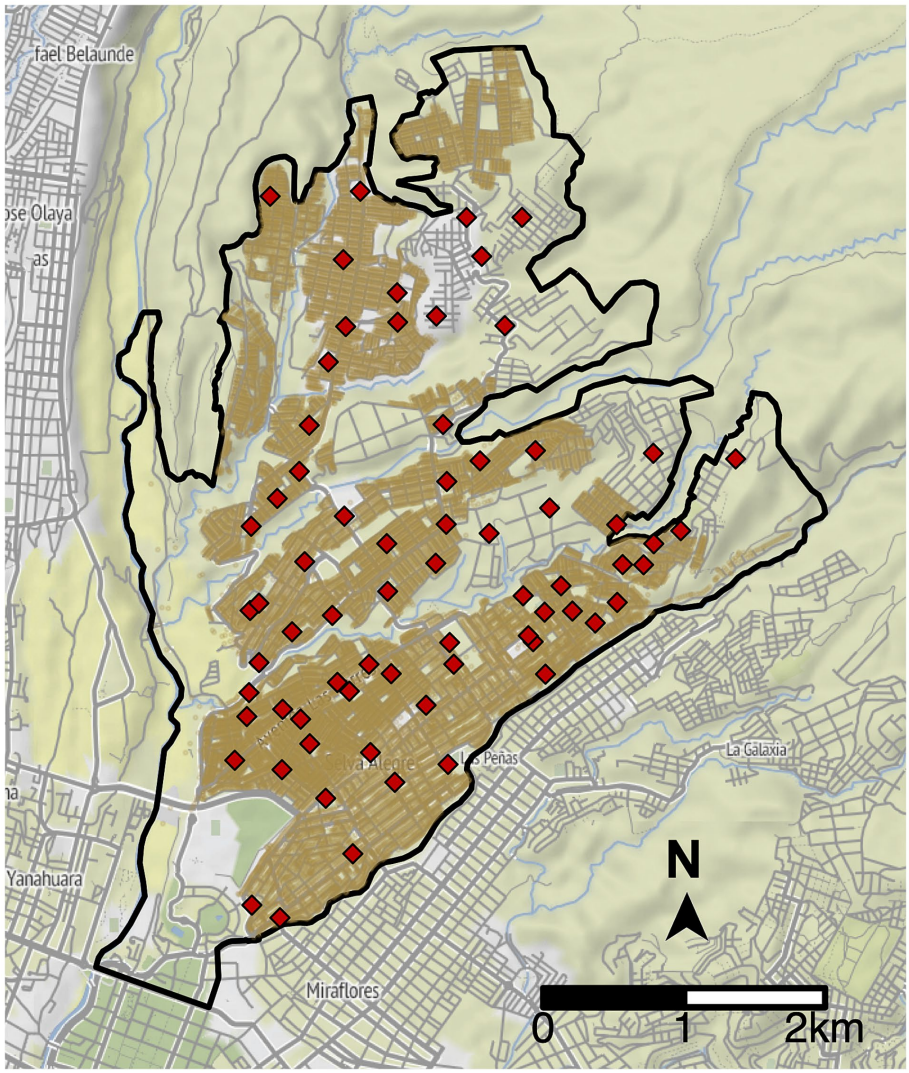

FIGURE 2
Potential vaccination site locations in Alto Selva Alegre. The boundaries of Alto Selva Alegre are depicted by the solid, black line. Candidate MDVC sites (N = 70) are indicated by red diamonds, and the locations of houses are shaded brown.

queue-conscious solutions were compared to the locations of actual sites used in the 2016 MDVC to evaluate how the performance of sites placed by the queue-conscious algorithm compared to a real-world baseline (28). Note that although the *queue-naïve* solution to the location problem was obtained assuming no attrition, its performance was assessed under the assumption of a low- or high-attrition parameter regime. Additionally, the optimized sites were mapped along with their catchments to compare how site placement varied between the queue-conscious and queue-naïve solutions.

2.3 Sensitivity analyses

To determine how our results may have been impacted by misspecification of α and β, we considered four possible scenarios for true balking and reneging propensities. In addition to the low- and high-attrition scenarios discussed previously ($\alpha = 0.01/\beta = 0.02$ and $\alpha = 0.1/\beta = 0.1$, respectively), we considered two additional scenarios for true balking and reneging propensities: (1) low balking and high reneging ($\alpha = 0.01$, $\beta = 0.1$) and (2) high balking and low reneging ($\alpha = 0.1$, $\beta = 0.02$). We applied the low- and high-attrition solutions to these four scenarios to evaluate performance (in terms of number of vaccinations and losses to attrition) for situations in which α and β are correctly and incorrectly specified. For each scenario and queue-conscious solution applied, performance was evaluated using the number vaccinated and losses to attrition achieved by the queue-naïve solution as a benchmark.

The optimization methods detailed above rely on the use of the closed-form equations for the queueing system, which assumes a constant arrival rate λ. We considered how this assumption impacted our results by allowing λ to vary in a step-wise manner to approximate time-varying arrival rates that have been observed in the field (Supplementary Figure S3). Four time-varying arrival densities were considered: (a) a steep unimodal peak density, (b) a wide unimodal density that is skewed right, (c) a wide unimodal density that is skewed left, and (d) a bimodal density distribution

(Supplementary Figure S4). Eight total scenarios were considered, representing all combinations of the four time-varying arrival densities and low- and high-attrition parameter regimes. Queueing simulations were performed for each scenario, and natural splines were used to summarize the behavior of the system over a range of arrival rates (Supplementary Text C and Supplementary Figure S5). Once again, the performance of the low- and high-attrition solutions were assessed for each scenario, using performance under the queue-naïve solution as a benchmark. Additionally, the different non-constant arrival rate densities were compared to the baseline assumption of a constant arrival rate to determine how this assumption impacted estimations of the number of vaccinations and losses to attrition.

3 Results

3.1 Queue-conscious optimization for MDVCs

As expected, the amount of balking and reneging was greater for higher arrival rates and for higher α and β values, representing greater attrition propensity (Figure 3). Although the closed-form expression for the expected number of vaccinations (Equation 6) was derived under steady-state assumptions, the results of the stochastic simulations closely approximated results obtained using Equation 6 across a range of arrival rates for both high- and low-attrition parameter regimes (root mean square percentage error < 2% for both regimes; Supplementary Figure S6). Thus, Equation 6 was used as the objective function in the hybrid algorithm that was used to optimize MDVC site placement.

Compared to the queue-naïve algorithm, the queue-conscious algorithm favored a more even distribution in the number of arrivals across all selected sites (Figure 4). The queue-conscious algorithm "flattens" the distribution of arrivals by placing more sites in densely populated areas to divide the higher vaccination workload across more vaccinators and placing fewer sites in less populous areas (Figure 5). This difference in site distribution is expected, because too many arrivals at a site result in the formation of long queues and more losses from balking and reneging; these losses are accounted for (penalized) by the queue-conscious algorithm but not by the queue-naïve algorithm, which assumes that all arrivals get vaccinated. This difference between the queue-naïve and queue-conscious algorithms also results in the queue-naïve algorithm yielding more arrivals, as it maximizes the number of participating households simply by maximizing the number of arrivals.

Within the low-attrition system ($\alpha = 0.01$, $\beta = 0.02$), vaccination sites that were placed using the queue-conscious algorithm achieved an expected vaccination coverage of 57.2% compared to 56.4% achieved by the queue-naïve algorithm (Table 1 and Figure 4). The amount of queueing attrition (i.e., the expected number of dog owners balked or reneged) was also lower for sites placed using the queue-conscious algorithm: 596 vs. 733 for the queue-naïve algorithm, representing a 19% reduction. Trends were similar for the high-attrition system ($\alpha = 0.1$, $\beta = 0.1$), in which the queue-conscious algorithm improved the expected vaccination coverage from 47.2 to 48% and reduced queueing attrition by 9% from 1,727 to 1,566. Queue-conscious optimization resulted in markedly superior performance when compared to that of historic MDVC sites, increasing expected vaccination coverage from 50.9 to 57.2% in the low-attrition regime and from 43.2 to 48% in the high-attrition regime; it also decreased queueing attrition by 32% (from 882 to 596) and 9% (from 1,721 to 1,566) in the low- and high-attrition regimes, respectively (Table 1 and Supplementary Figure S7).

3.2 Sensitivity analyses

These results were robust to misspecification of α and β, and the performance varied only slightly between the high- and low-attrition solutions for all combinations of α and β considered (Figure 6). When the true values of α and β are low ($\alpha = 0.01$ and $\beta = 0.02$), overestimating these parameters in the optimization did not result in a substantial loss in the number of dogs vaccinated compared to the correctly optimized solution (82 vs. 84 more dogs vaccinated beyond the queue-naïve solution). Similarly, when the true values of α and β are high ($\alpha = \beta = 0.1$), underestimating these parameters in the optimization did not markedly impact the number of dogs vaccinated compared to the correctly optimized solution (83 vs. 85 more dogs vaccinated beyond the queue-naïve solution). Moreover, applying the low- and high-attrition solutions resulted in a similar number of dogs vaccinated when the true value of α is low and the true value of β is high and vice-versa (Figure 6A). The high-attrition solution resulted in a greater reduction in queueing attrition than the low-attrition solution for all four attrition scenarios, though both solutions resulted in substantially fewer losses compared to the queue-naïve solution (Figure 6B). Taken together, these results demonstrate that the queue-conscious algorithm outperforms the queue-naïve algorithm even in the presence of mis-specified queueing parameters.

The superior performance of the queue-conscious algorithm compared to the queue-naïve algorithm was also robust to relaxation of the constant arrival rate assumption. For all four time-varying arrival densities and attrition regimes, both low- and high-attrition solutions substantially outperformed the queue-naïve solution in terms of the numbers vaccinated and lost to attrition (Supplementary Figure S7). Interestingly, with the exception of arrival density D under a low-attrition regime, for which the low- and high-attrition solutions yielded roughly equal numbers of vaccinations, the high-attrition solution outperformed the low-attrition solution in terms of the numbers vaccinated. The high-attrition solution also resulted in less queueing attrition than the low-attrition solution for all scenarios considered. In addition, non-constant arrival rates resulted in more queueing attrition and fewer dogs vaccinated compared to an otherwise equivalent scenario where the constant arrival rate assumption is met (Supplementary Figure S8).

4 Discussion

We developed an optimization algorithm that integrates queueing theory into a spatial optimization framework to improve the placement of mass vaccination sites. We applied our algorithm to the MDVC in Arequipa, Peru by simultaneously minimizing travel distance to MDVC sites and queueing attrition resulting from large arrival volumes at some sites. Our queue-conscious algorithm decreased queueing attrition by 9–32% and increased expected

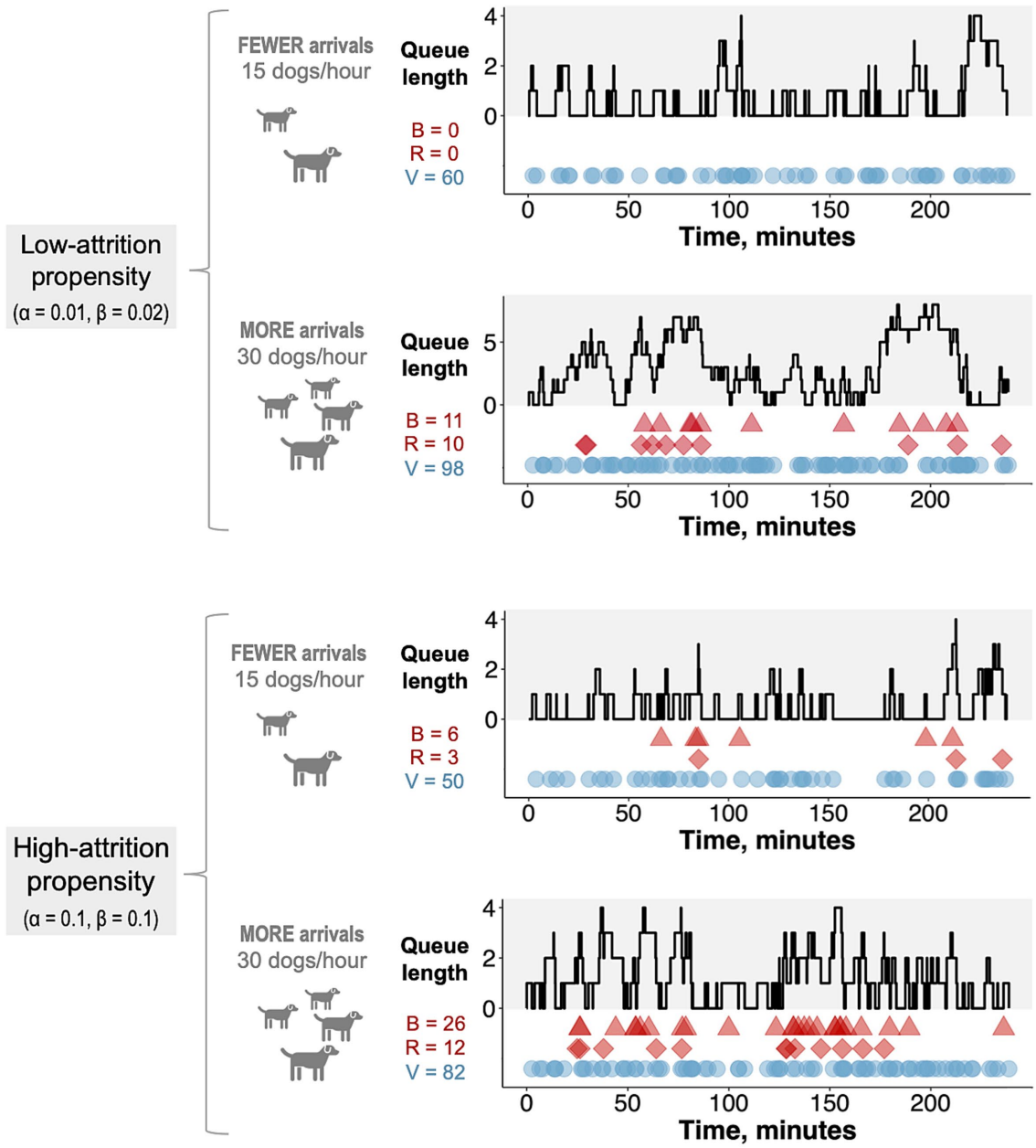

FIGURE 3
Realized trials of the stochastic queueing model. Each trial of the stochastic queueing simulation represents a single four-hour day at an MDVC site. The gray-shaded portion of each plot tracks the queue length over the four-hour period, and the colored shapes in the white portion of each plot tracks the occurrences of balking (red triangles), reneging (red diamonds) and vaccination (blue circles). The number of balking events (B), reneging events (R), and vaccinations (V) are reported for each trial. Trials are shown for two different α/β parameter regimes (low: $\alpha = 0.01$, $\beta = 0.02$ and high: $\alpha = 0.1$, $\beta = 0.1$) and two different arrival rates (15 and 30 dogs per hour).

vaccination coverage by 11–12% compared to actual sites used in a previous MDVC and decreased queueing attrition by 9–19% and increased expected vaccination coverage by 1–2% compared to a queue-naïve version of the same algorithm. MDVC site optimization that accounted for queueing placed more vaccination sites in densely populated areas to even out the number of expected arrivals across sites, and sensitivity analyses revealed that accounting for queueing resulted in improved MDVC performance, even in the absence of accurate parameter estimates. Moreover, the expected gains in vaccination coverage do not capture the indirect gains from reduced queueing and increased MDVC participant satisfaction, which is likely to improve turnout in subsequent campaigns.

Longer wait times have been negatively associated with patient satisfaction in a variety of healthcare contexts, and patients report being less likely to repeatedly patronize a medical practice with long wait times compared to one with shorter wait times (1, 31, 32). For dog rabies vaccination, individuals who must wait a long time before receiving vaccinations for their dogs may be far less likely to participate in subsequent vaccination campaigns. Furthermore, considering the

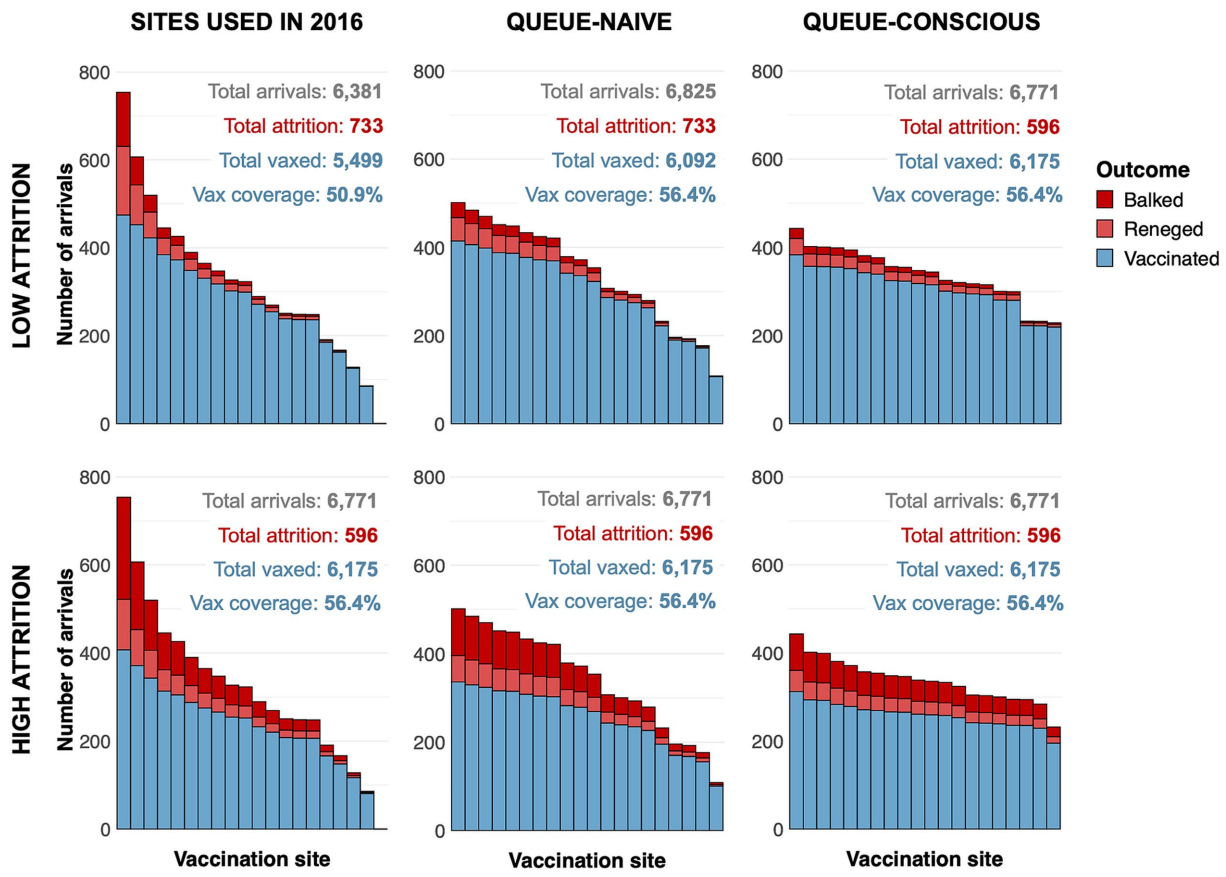

FIGURE 4
Arrivals histograms for sites selected by queue-naïve and queue-conscious optimization compared to actual sites used in the 2016 MDVC assuming low- and high-attrition parameter values. The height of each stacked bar represents the expected number of dogs that arrive at a selected vaccination site. Bars are subdivided by color according to whether dogs ultimately get vaccinated (blue) or are lost to attrition, either through balking (dark red) or reneging (light red). The text above the bars gives the total number of arrivals, total losses to attrition, and overall vaccination coverage achieved for each set of sites. Top row shows results assuming a low-attrition parameter regime, and bottom row shows results for a high-attrition parameter regime. The number of dogs vaccinated and the number of dogs lost to attrition for all situations were determined using Equation 6 and the equations outlined in the electronic Supplementary Text A.

evidence of social contagion around vaccines (33–37), dog owners could share their negative experiences waiting at an MDVC site with friends and neighbors, discouraging them from participating. The reduction of attrition resulting from well-placed vaccination sites may pay dividends in improving turnout and vaccination coverage in subsequent MDVCs; this is particularly important for dog rabies elimination, which requires sustained high levels of vaccination year after year (38–40).

We assumed that owners arrived with their dogs to MDVC sites at time-invariant rates. The rationale behind this assumption was twofold: (1) it ensured tractability of the queueing equations, and (2) it was unclear how to specify a non-constant arrival rate in the face of heterogeneity in the trajectory of rates observed at MDVC sites (Supplementary Figure S3). Our sensitivity analysis indicated that the queue-conscious solutions outperformed the queue-naïve solutions even when arrival rates varied over time (Supplementary Figure S7). We also found that non-constant arrival rates resulted in more queueing attrition and fewer dogs vaccinated than the baseline assumption of a constant arrival rate (Supplementary Figure S8). This result can be explained by the fact that a time-varying arrival density leads to swells of arrivals during peak intervals, when queue lengths would escalate and cause attrition to spike.

Surprisingly, the high-attrition solution performed as well as or better than the low-attrition solution for all time-varying arrival scenarios, even those in which the true attrition rates were low (Supplementary Figure S7). This result can be explained by the spikes in attrition that accompany time-varying arrival rates but are not captured by the low-attrition solution, which are obtained under the assumption of a constant arrival rate. As a result, even when α and β are low, the expected vaccination rate is higher with the high-attrition solution, as it favors a more even distribution in the number of arrivals across vaccination sites (compare top vs. bottom rows of Figures 4, 5). These results suggest that applying MDVC optimization in the real world is as much an art as it is a precise science. Even if the "true" balking and reneging rates could be determined, it may be beneficial to slightly overestimate these parameters to offset the reality of non-constant arrival rates.

The queue-conscious algorithm we employed decreases queue lengths across the study area, but some queueing is inevitable. Attrition can be minimized further by improving the waiting experience for queueing dog owners (41, 42). In the context of

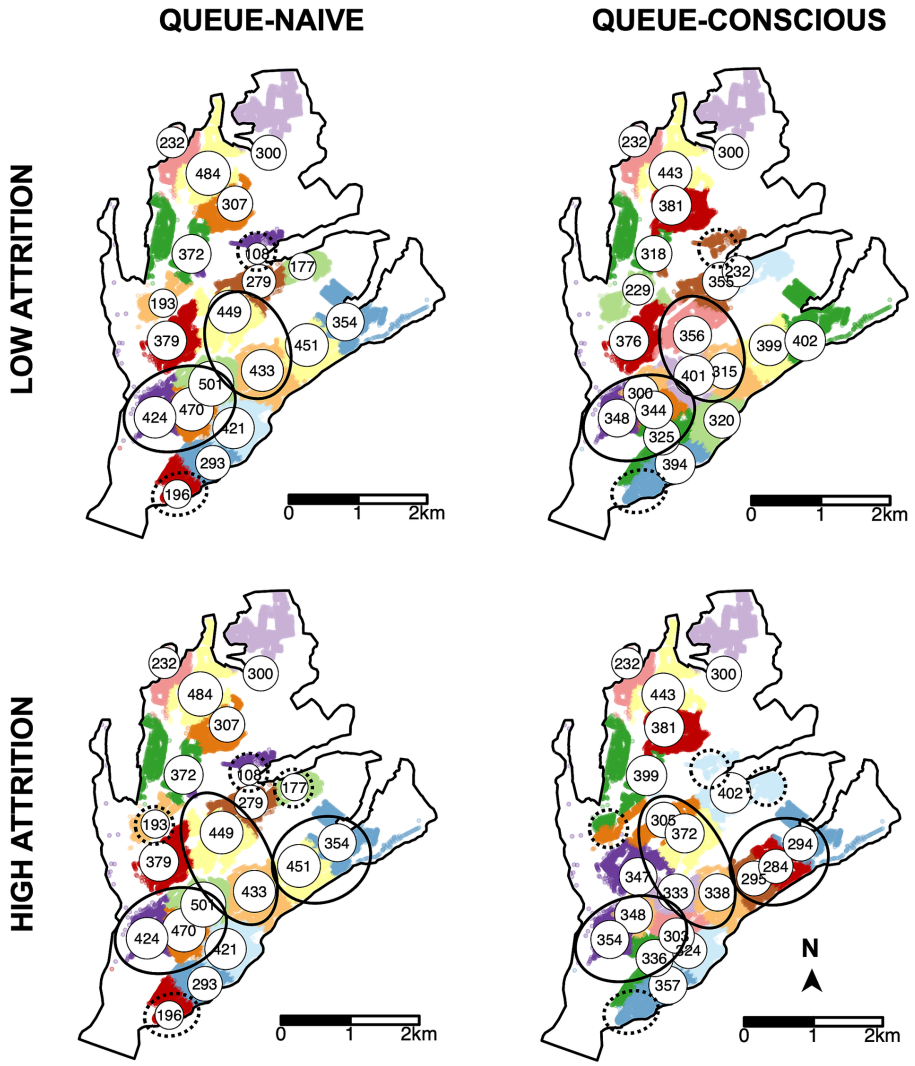

FIGURE 5
Locations of MDVC sites selected by the queue-naïve vs. queue-conscious algorithm for the low- and high-attrition systems. The locations of selected vaccination sites are indicated by white circles that are labeled and scaled according to the expected number of arriving dogs, which were calculated using Equation 6. Top row shows results for the low-attrition system, and bottom row shows results for the high-attrition system. Houses in the study area are small dots colored according to their catchment, representing the area in which a MDVC site is the closest site for houses in terms of travel distance. Areas in which the queue-conscious algorithm placed a higher density of vaccination sites compared to the queue-naïve algorithm are indicated by ellipses with solid lines, and areas in which the queue-conscious algorithm placed one fewer site are indicated by ellipses with dotted lines.

TABLE 1 Performance of vaccination sites placed by queue-naïve and queue-conscious optimization compared to actual sites used in 2016 for low- and high-attrition parameter regimes.

Parameter regime	Placement type	Expected arrivals, *n*	Losses to attrition, *n* (%)	Households vaccinated, *n* (%)	Est. vaccination coverage, %
Low attrition	Actual sites	6,381	882 (13.8)	5,499 (86.2)	50.9
Low attrition	Optimized, queue-naïve	6,825	733 (10.7)	6,092 (89.3)	56.4
Low attrition	Optimized, queue-conscious	6,771	596 (8.8)	6,175 (91.2)	57.2
High attrition	Actual sites	6,381	1721 (27.0)	4,660 (73.0)	43.2
High attrition	Optimized, queue-naïve	6,825	1727 (25.3)	5,098 (74.7)	47.2
High attrition	Optimized, queue-conscious	6,771	1,566 (23.1)	5,205 (76.9)	48.0

Losses to attrition and total vaccinated are expressed as the number of households lost or vaccinated, as well as a percentage of arriving households. The estimated vaccination coverage was calculated as the proportion of dog-owning households that are expected to participate in the MDVC.

10.3389/fpubh.2024.1440673

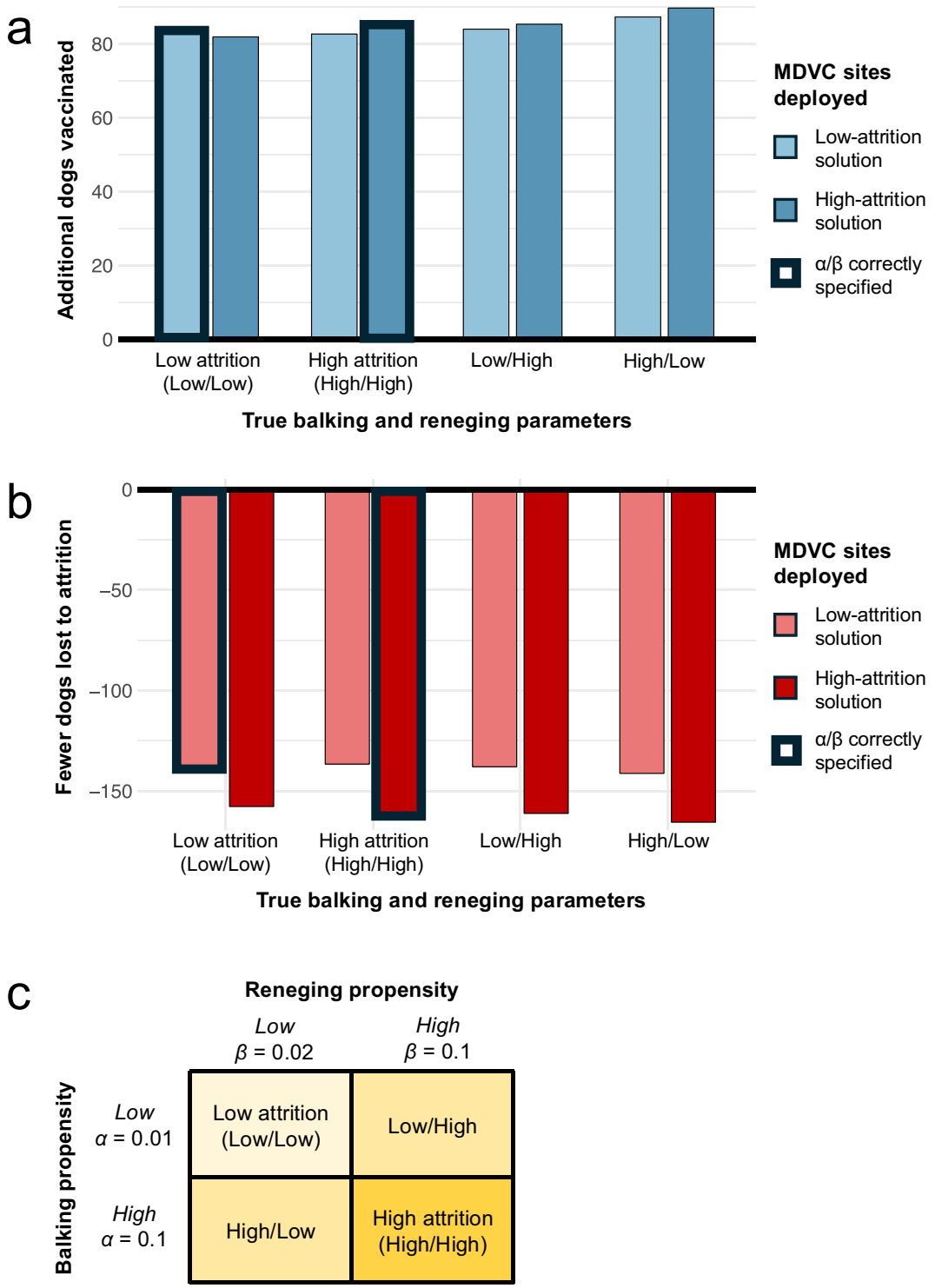

FIGURE 6
Sensitivity of results to misspecification of balking and reneging parameters. Panels a-b illustrate how misspecification of α and β impacts the expected number of dogs vaccinated **(A)** and the number of dogs lost to attrition **(B)**. The performance of the low- and high-attrition solutions are provided with the queue-naïve solution acting as a benchmark; thus **(A)** shows the additional number of dogs vaccinated beyond the expected number achieved with the queue-naïve solution, and **(B)** shows the reduction in attrition compared to the queue-naïve solution. Bars outlined in bold represent scenarios in which the balking and reneging parameters are correctly estimated in the optimization. **(C)** Provides a legend with the values of α and β for the four balking/reneging scenarios considered.

MDVCs, accommodations should be made for aggressive dogs, whose presence in a queue can cause other owners to balk or renege. Some vaccinators may choose to deviate from FIFO principles and vaccinate aggressive dogs first regardless of when they arrive to remove them from the queue more quickly. This strategy should be explained clearly to the owners present as violations of FIFO are generally perceived as

unfair (42, 43). MDVC participant satisfaction should be prioritized wherever possible, as it impacts whether individuals will continue to participate in future MDVCs. Other behavioral interventions that can minimize queueing attrition are messaging and incentives to flatten out the arrival rate. Field observations show arrival peaks, longer queue lengths, and greater attrition at midday (Supplementary Figure S3). Attrition during these peaks can be mitigated by communicating about shorter wait times early in the morning or incentivizing early arrivals by rewarding a limited quantity of "doorbuster" prizes (e.g., dog food or dewormer medication).

The expected vaccination coverage achieved by our optimization of fixed-location vaccination sites (57 and 48% for the low- and high-attrition scenarios, respectively) falls short of the 70–80% threshold recommended by World Health Organization (38) and Pan American Health Organization (44). This gap can be met, in part, by combining fixed-location vaccination sites with door-to-door vaccination in areas with low penetration by the fixed-location campaign. This two-pronged approach has been leveraged successfully in other MDVCs (45, 46) as well as pandemic-era COVID-19 vaccination programs (47, 48). A benefit of combining door-to-door vaccination with fixed-point vaccination is the ability to target high-risk or underserved areas, which not only increases total vaccine uptake but also promotes vaccine equity. We have previously found that the queue-naïve algorithm increases the spatial evenness of vaccine coverage, a dimension of vaccine equity, even though it does not explicitly optimize for spatial equity (28). By placing more vaccination sites in more populous areas and limiting the placement of sites in less populous ones, the queue-conscious algorithm inadvertently decreases the spatial equity of fixed-point vaccinations compared to the queue-naïve algorithm, which is a limitation of the queue-conscious approach. In many Latin American cities, including Arequipa, the less populous peri-urban areas also coincide with areas of greater socioeconomic disadvantage (25, 26); thus, it is crucial for peri-urban areas to be prioritized by door-to-door campaigns following the deployment of fixed-point vaccination sites to ensure vaccine equity. Disadvantaged groups face the greatest barriers in accessing health services and are thus least able to travel to vaccination sites and wait for service (49–51). They might benefit the most from this combined approach.

There are other limitations of our study. The balking and reneging parameters α and β were not estimated from data but selected to model two hypothetical parameter regimes that fell within the upper and lower bounds of values that could feasibly capture real-world dynamics. While this lack of empirical estimation is a study limitation, our sensitivity analyses also indicated that the performance of our optimization algorithm was robust to misspecification of these parameters. In addition, the MDVC participation probability function that was used to optimize vaccination site locations included distance to the nearest site as a sole predictor and did not consider other household-level factors such as socioeconomic status (SES) or local environment factors such as urban/peri-urban status. Future studies can investigate how travel distance to MDVC sites affect MDVC participation among different household SES levels and across urban and peri-urban areas to derive a more nuanced MDVC participation function. Doing so can also be a means of promoting vaccine equity; for example, if future investigations revealed that marginalized groups are less able to travel long distances to participate in the MDVC, then the algorithm using this "updated" function would favor placing more sites near marginalized populations. Additionally, deviations from a constant arrival rate in the real world may impact the generalizability of our results, though our sensitivity analyses suggested that the superior performance of the queue-conscious algorithm was robust to relaxation of the constant arrival rate assumption. Finally, our algorithm assumed that all MDVC sites were operated by a single vaccinator (i.e., M/M/1). As a result, the algorithm tended to place multiple, adjacent single-vaccinator sites in highly populous areas. There are generally efficiency gains associated with multi-server (i.e., multi-vaccinator) queueing systems (where multiple vaccinators serve a single queue) compared to single-server systems with designated queues (10). However, pooling vaccinators (i.e., placing k vaccinators across fewer than k sites) may also lead to performance loss, as reducing the number of sites could result in longer queues, which may increase perceived waiting times and result in greater attrition (52); reducing the number of sites may also increase travel distances for some dog owners and thus decrease their probability of participation. A possible extension of our work would be to examine the tradeoff between gains from pooling vaccinators and losses due to slightly longer travel distances and potentially longer queue lengths.

In summary, our spatial optimization framework that incorporates expected losses from queueing offers insights for current vaccine-preventable disease programs and for future pandemic preparedness efforts. We maximized the total vaccine uptake by enhancing the spatial accessibility of vaccination sites while mitigating excessive queue lengths to reduce losses due to queueing attrition. We found that explicitly modeling queueing behavior, even with imprecise parameter estimates, led to gains in vaccination coverage and fewer losses to attrition than optimization that ignores the effects of queueing. Combined with door-to-door outreach and targeted media campaigns, rational placement of fixed-point vaccination sites is expected to bring vaccine uptake closer to threshold levels recommended for the control and eventual elimination of dog rabies. Considering the impact of excessive wait times on other vaccination campaigns, including the early rollout of the COVID-19 vaccine, our spatial optimization framework that explicitly considers queueing attrition can be broadly adopted to support other mass vaccination programs.

Data availability statement

The datasets presented in this study can be found in online repositories. The names of the repository/repositories and accession number(s) can be found at: https://github.com/sherriexie/spatialoptimizationqueueing. Note that identifiable data (residential geocodes) have been removed from the data repository.

Ethics statement

The studies involving humans were approved by the Institutional Review Boards of Universidad Peruana Cayetano Heredia (approval number: 65369) and University of Pennsylvania (approval number: 823736). The studies were conducted in accordance with the local legislation and institutional requirements. The participants provided their written informed consent to participate in this study.

Author contributions

SX: Conceptualization, Formal analysis, Investigation, Methodology, Project administration, Software, Validation, Visualization, Writing – original draft, Writing – review & editing. MR: Conceptualization, Formal analysis, Methodology, Writing – review & editing. SC: Formal analysis, Writing – review & editing. BB: Methodology, Writing – review & editing. ED: Data curation, Writing – review & editing. ML: Conceptualization, Methodology, Writing – review & editing. RC-N: Conceptualization, Funding acquisition, Methodology, Project administration, Supervision, Writing – review & editing.

Funding

The author(s) declare that financial support was received for the research, authorship, and/or publication of this article. This study was supported by the National Institute of Allergy and Infectious Diseases (grant nos. K01AI139284 and R01AI168291) to RC-N.

Acknowledgments

We gratefully acknowledge the contributions of and the work done by the Gerencia Regional de Salud de Arequipa, the Red de Salud Arequipa Caylloma, the Laboratorio Referencial Regional Arequipa, and the Microredes of the city of Arequipa. We acknowledge the work of the members of the Zoonotic Disease Research Laboratory, One Health Unit, and their contribution collecting part of the data used in this study.

Conflict of interest

The authors declare that the research was conducted in the absence of any commercial or financial relationships that could be construed as a potential conflict of interest.

Publisher's note

All claims expressed in this article are solely those of the authors and do not necessarily represent those of their affiliated organizations, or those of the publisher, the editors and the reviewers. Any product that may be evaluated in this article, or claim that may be made by its manufacturer, is not guaranteed or endorsed by the publisher.

Supplementary material

The Supplementary material for this article can be found online at: https://www.frontiersin.org/articles/10.3389/fpubh.2024.1440673/full#supplementary-material

References

1. Bleustein C, Rothschild DB, Valen A, Valatis E, Schweitzer L, Jones R. Wait times, patient satisfaction scores, and the perception of care. *Am J Manag Care*. (2014) 20:393–400.

2. Ward PR, Rokkas P, Cenko C, Pulvirenti M, Dean N, Carney AS, et al. 'Waiting for' and 'waiting in' public and private hospitals: a qualitative study of patient trust in South Australia. *BMC Health Serv Res*. (2017) 17:333. doi: 10.1186/s12913-017-2281-5

3. Embrett M, Sim SM, Caldwell HAT, Boulos L, Yu Z, Agarwal G, et al. Barriers to and strategies to address COVID-19 testing hesitancy: a rapid scoping review. *BMC Public Health*. (2022) 22:750. doi: 10.1186/s12889-022-13127-7

4. Goralnick E, Kaufmann C, Gawande AA. Mass-vaccination sites — an essential innovation to curb the Covid-19 pandemic. *N Engl J Med*. (2021) 384:e67. doi: 10.1056/NEJMp2102535

5. Rosner E, Lapin T, Garger K. (2021). Hours-long waits reported at Javits center COVID vaccine site in NYC. New York Post. Available at: https://nypost.com/2021/03/02/hours-long-waits-reported-at-javits-center-covid-vaccine-site-in-nyc/ (Accessed March 2, 2021).

6. CBS Baltimore. As interest in COVID-19 vaccine rises, Baltimoreans face long lines, wait times. New York, NY, CBS News: (2021).

7. Di Pumpo M, Ianni A, Miccoli GA, Di Mattia A, Gualandi R, Pascucci D, et al. Queueing theory and COVID-19 prevention: model proposal to maximize safety and performance of vaccination sites. *Front Public Health*. (2022) 10:8406777. doi: 10.3389/fpubh.2022.840677

8. Orsi A, Butera F, Piazza MF, Schenone S, Canepa P, Caligiuri P, et al. Analysis of a 3-months measles outbreak in western Liguria, Italy: are hospital safe and healthcare workers reliable? *J Infect Public Health*. (2020) 13:619–24. doi: 10.1016/j.jiph.2019.08.016

9. Mo Y, Eyre DW, Lumley SF, Walker TM, Shaw RH, O'Donnell D, et al. Transmission of community- and hospital-acquired SARS-CoV-2 in hospital settings in the UK: a cohort study. *PLoS Med*. (2021) 18:e1003816. doi: 10.1371/journal.pmed.1003816

10. Shortle JF, Thompson JM, Gross D, Harris CM. Fundamentals of queueing theory. *5th* ed. New York, NY: John Wiley & Sons (2018).

11. Moreno-Carrillo A, Arenas LMÁ, Fonseca JA, Caicedo CA, Tovar SV, Muñoz-Velandia OM. Application of queuing theory to optimize the triage process in a tertiary emergency care ("ER") department. *J Emerg Trauma Shock*. (2019) 12:268–73. doi: 10.4103/JETS.JETS_42_19

12. Tucker JB, Barone JE, Cecere J, Blabey RG, Rha CK. Using queueing theory to determine operating room staffing needs. *J Trauma Acute Care Surg*. (1999) 46:71–9. doi: 10.1097/00005373-199901000-00012

13. Zonderland ME, Boucherie RJ, Litvak N, Vleggeert-Lankamp CLAM. Planning and scheduling of semi-urgent surgeries. *Health Care Manag Sci*. (2010) 13:256–67. doi: 10.1007/s10729-010-9127-6

14. de Bruin AM, Bekker R, van Zanten L, Koole GM. Dimensioning hospital wards using the Erlang loss model. *Ann Oper Res*. (2010) 178:23–43. doi: 10.1007/s10479-009-0647-8

15. Cayirli T, Veral E. Outpatient scheduling in health care: a review of literature. *Prod Oper Manag*. (2003) 12:519–49. doi: 10.1111/j.1937-5956.2003.tb00218.x

16. Lee EK, Li ZL, Liu YK, LeDuc J. Strategies for vaccine prioritization and mass dispensing. *Vaccine*. (2021) 9:506. doi: 10.3390/vaccines9050506

17. Kumar A, Kumar G, Ramane TV, Singh G. Optimal Covid-19 vaccine stations location and allocation strategies. *BIJ*. (2022) 30:3328–56. doi: 10.1108/BIJ-02-2022-0089

18. Hanly M, Churches T, Fitzgerald O, Caterson I, MacIntyre CR, Jorm L. Modelling vaccination capacity at mass vaccination hubs and general practice clinics: a simulation study. *BMC Health Serv Res*. (2022) 22:1059. doi: 10.1186/s12913-022-08447-8

19. Jahani H, Chaleshtori AE, Khaksar SMS, Aghaie A, Sheu JB. COVID-19 vaccine distribution planning using a congested queuing system—a real case from Australia. *Transp Res Part E Logistics Transp Rev*. (2022) 163:102749. doi: 10.1016/j.tre.2022.102749

20. Hirbod F, Eshghali M, Sheikhasadi M, Jolai F, Aghsami A. A state-dependent M/M/1 queueing location-allocation model for vaccine distribution using metaheuristic algorithms. *J Comput Design Eng*. (2023) 10:1507–30. doi: 10.1093/jcde/qwad058

21. Lee E. Modeling and optimizing the public-health infrastructure for emergency response. *Interfaces*. (2009) 39:476–90. doi: 10.1287/inte.1090.0463

22. Lee EK, Smalley HK, Zhang Y, Pietz F, Benecke B. Facility location and multi-modality mass dispensing strategies and emergency response for biodefence and infectious disease outbreaks. *IJRAM*. (2009) 12:311. doi: 10.1504/IJRAM.2009.025925

23. Lee EK, Pietz F, Benecke B, Mason J, Burel G. Advancing public health and medical preparedness with operations research. *Interfaces*. (2013) 43:79–98. doi: 10.1287/inte.2013.0676

24. Blank F. A spatial queuing model for the location decision of emergency medical vehicles for pandemic outbreaks: the case of Za'atari refugee camp. *JHLSCM*. (2021) 11:296–319. doi: 10.1108/JHLSCM-07-2020-0058

25. Castillo-Neyra R, Toledo AM, Arevalo-Nieto C, MacDonald H, De la Puente-León M, Naquira-Velarde C, et al. Socio-spatial heterogeneity in participation in mass dog rabies vaccination campaigns, Arequipa, Peru. *PLoS Negl Trop Dis*. (2019) 13:e0007600

26. Castillo-Neyra R, Brown J, Borrini K, Arevalo C, Levy MZ, Buttenheim A, et al. Barriers to dog rabies vaccination during an urban rabies outbreak: qualitative findings from Arequipa, Peru. *PLoS Negl Trop Dis*. (2017) 11:e0005460

27. Raynor B, Díaz EW, Shinnick J, Zegarra E, Monroy Y, Mena C, et al. The impact of the COVID-19 pandemic on rabies reemergence in Latin America: the case of Arequipa, Peru. *PLoS Negl Trop Dis*. (2021) 15:e0009414. doi: 10.1371/journal.pntd.0009414

28. Castillo-Neyra R, Xie S, Bellotti BR, Diaz EW, Saxena A, Toledo AM, et al. Optimizing the location of vaccination sites to stop a zoonotic epidemic. *Sci Rep*. (2024) 14:15910. doi: 10.1038/s41598-024-66674-x

29. Kulkarni VG. Modeling and analysis of stochastic systems. *3rd* ed. New York, NY: Chapman and Hall/CRC (2016).

30. Teitz MB, Bart P. Heuristic methods for estimating the generalized vertex median of a weighted graph. *Oper Res*. (1968) 16:955–61. doi: 10.1287/opre.16.5.955

31. Anderson RT, Camacho FT, Balkrishnan R. Willing to wait?: the influence of patient wait time on satisfaction with primary care. *BMC Health Serv Res*. (2007) 7:31. doi: 10.1186/1472-6963-7-31

32. Camacho F, Anderson R, Safrit A, Jones AS, Hoffmann P. The relationship between Patient's perceived waiting time and office-based practice satisfaction. *N C Med J*. (2006) 67:409–13. doi: 10.18043/ncm.67.6.409

33. Konstantinou P, Georgiou K, Kumar N, Kyprianidou M, Nicolaides C, Karekla M, et al. Transmission of vaccination attitudes and uptake based on social contagion theory: a scoping review. *Vaccine*. (2021) 9:607. doi: 10.3390/vaccines9060607

34. Karashiali C, Konstantinou P, Christodoulou A, Kyprianidou M, Nicolaou C, Karekla M, et al. A qualitative study exploring the social contagion of attitudes and uptake of COVID-19 vaccinations. *Hum Vaccin Immunother*. (2023) 19:2260038. doi: 10.1080/21645515.2023.2260038

35. Fu F, Christakis NA, Fowler JH. Dueling biological and social contagions. *Sci Rep*. (2017) 7:43634. doi: 10.1038/srep43634

36. Alvarez-Zuzek LG, Zipfel CM, Bansal S. Spatial clustering in vaccination hesitancy: the role of social influence and social selection. *PLoS Comput Biol*. (2022) 18:e1010437. doi: 10.1371/journal.pcbi.1010437

37. Buttenheim AM, Paz-Soldan V, Barbu C, Skovira C, Quintanilla Calderón J, Mollesaca Riveros LM, et al. Is participation contagious? Evidence from a household vector control campaign in urban Peru. *J Epidemiol Community Health*. (2014) 68:103–9. doi: 10.1136/jech-2013-202661

38. World Health Organization. WHO expert consultation on rabies: Third Report. Geneva: World Health Organization (2018).

39. Cleaveland S. A dog rabies vaccination campaign in rural Africa: impact on the incidence of dog rabies and human dog-bite injuries. *Vaccine*. (2003) 21:1965–73. doi: 10.1016/S0264-410X(02)00778-8

40. Vigilato MAN, Clavijo A, Knobl T, Silva HMT, Cosivi O, Schneider MC, et al. Progress towards eliminating canine rabies: policies and perspectives from Latin America and the Caribbean. *Philos Trans R Soc B*. (2013) 368:20120143. doi: 10.1098/rstb.2012.0143

41. Liang CC. Queueing management and improving customer experience: empirical evidence regarding enjoyable queues. *J Consum Mark*. (2016) 33:257–68. doi: 10.1108/JCM-07-2014-1073

42. Allon G, Kremer M. Behavioral foundations of queueing systems In: K Donohue, E Katok and S Leider, editors. The handbook of behavioral operations [internet]. Hoboken, NJ, USA: John Wiley & Sons, Inc. (2018). 323–66.

43. Zhou R, Soman D. Consumers' waiting in queues: the role of first-order and second-order justice. *Psychol Mark*. (2008) 25:262–79. doi: 10.1002/mar.20208

44. Pan American Health Organization. República Dominicana: Elimination of dog-transmitted rabies in Latin America: Situation analysis. Washington, DC: OPS (2004).

45. Sánchez-Soriano C, Gibson AD, Gamble L, Burdon Bailey JL, Green S, Green M, et al. Development of a high number, high coverage dog rabies vaccination programme in Sri Lanka. *BMC Infect Dis*. (2019) 19:977. doi: 10.1186/s12879-019-4585-z

46. Gibson AD, Handel IG, Shervell K, Roux T, Mayer D, Muyila S, et al. The vaccination of 35,000 dogs in 20 working days using combined static point and door-to-door methods in Blantyre, Malawi. *PLoS Negl Trop Dis*. (2016) 10:e0004824

47. le-Morawa N, Kunkel A, Darragh J, Reede D, Chidavaenzi NZ, Lees Y, et al. Effectiveness of a COVID-19 vaccine rollout in a highly affected American Indian community, San Carlos apache tribe, December 2020-February 2021. *Public Health Rep*. (2023) 138:23S–9S. doi: 10.1177/00333549221120238

48. Sethy G, Chisema MN, Sharma L, Singhal S, Joshi K, Nicks PO, et al. 'Vaccinate my village' strategy in Malawi: an effort to boost COVID-19 vaccination. *Expert Rev Vaccines*. (2023) 22:180–5. doi: 10.1080/14760584.2023.2171398

49. Whitehead J, Carr P, Scott N, Lawrenson R. Structural disadvantage for priority populations: the spatial inequity of COVID-19 vaccination services in Aotearoa. *N Z Med J*. (2022) 135:54–67.

50. Hawkins D. Disparities in access to paid sick leave during the first year of the COVID-19 pandemic. *J Occup Environ Med*. (2023) 65:370–7. doi: 10.1097/JOM.0000000000002784

51. Schnake-Mahl AS, O'Leary G, Mullachery PH, Skinner A, Kolker J, Diez Roux AV, et al. Higher COVID-19 vaccination and narrower disparities in US cities with paid sick leave compared to those without. *Health Aff*. (2022) 41:1565–74. doi: 10.1377/hlthaff.2022.00779

52. Sunar N, Tu Y, Ziya S, Pooled VS. Dedicated queues when customers are delay-sensitive. *Manag Sci*. (2021) 67:3785–802. doi: 10.1287/mnsc.2020.3663

frontiers | Frontiers in Public Health

TYPE Original Research
PUBLISHED 06 June 2025
DOI 10.3389/fpubh.2025.1603158

OPEN ACCESS

EDITED BY
Hazel Stewart,
University of Cambridge, United Kingdom

REVIEWED BY
Victor C. Huber,
University of South Dakota, United States
Cheng Zhang,
Hebei Agricultural University, China

*CORRESPONDENCE
Chongkun Xiao
✉ fangy27001@163.com
Heng Yuan
✉ 447843610@qq.com

†These authors have contributed equally to this work and share first authorship

RECEIVED 31 March 2025
ACCEPTED 23 May 2025
PUBLISHED 06 June 2025

CITATION
Zhou L, Li Z, Zhou X, Zhao L, Peng H, Du X, Yang J, Hu F, Dong S, Li B, Liu G, Tang H, Lei X, Wang X, Zhao S, Zhou P, Yuan H and Xiao C (2025) Investigation of human infection with H5N6 avian influenza cases in Sichuan Province from 2014 to 2024: a retrospective study.
Front. Public Health 13:1603158.
doi: 10.3389/fpubh.2025.1603158

Investigation of human infection with H5N6 avian influenza cases in Sichuan Province from 2014 to 2024: a retrospective study

Lijun Zhou[1†], Zhirui Li[1†], Xingyu Zhou[1], Lin Zhao[2], Huanwen Peng[3], Xunbo Du[4], Jianping Yang[5], Fengmiao Hu[1], Shuang Dong[1], Baisong Li[6], Guidan Liu[7], Hongyu Tang[8], Xiao Lei[9], Xiaojuan Wang[10], Shunning Zhao[11], Ping Zhou[12], Heng Yuan[1*] and Chongkun Xiao[1*]

[1]Department of Disease Control and Prevention, Sichuan Provincial Center for Disease Control and Prevention, Chengdu, China, [2]Nanchong Center for Disease Control and Prevention, Nanchong, China, [3]Dazhou Center for Disease Control and Prevention, Nanchong, China, [4]Chengdu Center for Disease Control and Prevention, Chengdu, China, [5]Bazhong Center for Disease Control and Prevention, Bazhong, China, [6]Chongqing Center for Disease Control and Prevention, Chongqing, China, [7]Zigong Center for Disease Control and Prevention, Zigong, China, [8]Deyang Center for Disease Control and Prevention, Deyang, China, [9]Leshan Municipal Center for Disease Control and Prevention, Leshan, China, [10]Luzhou Center for Disease Control and Prevention, Luzhou, China, [11]Ziyang Center for Disease Control and Prevention, Ziyang, China, [12]Yibin Center for Disease Control and Prevention, Yibin, China

Objective: The objective is to examine the epidemiology and clinical features of human cases infected with H5N6 avian influenza in Sichuan Province from 2014 to 2024, and to offer guidance for the prevention and management of human infections with H5N6 avian influenza.

Methods: Epidemiological survey reports of H5N6 avian influenza cases in Sichuan Province from 2014 to 2024 were compiled, and the epidemiological context and characteristics of 16 human cases infected with H5N6 avian influenza in the province were summarized and analyzed using descriptive epidemiological methods.

Results: From 2014, when the initial human case ofH5N6 infection was documented in Sichuan Province, to 2024, there have been 16 human cases of H5N6 avian influenza in the region, resulting in 12 fatalities and a case fatality rate of 75%. The instances were predominantly located in the Chengdu Plain, eastern Sichuan, and southern Sichuan.

Conclusion: Human instances of H5N6 avian influenza in Sichuan Province exhibit no discernible periodicity, and entail significant fatality rates. It is essential to enhance the early diagnosis and treatment of avian influenza cases in medical facilities, prioritize farmers with preexisting conditions who have been in contact with deceased poultry, conduct influenza virus testing promptly, and administer antiviral medications at the earliest opportunity. Simultaneously, we must effectively engage in public awareness and education for the populace, manage poultry scientifically, and prevent direct contact with deceased poultries.

KEYWORDS

influenza, epidemiology, avian, H5N6, poultry diseases

1 Introduction

The initial human instance of H5N6 influenza was documented in Sichuan Province in 2014, with a resurgence occurring in 2021. By December 31, 2024, there had been 16 documented cases of human infection with H5N6 avian influenza (1). Avian influenza viruses (AIVs) are zoonotic and provide a continual public health risk globally (2). The World Organization for Animal Health characterizes avian influenza as a highly transmissible illness resulting from several subtypes that persistently develop, impacting poultry, avian species, mammals, and, on occasion, humans (3).

The influenza virus is a single-stranded Ribonucleic Acid (RNA) virus categorized into types A, B, C, and D based on antigenic variations in the matrix protein and nucleoprotein (4). The avian influenza virus is classified as type A (5). The avian influenza virus mostly affects avians and sometimes humans. The incubation time for human infection with avian influenza typically ranges from 2 to 5 days, but the incubation period for H5N6 spans from 1 to 13 days, averaging 4.3 days (6). H5N6 avian influenza is a severe respiratory illness. The severity of avian influenza virus infection in humans can vary from asymptomatic or moderate flu-like symptoms to severe respiratory infections, including pneumonia, multiple organ failure, or death (7, 8). The severity of the sickness is contingent upon the subtype of the avian influenza virus responsible for the infection and the physical state of the afflicted individual (9).

While the majority of documented human H5N6 cases have transpired in China, isolated instances of H5N6 viruses have also been detected in poultry and wild avifauna throughout other Southeast Asian nations, including Vietnam and Laos, underscoring the regional dissemination of the virus (10, 11). The H5N6 virus emerged from the reassortment of H5N1 and H5N2 with H6N6 viruses. The hemagglutinin (HA) gene is classified under the H5 evolutionary lineage 2.3.4.4, although its neuraminidase (NA) gene is derived from the H6N6 strain commonly seen in Asian poultry (12, 13). The preliminary reassortment event likely transpired in ducks, who serve as primary hosts for viral amalgamation owing to their vulnerability to various influenza subtypes (14). Following the introduction of the H5N6 virus, genetic reassortment transpired with low pathogenic avian influenza viruses, leading to the selection and evolution of dominant genotypes (G1, G2, G1.1, G1.2) (13). The reassortment events increased the adaptability and transmissibility of the H5N6 virus. Recent research in Sichuan Province identified new triple reassortant H5N6 strains, including genes from H5N8, H6N6, and H9N2, underscoring continuous genetic evolution (15, 16). Moreover, H5N6 viruses have been identified in animals including pigs, cats, and wild birds, suggesting their capacity for interspecies transmission (17).

The H5N6 avian influenza virus continues to represent a significant risk to both poultry and humans (18). A conceptual framework for the dissemination of H5N6 is illustrated in Figure 1. Current reports indicate that, as of April 30, 2025, all documented H5N6 infections originated from China, with the exception of a single case identified in Laos (19). Sichuan Province is the inaugural location where H5N6 was identified globally. This can be elucidated from the following perspectives: (1) Ecological characteristics: Sichuan Province features a diverse terrain with basins, mountains, and plateaus. The climatic classifications encompass subtropical to cold zones, primarily comprising subtropical humid and high-cold climates. This habitat may facilitate the proliferation and dissemination of avian influenza viruses; Sichuan serves as a crucial water supply in the upper sections of the Yangtze and Yellow Rivers, boasting abundant wetland and forest resources that attract numerous migratory birds. Nevertheless, migratory birds may have viruses, heightening the danger of cross-regional transmission of avian influenza (20). (2) Agricultural attributes: Sichuan is a significant rice cultivation region, necessitating substantial water resources. The mixed farming model of rice cultivation and poultry is prevalent, enhancing the likelihood of interaction between poultry and people; live poultry markets and poultry farming are widespread in rural Sichuan, with mixed farming practices present in certain regions. This approach elevates the likelihood of viral reassortment in avian species and its transfer to humans (21). (3) Population characteristics: Sichuan possesses a significant rural demographic, with rural inhabitants exhibiting a lack of awareness regarding avian influenza, hence enhancing the danger of outbreaks (22). (4) Additional factors: AIVs are primarily spread among birds, poultry, and people via migratory bird movements, poultry farms, and transactions in live poultry markets (22, 23). Wild birds serve as natural reservoirs for avian influenza and may disseminate the genetic material of all influenza A virus strains (24). China acts as a significant transit hub for worldwide migratory avifauna. China has three major international migration routes, with two traversing Sichuan Province: the Central Asian Migration Route and the East Asian-Australasian Migration Route (25–27). Two of the three migration routes in China, namely the central and western routes, traverse the Sichuan Basin, where the East Asian-Australasian

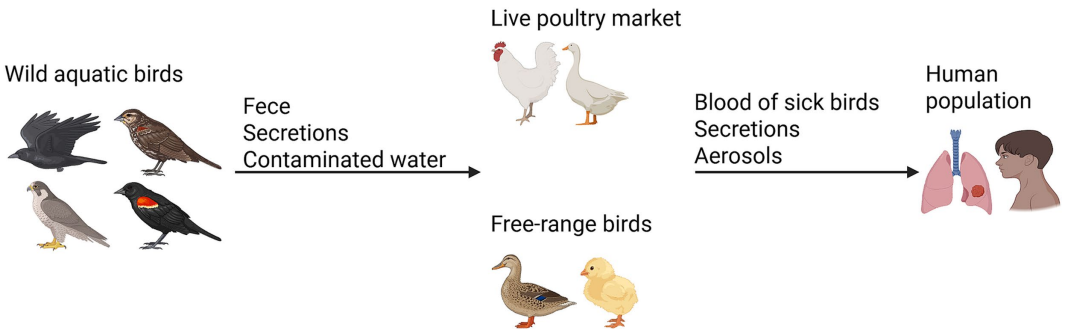

FIGURE 1
A conceptual framework for the dissemination of H5N6.

Migration Route intersects with the Central Asian Migration Route (28, 29). Sichuan Province has emerged as a significant stopover location for several migrating birds, owing to its elevated wetland habitats, diverse wetland ecosystems, and vertical migration pathways (Figure 2). Consequently, the species variety of wild avifauna is greater (30, 31). Migratory birds typically migrate from March to May during spring and from September to November in fall (32, 33).

The primary risk factors for avian influenza infection in poultry farms are wild birds and associated environments, unprotected water sources, and vulnerable animals (34, 35). Fecal-oral transmission constitutes the primary pathway for avian influenza dissemination in poultry, with the virus expelled in elevated titers via feces (36, 37). In regions where poultry farming land coincides with migratory bird pathways, there exists a conduit for the transmission and interchange of viruses between domesticated fowl and wild avians (38). A significant flow of viruses transpires between poultry and adjacent wild birds, potentially resulting in antigenic drift and antigenic shift, finally culminating in the modification of the avian influenza virus (39). The altered novel virus may possess an enhanced capacity to infect animals, including humans. While the transmission pathway and infection mechanism of the avian influenza virus in mammals remain ambiguous, data indicates that several mammalian species have been infected with the virus (40, 41). Future hazards of avian influenza pandemics may arise from frequent genetic recombination and interspecies transmission, necessitating more effective measures to mitigate the risk posed by AIVs (2).

The ecological and geomorphological variety, agricultural structural attributes, and demographic features of Sichuan Province have collectively fostered an environment conducive to the proliferation of avian influenza viruses. This publication analyses and categorizes human cases of H5N6 avian influenza identified in Sichuan Province throughout the years to serve as a reference for the prevention and management of human avian influenza. We further suggested evidence-based solutions to enhance the surveillance system, particularly at high-frequency interaction places between people and poultry, and to priorities preventative interventions for high-risk groups.

2 Methods

2.1 Patients

The cases were individuals infected with the influenza A(H5N6) virus reported in Sichuan Province from January 1, 2014, to April 30,

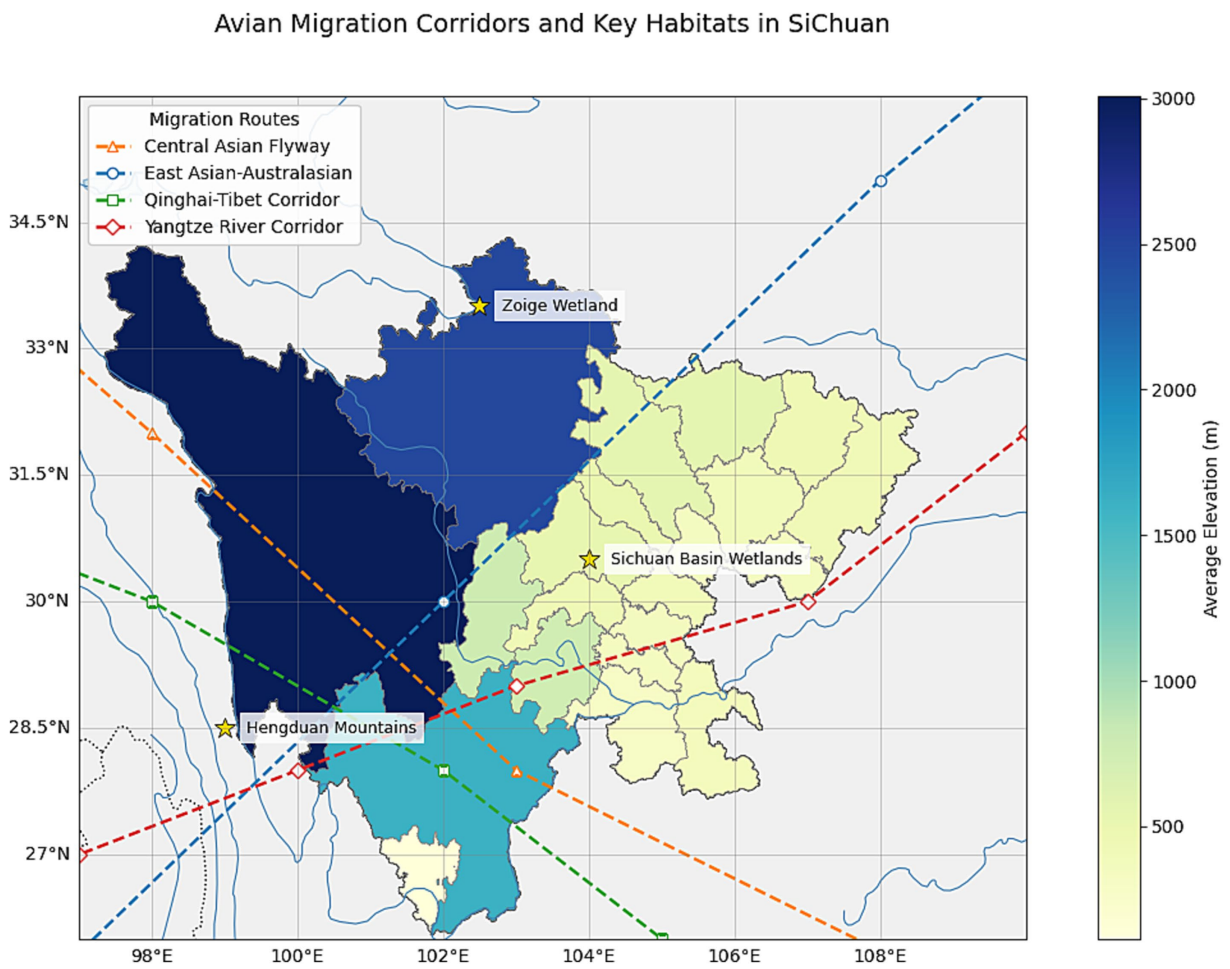

FIGURE 2
Key time intervals in H5N6 cases, Sichuan Province, 2014–2024.

2025. The case data were obtained from the infectious illness monitoring and reporting system and case survey reports of the China Disease Prevention and Control Information System. The primary information encompassed age, gender, employment, domicile, onset time, hospitalization duration, medical history, poultry exposure history, specimen collection, and laboratory test findings etc. The data were derived from epidemiological surveys and laboratory testing performed by medically trained investigators and physicians, after patient consent. Sichuan Province has implemented a sentinel hospital monitoring network including all cities since 2009. Each sentinel hospital gathers 10–40 specimens of influenza-like cases weekly and does nucleic acid testing for the influenza virus. No mild cases of H5N6 avian influenza have been identified to yet.

2.2 Environmental monitoring

According to the Technical Guidelines for the Prevention and Control of Influenza of Human Infection of Animal Origin, all cities (21) within the province are implementing external environmental surveillance for avian influenza. Two or more locations are designated, encompassing live poultry market, Family poultry farm, Poultry processing plants, Wild migratory bird habitat, with monitoring conducted monthly (42). A minimum of 10 specimens are gathered monthly, totaling 120 specimens each city year.

2.3 Research methods

Real-time Quantitative PCR was employed to identify influenza virus nucleic acid in environmental samples from confirmed patients and probable exposure locations. The case definition and monitoring techniques have remained unchanged over the past decade. A case is characterized by the isolation of the avian influenza virus from an individual's respiratory secretions or other pertinent materials, or the detection of the virus using nucleic acid testing or deep sequencing. In Sichuan Province, case confirmation mostly relies on positive nucleic acid test findings and associated clinical signs. Close contacts were identified as those who interacted with cases and personnel who failed to implement adequate protective measures throughout the diagnosis and treatment of cases; this includes individuals who had close contact with cases from 1 day prior to the start of symptoms to the initiation of isolation. We gathered patients' medical records and performed verification, monitoring, and medical assessment in compliance with the Technical Guidelines for the Prevention and Control of Animal-Origin Influenza in Human Infection. Close contacts were monitored according to the comprehensive range of activities from the day preceding the commencement of the case until isolation treatment or death. Close contacts encompass: medical personnel who inadequately safeguarded themselves while diagnosing and treating suspected, clinically diagnosed, or confirmed cases, as well as other individuals who attended to these cases; individuals residing with or having close interactions with suspected, clinically diagnosed, or confirmed cases from 1 day prior to the onset of the illness until isolation treatment or death; and additional individuals requiring management following an on-site investigation.

In order to more accurately represent the central trend and variations, we employed box plots to emphasize the distribution of three distinct time periods: (a) time from onset to hospitalization, (b) time from hospitalization to commencement of treatment, and (c) time from treatment to outcome.

2.4 Statistical analysis

The monitoring data were compiled using Excel 2019, and the descriptive epidemiological approach was employed to examine the outcomes of human infections with H5N6 avian influenza. The statistical analysis software employed was R version 4.2.1. Owing to the exceedingly limited sample size of our study (e.g., survival group $n = 4$), the p value may not accurately represent the genuine difference; hence, the effect size is illustrated through the confidence interval. Continuous variables are expressed as mean ± SD (95% CI), with group differences indicated by the mean difference via Welch's t test; categorical variables are represented as proportions % (95% CI), with group differences denoted by the proportion difference using the Newcombe-Wilson method. Data visualization and visuals were created using the VS Code editor and the Python programming language, using relevant libraries like Matplotlib 3.5.1 and Seaborn 0.11.2.

3 Results

3.1 Demographic distribution

Table 1 presents the fundamental details of the 16 instances. The male-to-female ratio among the patients was 1:1, and the case fatality rate was 75%; the median age was 54.5 years (IQR: 27–75); the occupational distribution predominantly consisted of farmers, accounting for 12 cases (75%). Of the 16 patients, 12 (75%) had preexisting conditions, while 4 cases (25%) were previously healthy. The case fatality rate for patients with underlying conditions was 83.33%, above that of individuals without such conditions, which was 50.00%.

3.2 Geographical allocation

Figure 3 illustrates 16 instances of human infection with H5N6 avian influenza identified in Sichuan Province between 2014 and 2024. The instances were predominantly located in the Chengdu Plain, as well as eastern and southern Sichuan. Nanchong and Dazhou had the highest incidence, with 3 instances apiece; followed by Chengdu and Bazhong, each with 2 cases; and Deyang, Leshan, Luzhou, Yibin, Ziyang, and Zigong, each with 1 case.

3.3 Onset and treatment

Figures 4, 5 illustrate the timings of the three critical nodes: "onset to hospitalization," "hospitalization to treatment," and "treatment to outcome" for the 16 patients, along with the disparities in the distribution of these three indicators between the mortality group and the survival group. The median duration from beginning to hospitalization was 4 days (range: 0–13 days), suggesting that while some patients were treated promptly, others had significant delays. The

10.3389/fpubh.2025.1603158

TABLE 1 Basic information on human infections of H5N6 avian influenza in Sichuan Province from 2014 to 2024.

Characteristics	Deceased (*n* = 12) (95% CI)	Survived (*n* = 4) (95% CI)	Between-group difference (95% CI)
Age (year, mean ± SD)	52.8 ± 15.7 (42.3–63.2)	55.8 ± 7.9 (44.9–66.6)	Δ-3.0 (−20.1–14.1)
Gender n (%)			
Female	3 (25.0%, 5.5–57.2%)	2 (50.0%, 6.7–93.3%)	Δ-25.0% (−64.1–14.1%)
Male	9 (75.0%, 42.8–94.5%)	2 (50.0%, 6.7–93.3%)	Δ25.0% (−14.1–64.1%)
Occupation n (%)			
Farmer	9 (75.0%, 42.8–94.5%)	3 (75.0%, 19.4–99.4%)	Δ0.0% (−48.1–48.1%)
Others	3 (25.0%, 5.5–57.2%)	1 (25.0%, 0.6–80.6%)	Δ0.0% (−48.1–48.1%)
Time Intervals (days, mean ± SD)			
Onset to hospital admission	5.4 ± 4.3 (2.6–8.3)	3.3 ± 1.5 (0.9–5.6)	Δ2.1 (−2.3–6.5)
Hospital admission to ICU entry	1.6 ± 1.2 (0.8–2.4)	3.0 ± 2.2 (0.0–6.5)	Δ-1.4 (−3.9–1.1)
Onset to diagnosis	11.2 ± 6.5 (6.9–15.4)	9.5 ± 4.4 (2.7–16.3)	Δ1.7 (−6.1–9.5)
Hospital admission to initiation of antiviral treatment	2.1 ± 3.0 (0.1–4.1)	1.3 ± 0.5 (0.0–2.5)	Δ0.8 (−1.8–3.4)
Interventions			
ECMO* use (%)	33.3 (9.9–65.1)	25.0 (0.6–80.6)	Δ8.3 (−34.1–50.7)
Antiviral treatment use (%)	83.3 (51.6–97.9)	100.0 (39.8–100.0)	Δ-16.7 (−44.4–11.0)
Exposure history			
Contact with sick/dead poultry (%)	58.3 (27.7–84.8)	75.0% (19.4–99.4%)	Δ-16.7% (−54.1–20.7%)

* ECMO: Extracorporeal Membrane Oxygenation.

median duration from hospitalization to the initiation of antiviral medication was 3 days (range: 1–10 days), indicating a potential delay in commencing treatment post-hospitalization. The median period from therapy to result was 6 days (range: 1–11 days), reflecting variability in illness regression.

The findings on the duration from beginning to hospitalization indicated that the median disparity between the mortality group and the survival group was minimal, with a significant overlap in distribution, predominantly concentrated between 5 to 10 days. The analysis of the duration from hospitalization to the initiation of antiviral therapy indicated that the survival cohort commenced treatment more uniformly and somewhat sooner, whereas the timing of treatment initiation in the mortality cohort exhibited greater variability, with notable delays in certain instances. The duration from antiviral therapy to outcome was shorter in the mortality group, suggesting fast disease progression. The duration from antiviral therapy to discharge/recovery in the survival cohort was comparatively prolonged, aligning with the clinical recovery trajectory. Our findings indicated a tendency of differences between the mortality group and the survival group; however, none achieved statistical significance, likely attributable to the limited sample size impacting statistical power. The occurrence of delayed treatment and subsequent quick mortality in the deceased cohort is noteworthy and will be further examined in a larger sample in the future.

3.4 Poultry exposure

Table 2 presents the poultry exposure history associated with the patients. Following epidemiological research and laboratory analysis, 10 of the 16 patients exhibited a history of contact with deceased poultry, representing 62.5%; 12 cases, or 75.00%, tested positive for H5N6 or H5 subtypes in chicken specimens at their residences. A total of 203 close connections of the 16 patients were identified, and all close contacts received health monitoring for a minimum of 10 days. No anomalies were identified during the health monitoring period, and no influenza virus was discovered in respiratory specimens at the commencement and conclusion of the monitoring.

3.5 Environmental monitoring

Environmental monitoring in Sichuan Province is conducted in line with the Sichuan Provincial Avian Influenza Environmental Monitoring Program. Every city gathers a minimum of 10 poultry-related samples monthly. Sampling stations are designated in regions with elevated exposure concerns, including poultry drinking water, faeces, and areas of intense poultry operations. The gathered specimens are preserved at 4°C, dispatched to the laboratory within 48 h, and the viral nucleic acid assay is finalized within 1 week. Between 2019 and 2024, 14,397 external environmental samples were collected, of which 1,362 tested positives for the H5 subtype, resulting in a positivity rate of 9.46%. Figure 6 illustrates the monthly distribution of positive test results for the H5 subtype. The months with the highest number of H5 positive samples are July, October, and December. Figure 6 provide the sources of H5 positive samples, respectively. Among the monitored sites, the poultry slaughter board (400 instances) and the sewage used for washing poultry (300 cases) exhibited the highest number of positive samples; regarding sample

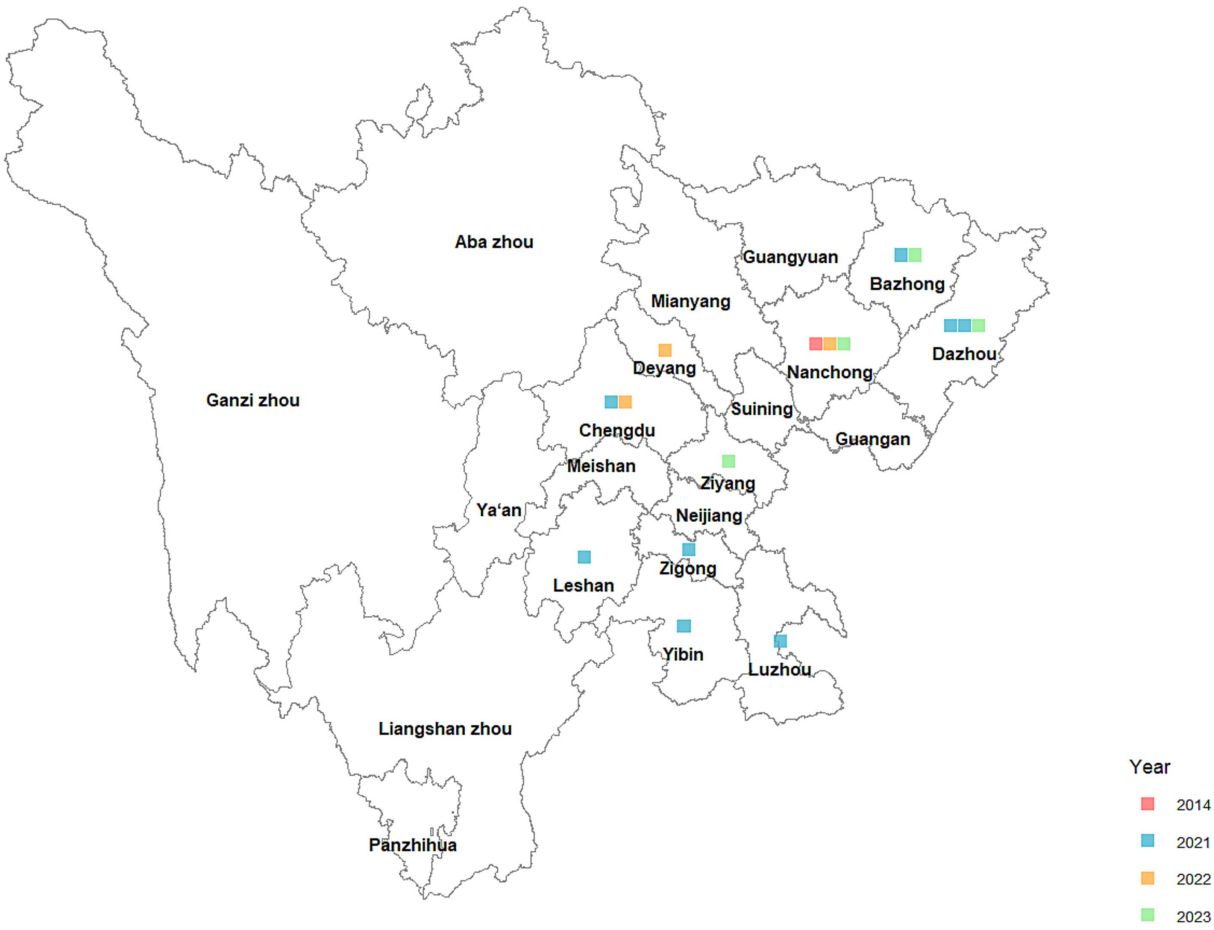

FIGURE 3
Geographical distribution of human infections with H5N6 avian influenza in Sichuan Province, 2014–2024.

sources, the live poultry market recorded the most positive samples (303 cases).

4 Discussion

The cases identified in Sichuan Province placed second, constituting 17.39% of all H5N6 cases. Prior research indicates that the death rate for human infections with H5N6 avian influenza can reach 55.4%, predominantly affecting older individuals, with a median age of around 51 years (9). Our study findings support this perspective. The case fatality rate for human infections with H5N6 avian influenza in Sichuan Province was 75%, with a median age of 54.5 years. The initial human infection strain in Sichuan Province in 2014 (A/Sichuan/1/2014) was a reassortant of H5N1 and H6N6, with its HA gene classified under Clade 2.3.4.4 (1). The HA gene of the strain predominant in Guangdong Province is classified within Clade 2.3.4.4, but the origin of the NA gene is intricate. In contrast to the strain in Sichuan Province, the strain in Jiangsu Province has a V100A mutation in the PB1-F2 protein (43, 44). The H5N6 strain isolated in early Europe (Germany A/duck/Germany/AR844/2007) has minimal pathogenicity, with its HA gene classified under Clade 2.2.1, distinct from the evolutionary lineage of highly pathogenic strains in Asia (45).

The primary route of transmission of AIVs often occurs in wild birds (46). AIVs and genetic pieces can sustain viral genetic variety via the dissemination of wild birds (47). Sichuan Province serves as a significant nexus in the migratory pathway of avian species in western China, boasting a diverse array of bird species. The China Bird Watching Record Center[1] reports that Sichuan Province is the second most species-rich area in the nation, with 699 species documented. This establishes the conditions for the dissemination and genetic recombination of AIVs among various wild bird species (46). The capacity of viruses to traverse species boundaries is generally restricted, and AIVs cannot swiftly multiply in humans directly (48). Nonetheless, avian transmission may indirectly elevate the risk of human infection, particularly in regions exhibiting significant genetic variety of the virus, where variants capable of circumventing barriers may be more prone to emergence (49). Despite the seldom positive tests for the H5 subtype in specimens gathered from wild bird habitats in Sichuan Province, the unique ecological attributes may still be linked to the elevated occurrence of H5N6 infections. The virus's genetic variety may be perpetually augmented by transmission by

1 http://www.birdreport.cn

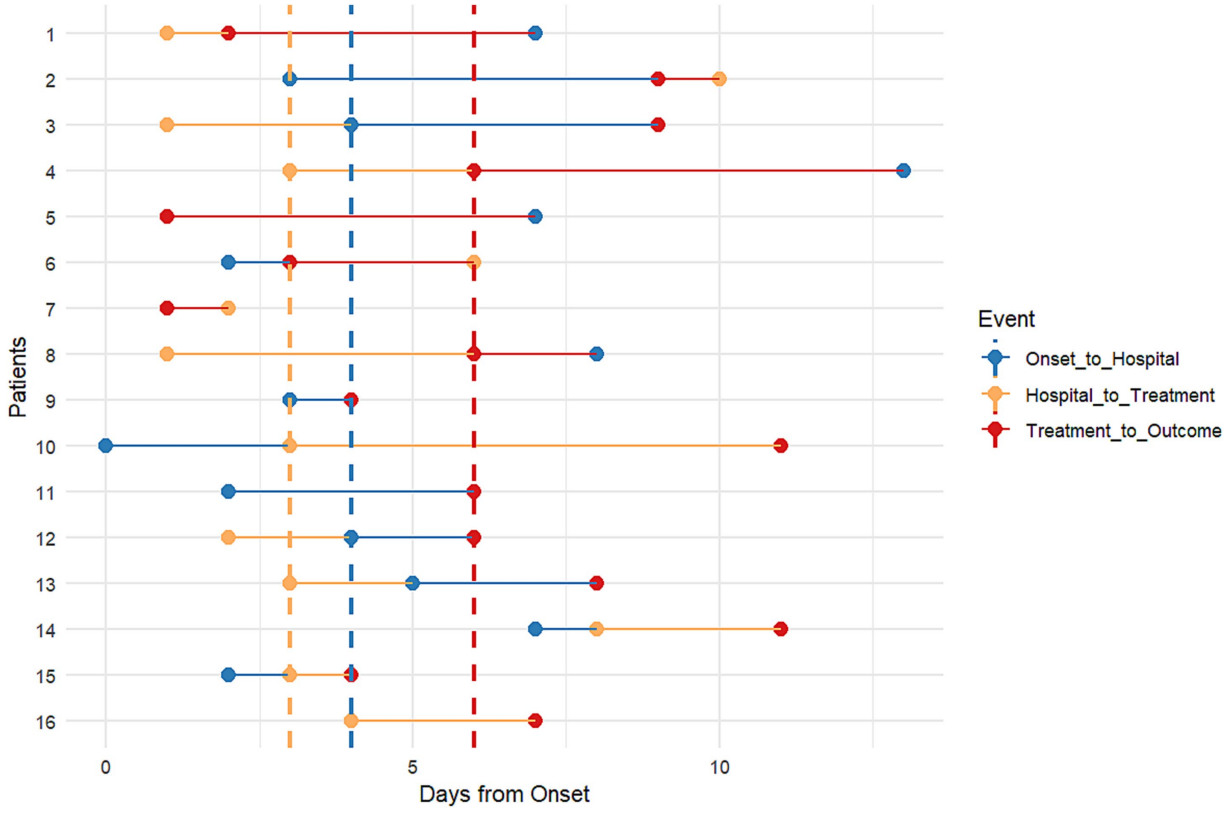

FIGURE 4
Avian migration corridors and key habitats in Sichuan.

migrating birds, leading to Sichuan Province having one of the highest incidences of H5N6 case reports in the nation. Future collaborative ecological-epidemiological investigations are necessary to further substantiate the causal link.

Avian influenza is a secondary transmission pathway via poultry farms and associated transportation networks (50). The cumulative monthly case distribution exhibited a bimodal pattern in winter and summer, aligning with the H5 positivity distribution results seen in our external environment. The winter peak may result from low temperatures facilitating the prolonged survival of the avian influenza virus in external environments, such as feces, whereas the summer peak may stem from a decrease in poultry immunity under high-temperature and high-humidity conditions, hence triggering the epidemic (36, 51). Results from environmental monitoring indicate that live poultry markets are the primary source of avian influenza virus detection. Poultry slaughtering boards and washing wastewater are the two sample classes with the highest number of positive specimens, indicating a significantly elevated risk of viral transmission during poultry slaughtering and washing processes (52). The affirmative identification of cage surface and fecal samples indicates that the transportation of live poultry and fecal contamination remain significant transmission pathways, and inadequate sanitation of transport cages may result in cross-regional transmission (52). The prevalence of positives on family poultry farm and natural migratory bird habitats is comparatively low, maybe because to the limited size of breeding or inadequate monitoring of migratory bird habitats. Despite the low incidence of positive detections, the potential for farmed poultries to interact with wild birds may facilitate viral mutation and recombination (53).

The investigation's findings indicated that contact with deceased poultry or their feces was the primary mode of infection for the case, succeeded by exposure to live poultry markets. The eastern and southern districts of Sichuan Province exhibit a substantial volume of poultry breeding and commerce, facilitating the maintenance and dissemination of the virus to a considerable degree (54). Temporary market closures in Guangdong, Shanghai, and other regions have markedly diminished the probability of H7N9 pandemic spread (55). The epidemic was contained after Guangdong halted live poultry trading during the Spring Festival in 2015, and the Xuhui District of Shanghai has not reported any human infection cases since the permanent closure of its live poultry market in 2013, demonstrating that prolonged closure can effectively impede the virus's transmission (50, 56). Nevertheless, owing to inadequate law enforcement and the populace's love for live poultry in Nanjing and other locales, illicit commerce has persisted despite several prohibitions, undermining the efficacy of preventative and control measures (57). This indicates that market closure regulations must be supplemented by rigorous law enforcement and public education initiatives. In rural regions, altering entrenched consumption patterns or constrained resources poses challenges for policy implementation. Future interventions in live poultry markets will necessitate a more adaptable approach (50, 55).

Chickens and ducks constituted the predominant species among the deceased poultry with whom the cases had contact, reflecting the

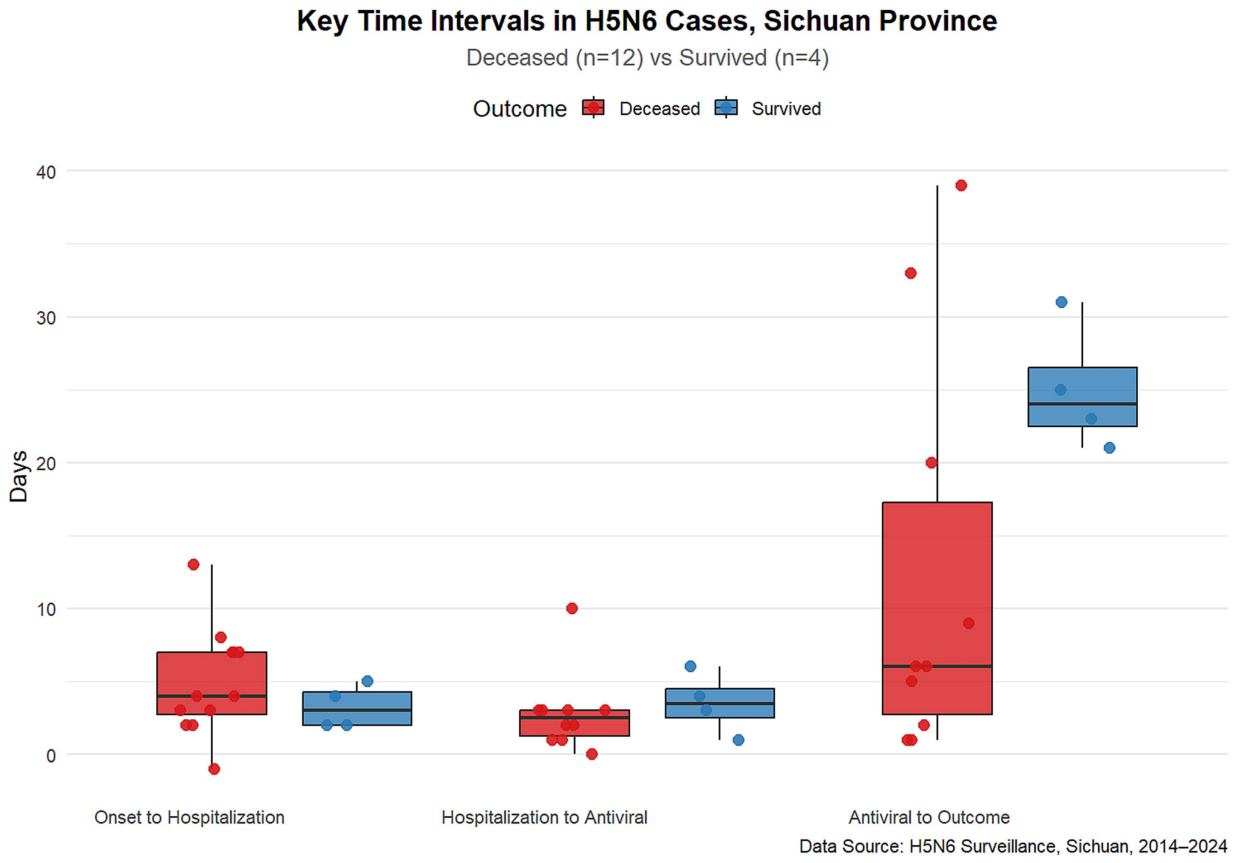

FIGURE 5
Timeline of "Onset to Hospital," "Hospital to Treatment," "Treatment to Outcome" of human cases of avian influenza H5N6 in Sichuan Province, 2014–2024.

prevalent breeding practices in Sichuan Province. The high-density breeding might have resulted in frequent interactions among birds, facilitating the fast transmission of the virus through feces, respiratory secretions, and other means (58). It is important to recognize that migrating birds may interact with the environments around farms throughout their migration paths, potentially introducing wild diseases to chicken populations. Should wild viruses exchange genetic material with AIVs in poultry, new strains potentially more transmissible to humans may emerge (46). Of the cases with positive specimens identified in the market, 85.7% (6/7) of the samples from domestic fowl were positive. This indicates that the virus might be spread indirectly via environmental contamination, necessitating an expansion of the monitoring parameters for the external environment in the future. In 2021, the market conditions for cases in Bazhong and Zigong were unexamined or the outcomes were indeterminate; nonetheless, the home specimens yielded positive findings, suggesting inadequate testing coverage. In 2022, a case in Nanchong City had no history of exposure; yet, house specimens tested positive, suggesting the existence of an unidentified transmission chain. In the future, it is essential to address surveillance deficiencies and explore the potential for asymptomatic poultry to harbor the virus.

Individuals with preexisting conditions, pregnant women, and other demographics are at elevated risk of severe illness and mortality due to zoonotic avian influenza (59). Epidemiological survey data from 16 cases in Sichuan Province indicated a significant prevalence of underlying disorders, with just 3 instances lacking such conditions, of which 2 were successfully treated. The cure rate for individuals without comorbidities was much superior to that of those with comorbidities. Individuals infected with H5N6 in Sichuan Province typically have a tendency to postpone medical intervention following the commencement of the illness. The box plot results indicate significant disparities in the time of treatment across various instances, implying the absence of a cohesive and standardized protocol to govern the commencement timing of antiviral therapy. This may occur due to their frequent misidentification as typical colds in the first phases of the illness. The mean duration from the beginning of symptoms to hospital admission was 4.6 days, surpassing the advised treatment duration for antiviral medications against influenza (60). The elevated case fatality rate of human H5N6 virus infections in Sichuan Province is mostly attributable to delayed diagnosis and treatment. The majority of patients reside in rural regions and initially pursue medical care at primary healthcare facilities or self-medicate, leading to lost chances for early intervention. Simultaneously, as human infections with avian influenza are few, medical institutions have limited exposure to such cases, resulting in a deficiency of experience in early detection. The duration from beginning to diagnosis is prolonged, hence hindering the prompt administration of anti-influenza medications.

During the 10-day monitoring period for close contact tracking, no abnormal symptoms were observed, and all respiratory specimens

10.3389/fpubh.2025.1603158

TABLE 2 Environmental exposure history of H5N6 avian influenza cases in Sichuan Province from 2014 to 2024.

Year	Region	Live Poultry Market Exposure	Positive specimens detected in the market	Diseased or dead birds in and around your residence	Exposure to diseased or dead birds	Consumption of diseased or dead birds	Types of sick and dead birds	Positive avian specimens in residential environment
2014	Nanchong[1]	Yes	No	Yes	Yes	Yes	Chicken, Duck, Goose	Yes
2021	Chengdu[1]	Yes	Yes	No	No	No	—	No
2021	Bazhong[1]	No	Untested	Yes	Yes	No	Chicken, Duck, Goose	Yes
2021	Dazhou[1]	Yes	Yes#	Yes	Yes	Yes	Chicken, Duck	Yes#
2021	Dazhou[2]	Yes	Yes	Yes	Yes	Unknown	Chicken, Duck	Yes#
2021	Yibin	Yes	Yes	Yes	Yes	Yes	Chicken	Yes#
2021	Zigong	Unknown	Untested	Yes	Yes	Yes	Chicken, Duck	Yes
2021	Leshan	Unknown	Untested	Yes	Yes	Yes	Chicken	Yes
2021	Luzhou	Unknown	Yes	Yes	Yes	Yes	Chicken, Duck	Yes
2022	Nanchong[2]	No	No	No	No	No	—	Yes
2022	Chengdu[2]	Yes	Yes	No	No	No	—	No
2022	Deyang	No	No	No	Yes	No	Chicken	No
2023	Nanchong[3]	Yes	Yes	Yes	Yes	No	Chicken, Goose	Yes
2023	Dazhou[3]	No	Yes#	No	No	No	—	Yes#
2023	Bazhong[2]	Yes	Yes	No	No	No	—	No
2023	Ziyang	Yes	Yes	No	No	No	—	Yes

* a for farm exposures, # for positive detections of H5 only.

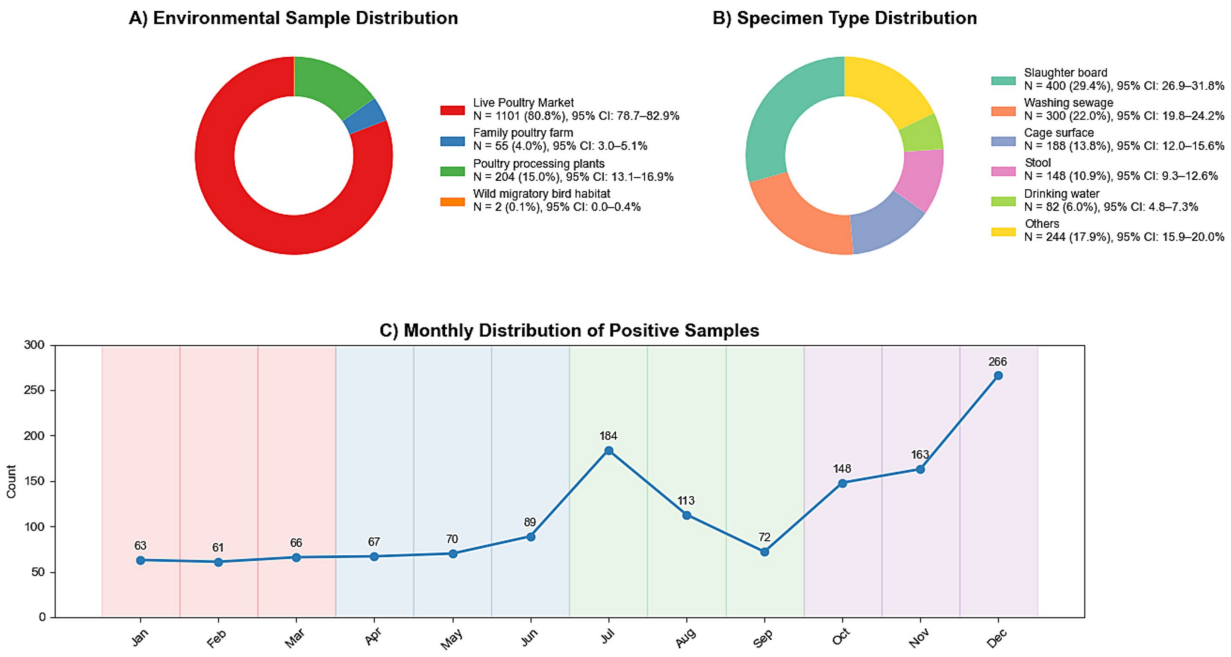

FIGURE 6
Pie chart of sample sources and locations for testing positive for subtype H5. **(A)** Environmental sample distribution; **(B)** Specimen type distribution; **(C)** Monthly distribution of positive samples.

tested negative, indicating that the H5N6 avian influenza virus is not yet capable of human-to-human transmission, consistent with the characteristic difficulty AIVs have in overcoming the "bird-to-human" transmission barrier (9, 61). H5N6 strains exhibit a pronounced affinity for the α2-3 sialic acid receptor (SAα2-3Gal), prevalent in the respiratory and gastrointestinal systems of avian species (62). While several strains exhibit partial affinity for human-like α-2,6-linked sialic acid receptors *in vitro*, their binding rate remains markedly inferior to that of influenza viruses adapted to humans. In comparison to other avian influenza viruses (such as H7N9 and H5N1), H5N6 strains predominantly remain exclusive to avian receptors and seldom propagate in clusters (62, 63). Certain mutations indicate that H5N6 may possess the capability to adapt to certain animals. The E627K mutation in the PB2 gene can augment the virus's replication capacity in mammalian cells, while the HA-T160A mutation may result in the elimination of glycosylation sites, hence enhancing the virus's evasion of host protection (64, 65). The existing receptor binding range and gene mutation pattern collectively provide the constraints on human-to-human transmission, and the critical location (HA-Q226L/G228S) remains unmutated. Consequently, the immediate pandemic threat posed by the H5N6 virus is quite minimal (66, 67). The significant diversity of the virus and its strong connection to chicken markets will persist in necessitating enhanced viral surveillance and interdisciplinary collaboration to mitigate possible pandemic threats. Despite the virus's now restricted transmissibility among individuals, ongoing surveillance of its genetic alterations is essential.

Currently, China lacks an avian influenza immunization initiative for high-risk populations. Nevertheless, several nations have previously used these techniques on an international scale. In 2024, Finland initially revealed intentions to immunize persons at occupational risk of avian influenza, including veterinarians and laboratory technicians (68). In 2025, Canada announced the acquisition of 500,000 doses of the human avian influenza vaccine, distributing them to high-risk populations, including laboratory personnel, close connections, and agricultural workers (69). These initiatives underscore the potential of vaccination as a crucial preventative measure for humans in the future, and tailored vaccination efforts for high-risk populations may also be executed in China thereafter.

The limitation of our analysis is that 16 cases insufficiently represent the whole risk profile of the province, necessitating the integration of additional epidemiological data about subtypes and locations. Considering our limited sample size, a non-significant *p*-value does not inherently indicate an absence of practical or therapeutic significance; rather, we must interpret these findings with care. Future research should integrate data from other locations to enhance statistical power and the generalizability of the findings. Nucleic acid testing has only been performed on environmental samples; research such as viral load measurement, genetic identification of isolates, and comparative study of viral sequences between poultry and human cases have not yet been done. Subsequent experiments may be undertaken to investigate the kinetics of viral transmission.

In the short term, we intend to enhance our findings by offering specific policy recommendations that might directly inform public health policy. We propose the implementation of advanced surveillance systems focused on regions with substantial chicken supply and closeness to live poultry markets, alongside systematic monitoring of wild bird populations and poultry farms, while also tracking human cases. These tools will facilitate the early detection of epidemics and inform targeted interventions. Furthermore, we endorse the development of explicit and succinct risk communication materials aimed at vulnerable populations and healthcare professionals, as well as the use of several communication channels to guarantee extensive distribution. We advocate for the creation of clinical management algorithms to assist healthcare professionals in the timely identification and treatment of H5N6 infections, highlighting the importance of early antiviral therapy for high-risk populations and the use of extracorporeal membrane oxygenation (ECMO) in severe instances. Prolonged investigation for forthcoming developments, we advocate for the establishment of targeted vaccination initiatives for high-risk populations, regular disinfection procedures for poultry farms and live poultry markets, and cost-effectiveness assessments to identify the most economically viable strategies for preventing outbreaks and alleviating social repercussions. The integration of human and animal monitoring systems is still constrained, and mechanisms for direct data sharing with agricultural authorities have not been completely realized. In light of the rise in instances, further study will incorporate additional socio-demographic characteristics, socio-economic status, and health literacy levels. We also promote the enhancement of interdepartmental data connectivity to bolster early warning systems and augment the surveillance of avian influenza under the "One Health" plan.

5 Conclusion

Sichuan Province has a significant prevalence of H5N6, and the cases with elevated fatality rates are of considerable concern. The infection risk of avian influenza in the province is mostly associated with exposure to live poultry markets, contact with deceased poultry, and environmental contamination, with chickens and ducks serving as the principal hosts. The province serves as a migratory habitat for avian species. In the future, it may be essential to disrupt the transmission chain through comprehensive interventions involving "wild birds-live poultry trading markets-breeding areas-households," and to address the threat of potential avian influenza variants by enhancing environmental monitoring and virus traceability research.

Data availability statement

The raw data supporting the conclusions of this article will be made available by the authors, without undue reservation.

Ethics statement

Written informed consent was obtained from the individual(s) for the publication of any potentially identifiable images or data included in this article.

Author contributions

LijZ: Conceptualization, Data curation, Formal analysis, Investigation, Methodology, Project administration, Resources, Software,

Validation, Visualization, Writing – original draft, Writing – review & editing. ZL: Investigation, Methodology, Project administration, Resources, Software, Validation, Visualization, Writing – original draft, Writing – review & editing. XZ: Investigation, Methodology, Supervision, Writing – review & editing. LinZ: Data curation, Resources, Writing – review & editing. HP: Data curation, Resources, Writing – review & editing. XD: Data curation, Resources, Writing – review & editing. JY: Data curation, Resources, Writing – review & editing. FH: Data curation, Resources, Writing – review & editing. SD: Data curation, Resources, Software, Writing – review & editing. BL: Data curation, Resources, Writing – review & editing. GL: Data curation, Resources, Writing – review & editing. HT: Data curation, Resources, Writing – review & editing. XL: Data curation, Resources, Writing – review & editing. XW: Data curation, Resources, Writing – review & editing. SZ: Data curation, Resources, Writing – review & editing. PZ: Data curation, Resources, Writing – review & editing. HY: Methodology, Supervision, Writing – original draft, Writing – review & editing. CX: Formal analysis, Methodology, Supervision, Writing – original draft, Writing – review & editing.

Funding

The author(s) declare that no financial support was received for the research and/or publication of this article.

Acknowledgments

This study was supported by Sichuan center for disease control and prevention.

Conflict of interest

The authors declare that the research was conducted in the absence of any commercial or financial relationships that could be construed as a potential conflict of interest.

Generative AI statement

The authors declare that no Gen AI was used in the creation of this manuscript.

Publisher's note

References

1. Pan M, Gao R, Lv Q, Huang S, Zhou Z, Yang L, et al. Human infection with a novel, highly pathogenic avian influenza A (H5N6) virus: virological and clinical findings. *J Infect*. (2016) 72:52–9. doi: 10.1016/j.jinf.2015.06.009

2. Kang M, Wang LF, Sun BW, Wan WB, Ji X, Baele G, et al. Zoonotic infections by avian influenza virus: changing global epidemiology, investigation, and control. *Lancet Infect Dis*. (2024) 24:e522–31. doi: 10.1016/S1473-3099(24)00234-2

3. Li YT, Linster M, Mendenhall IH, Su YC, Smith GJ. Avian influenza viruses in humans: lessons from past outbreaks. *Br Med Bull*. (2019) 132:81–95. doi: 10.1093/bmb/ldz036

4. Skelton RM, Huber VC. Comparing influenza virus biology for understanding influenza d virus. *Viruses*. (2022) 14:1036. doi: 10.3390/v14051036

5. Bi Y, Yang J, Wang L, Ran L, Gao GF. Ecology and evolution of avian influenza viruse. *Curr Biol*. (2024) 34:R716–21. doi: 10.1016/j.cub.2024.05.053

6. Li F, Sun Z, Tao M, Song K, Wang Z, Ren X. Epidemiological characterization of human infection with H5N6 avian influenza. *Front Public Health*. (2024) 12:1398365. doi: 10.3389/fpubh.2024.1398365

7. Guan W, Qu R, Shen L, Mai K, Pan W, Lin Z, et al. Baloxavir marboxil use for critical human infection of avian influenza A H5N6 virus. *Medicine*. (2024) 5:32–41. doi: 10.1016/j.medj.2023.11.001

8. Zhu W, Li X, Dong J, Bo H, Liu J, Yang J, et al. Epidemiologic, clinical, and genetic characteristics of human infections with influenza A (H5N6) viruses, China. *Emerg Infect Dis*. (2022) 28:1332. doi: 10.3201/eid2807.212482

9. Tiwari A, Meriläinen P, Lindh E, Kitajima M, Österlund P, Ikonen N, et al. Avian influenza outbreaks: human infection risks for beach users-one health concern and environmental surveillance implications. *Sci Total Environ*. (2024) 943:173692. doi: 10.1016/j.scitotenv.2024.173692

10. Sengkeopraseuth B, Co KC, Leuangvilay P, Mott JA, Khomgsamphanh B, Somoulay V, et al. First human infection of avian influenza A (H5N6) virus reported in Lao People's Democratic Republic, February–march 2021. *Influenza Other Respir Viruses*. (2022) 16:181–5. doi: 10.1111/irv.12934

11. Tsunekuni R, Sudo K, Nguyen PT, Luu BD, Phuong TD, Tan TM, et al. Isolation of highly pathogenic H5N6 avian influenza virus in southern Vietnam with genetic similarity to those infecting humans in China. *Transbound Emerg Dis*. (2019) 66:2209–17. doi: 10.1111/tbed.13294

12. Zhao W, Liu X, Zhang X, Qiu Z, Jiao J, Li Y, et al. Virulence and transmission characteristics of clade 2.3. 4.4 b H5N6 subtype avian influenza viruses possessing different internal gene constellations. *Virulence*. (2023) 14:2250065. doi: 10.1080/21505594.2023.2250065

13. Li H, Li Q, Li B, Guo Y, Xing J, Xu Q, et al. Continuous reassortment of clade 2.3.4.4 H5N6 highly pathogenetic avian influenza viruses demonstrating high risk to public health. *Pathogens*. (2020) 9:670. doi: 10.3390/pathogens9080670

14. Shehata AA, Hafez HM. Avian influenza In: H. M. Hafez, editor. Turkey diseases and disorders volume 2: Infectious and nutritional diseases diagnostics and control strategies. (Berlin, Germany: Springer Nature, Institute of Poultry Diseases, Free University of Berlin). (2024). 3–20. doi: 10.1007/978-3-031-63322-5

15. Sun R, Jiang W, Liu S, Peng C, Yin X, Liu H, et al. Emergence of novel reassortant H5N6 influenza viruses in poultry and humans in Sichuan Province, China. *J Infect*. (2022) 84:e50–2. doi: 10.1016/j.jinf.2022.03.003

16. Ke YK, Han XY, Lin SR, Wu HG, Li YX, Liu RQ, et al. Emergence of a triple reassortment avian influenza virus (A/H5N6) from wild birds. *J Infect*. (2024) 88:5. doi: 10.1016/j.jinf.2024.01.005

17. Shao JW, Zhang XL, Sun J, Liu H, Chen JM. Infection of wild rats with H5N6 subtype highly pathogenic avian influenza virus in China. *J Infect*. (2023) 86:e117–9. doi: 10.1016/j.jinf.2023.03.007

18. Li J, Fang Y, Qiu X, Yu X, Cheng S, Li N, et al. Human infection with avian-origin H5N6 influenza a virus after exposure to slaughtered poultry. *Emerg Microbes Infect*. (2022) 11:807–10. doi: 10.1080/22221751.2022.2048971

19. EB/OL Centre for Health Protection (2025).

20. Bui CM, Gardner L, Macintyre R, Sarkar S. Influenza A H5N1 and H7N9 in China: A spatial risk analysis. *PLoS One*. (2017) 12:e0174980. doi: 10.1371/journal.pone.0174980

21. Xiao C, Xu J, Lan Y, Huang Z, Zhou L, Guo Y, et al. Five independent cases of human infection with avian influenza H5N6—Sichuan Province, China. *China CDC Wkly*. (2021) 3:751. doi: 10.46234/ccdcw2021.187

22. Sun Z, Li YP, An Q, Gao X, Wang HB. Risk factors contributing to highly pathogenic avian influenza H5N6 in China, 2014–2021: based on a MaxEnt model. *Transbound Emerg Dis*. (2023) 2023:6449392. doi: 10.1155/2023/6449392

23. Tawakol MM, Nabil NM, Samir A, Yonis AE, Shahein MA, Elsayed MM. The potential role of migratory birds in the transmission of pathogenic *Campylobacter* species to broiler chickens in broiler poultry farms and live bird markets. *BMC Microbiol*. (2023) 23:66. doi: 10.1186/s12866-023-02794-0

24. Hill NJ, Bishop MA, Trovão NS, Ineson KM, Schaefer AL, Puryear WB, et al. Ecological divergence of wild birds drives avian influenza spillover and global spread. *PLoS Pathog*. (2022) 18:e1010062. doi: 10.1371/journal.ppat.1010062

25. Yong DL, Liu Y, Low BW, Espanola CP, Choi CY, Kawakami K. Migratory songbirds in the east Asian-Australasian flyway: a review from a conservation perspective. *Bird Conserv Int*. (2015) 25:1–37. doi: 10.1017/S0959270914000276

26. Liang M, Ran J, Liang S, Wu Y, Yu X. Diversity and migration routes of raptors in Sichuan Province. *Biodivers Sci*. (2016) 24:1408. doi: 10.17520/biods.2016238

27. Chen W, Lu S, Xiong H, Xiang Z, Wang Y, Hu J, et al. Gene flow and its sporadic spillover: H10 and N5 avian influenza viruses from wild birds and the H10N5 human cases in China. *Virol Sin*. (2024) 18:198. doi: 10.1016/j.virs.2024.12.002

28. Nam NT, Chi NH, Ha CH, Nga NTB. Evolutionary characterization of clades 2.3.4.4 H5N6 and 2.3.2.1c H5N1 HPAI viruses in Vietnam (2013–2019) revealed distinct reassortants from distant spillovers. *Vietnam J Biotechnol*. (2022) 20:231–43. doi: 10.15625/1811-4989/15325

29. Seri NA, Rahman AA. Impact of climate change on migratory birds in Asia. *Pertanika J Sci Technol*. (2021) 29:2937–65. doi: 10.47836/pjst.29.4.38

30. Wang F, Yang Y, Song G, Shi X, Pu B, Yang L. Mangcuo lake in hengduan mountains: an important alpine breeding and stopover site along central Asian flyway. *Animals*. (2023) 13:1139. doi: 10.3390/ani13071139

31. Li D, Zhu S, Gao J, Jiang H, Deng G, Sheng L, et al. The influence of ecological engineering on waterbird diversity in different habitats within the Xianghai nature reserve. *Diversity*. (2022) 14:1016. doi: 10.3390/d14121016

32. Sawa Y, Sugawa H, Wada T, Sato T, Arima H, Yomoda N, et al. Variation in seasonal movement and body size of wintering populations of black-headed gull in Japan. *Ornithol Sci*. (2025) 24:55–68. doi: 10.2326/osj.24.55

33. Butler MJ, Bidwell MT. Long-term migratory alterations to whooping crane arrival and departure on the wintering and staging grounds. *Endangered Species Res*. (2024) 53:481–91. doi: 10.3354/esr01315

34. Das Gupta S, Barua B, Fournié G, Hoque MA, Henning J. Village and farm-level risk factors for avian influenza infection on backyard chicken farms in Bangladesh. *Sci Rep*. (2022) 12:13009. doi: 10.1038/s41598-022-16489-5

35. Liu Y, Kjær LJ, Boklund AE, Hjulsager CK, Larsen LE, Kirkeby CT. Risk factors for avian influenza in Danish poultry and wild birds during the epidemic from June 2020 to may 2021. *Front Vet Sci*. (2024) 11:1358995. doi: 10.3389/fvets.2024.1358995

36. de Vos CJ, Elbers ARW. Quantitative risk assessment of wind-supported transmission of highly pathogenic avian influenza virus to Dutch poultry farms via fecal particles from infected wild birds in the environment. *Pathogens*. (2024) 13:571. doi: 10.3390/pathogens13070571

37. Ahrens AK, Selinka HC, Wylezich C, Wonnemann H, Sindt O, Hellmer HH, et al. Investigating environmental matrices for use in avian influenza virus surveillance—surface water, sediments, and avian fecal samples. *Microbiol Spectr*. (2023) 11:e02664-22. doi: 10.1128/spectrum.02664-22

38. Velkers FC, Manders TT, Vernooij JC, Stahl J, Slaterus R, Stegeman JA. Association of wild bird densities around poultry farms with the risk of highly pathogenic avian influenza virus subtype H5N8 outbreaks in the Netherlands, 2016. *Transbound Emerg Dis*. (2021) 68:76–87. doi: 10.1111/tbed.13595

39. Zhang L, Zhou E, Liu C, Tian X, Xue B, Zhang K, et al. Avian influenza and gut microbiome in poultry and humans: A "one health" perspective. *Fundamental Res*. (2024) 4:455–62. doi: 10.1016/j.fmre.2023.10.016

40. Branda F, Giovanetti M, Scarpa F, Ciccozzi M. Monitoring avian influenza in mammals with real-time data. *Pathogens Global Health*. (2024) 118:280–4. doi: 10.1080/20477724.2024.2323843

41. Venkatesan P. Avian influenza spillover into mammals. *Lancet Microbe*. (2023) 4:e492. doi: 10.1016/S2666-5247(23)00173-8

42. Yang J. Technical guidelines for the prevention and control of human infection with animal-borne influenza (trial version) - a brief analysis: animal-borne influenza and influenza pandemics. *Trop Dis Parasitol*. (2021) 19:301. doi: 10.3760/cma.j.issn.0253-9624.2019.11.003

43. Yang L, Zhu W, Li X, Bo H, Zhang Y, Zou S, et al. Genesis and dissemination of highly pathogenic H5N6 avian influenza viruses. *J Virol*. (2017) 91:10–1128. doi: 10.1128/JVI.02199-16

44. Mok CKP, Da Guan W, Liu XQ, Lamers MM, Li XB, Wang M, et al. Genetic characterization of highly pathogenic avian influenza A (H5N6) virus, Guangdong, China. *Emerg Infect Dis*. (2015) 21:2268–71. doi: 10.3201/eid2112.150809

45. Pohlmann A, Hoffmann D, Grund C, Koethe S, Hüssy D, Meier SM, et al. Genetic characterization and zoonotic potential of highly pathogenic avian influenza virus A (H5N6/H5N5), Germany, 2017–2018. *Emerg Infect Dis*. (2019) 25:1973. doi: 10.3201/eid2510.181931

46. Blagodatski A, Trutneva K, Glazova O, Mityaeva O, Shevkova L, Kegeles E, et al. Avian influenza in wild birds and poultry: dissemination pathways, monitoring methods, and virus ecology. *Pathogens*. (2021) 10:630. doi: 10.3390/pathogens10050630

47. Ganti K, Bagga A, DaSilva J, Shepard SS, Barnes JR, Shriner S, et al. Avian influenza A viruses reassort and diversify differently in mallards and mammals. *Viruses*. (2021) 13:509. doi: 10.3390/v13030509

48. Kanaujia R, Bora I, Ratho RK, Thakur V, Mohi GK, Thakur P. Avian influenza revisited: concerns and constraints. *Virus*. (2022) 33:456–65. doi: 10.1007/s13337-022-00800-z

49. Byrne AM, James J, Mollett BC, Meyer SM, Lewis T, Czepiel M, et al. Investigating the genetic diversity of H5 avian influenza viruses in the United Kingdom from 2020–2022. *Microbiol Spectr*. (2023) 11:e04776-22. doi: 10.1128/spectrum.04776-22

50. Zhang R, Lei Z, Liu C, Zhu Y, Chen J, Yao D, et al. Live poultry feeding and trading network and the transmission of avian influenza A (H5N6) virus in a large city in China, 2014–2015. *Int J Infect Dis*. (2021) 108:72–80. doi: 10.1016/j.ijid.2021.05.022

51. Ellis JW, Root JJ, McCurdy LM, Bentler KT, Barrett NL, VanDalen KK, et al. Avian influenza A virus susceptibility, infection, transmission, and antibody kinetics in European starlings. *PLoS Pathog*. (2021) 17:e1009879. doi: 10.1371/journal.ppat.1009879

52. Huneau-Salaün A, Scoizec A, Thomas R, Martenot C, Schmitz A, Pierre I, et al. Avian influenza outbreaks: evaluating the efficacy of cleaning and disinfection of vehicles and transport crates. *Poult Sci*. (2022) 101:101569. doi: 10.1016/j.psj.2021.101569

53. Martelli L, Fornasiero D, Scarton F, Spada A, Scolamacchia F, Manca G, et al. Study of the Interface between wild bird populations and poultry and their potential role in the spread of avian influenza. *Microorganisms*. (2023) 11:2601. doi: 10.3390/microorganisms11102601

54. Gang Y, Jie H. Timing and quantity changes of winter migratory Waterbirds in the Nanchong section of the Jialing River. *Zoology*. (2011) 30:638–43. doi: 10.3969/j.issn.1000-7083.2011.04.022

55. Chen Y, Cheng J, Xu Z, Hu W, Lu J. Live poultry market closure and avian influenza A (H7N9) infection in cities of China, 2013–2017: an ecological study. *BMC Infect Dis*. (2020) 20:1–10. doi: 10.1186/s12879-020-05091-7

56. Wu J, Lu J, Faria NR, Zeng X, Song Y, Zou L, et al. Effect of live poultry market interventions on influenza A (H7N9) virus, Guangdong, China. *Emerg Infect Dis*. (2016) 22:2104. doi: 10.3201/eid2212.160450

57. Li R, Zhang T, Bai Y, Li H, Wang Y, Bi Y, et al. Live poultry trading drives China's H7N9 viral evolution and geographical network propagation. *Front Public Health*. (2018) 6:210. doi: 10.3389/fpubh.2018.00210

58. Mahendra P, Lema AG, Megersa AT. Current understanding on avian influenza and its public health impact: a comprehensive review. *Int Jr Infect Dis Epidemlgy*. (2023) 23:1–58. doi: 10.51626/ijide.2023.04.00043

59. Valensia R, Hilmi IL, Salman S. Analysis of the effectiveness of avian influenza treatment in humans: literature review. *J Eduhealth*. (2022) 13:1137–42. doi: 10.1093/infdis/jiz372

60. Fiore AE, Shay D, Gubareva L, Bresee JS, Uyeki TM, et al. Antiviral agents for the treatment and chemoprophylaxis of influenza—recommendations of the advisory committee on immunization practices (ACIP). *MMWR Recomm Rep*. (2011) 60:1–24.

61. Petersen E, Memish ZA, Hui DS, Scagliarini A, Simonsen L, Simulundu E, et al. Avian 'Bird'Flu–undue media panic or genuine concern for pandemic potential requiring global preparedness action? *IJID Regions*. (2024) 11:100367. doi: 10.1016/j.ijregi.2024.100367

62. Sun H, Pu J, Wei Y, Sun Y, Hu J, Liu L, et al. Highly pathogenic avian influenza H5N6 viruses exhibit enhanced affinity for human type sialic acid receptor and in-contact transmission in model ferrets. *J Virol*. (2016) 90:6235–43. doi: 10.1128/JVI.00127-16

63. Zhang C, Cui H, Zhang C, Zhao K, Kong Y, Chen L, et al. Pathogenicity and transmissibility of clade 2.3.4.4 h H5N6 avian influenza viruses in mammals. *Animals*. (2022) 12:3079. doi: 10.3390/ani12223079

64. Peng X, Liu F, Wu H, Peng X, Xu Y, Wang L, et al. Amino acid substitutions HA A150V, PA A343T, and PB2 E627K increase the virulence of H5N6 influenza virus in mice. *Front Microbiol*. (2018) 9:453. doi: 10.3389/fmicb.2018.00453

65. Hui KP, Chan LL, Kuok DI, Mok CK, Yang ZF, Li RF, et al. Tropism and innate host responses of influenza A/H5N6 virus: an analysis of ex vivo and in vitro cultures of the human respiratory tract. *Eur Respir J*. (2017) 49:16. doi: 10.1183/13993003.01710-2016

66. Chen P, Xie JF, Lin Q, Zhao L, Zhang YH, Chen HB, et al. A study of the relationship between human infection with avian influenza A (H5N6) and environmental avian influenza viruses in Fujian, China. *BMC Infect Dis*. (2019) 19:1–8. doi: 10.1186/s12879-019-4145-6

67. Yamaji R, Saad MD, Davis CT, Swayne DE, Wang D, Wong FY, et al. Pandemic potential of highly pathogenic avian influenza clade 2.3. 4.4 A (H5) viruses. *Rev Med Virol*. (2020) 30:e2099. doi: 10.1002/rmv.2099

68. Hanna O, Helve OM. "One health, many interpretations: vaccinating risk groups against H5 avian influenza in Finland." *Eurosurveillance* (2024) 29.25:2400383.

69. Government of Canada (2025) Purchases avian influenza vaccine to protect individuals most at risk. Ottawa, ON: Public Health Agency of Canada. Available at: https://www.canada.ca/en/public-health/news/2025/02/government-of-canada-purchases-avian-influenza-vaccine-to-protect-individuals-most-at-risk.html

frontiers | Frontiers in Cellular and Infection Microbiology

TYPE Original Research
PUBLISHED 12 June 2025
DOI 10.3389/fcimb.2025.1603369

OPEN ACCESS

EDITED BY
Sneha Vishwanath,
University of Cambridge, United Kingdom

REVIEWED BY
Hala Abou El Naja,
Independent Researcher, Cairo, Egypt
Srivatsan Parthasarathy,
Diosynvax Ltd., United Kingdom

*CORRESPONDENCE
Zhongliang Hu
zhonglianghu@abtu.edu.cn

RECEIVED 31 March 2025
ACCEPTED 28 May 2025
PUBLISHED 12 June 2025

CITATION
Li X, Yang C, Chen L, Ma J and Hu Z (2025) Epidemiological trends of influenza A and B in one hospital in Chengdu and national surveillance data (2019–2024).
Front. Cell. Infect. Microbiol. 15:1603369.
doi: 10.3389/fcimb.2025.1603369

Epidemiological trends of influenza A and B in one hospital in Chengdu and national surveillance data (2019–2024)

Xiang Li[1], Chenlijie Yang[2], Lu Chen[2], Jian Ma[1] and Zhongliang Hu[2*]

[1]Department of Laboratory Medicine, Sichuan Jinxin Xinan Women and Children Hospital, Chengdu, China, [2]College of Resources and Environment, Aba Teachers College, Wenchuan, China

Background: Influenza A (Flu A) and Influenza B (Flu B) are major contributors to seasonal epidemics, causing significant morbidity and mortality worldwide. Understanding their epidemiological trends is essential for optimizing prevention and control strategies.

Objective: This study aims to analyze the epidemiological trends of Flu A and Flu B, compare hospital-based and national surveillance data, and evaluate the impact of COVID-19 on influenza transmission to provide scientific evidence for influenza control measures.

Methods: We analyzed influenza positivity rates from Sichuan Jinxin Xinan Women and Children Hospital data (HD) and Chinese National Influenza Center (CNIC) between 2019 and 2024. Temporal trends, subtype distributions, and the effects of non-pharmaceutical interventions (NPIs) were assessed.

Results: Influenza activity exhibited significant temporal variations. In HD, the highest cumulative positivity rate of Flu A + Flu B was observed in 2023 (31.9%), whereas the lowest rate occurred during the COVID-19 pandemic (2020–2022), with a nadir in 2021 (2.0%). Flu A remained the predominant subtype in HD except in 2021, whereas CNIC data showed a relatively higher proportion of Flu B. Weekly positivity rates displayed distinct seasonal trends in CNIC data but not in HD. A comparative analysis of pre-pandemic (2019), pandemic (2020–2022), and post-pandemic (2023–2024) phases indicated that NPIs had a stronger suppressive effect on Flu A than on Flu B.

Conclusion: Hospital-based and national influenza surveillance data showed heterogeneity in subtype proportions, seasonal trends, and pandemic-related impacts. These findings underscore the importance of integrating multiple

surveillance sources for a comprehensive understanding of influenza dynamics. Enhancing vaccine coverage, implementing targeted public health interventions, and optimizing resource allocation are crucial for mitigating the influenza burden in the post-pandemic era.

KEYWORDS

influenza A, influenza B, epidemiology, non-pharmaceutical interventions, COVID-19

Introduction

Influenza, commonly known as the flu, is an acute viral respiratory disease caused by infection with influenza viruses, primarily seasonal influenza A (Flu A) and B (Flu B) viruses (Uyeki, 2021; Bi et al., 2024). These viruses circulate globally, leading to seasonal epidemics that significantly impact public health (Uyeki et al., 2022). Hospitalization rates are particularly elevated among vulnerable populations, including children, the elderly, and individuals with underlying health conditions (Thomas, 2023). The elderly population, particularly those aged 65 and older, experiences the highest mortality rates (approximately 90%) due to influenza (Mi et al., 2025). It is estimated that seasonal influenza causes between 290,000 and 650,000 deaths worldwide each year (Cozza et al., 2021). Studying the epidemiological trends of influenza can provide valuable insights for future prevention and control measures.

In China, influenza remains a significant public health concern. The epidemiological trends of Flu A and Flu B in the Chinese population exhibit a certain pattern. Overall, Flu A infection rates are generally higher than those of Flu B, with Flu A peaking during the winter and early spring months (December to March of the following year). In contrast, Flu B tends to peak later, sometimes emerging at the end of winter or in spring (Huang W-J. et al., 2022; Lei et al., 2022; Xie et al., 2024; Qu et al., 2025). In recent years, the COVID-19 pandemic has influenced influenza transmission patterns. Non-pharmaceutical interventions (e.g., mask-wearing, social distancing) led to a decline in influenza activity in certain years (Feng et al., 2021; Huang Q-M. et al., 2022). However, as control measures eased, Flu A and Flu B circulation gradually rebounded (Zhang et al., 2024; Cowling et al., 2020).

Existing studies may lack long-term surveillance data for specific regions (Hammond et al., 2022; Soudani et al., 2022; Langer et al., 2023). While the National Influenza Center provides nationally representative data, it does not include detailed analyses of case positivity rates in regional healthcare facilities. Additionally, influenza transmission patterns may have been disrupted during the COVID-19 pandemic and subsequent recovery period, yet research on this impact remains limited.

Here we analyzed the trends in Flu A and Flu B positivity rates at Sichuan Jinxin Xinan Women and Children Hospital from 2019 to 2024 and compared them with data from the Chinese National Influenza Center (CNIC). Our findings revealed notable heterogeneity between hospital data (HD) and CNIC influenza surveillance data in terms of influenza subtype proportions, seasonal fluctuations, and the impact of COVID-19, highlighting the potential limitations of relying on a single data source for assessing influenza dynamics. Additionally, we examined influenza trends across the pre-pandemic, pandemic, and post-pandemic periods and found that non-pharmaceutical interventions (NPIs) during COVID-19 had a stronger suppressive effect on Flu A than on Flu B. These findings underscore the need for enhanced influenza vaccine coverage, precise surveillance, and adaptive resource allocation in the post-pandemic era, particularly in response to Flu B's seasonal peaks and the risk of mixed influenza outbreaks.

Materials and methods

HD data collection

Virus detection reagents and instruments

FluA and FluB antigens were detected using a colloidal gold-based influenza antigen detection kit (Product Registration Number: National Medical Device Registration Certificate Number: 20143401922) manufactured by InTec (https://www.asintec.com/product/30). This rapid immunochromatographic assay utilizes a double-antibody sandwich principle. The test strip is pre-coated with monoclonal antibodies targeting the nucleoproteins of FluA and FluB at detection zones A and B, respectively, and with goat anti-mouse IgG antibodies in the control zone (C). If viral antigens are present in the sample, they bind to colloidal gold-labeled antibodies, forming antigen-antibody complexes that migrate along the nitrocellulose membrane and produce visible color bands, allowing for qualitative detection of FluA and FluB.

Sample collection and processing

Sample type: Throat swabs were collected from patients with influenza-like illness (ILI) at Sichuan Jinxin Xinan Women and Children Hospital from 2019 to 2024. The swabs were gently rubbed against the posterior pharyngeal wall and bilateral tonsils, rotated, and held in place for 10 seconds to ensure sufficient sample collection.

Sample preservation: Immediately after collection, swabs were immersed in the provided lysis buffer (0.01 M phosphate-buffered solution, pH 7.2 ± 0.2), stirred thoroughly 10 times, and squeezed against the tube wall to release the antigens. Samples were tested

within 2 hours of collection to avoid degradation, and repeated freeze-thaw cycles were avoided.

Detection procedure

Reagent preparation: Prior to testing, unopened reagent kits were equilibrated to room temperature (15–30°C). Once opened, test cassettes were used within 1 hour to prevent moisture interference.

Sample application:

A micropipette was used to transfer 80 µL (approximately 2–3 drops) of the lysed sample solution into the sample well of the test cassette.

A timer was started, and the test was incubated at room temperature for 10–15 minutes before result interpretation. Results read beyond this time frame were considered invalid.

Result interpretation:

Positive: A red band appeared in detection zone A (FluA) and/or B (FluB), with a visible control band (C).

Negative: Only the control band (C) appeared, with no visible bands in zones A or B.

Invalid: No control band (C) appeared, indicating a failed test requiring retesting.

This study was approved by the Ethics Committee of Sichuan Jinxin Xinan Women and Children Hospital.

CNIC data collection

Influenza surveillance data were obtained from CNIC, which systematically collects and reports influenza activity across China. The dataset includes weekly influenza positivity rates and subtype distributions from sentinel hospitals and laboratories nationwide. For this study, we extracted relevant data from the CNIC database covering the period from 2019 to 2024. Data were accessed through official CNIC (https://ivdc.chinacdc.cn/cnic/zyzx/lgzb/202411/t20241115_302662.htm).

Statistical analysis

Data were analyzed using GraphPad Prism 9.0. Group differences were assessed using the Kruskal-Wallis test followed by Dunn's multiple comparison test. Bar graphs were presented as mean ± SD and generated using GraphPad Prism 9.0. Polar coordinate plots were created by https://www.bioinformatics.com.cn, an online platform for data analysis and visualization. A p-value of <0.05 was considered statistically significant.

Results

Influenza positivity rates in HD and CNIC from 2019 to 2024

We analyzed the positivity rates of Flu A and Flu B in HD from 2019 to 2024 and found that the highest cumulative positivity rate of Flu A + Flu B was observed in 2023 (31.9%), followed by 2019 (25.0%) and 2024 (18.4%). In contrast, the cumulative positivity rates were recorded during the COVID-19 pandemic period, with 2020 at 10.3%, 2021 at 2.0%, and 2022 at 11.4%, indicating a substantial decline during the peak pandemic years and a gradual rebound thereafter. Flu A was the predominant subtype in the cumulative positivity rates (Figures 1A, C). Additionally, an analysis of influenza surveillance data from CNIC during the same period revealed a slightly different trend. The cumulative positivity rates of Flu A + Flu B, ranked from highest to lowest, were as follows: 2019 (20.8%), 2023 (17.8%), 2022 (15.0%), 2024 (12.5%), 2020 (5.9%), and 2021 (5.8%). Notably, the proportion of Flu B appeared to be slightly higher in the CNIC dataset compared to HD (Figures 1B, C). Further analysis of the weekly average positivity rates in HD revealed that Flu A maintained an average of approximately 10% in 2019, 2023, and 2024, while in 2020 and 2021, the average dropped to around 1%, with a moderate increase observed in 2022 (approximately 5%). For Flu B, the average positivity rate was 6.1% in 2019, with significantly lower rates ($p<0.05$) observed in the subsequent years (Figure 1D). Analysis of CNIC data revealed that the weekly average positivity rate for Flu A peaked in 2023 at 14.7%, followed by 11.6% in 2019, with the lowest rate observed in 2021 (<0.1%). For Flu B, lower average positivity rates were noted in 2020 (1.5%) and 2023 (1.3%), while in other years, the rates exceeded 4% (Figure 1E). In addition, we compared the average positivity rates of Flu A and Flu B between the HD and CNIC datasets from 2019 to 2024. The results showed that there were no statistically significant differences in the average positivity rates of Flu A between HD and CNIC. For Flu B, however, the positivity rates in CNIC were significantly higher than those in HD in both 2021 ($p<0.01$) and 2022 ($p<0.0001$) (Figure 1F).

Proportional analysis of influenza A and B positivity rates in HD and CNIC datasets

Analysis of influenza data from both HD and CNIC revealed notable differences in the positivity rates of Flu A and Flu B. To further investigate the relationship between these subtypes among positive cases, we examined their respective proportions. In the HD dataset, Flu A predominated in all years except 2021, with its proportion exceeding 80% in 2019, 2022, 2023, and 2024 (Figure 2A). Conversely, in the CNIC dataset, only in 2023 did Flu A's proportion surpass 80%. Notably, in 2021, Flu B accounted for an overwhelming 99.87% of positive cases (Figure 2B).

Weekly trends in influenza A and B positivity rates in HD and CNIC datasets (2019–2024)

To investigate the annual trends in Flu A positivity rates, we analyzed their weekly variations from 2019 to 2024. In the HD dataset, no distinct seasonal patterns were observed in Flu A positivity rates during this period (Figure 3A). Conversely, the CNIC data exhibited more defined seasonal trends, with notable

10.3389/fcimb.2025.1603369

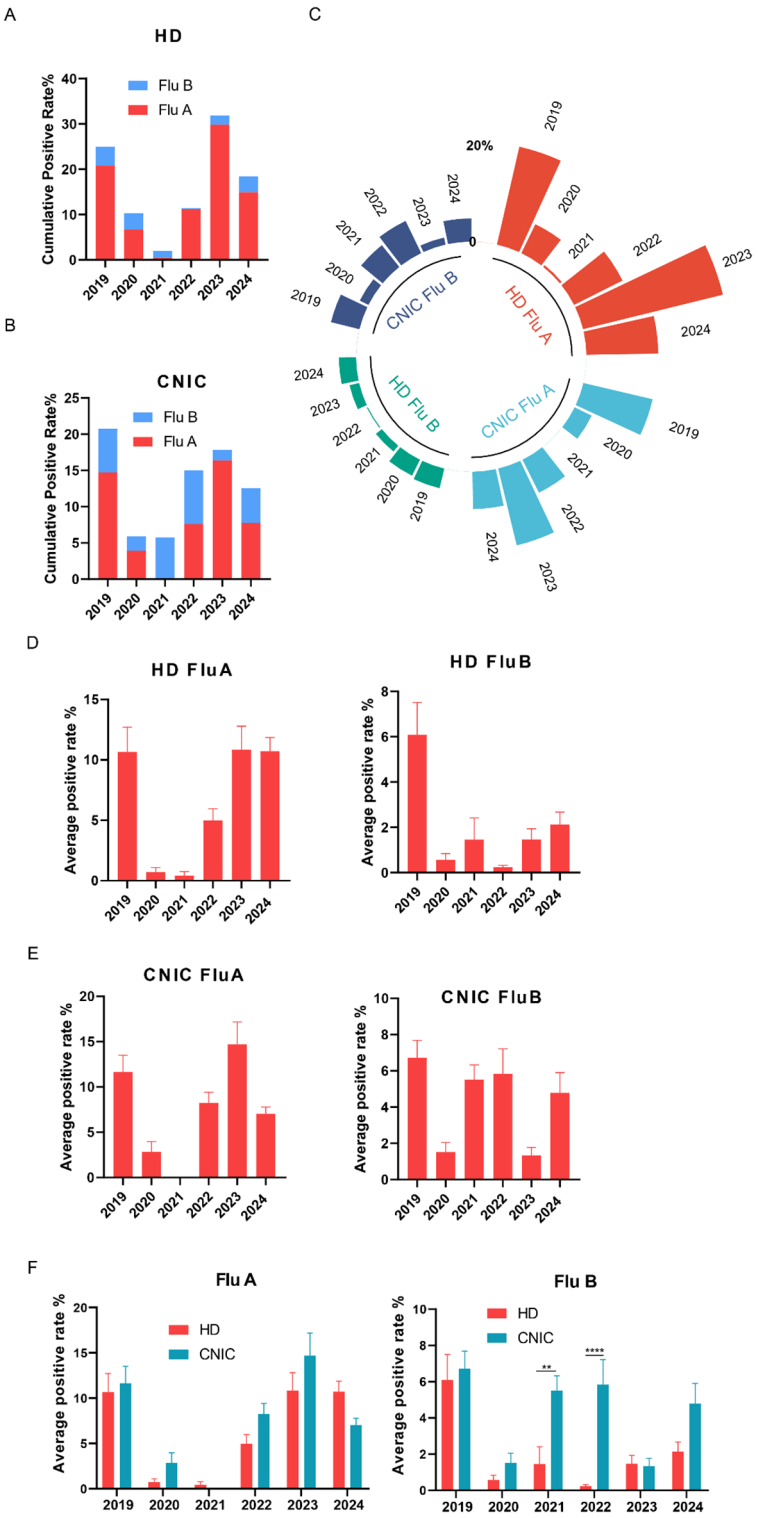

FIGURE 1
Analysis of influenza A and B positivity rates in HD and CNIC datasets. **(A)** Cumulative positivity rates of influenza A and B in HD. This figure illustrates the cumulative positivity rates of influenza A (Flu A) and influenza B (Flu B) cases in the HD (hospital data) over the study period. **(B)** Cumulative positivity rates of Flu A and Flu B in CNIC data. This figure illustrates the cumulative positivity rates of Flu A and Flu B cases in the CNIC (Chinese National Influenza Center) dataset over the study period. **(C)** Polar plot of Flu A and Flu B positivity rates in HD and CNIC data from 2019 to 2024. This figure presents a polar plot comparing the positivity rates of Flu A and Flu B in both HD and CNIC datasets over the period from 2019 to 2024. **(D)** Bar chart of average weekly positivity rates for Flu A and Flu B in HD data. This figure presents a bar chart depicting the average weekly positivity rates of Flu A and Flu B cases within the HD. **(E)** Bar chart of average weekly positivity rates for Flu A and Flu B in CNIC data. This figure presents a bar chart depicting the average weekly positivity rates of Flu A and Flu B cases within the CNIC dataset. **(F)** Comparison of average positivity rates of Flu A and Flu B between HD and CNIC datasets, shown as paired bars by year. ** indicates $p<0.01$; ****indicates $p<0.0001$.

10.3389/fcimb.2025.1603369

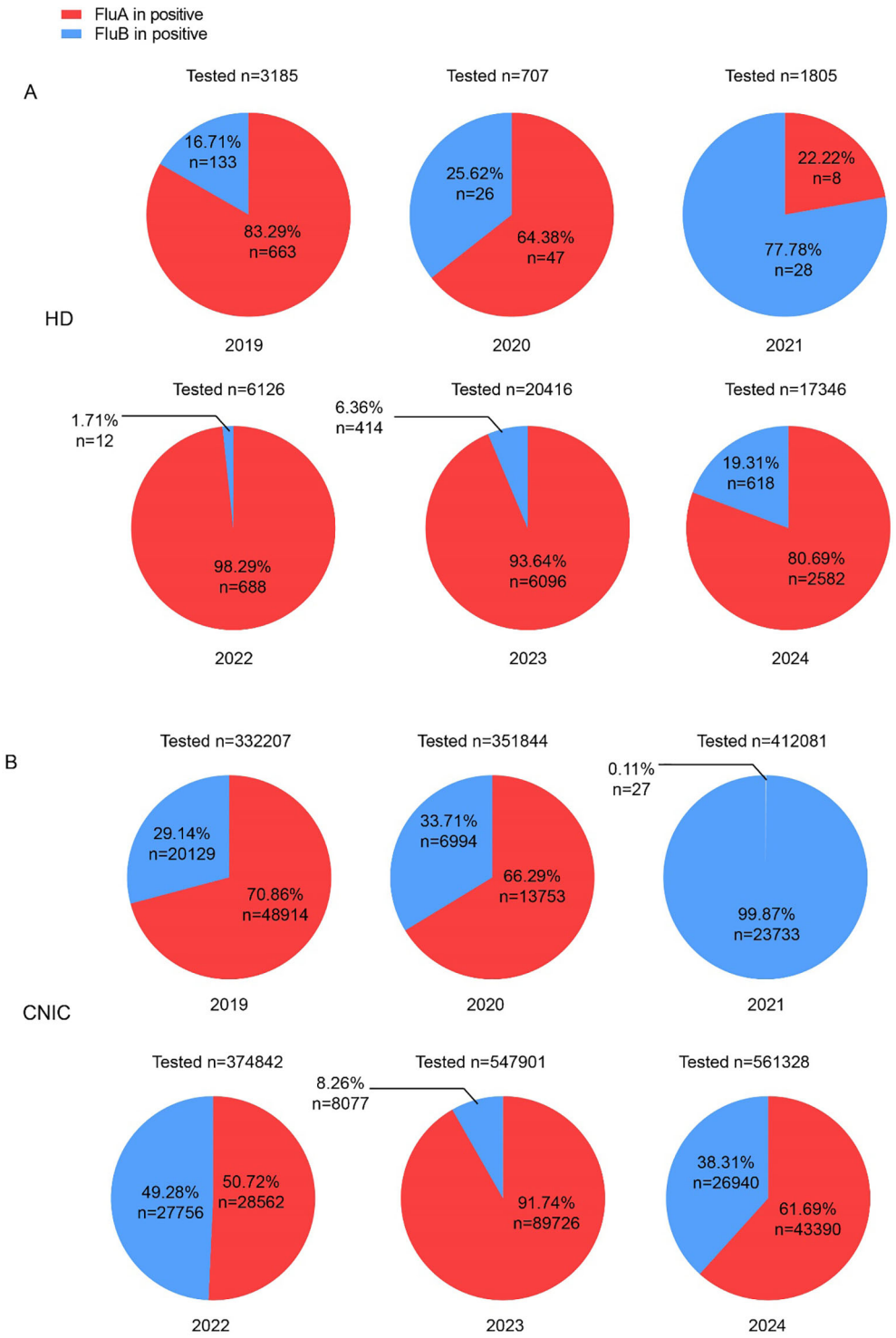

FIGURE 2
Proportions of influenza A and B cases among influenza-positive cases in HD and CNIC datasets. **(A)** Pie chart depicting the proportion of influenza A and B cases among influenza-positive cases in HD. **(B)** Pie chart depicting the proportion of influenza A and B cases among influenza-positive cases in CNIC data. HD, hospital data; CNIC, Chinese National Influenza Center.

peaks occurring during the first 15 weeks and the last 10 weeks of 2019, 2023, and 2024 (Figure 3B).

Similarly, we analyzed the weekly variations in Flu B positivity rates across different years. In the HD dataset from 2022 to 2024, Flu B positivity rates peaked during the initial 10 weeks and the final 10 weeks of each year (Figure 4A). The CNIC data exhibited a comparable pattern, with significant peaks in Flu B positivity rates occurring within the first and last 10 weeks of the year (Figure 4B).

10.3389/fcimb.2025.1603369

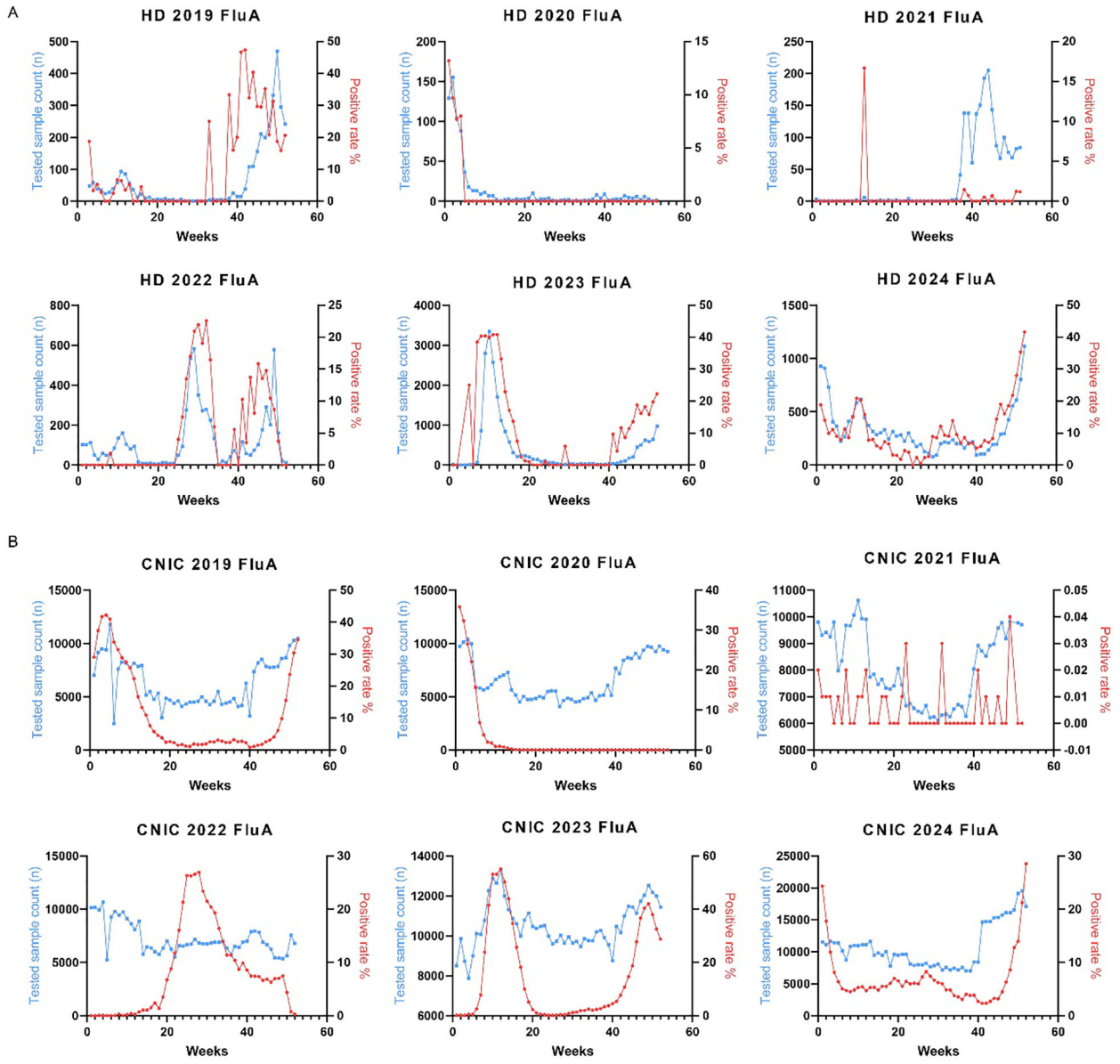

FIGURE 3
Weekly distribution of influenza A testing samples and positivity rates in HD and CNIC datasets. **(A)** Weekly distribution of influenza A testing samples and positivity rates in HD. **(B)** Weekly distribution of influenza A testing samples and positivity rates in CNIC. HD, hospital data; CNIC, Chinese National Influenza Center.

Impact of the COVID-19 pandemic on influenza positivity rates in HD and CNIC datasets

Studies have suggested that the COVID-19 pandemic has influenced influenza transmission patterns. To explore this hypothesis, we analyzed influenza data from HD and CNIC, categorizing the periods based on COVID-19 control measures into pre-pandemic (Pre, 2019), pandemic (Pan, 2020–2022), and post-pandemic (Post, 2023–2024) phases. Our analysis revealed a significant decrease in the cumulative positivity rates of Flu A and Flu B during the Pan period in both HD and CNIC datasets (Figures 5A, B). Specifically, the positivity rates of Flu A in both HD and CNIC declined markedly during the Pan phase. In HD, Flu B positivity rates were lower in the Pan period compared to the Pre and Post phases. However, in the CNIC dataset, Flu B positivity during the Pan phase was higher than in the Post phase (Figure 5B).

Further analysis of the average weekly positivity rates indicated that, in HD, both Flu A and Flu B had significantly lower values during the Pan period compared to the Pre and Post periods. In the CNIC dataset, Flu A followed a similar trend, while Flu B showed no significant difference between the Pan and Post periods. Notably, in both HD and CNIC datasets, Flu B positivity rates were significantly higher in the Pre phase compared to the Post phase (Figure 5C).

10.3389/fcimb.2025.1603369

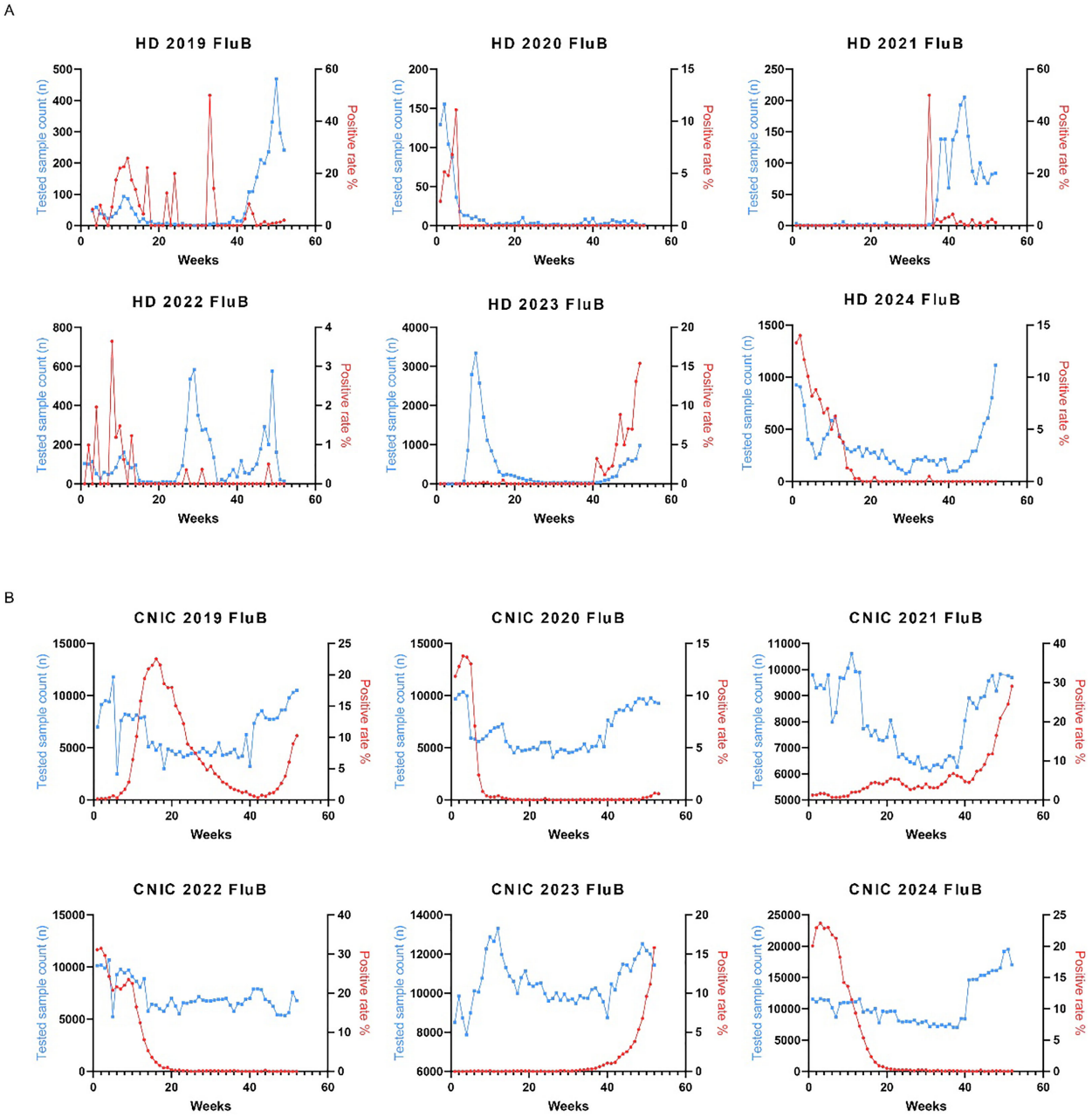

FIGURE 4
Weekly distribution of influenza B testing samples and positivity rates in HD and CNIC datasets. **(A)** Weekly distribution of influenza B testing samples and positivity rates in HD. **(B)** Weekly distribution of influenza B testing samples and positivity rates in CNIC. HD, hospital data; CNIC, Chinese National Influenza Center.

Examining the proportions of Flu A and Flu B among influenza-positive cases, we found that in HD, Flu A dominated during the Pre, Pan, and Post periods, consistently accounting for over 80% of cases. In contrast, within the CNIC dataset, although Flu A had a higher proportion during the Pre and Post phases, it remained below 80%. Notably, during the Pan period, Flu B became the predominant pathogen, comprising 58% of influenza-positive cases (Figure 5D).

Discussion

In this study, we analyzed the trends in Flu A and Flu B positivity rates from 2019 to 2024 at Sichuan Jinxin Xinan Women and Children Hospital and compared them with national surveillance data from the CNIC. Our findings revealed significant heterogeneity between local and national datasets in terms of influenza subtype distribution, seasonal patterns, and the impact

10.3389/fcimb.2025.1603369

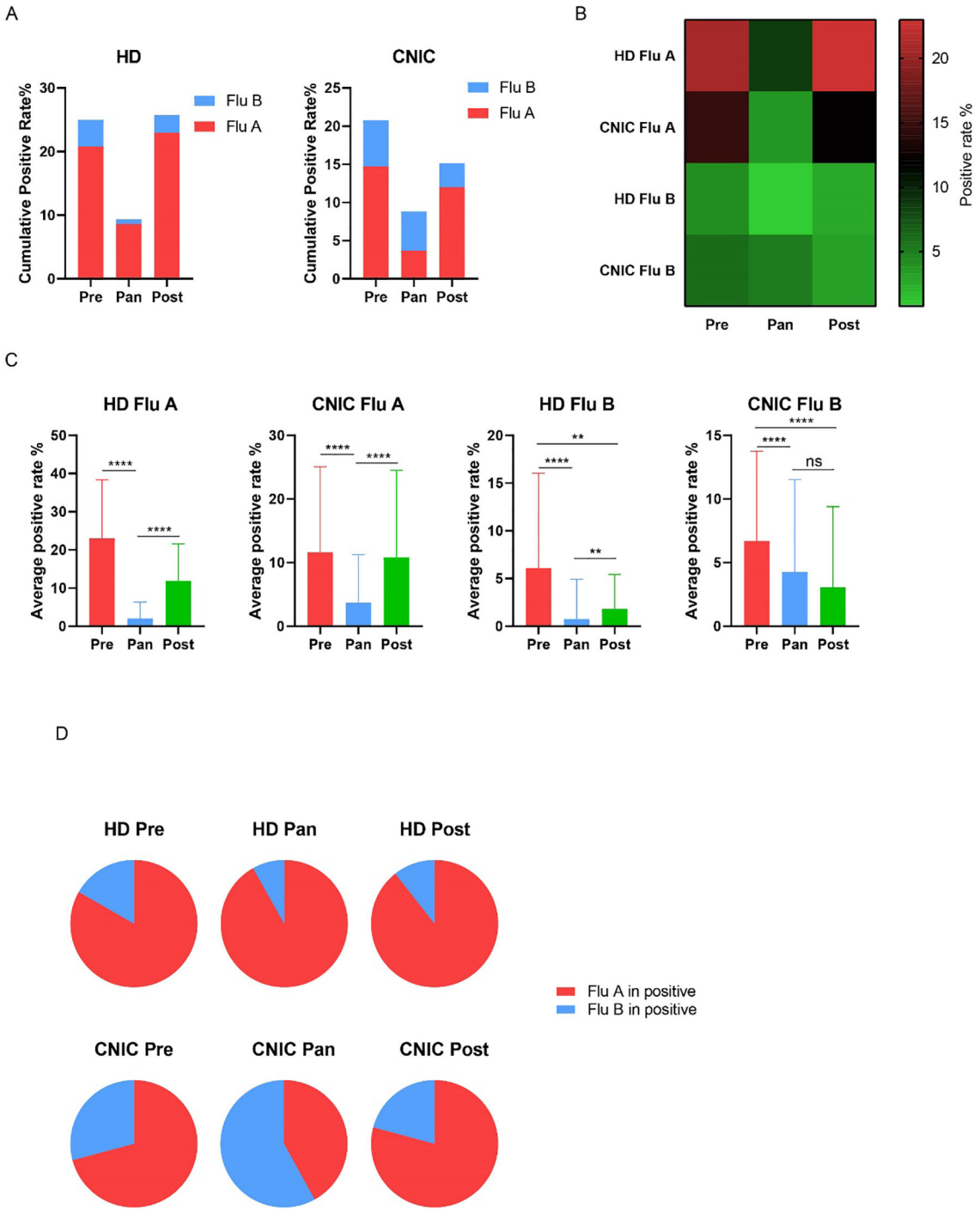

FIGURE 5
Analysis of influenza A and B positivity rates in HD and CNIC datasets during the Pre, Pan, and Post COVID-19 periods. **(A)** Bar charts depict the cumulative positivity rates of influenza A and B in HD and CNIC datasets during the pre-pandemic (Pre), pandemic (Pan), and post-pandemic (Post) COVID-19 periods. **(B)** Heatmap depicting the positivity rates of influenza A and B in HD and CNIC datasets during the Pre, Pan, and Post COVID-19 periods. **(C)** Bar charts depicting the weekly average positivity rates of influenza A and B in HD and CNIC datasets during the P Pre, Pan, and Post COVID-19 periods. **(D)** Pie charts depicting the proportions of influenza A and B cases among influenza-positive cases in HD and CNIC datasets during the Pre, Pan, and Post COVID-19 periods. HD, hospital data; CNIC, Chinese National Influenza Center. ns indicates no significant; ** indicates $p<0.01$; ****indicates $p<0.0001$.

of the COVID-19 pandemic. Notably, the suppression of influenza activity during the pandemic period was more pronounced for Flu A than for Flu B, with Flu B emerging as the dominant subtype in the CNIC dataset. Additionally, we observed a resurgence of influenza positivity rates in 2023, underscoring the need for strengthened post-pandemic surveillance and vaccination strategies. These findings highlight the importance of integrating both local and national data to obtain a comprehensive understanding of influenza dynamics and inform targeted public health interventions.

We found that both HD and CNIC data indicated that Flu A was the predominant type in 2019, with an average positivity rate exceeding 10%. This finding is consistent with results from multiple studies. A study in Yichang, a subtropical city in China, found an overall influenza virus positive rate of 16.6% among 8693 ILI cases, with a higher positive rate for Flu A (10.6%) than Flu B (5.9%) (Zhu et al., 2020). Another study in China, focusing on the period 2014-2018, reported an overall positive rate of 17.2% among 1,890,084 ILI cases, with Flu A detected in 62% of cases and Flu B in 38% (Zhu et al., 2023). In Cameroon, a study spanning from 2009 to 2018 indicated an influenza virus positivity rate of 24.0% among 11,816 participants with ILI (Monamele et al., 2020). These results suggest that before the COVID-19 pandemic, Flu A was the dominant strain of influenza.

The outbreak of the COVID-19 pandemic led to significant changes in influenza transmission patterns. A study reported that during the 2020–2021 influenza season, the global incidence of Flu A and B declined dramatically to just 0.0015 and 0.0028 times pre-pandemic levels (Lampejo, 2022). In the United States, reported influenza cases dropped sharply to only 1,899 during the 2020–2021 season, compared to millions of cases in previous years (Shaghaghi et al., 2021). Time-series analyses also indicate changes in influenza prevalence in China during the pandemic. One study found that during the 2020–2021 influenza season, the proportion of influenza-positive samples in southern China fell to 0.7%, whereas in previous seasons, this proportion ranged from 11.8% to 21.1% (Cao et al., 2023). From February 2020 to January 2021, the influenza positivity rate in China dropped to 0.2%, representing a significant decline compared to the same period in 2019 (Lei et al., 2020). The Chinese government established a Joint Prevention and Control Mechanism on January 2020, marking the beginning of its comprehensive response to the COVID-19 outbreak. This mechanism facilitated the rapid implementation of NPIs, including travel restrictions, quarantine measures, and public health campaigns aimed at educating the population about the virus (Deng and Grépin, 2024). On January 2023, China officially transitioned from a Class A to a Class B infectious disease management approach, signaling the end of the dynamic zero-COVID policy (Ge, 2023). This is why we defined 2019 as the Pre period, 2020–2022 as the Pan period, and 2023–2024 as the Post period in our study. In our study, HD results showed that during the COVID-19 pandemic, the influenza positivity rate dropped from approximately 25% before the outbreak to below 10%. After the pandemic, it rebounded to pre-pandemic levels. Similar findings were also observed in the CNIC data. These changes may be attributed to the stringent public health measures implemented to control the spread of COVID-19, such as lockdowns, social distancing, and mask mandates, which inadvertently reduced the transmission of influenza viruses. These non-pharmaceutical interventions significantly lowered influenza incidence during the 2020–2021 flu season (Chan et al., 2020; Itaya et al., 2020).

An important finding in our study is that, compared to Flu A, the COVID-19 pandemic appeared to have a lesser impact on Flu B. Our results show that, in 2021, Flu B was the dominant influenza type in both HD and CNIC data. While the limited sample size in HD might raise concerns about the reliability of the results, the CNIC dataset, which included over 400,000 tested samples, showed a similar pattern, with Flu B accounting for 99.87% of positive cases. This phenomenon had not been observed in previous studies. In the comparative analysis of the Pre, Pan, and Post periods, we also found that in the Pan period, Flu B accounted for more than 50% in the CNIC data, and in the Post period, the average positive rate for Flu B was slightly lower (though not statistically significant). During the COVID-19 pandemic, we observed that Influenza B (Flu B) replaced Influenza A (Flu A) as the predominant type of influenza. We speculate that this shift may be attributed to the following reasons:

The COVID-19 pandemic led to a significant decline in Flu A cases, with reports from many regions indicating that A/H1N1 and A/H3N2 strains were nearly eliminated. In contrast, Influenza B—particularly the Victoria lineage—persisted and even became dominant (Chang et al., 2023; Zhou et al., 2023); Compared to Influenza B, preventive measures such as social distancing and mask-wearing may have been more effective in reducing the transmission of Influenza A, allowing Influenza B to thrive (Wan and Zhang, 2022); The COVID-19 pandemic significantly altered the competitive dynamics of influenza viruses. As the prevalence of Flu A declined, Flu B filled the epidemiological niche and became increasingly prominent in the influenza landscape (Zeng et al., 2024).

Additionally, our study revealed discrepancies between HD and CNIC data. For example, an analysis of the weekly average Flu A positivity rate in the most recent year (2024) showed that the HD Flu A positivity rate was significantly higher than that of CNIC ($p = 0.0008$). Similar differences can also be observed in the figures from our study, highlighting the necessity of monitoring influenza trends at both the regional level and within individual centers. Furthermore, a comparative analysis between regional data and national influenza center data is crucial for understanding the characteristics of influenza epidemics and optimizing prevention and control strategies.

This study has several limitations that warrant further discussion. First, our dataset is derived from a single tertiary maternal and pediatric hospital in Chengdu, which may introduce selection bias. The patient population is primarily composed of children and women of childbearing age, who may have different healthcare-seeking behaviors, immune status, and vaccination coverage compared to the general population. Consequently, our findings may not be fully representative of the broader community, limiting the generalizability of the results. In our previous work on

respiratory pathogen epidemiology in this hospital, we observed similar demographic limitations, emphasizing the need for caution when extrapolating hospital-based findings to population-level inferences (Li et al., 2025). Second, while national data from the Chinese National Influenza Center (CNIC) was used for comparison, a lack of transparency regarding critical surveillance parameters—such as catchment population size, geographic coverage, case definition, and laboratory protocols—limits our ability to draw direct comparisons between the HD and CNIC datasets. These system-level differences could contribute to the observed discrepancies in influenza subtype prevalence and seasonality. Third, vaccination coverage was not captured in the HD dataset, and reliable population-level estimates were not available. This presents a critical gap, as influenza vaccination is known to influence both individual susceptibility and transmission dynamics (Alexander et al., 2004). Without such data, we cannot assess whether the observed patterns were influenced by differential vaccine uptake, particularly in vulnerable populations such as children or the elderly. Fourth, changes in healthcare-seeking behavior during and after the COVID-19 pandemic may have influenced testing patterns and positivity rates. For example, reduced outpatient visits during the pandemic may have led to under-detection of mild influenza cases, while heightened awareness of respiratory symptoms in the post-pandemic period may have led to increased testing (Li et al., 2024). These shifts could introduce temporal bias in surveillance data. Fifth, our study focused exclusively on influenza positivity rates and did not include clinical outcomes such as hospitalization rates, ICU admission, or disease severity. These indicators would provide important context regarding the public health burden of influenza across different time periods and viral subtypes (Caini et al., 2018). Lastly, environmental and behavioral changes due to non-pharmaceutical interventions (NPIs) varied significantly across regions and time, potentially influencing the transmission dynamics of different influenza subtypes in ways not fully captured by surveillance data. Future studies should incorporate multi-center data with diverse population profiles, standardized surveillance protocols, individual-level clinical and vaccination data, and longitudinal follow-up to improve the accuracy, comparability, and public health relevance of influenza epidemiological assessments. Addressing these limitations will be crucial for optimizing influenza control strategies and improving our preparedness for future respiratory virus outbreaks.

In conclusion, our study reveals significant temporal variations in influenza activity, with notable differences in subtype distribution and seasonal trends between hospital-based and national surveillance data. The impact of COVID-19-related non-pharmaceutical interventions was more pronounced on Flu A than Flu B, highlighting the differential sensitivity of influenza subtypes to public health measures. These findings underscore the importance of integrating multiple surveillance sources for a comprehensive understanding of influenza dynamics. Strengthening vaccination coverage and adaptive public health strategies will be essential for mitigating the influenza burden in the post-pandemic era.

Data availability statement

The raw data supporting the conclusions of this article will be made available by the authors, without undue reservation.

Ethics statement

The studies involving humans were approved by Ethics Committee of Sichuan Jinxin Xinan Women and Children Hospital. The studies were conducted in accordance with the local legislation and institutional requirements. The ethics committee/institutional review board waived the requirement of written informed consent for participation from the participants or the participants' legal guardians/next of kin because Written informed consent was waived because the data used in the study were anonymized and did not involve direct interaction with participants.

Author contributions

XL: Formal Analysis, Investigation, Methodology, Writing – review & editing. CY: Validation, Visualization, Writing – review & editing. LC: Formal Analysis, Methodology, Writing – review & editing. JM: Funding acquisition, Project administration, Resources, Supervision, Writing – review & editing. ZH: Conceptualization, Data curation, Formal Analysis, Funding acquisition, Investigation, Methodology, Project administration, Resources, Software, Supervision, Validation, Visualization, Writing – original draft, Writing – review & editing.

Funding

The author(s) declare that no financial support was received for the research and/or publication of this article.

Conflict of interest

The authors declare that the research was conducted in the absence of any commercial or financial relationships that could be construed as a potential conflict of interest.

Generative AI statement

The author(s) declare that no Generative AI was used in the creation of this manuscript.

Publisher's note

References

Alexander, M. E., Bowman, C., Moghadas, S. M., Summers, R., Gumel, A. B., and Sahai, B. M.. (2004). A vaccination model for transmission dynamics of influenza. *SIAM J. Appl. Dynamical Syst.* 3, 503–524. doi: 10.1137/030600370

Bi, Y., Yang, J., Wang, L., Ran, L., and Gao, G. F. (2024). Ecology and evolution of avian influenza viruses. *Curr. Biol.* 34, R716–r721. doi: 10.1016/j.cub.2024.05.053

Caini, S., Kroneman, M., Wiegers, T., El Guerche-Séblain, C., and Paget, J. (2018). Clinical characteristics and severity of influenza infections by virus type, subtype, and lineage: a systematic literature review. *Influenza Other Respir. Viruses* 12, 780–792. doi: 10.1111/irv.2018.12.issue-6

Cao, G., Guo, Z., Liu, J., and Liu, M. (2023). Change from low to out-of-season epidemics of influenza in China during the COVID-19 pandemic: A time series study. *J. Med. Virol.* 95, e28888. doi: 10.1002/jmv.28888

Chan, K. S., Liang, F. W., Tang, H. J., Toh, H. S., and Yu, W. L. (2020). Collateral benefits on other respiratory infections during fighting COVID-19. *Med. Clin. (Barc)* 155, 249–253. doi: 10.1016/j.medcli.2020.05.026

Chang, D., Lin, M., Song, N., Zhu, Z., Gao, J., Li, S., et al. (2023). The emergence of influenza B as a major respiratory pathogen in the absence of COVID-19 during the 2021–2022 flu season in China. *Virol. J.* 20, 189. doi: 10.1186/s12985-023-02115-x

Cowling, B. J., Ali, S. T., Ng, T. W., Tsang, T. K., Li, J. C., Fong, M. W., et al. (2020). Impact assessment of non-pharmaceutical interventions against coronavirus disease 2019 and influenza in Hong Kong: an observational study. *Lancet Public Health* 5, e279–e288. doi: 10.1016/s2468-2667(20)30090-6

Cozza, V., Campbell, H., Chang, H. H., Iuliano, A. D., Paget, J., Patel, N. N., et al. (2021). Global seasonal influenza mortality estimates: A comparison of 3 different approaches. *Am. J. Epidemiol.* 190, 718–727. doi: 10.1093/aje/kwaa196

Deng, Z., and Grépin, K. A. (2024). Achilles' heel: elderly COVID-19 vaccination policy in China. *Health Res. Policy Syst.* 22, 90. doi: 10.1186/s12961-024-01155-1

Feng, L., Zhang, T., Wang, Q., Xie, Y., Peng, Z., Zheng, J., et al. (2021). Impact of COVID-19 outbreaks and interventions on influenza in China and the United States. *Nat. Commun.* 12, 3249. doi: 10.1038/s41467-021-23440-1

Ge, J. (2023). The COVID-19 pandemic in China: from dynamic zero-COVID to current policy. *Herz* 48, 226–228. doi: 10.1007/s00059-023-05183-5

Hammond, A., Kim, J. J., Sadler, H., and Vandemaele, K. (2022). Influenza surveillance systems using traditional and alternative sources of data: A scoping review. *Influenza Other Respir. Viruses* 16, 965–974. doi: 10.1111/irv.13037

Huang, W.-J., Cheng, Y. H., Tan, M. J., Liu, J., Li, X. Y., Zeng, X. X., et al. (2022). Epidemiological and virological surveillance of influenza viruses in China during 2020–2021. *Infect. Dis. Poverty* 11, 74. doi: 10.1186/s40249-022-01002-x

Huang, Q.-M., Song, W. Q., Liang, F., Ye, B. L., Li, Z. H., Zhang, X. R., et al. (2022). Non-pharmaceutical interventions implemented to control the COVID-19 were associated with reduction of influenza incidence. *Front. Public Health* 10, 773271. doi: 10.3389/fpubh.2022.773271

Itaya, T., Furuse, Y., and Jindai, K. (2020). Does COVID-19 infection impact on the trend of seasonal influenza infection? 11 countries and regions, from 2014 to 2020. *Int. J. Infect. Dis.* 97, 78–80. doi: 10.1016/j.ijid.2020.05.088

Lampejo, T. (2022). The impact of the COVID-19 pandemic on the global burden of influenza. *J. Med. Virol.* 94, 2357. doi: 10.1002/jmv.27653

Langer, J., Welch, V. L., Moran, M. M., Cane, A., Lopez, S. M., Srivastava, A., et al. (2023). High clinical burden of influenza disease in adults aged ≥65 years: can we do better? A systematic literature review. *Adv. Ther.* 40, 1601–1627. doi: 10.1007/s12325-023-02432-1

Lei, H., Xu, M., Wang, X., Xie, Y., Du, X., Chen, T., et al. (2020). Nonpharmaceutical interventions used to control COVID-19 reduced seasonal influenza transmission in China. *J. Infect. Dis.* 222, 1780–1783. doi: 10.1093/infdis/jiaa570

Lei, H., Yang, L., Wang, G., Zhang, C., Xin, Y., Sun, Q., et al. (2022). Transmission patterns of seasonal influenza in China between 2010 and 2018. *Viruses* 14, 2063. doi: 10.3390/v14092063

Li, L., Fu, L., Li, H., Liu, T., and Sun, J. (2024). Emerging trends and patterns in healthcare-seeking behavior: A systematic review. *Medicine* 103, e37272. doi: 10.1097/MD.0000000000037272

Li, X., Ma, J., Li, Y., and Hu, Z. (2025). One-year epidemiological patterns of respiratory pathogens across age, gender, and seasons in Chengdu during the post-COVID era. *Sci. Rep.* 15, 357. doi: 10.1038/s41598-024-84586-8

Mi, S., Yang, Y., and Li, T. (2025). Epidemiological changes of common respiratory viruses in Shanghai, during 2021–2023. *Clin. Epidemiol. Global Health* 31, 101905. doi: 10.1016/j.cegh.2024.101905

Monamele, C. G., Kengne-Nde, C., Munshili Njifon, H. L., Njankouo, M. R., Kenmoe, S., and Njouom, R.. (2020). Clinical signs predictive of influenza virus infection in Cameroon. *PloS One* 15, e0236267. doi: 10.1371/journal.pone.0236267

Qu, H., Guo, Y., Guo, X., Fang, K., Wu, J., Li, T., et al. (2025). Predicting influenza in China from October 1, 2023, to February 5, 2024: A transmission dynamics model based on population migration. *Infect. Dis. Model.* 10, 139–149. doi: 10.1016/j.idm.2024.09.007

Shaghaghi, N., Karishetti, S., and Ma, N. (2021). *4th International Conference on Bio-Engineering for Smart Technologies (BioSMART)* (IEEE), 1–5.

Soudani, S., Mafi, A., Al Mayahi, Z., Al Balushi, S., Dbaibo, G., Al Awaidy, S., et al. (2022). A systematic review of influenza epidemiology and surveillance in the eastern mediterranean and North African region. *Infect. Dis. Ther.* 11, 15–52. doi: 10.1007/s40121-021-00534-3

Thomas, C. M. (2023). Early and increased influenza activity among children-tennessee, 2022-23 influenza season. *MMWR Morb. Mortal. Wkly. Rep.* 72, 49–54. doi: 10.15585/mmwr.mm7203a1

Uyeki, T. M. (2021). Influenza. *Ann. Intern. Med.* 174, Itc161–itc176. doi: 10.7326/aitc202111160

Uyeki, T. M., Hui, D. S., Zambon, M., Wentworth, D. E., and Monto, A. S. (2022). Influenza. *Lancet* 400, 693–706. doi: 10.1016/s0140-6736(22)00982-5

Wan, J., and Zhang, R. (2022). Positivity rate, risk factors and symptom characteristics of influenza virus in a tertiary hospital meeting COVID-19, Hangzhou, China. *Authorea Preprints*. doi: 10.22541/au.166236122.20225546/v2

Xie, Y., Lin, S., Zeng, X., Tang, J., Cheng, Y., Huang, W., et al. (2024). Two peaks of seasonal influenza epidemics - China, 2023. *China CDC Wkly.* 6, 905–910. doi: 10.46234/ccdcw2024.069

Zeng, Z., Jia, L., Zheng, J., Nian, X., Zhang, Z., Chen, L., et al. (2024). Molecular epidemiology and vaccine compatibility analysis of seasonal influenza A viruses in the context of COVID-19 epidemic in Wuhan, China. *J. Med. Virol.* 96, e29858. doi: 10.1002/jmv.29858

Zhang, L., Duan, W., Ma, C., Zhang, J., Sun, Y., Ma, J., et al. (2024). *Open forum infectious diseases* (US: Oxford University Press), ofae163.

Zhou, X., Lin, Z., Tu, J., Zhu, C., and Li, H. (2023). Persistent predominance of the Victoria lineage of influenza B virus during COVID-19 epidemic in Nanchang, China. *Influenza Other Respir. Viruses* 17, e13226. doi: 10.1111/irv.13226

Zhu, A., Liu, J., Ye, C., Yu, J., Peng, Z., Feng, L., et al. (2020). Characteristics of seasonal influenza virus activity in a subtropical city in China, 2013–2019. *Vaccines* 8, 108. doi: 10.3390/vaccines8010108

Zhu, A.-Q., Li, Z.-J., and Zhang, H.-J. (2023). Spatial timing of circulating seasonal influenza A and B viruses in China from 2014 to 2018. *Sci. Rep.* 13, 7149. doi: 10.1038/s41598-023-33726-7

frontiers | Frontiers in Public Health

TYPE Original Research
PUBLISHED 02 July 2025
DOI 10.3389/fpubh.2025.1588760

OPEN ACCESS

EDITED BY
Sneha Vishwanath,
University of Cambridge, United Kingdom

REVIEWED BY
Daniele Melo Sardinha,
Evandro Chagas Institute, Brazil
Sruthika K. Ashokan,
Diosynvax Ltd., United Kingdom

*CORRESPONDENCE
Haimei Jia
✉ haimei1103@126.com

RECEIVED 06 March 2025
ACCEPTED 12 June 2025
PUBLISHED 02 July 2025

CITATION
Jia H, Gao W, Huang X, Wang Q, Huang Y, Chen L, Zheng D, Zhang Y and Xu L (2025) Exploring influenza vaccination coverage and barriers to influenza vaccine uptake among preschool children in Fuzhou in 2022: a cross-sectional study. *Front. Public Health* 13:1588760. doi: 10.3389/fpubh.2025.1588760

Exploring influenza vaccination coverage and barriers to influenza vaccine uptake among preschool children in Fuzhou in 2022: a cross-sectional study

Haimei Jia[1]*, Wenyan Gao[1], Xun Huang[1], Qinghua Wang[1], Yonghan Huang[1], Liang Chen[2], Desi Zheng[3], Yinchuan Zhang[4] and Lifei Xu[5]

[1]Fuzhou Center for Disease Control and Prevention, Affiliated with Fujian Medical University, Fuzhou, China, [2]Gulou District Center for Disease Control and Prevention, Fuzhou, China, [3]Fuqing Center for Disease Control and Prevention, Fuzhou, China, [4]Minqing County Center for Disease Control and Prevention, Fuzhou, China, [5]Yongtai County Center for Disease Control and Prevention, Fuzhou, China

Background: Children are vulnerable to influenza virus due to their developing immune systems, particularly children aged 6 months-5 years (preschool children). To improve the uptake of influenza vaccine in preschool children, it is important to determine the influencing factors of Chinese parents/guardians' (P/Gs) intention and behavior for children to receive. We implemented an investigation to determine coverage of influenza vaccination in preschool children and the influencing factors of being vaccinated against influenza among preschool children in Fuzhou.

Methods: This is a cross-sectional study. Using a hierarchical approach, based on the coverage of influenza vaccination in preschool children, the 12 districts/counties in Fuzhou were divided into two levels. In each level, two urban districts and two counties were selected, including 2 randomly selected vaccination clinics and 2 kindergartens. A standardized anonymous questionnaire was used to collect information on P/Gs. Chi-square testing and multivariate logistic regression were used to analyze factors that may be associated with influenza.

Results: The coverage rate of influenza vaccination was 7.38% among preschool children in 2022 in Fuzhou City. A total of 8,768 guardians completed the questionnaire. 54.70% of the responders had received at least one dose of flu. Only 23.56% of the P/Gs involved were able to correctly list the influenza clinical feature. Higher education status had higher coverage (p-values < 0.05). Multivariate analysis showed birth order [odds ratio (OR) = 0.76, 95% confidence interval (CI): 0.63, 0.92], medical insurance [OR = 1.42, 95% CI: 1.22, 1.65], occupation [OR = 0.84, 95% CI: 0.75, 0.93], average monthly household income ≥ 10,000 [OR = 0.66, 95% CI: 0.56, 0.79], vaccine prices > 200 [OR = 1.66, 95% CI: 1.41, 1.97], and total duration of each vaccination session [OR = 0.49, 95% CI: 0.42, 0.58] were associated with flu vaccination.

Conclusion: Influenza vaccination coverage among preschoolers was low, and parental/guardian knowledge regarding influenza prevention was inadequate. Enhanced awareness, vaccine understanding, and recommendation policies correlated with higher coverage. Authorities should implement sustainable

financing and incentives to ensure access and affordability, while promoting education to convert vaccination intentions into actual uptake.

KEYWORDS

influenza, preschool children, parental attitudes, influenza vaccination coverage, questionnaire survey

Introduction

Influenza remains a major cause of morbidity, mortality, and economic burden worldwide each year. There are approximately 1 billion cases of influenza worldwide each year, of which 3 to 5 million are severe cases, resulting in 290,000–650,000 deaths globally (1). Children are relatively immunologically naive to influenza virus, leading to increased morbidity on infection (2). Among children under 5 years globally, there were an estimated one hundred million influenza virus episodes, and results in a substantial burden on health services worldwide (3). Lai et al. (4) indicated that the average economic burden of children due to influenza-like illness was 1,647 yuan (237.2 dollars) per episode, and the indirect economic burden due to the loss of caregivers' labor time also was fairly large. The estimated overall attack rate in China was reported to be approximately 5.5% in all age groups, with the highest attack rate observed in 0–4 years old preschool children (31.9%). However, influenza vaccination coverage among children in China is low, remaining at approximately 25% (5).

World Health Organization (WHO) and European Union targets for immunization rates for at-risk populations are 75% (6). Both the Advisory Committee on Immunization Practices and Chinese Center for Disease Control and Prevention were simultaneously recommending universal influenza vaccination for preschool children (between the ages of 6 and 59 months), as well as those with high-risk conditions (7, 8). Vaccinating children against influenza could not only protect children themselves but also protect the whole community and reduce influenza incidence in the general population (9).

Parents/guardians (P/Gs) are the primary decision-makers for all family behaviors, it is critical to understand the factors that influence P/Gs' intentions to vaccinate their children. Low MSF's article showed that P/Gs' willingness to vaccinate is a strong predictor of child influenza vaccination (10). Thus, a comprehensive survey of P/Gs is warranted to assess vaccination willingness and identify potential determinants influencing their decision-making.

In order to better control the influenza prevalent among preschool children, Fuzhou Health Commission and Fuzhou Center for Disease Control and Prevention provide health reminders and recommend getting vaccinated against influenza each year. However, the actual vaccination willingness of preschool children and the factors influencing their vaccination remain unclear. During 2022 through 2023, we conducted a field investigation to evaluate the knowledge, attitudes of P/Gs regarding this influenza vaccination, and assess their status of influenza vaccination. This study was designed to identify factors affecting influenza vaccination among preschool children and provide evidence increasing influenza vaccination rates among preschool children.

Methods

Study design and setting

Data on influenza vaccinations of children aged 6 months-5 years (preschool children) in 2022 were obtained from the Fujian Province Immunization Information System, which contains vaccination data for all citizens living in Fuzhou. Population data used in this study were obtained from the China Information System for Disease Control and Prevention.

Setting and subjects

Fuzhou area is made of 12 urban districts (counties). Based on the coverage of influenza vaccination in preschool children, the 12 districts/counties in Fuzhou were divided into two levels A and B (A: high coverage rate > 8.0%; B: low coverage rate < 8.0%) In each level, two urban districts and two counties were selected, including 2 randomly selected vaccination clinics and 2 kindergartens. There was no specific influenza vaccination campaign during the investigation period. At least 2,700 P/Gs of preschool children were investigated in each level. P/Gs who were unwilling to participate in the study and children with contraindications of influenza vaccines were excluded.

Data collection

A standardized anonymous questionnaire designed specifically for the study was used to collect information, including fundamental demographic details concerning the infants and their families (sex, age, household composition, education status of the P/Gs, health status of children, health insurance status, P/Gs occupation, average monthly household income, birth information of children), influenza vaccination status of children, health-related beliefs and attitudes to influenza vaccination knowledge to influenza and influenza vaccination, and the demand for vaccination services (trust and satisfaction with vaccination staff, schedule of clinics, medical service environment). The questionnaire was distributed by investigators, filled in, and retrieved immediately at the field.

Data analysis

Knowledge of influenza and influenza vaccination: Assign 1 point to each question, 1 point for correct answers, and 0 points for errors, the total score is 14. The scores were categorized into three groups: 0–5 unknown, 6–10 general know, 11–14 good know, with a hierarchy describing the respondent's state of knowledge. We established a database for analysis with SPSS version 26.0. Coverage of influenza

10.3389/fpubh.2025.1588760

TABLE 1 Demographic characteristics of parents/guardians and children.

Variable	Levels	Number of respondents	Percent %
Parents/guardians			
Age group (years)	20-30	2,598	29.63
	31-40	5,290	60.33
	>41	880	10.04
Fill the questionnaire	Mother	7,123	81.23
	Father	1,385	15.80
	Grandparents	138	1.57
	Other	122	1.39
Occupation	Enterprises and public institutions	3,947	45.02
	Self-employed/farmer	1,599	18.24
	Unemployed/other	3,222	36.75
Education level	Middle school or below	1,273	14.52
	High school	2,261	25.79
	Three-year college/ university	4,944	56.39
	Master and above	290	3.31
Average monthly household income (RMB)	<3,000	870	9.92
	3,000-4,999	2,344	26.73
	5,000-9,999	3,379	38.54
	≥10,000	2,175	24.81
Rest according to legal holidays	Yes	5,396	61.54
	Occasional overtime	2,389	27.25
	Frequent overtime	983	11.21
Transportation to the Vaccination Clinic	Walking	1,065	12.15
	Bicycle	104	1.19
	Motorcycle/electric vehicle	4,089	46.64
	Public transportation	301	3.43
	Self-driving	3,209	36.60
One-way inoculation time (minutes)	<30	7,540	85.99
	30-60	1,143	13.04
	>60	85	0.97
Children			
Age group	6-11 months	684	7.80
	1-2 years	1,822	20.78
	3-6 years	6,262	71.42
Gender	Male	4,573	52.16
	Female	4,195	47.84
Birth order	First	3680	41.97
	Second	4511	51.45
	Third or more	577	6.58
Common cold	Often	1220	13.91
	Infrequent	6011	68.56
	Seldom	1537	17.53
Medical insurance	No	806	9.19
	Purchased	7962	90.81

vaccination, demographics, knowledge about influenza and influenza vaccination, and health-related beliefs and attitudes to influenza vaccination were analyzed descriptively. Chi-square testing and multivariate logistic regression were used to analyze factors that may be associated with influenza vaccination. We used a 2-tail *p*-value (*p*) significance level of 0.05.

Results

Vaccination rates for flu in Fuzhou

Data obtained from the Fujian province immunization information system showed the total coverage of influenza vaccination (at least one dose) among preschool children in 2022 was 7.38%. The coverage was between 4.38–10.76% among 12 urban districts (counties). The coverage of influenza vaccination in preschool children among A (8.77%) was higher than in level B (6.10%) ($p < 0.05$).

Demographic characteristics

A total of 8,768 P/Gs were surveyed, their median age was 33 years (range: 20–99), and most participants were mothers (81.23%). According to occupational categorization, 45.02% of the respondents were enterprises and institutions, 59.39% were three-year college/ university, and 61.54% had legal holidays.

7.80% (684) were 6–11 months children, 20.78% (1,822) were between 1–2 years, 71.42% (6,262) were 3–6 years, 52.16% (4,573) were males. 51.45% of these were from the second birth, 90.81% had health insurance. Demographics and other characteristics are illustrated in Table 1.

Knowledge regarding influenza

Almost all of the respondents (97.54%) answered they knew the flu, however, 23.56% of the P/Gs involved were able to correctly list the influenza clinical feature. And the percentage with correct knowledge of transmission mode, complication, and the infectiousness of influenza were 94.66, 93.68, and 91.97%, respectively (Figure 1).

31–40 years old P/Gs had better knowledge about influenza than younger P/Gs and older P/Gs (24.40, 21.86, and 23.52%, respectively, $p < 0.05$). When we compared the education status, there were differences among P/Gs, 28% of P/Gs with Three-year college/ university and above had answered correctly, which was higher than

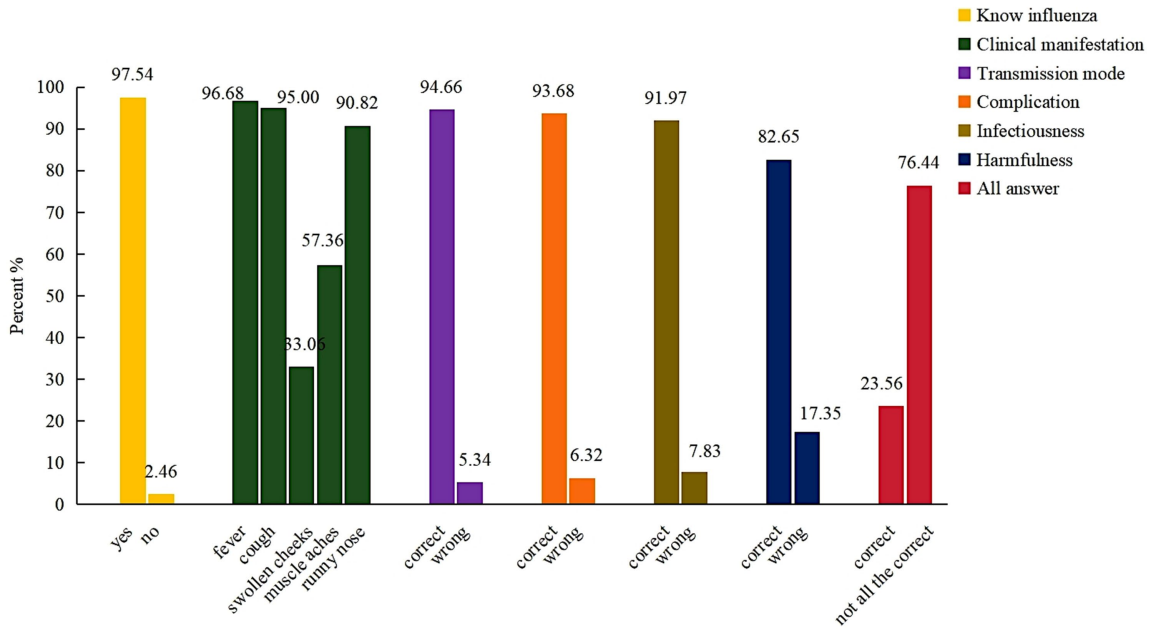

FIGURE 1
Respondents' answers about influenza knowledge.

TABLE 2 Main reasons influencing respondents' knowledge of influenza.

Variable	Levels	The rate of correct answer (%)	χ^2	*p*
Hierarchy	A	23.29	0.38	0.54
	B	23.86		
P/Gs age	20–30	21.86	6.21	0.04
	31–40	24.40		
	>41	23.52		
Education level	Middle school or below	13.12	152.75	0.00
	High school	19.46		
	Three-year college/ university	27.97		
	Master's degree and above	26.21		

those with a high school education (19.46%) and middle school or below (13.12%; $p < 0.05$) (Table 2).

Influenza vaccination and vaccination rates for flu

Figure 2 showed almost P/Gs knew the flu vaccine (95.38%), and knew that it protects against the flu (88.50%). However, only 1.49% P/Gs and 2.74% P/Gs answered "YES" about the safety and effectiveness of the influenza vaccine. When asked about the source of knowledge of flu vaccine, the main source of information about flu was vaccinators (55.34%), followed by Center for Disease Control and Prevention (CDC) (47.57%), and social media (47.67%).

Table 3 showed that almost all of P/Gs were willing to vaccinate against influenza (90.02%), main reasons for refusing the flu vaccine were concerns about the safety (47.20%), not effective (36.69%), no knowledge of vaccines (31.77%), and adverse reactions have occurred of the influenza vaccine (13.87%).

Factors associated with influenza uptake

Among preschool children respondents, 4,796 (54.70%) had received at least one dose of flu vaccine (Table 4).

The coverage rate of preschool children was no significant difference between strata A and B (56.33 and 55.50%, $p > 0.05$). 20–30 years old (60.70%) have higher vaccination rate for their children than 31–40 years old (51.63%) and older P/Gs (55.45%) ($p < 0.05$). The higher the education level of parents, the higher the flu vaccination rate of their children (the detailed data are in Tables 5, $p < 0.05$). The P/Gs working in state enterprises and public institutions (57.36%) had higher coverage for their children than self-employed/farmer (52.66%) and unemployed/other occupations (52.45%, $p < 0.05$). However, when we compared the household income, it showed the lower household income had higher coverage rate ($p < 0.05$). Total duration of each vaccination session < 30 min (58.72%) had a higher vaccination rate than 30–60 (52.66%) and > 60 (39.77%, $p < 0.05$) (Table 5).

Summary of children characteristics is shown in Table 5. 1–2 years old had higher vaccination rate than 6–11 months and 3–6 years old (65.86, 60.53, and 50.81%, respectively, $p < 0.05$). Furthermore, the first-born child had a higher vaccination rate than second-born and born later (58.40, 52.76, and 46.27%, respectively, $p < 0.05$). The coverage of preschool children with medical insurance was higher than that of children without (55.53 and 46.53%, respectively, $p < 0.05$).

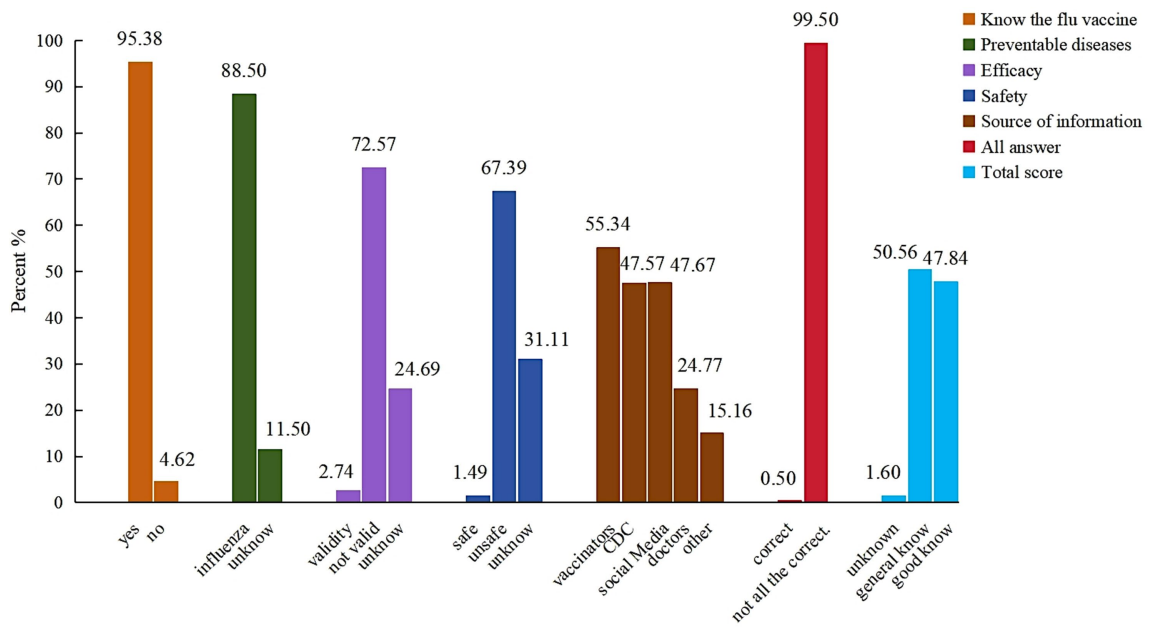

FIGURE 2
Respondents' answers about influenza vaccine knowledge.

TABLE 3 Attitude toward influenza illness and influenza vaccine.

Variable	Levels	Number of respondents	Percent %
Willingness to vaccinate	Yes	7,893	90.02
	No	875	9.98
Reasons for reluctance to vaccinate (N = 875)	No time	59	6.74
	Self-payment required	153	17.49
	No knowledge of vaccines	278	31.77
	Worried about the safety	413	47.20
	Not effective	321	36.69
	Poor physical of children	158	18.06
	Other	138	15.77
Adverse reaction (N = 4,796)	No	4,131	86.13
	Fever	370	7.71
	Redness, swelling and pain at the vaccination site	340	7.09
	Hard nodules at the vaccination site	191	3.98
	Rash	83	1.73
	Other	120	2.50

TABLE 4 Vaccination rates in districts/counties in this study sample.

Variable	Levels	Vaccination n (%)	Average rate %
A level	Fuqing City	1,216 (52.60)	56.33
	Jinan District	461 (54.24)	
	Taijiang District	477 (58.24)	
	Yongtai County	356 (60.24)	
B level	Gulou District	465 (57.20)	55.50
	Cangshan District	520 (65.16)	
	Minhou County	932 (51.04)	
	Minqing County	369 (48.62)	
Total	Fuzhou City	4,796 (54.70)	54.70

The multivariate analysis of factors influencing flu vaccination showed that children's birth order, medical insurance, P/G's occupation, average monthly household income, vaccine prices, and total duration of each vaccination session were associated with flu vaccination.

Children birthed third or late [odds ratio (OR) = 0.76, 95% confidence interval (CI): 0.63, 0.92]; medical insurance [OR = 1.42, 95% CI: 1.22, 1.65]; P/Gs occupation [OR = 0.86, 95% CI: 0.76, 0.98 and OR = 0.84, 95% CI: 0.75, 0.93]; average monthly household income ≥ 10,000 [OR = 0.66, 95% CI: 0.56, 0.79]; acceptable vaccine prices > 200 [OR = 1.66, 95% CI: 1.41, 1.97]; total duration of each vaccination session > 60 min [OR = 0.49, 95% CI: 0.42, 0.58] (Table 6).

Discussion

Our study showed the total coverage of influenza vaccination (at least one dose) among preschool children in 2022 was 7.38%. The coverage was between 4.38–10.76% among 12 urban districts (counties). 31–40 years old P/Gs had better knowledge about influenza than younger P/Gs and older P/Gs (24.40, 21.86, and 23.52%, respectively, $p < 0.05$), but almost P/Gs were unaware of the safety and effectiveness of the influenza vaccine. This investigation showed

10.3389/fpubh.2025.1588760

TABLE 5 Univariate analysis of factors influencing influenza vaccination.

Factors	Category	Vaccination rate (%)	β	p	OR (95% CI)
Hierarchies	A	56.33			
	B	55.50	−0.02	0.69	0.94 (0.90, 1.07)
Fill the questionnaire	Mother	54.43			
	Father	54.87	0.02	0.76	1.02 (0.91, 1.14)
	Grandparents	64.49	0.42	0.02	1.52 (1.07, 2.16)
	Other	57.38	0.12	0.52	1.13 (0.79, 1.62)
Age group (years)	20–30	60.70			
	31–40	51.63	−0.37	0.00	0.69 (0.63, 0.76)
	>41	55.45	−0.22	0.01	0.81 (0.69, 0.94)
Education level	Middle school or below	52.71			
	High school	52.10	−0.02	0.73	0.98 (0.85, 1.12)
	Three-year college/university	56.01	0.13	0.04	1.14 (1.01, 1.29)
	Master and above	61.38	0.36	0.01	1.43 (1.10, 1.85)
Occupation	Enterprises and public institutions	57.36			
	Self-employed/farmer	52.66	−0.19	0.00	0.83 (0.74, 0.93)
	Unemployed/other	52.45	−0.20	0.00	0.82 (0.75, 0.90)
Average monthly household income (RMB)	<3,000	57.59			
	3,000-4,999	57.00	−0.02	0.76	0.98 (0.83, 1.14)
	5,000-9,999	53.42	−0.17	0.03	0.85 (0.73, 0.98)
	≥10,000	53.06	−0.18	0.02	0.83 (0.71, 0.98)
Rest according to legal holidays	Yes	56.60			
	Occasional overtime	52.74	−0.16	0.00	0.86 (0.78, 0.94)
	Frequent overtime	49.03	−0.30	0.00	0.74 (0.64, 0.85)
Transportation	Walking	59.72			
	Bicycle	71.15	0.51	0.02	1.66 (1.07, 2.59)
	Motorcycle/electric vehicle	54.83	−0.20	0.00	0.82 (0.71, 0.94)
	Public transport	54.15	−0.23	0.08	0.80 (0.62, 1.03)
	Self-driving	52.38	−0.30	0.00	0.74 (0.65, 0.85)
One-way inoculation time (minutes)	<30	55.16			
	30–60	52.49	−0.11	0.09	0.90 (0.79, 1.02)
	>60	43.53	−0.47	0.03	0.63 (0.41, 0.96)
Acceptable vaccine prices (RMB)	≤50	49.15			
	50–100	53.33	0.17	0.01	1.18 (1.05, 1.33)
	100–200	58.01	0.36	0.00	1.43 (1.27, 1.61)
	>200	59.50	0.42	0.00	1.52 (1.30, 1.74)
Total duration of each vaccination session	<30	58.72			
	30–60	52.66	−0.25	0.00	0.78 (0.72, 0.85)
	>60	39.77	−0.77	0.00	0.46 (0.39, 0.55)
Total score	Unknown	55.00			
	General know	57.31	0.00	0.99	1.00 (0.71, 1.41)
	Good know	53.87	−0.03	0.88	0.97 (0.69, 1.37)
Children's characteristics					
Gender	Male	54.65			
	Female	54.76	0.00	0.92	1.00 (0.92, 1.09)

(Continued)

TABLE 5 (Continued)

Factors	Category	Vaccination rate (%)	β	p	OR (95% CI)
Age group	6–11 months	60.53			
	1–2 years	65.86	0.23	0.01	1.26 (1.05, 1.51)
	3–6 years	50.81	−0.40	0.00	0.67 (0.57, 0.79)
Birth order	First	58.40			
	Second	52.76	−0.23	0.00	0.80 (0.73, 0.87)
	Third or more	46.27	−0.49	0.00	0.61 (0.51, 0.73)
Cold condition	Often	55.82			
	Infrequent	54.17	−0.07	0.29	0.94 (0.83, 1.06)
	Seldom	55.89	0.00	0.97	1.00 (0.86, 1.17)
Medical insurance	No	46.53			
	Purchased	55.53	0.36	0.00	1.44 (1.24, 1.66)

TABLE 6 Multivariate analysis of the impact of influenza vaccination.

Factors	Category	β	p	OR (95% CI)
Birth order	First			
	Second	−0.11	0.02	0.89 (0.81, 0.98)
	Third or more	−0.27	0.01	0.76 (0.63, 0.92)
Medical insurance	No			
	Purchased	0.35	0.00	1.42 (1.22, 1.65)
Age group (years)	20–30			
	31–40	−0.30	0.00	0.74 (0.67, 0.82)
	>41	−0.10	0.22	0.90 (0.77, 1.06)
Education level	Middle school or below			
	High school	−0.07	0.33	0.93 (0.81, 1.08)
	Three-year college/university	0.03	0.69	1.03 (0.89, 1.19)
	Master and above	0.29	0.05	1.33 (1.00, 1.77)
Occupation	Enterprises and public institutions			
	Self-employed/farmer	−0.15	0.02	0.86 (0.76, 0.98)
	Unemployed/other	−0.18	0.00	0.84 (0.75, 0.93)
Average monthly household income (RMB)	<3,000			
	3,000–4,999	−0.16	0.05	0.85 (0.72, 1.00)
	5,000–9,999	−0.36	0.00	0.70 (0.59, 0.82)
	≥10,000	−0.41	0.00	0.66 (0.56, 0.79)
One-way inoculation time (minutes)	<30			
	30–60	−0.04	0.54	0.96 (0.84, 1.09)
	>60	−0.27	0.23	0.76 (0.49, 1.19)
Acceptable vaccine prices (RMB)	<50			
	50–100	0.22	0.00	1.25 (1.11, 1.41)
	100–200	0.43	0.00	1.54 (1.36, 1.73)
	>200	0.51	0.00	1.66 (1.41, 1.97)
Total duration of each vaccination session	<30			
	30–60	−0.24	0.00	0.79 (0.72, 0.86)
	>60	−0.71	0.00	0.49 (0.42, 0.58)

children's age, birth order, medical insurance, P/G's age, occupation, average monthly household income, overtime work, transportation, vaccine prices, and total duration of each vaccination session were associated with flu vaccination.

Data obtained from the Fujian Province Immunization Information System showed the total coverage of influenza vaccination (at least one dose) among preschool children in 2022 was 7.38%, which is far below Germany (40%) (11), and England (48%) (12) who provide specialized and effective policy support for vaccination. Currently, influenza vaccination in Fuzhou operates solely on a voluntary, self-paid basis without any complementary support measures such as government subsidies or insurance coverage. This suggested deficiencies in establishing or implementing influenza vaccine policies for Fuzhou.

This investigation showed 54.70% children had received at least one dose of the influenza vaccine, which was far below the WHO's target of 75% and domestic of 28% (13) flu vaccination coverage. However, almost P/Gs (90.02%) were willing to have their children vaccinated against the flu, which suggested they knew it's good to get vaccinated. If all P/Gs implemented the "Willingness," children can be protected against flu through vaccination. In this study. Higher-degree of parental had higher influenza vaccination rates among preschoolers. Larson HJ's article indicated that parental education level is a significant predictor of vaccine uptake (14). P/Gs with high education are more likely to vaccinate their children against influenza (15). However, European study reported that lower influenza vaccination rates among highly educated individuals in Ireland, Italy, and Spain (16). This discrepancy may be attributed to cultural and cognitive differences across regions. Extensive research has established that P/Gs knowledge significantly influences childhood influenza vaccination rates (17–19). Enhancing parental understanding of influenza may consequently improve vaccination rates among children. Our research showed only 1.49% P/Gs and 2.74% P/Gs answered "YES" about the safety and effectiveness of the influenza vaccine, indicating a substantial gap in influenza- and vaccine-related knowledge. When asked about the source of knowledge of flu vaccine, the main source of information about flu was vaccinators (55.34%), followed by CDC (47.57%), and social media (47.67%). So vaccinators must provide strong advice and vaccine knowledge to P/Gs who visit vaccination clinics. Above results showed influenza coverage among preschool children was low, good knowledge of influenza and influenza vaccine were linked to improved immunization coverage. These hinted that there was still a lack of publicity about influenza.

In addition to knowledge, the convenience and feasibility of influenza vaccination are also important influencing factors. Multivariate regression analyses showed that extended vaccination time negatively impacted compliance ($\beta = -0.71$, $p < 0.05$). The vaccination rate was higher among the respondents who could be vaccinated within 30 min. This disparity may reflect logistical challenges P/Gs face when coordinating clinic visits with children's schedules. Distance between outpatient clinic and home also affect the convenience of vaccination ($p < 0.05$). Furthermore, parental occupational constraints and overtime status were identified as additional barriers, Goldman (20) and Ding's (21) articles show that it is more difficult for P/Gs to coordinate the time of vaccination for children and their work leading to low vaccination.

Furthermore, some P/Gs also showed dissatisfaction with the vaccination process, including difficulties in making vaccine appointments, long queues, and cumbersome processes. These findings suggest current influenza vaccination procedures in Fuzhou create accessibility barriers. If individuals perceive the process of getting vaccinated to be complicated or cumbersome, they may be less likely to seek it out or delay it (22, 23). To boost children influenza vaccination coverage, public health authorities should prioritize service optimization through streamlined scheduling systems, extended clinic hours, digital appointment platforms, and strengthen cooperation with the school authorities (getting vaccinated before the flu season or strengthening the promotion of flu vaccination in schools).

Our results showed there was a significant inverse correlation between household income and influenza vaccination rates ($\beta = -0.41$, $p < 0.05$), which coincides with previous findings that vaccination rates among children tend to be higher in families with lower economic status (24). This phenomenon may be attributed to the greater perceived cost-effectiveness of immunization for economically disadvantaged families, where disease prevention represents a more substantial economic benefit. Health insurance coverage among preschool children is significantly associated with increased influenza vaccination uptake ($p < 0.05$). In addition, Fuzhou's self-funded vaccination policy makes socially and economically disadvantaged groups have the burden of vaccination. The price of vaccines is an important deterrent to vaccination behavior. Comparative analyses of vaccination policies reveal that regions implementing free vaccination programs, such as Beijing and Hong Kong, achieve significantly higher coverage rates. Comparative analyses of vaccination policies reveal that regions such as Beijing (25) and Hong Kong (26), which implement free vaccination policy achieved significantly higher coverage rates than Fuzhou. Empirical evidence from national policy evaluations confirms that free vaccination policies yield the highest coverage rates, followed by medical insurance reimbursement systems (27, 28). These findings underscore the critical role of policy interventions and financial support mechanisms in enhancing vaccination uptake. In order to comprehensively increase influenza vaccine coverage among school-aged children in Fuzhou, we recommend implementing comprehensive strategies including: (1) establishment of free or subsidized vaccination programs, (2) integration with existing healthcare insurance systems, and (3) development of targeted initiatives for vulnerable populations.

Our study had a few limitations. First, the data on vaccination were self-reported, and not verified by immunization certificate, document, or serological testing. Second, the survey is a self-administered questionnaire by the respondents, we relied on respondents to fill out the questionnaire themselves to complete the survey, which may have limited a small percentage of P/Gs from responding.

In conclusion, our study offers valuable insights into the determinants influencing Chinese P/Gs' willingness to vaccinate influenza vaccine for their children. The findings demonstrate that as factors such vaccine knowledge, medical insurance, occupation, household income, overtime work, transportation, vaccine prices, and total duration of each vaccination session play a pivotal role in shaping P/Gs' intentions to influenza vaccine. Public health campaigns and educational initiatives should emphasize the benefits associated with the influenza vaccine. First, public health authorities should establish sustainable financing mechanisms and incentive programs to ensure vaccine accessibility and affordability, health and education departments can do a good job of health education on influenza and vaccination in advance, improve the

corresponding cognitive level of the target population, convert vaccination intentions into actual uptake. These integrated measures, when implemented prior to influenza seasons, could significantly improve vaccination rates among preschool children, thereby establishing herd immunity and reducing influenza-related morbidity.

Data availability statement

The original contributions presented in the study are included in the article/supplementary material, further inquiries can be directed to the corresponding author.

Ethics statement

The studies involving humans were approved by Fuzhou Center for Disease Control and Prevention's Ethics Committee. The studies were conducted in accordance with the local legislation and institutional requirements. Written informed consent for participation in this study was provided by the participants' legal guardians/next of kin.

Author contributions

HJ: Writing – review & editing, Investigation, Project administration, Writing – original draft, Data curation, Methodology. WG: Data curation, Formal analysis, Software, Writing – original draft, Writing – review & editing. XH: Project administration, Writing – review & editing, Investigation. QW: Project administration, Writing – review & editing, Investigation. YH: Project administration, Writing – review & editing, Investigation. LC: Investigation, Data curation, Writing – review & editing. DZ: Investigation, Data curation, Writing – review & editing. YZ: Investigation, Data curation, Writing – review & editing. LX: Investigation, Data curation, Writing – review & editing.

Funding

The author(s) declare that financial support was received for the research and/or publication of this article. This research received funding came from Vaccine and Immunization Young Talent Promotion Project of Chinese Preventive Medicine Association grant number CPMAQT_YM0320.

Acknowledgments

We thank the respondents, the vaccinators, and investigation teams, in Fuzhou CDC, Gulou District CDC, Fuqing CDC, Minqing County CDC, Minhou County CDC, and Yongtai County for their support and assistance with this investigation. We would also like to kindly thank all the participants for their time and contribution to this research.

Conflict of interest

The authors declare that the research was conducted in the absence of any commercial or financial relationships that could be construed as a potential conflict of interest.

Generative AI statement

The authors declare that no Gen AI was used in the creation of this manuscript.

Publisher's note

References

1. World Health Organization. Global influenza strategy 2019–2030. WHO. (2023). Available online at: https://apps.who.int/iris/handle/10665/311184. (Accessed 18 February 2023).

2. Nayak J, Hoy G, Gordon A. Influenza in Children. *Cold Spring Harb Perspect Med*. (2021) 11:a038430. doi: 10.1101/cshperspect.a038430

3. Wang X, Li Y, O'Brien KL, Madhi SA, Widdowson MA, Byass P, et al. Global burden of respiratory infections associated with seasonal influenza in children under 5 years in 2018: a systematic review and modelling study. *Lancet Glob Health*. (2020) 8:e497–510. doi: 10.1016/S2214-109X(19)30545-5

4. Lai X, Rong H, Ma X, Hou Z, Li S, Jing R, et al. The economic burden of influenza-like illness among children, chronic disease patients, and the elderly in China: a National Cross-Sectional Survey. *Int J Environ Res Public Health*. (2021) 18:6277. doi: 10.3390/ijerph18126277

5. Wu S, VAN Asten L, Wang L, SA MD, Pan Y, Duan W, et al. Estimated incidence and number of outpatient visits for seasonal influenza in 2015-2016 in Beijing. *China Epidemiol Infect*. (2017) 145:3334–44. doi: 10.1017/S0950268817002369

6. World Health Assembly. Resolution WHA56.19. Prevention and control of influenza pandemics and annual epidemics (2003) Available online at: http://apps.who.int/gb/archive/pdf_files/WHA56/ea56r19.pdf. (Accessed February 8, 2013).

7. Grohskopf LA, Alyanak E, Ferdinands JM, Broder KR, Blanton LH, Talbot HK, et al. Prevention and control of seasonal influenza with vaccines: recommendations of the advisory committee on immunization practices, United States, 2021-22 influenza season. *MMWR Recomm Rep*. (2021) 70:1–28. doi: 10.15585/mmwr.rr7005a1

8. National Immunization Advisory Committee Technical Working Group IVTWG. Technical guidelines for seasonal influenza vaccination in China (2021-2022). *Zhonghua Liu Xing Bing Xue Za Zhi*. (2021) 42:1722–49. doi: 10.3760/cma.j.cn112338-20210913-00732

9. Shono A, Kondo M. Factors associated with seasonal influenza vaccine uptake among children in Japan. *BMC Infect Dis*. (2015) 18:72. doi: 10.1186/s12879-015-0821-3

10. Low MSF, Tan H, Hartman M, Tam CC, Hoo C, Lim J, et al. Parental perceptions of childhood seasonal influenza vaccination in Singapore: a cross-sectional survey. *Vaccine*. (2017) 35:6096–102. doi: 10.1016/j.vaccine.2017.09.060

11. Molnar D, Anastassopoulou A, Poulsen Nautrup B, Schmidt-Ott R, Eichner M, Schwehm M, et al. Cost-utility analysis of increasing uptake of universal seasonal quadrivalent influenza vaccine (QIV) in children aged 6 months and older in Germany. *Hum Vaccin Immunother*. (2022) 18:2058304. doi: 10.1080/21645515.2022.2058304

12. Boddington NL, Mangtani P, Zhao H, Verlander NQ, Ellis J, Andrews N, et al. Live-attenuated influenza vaccine effectiveness against hospitalization in children aged 2-6 years, the first three seasons of the childhood influenza vaccination program in England, 2013/14-2015/16. *Influenza Other Respir Viruses*. (2022) 16:897–905. doi: 10.1111/irv.12990

13. Wang Q, Yue N, Zheng M, Wang D, Duan C, Yu X, et al. Influenza vaccination coverage of population and the factors influencing influenza vaccination in mainland China: a meta-analysis. *Vaccine*. (2018) 36:7262–9. doi: 10.1016/j.vaccine.2018.10.045

14. Larson HJ, Jarrett C, Eckersberger E, Smith DM, Paterson P. Understanding vaccine hesitancy around vaccines and vaccination from a global perspective: a systematic review of published literature, 2007-2012. *Vaccine*. (2014) 32:2150–9. doi: 10.1016/j.vaccine.2014.01.081

15. Ghazy RM, Ibrahim SA, Taha SHN, Elshabrawy A, Elkhadry SW, Abdel-Rahman S, et al. Attitudes of parents towards influenza vaccine in the eastern Mediterranean region: a multilevel analysis. *Vaccine*. (2023) 41:5253–64. doi: 10.1016/j

16. Endrich MM, Blank PR, Szucs TD. Influenza vaccination uptake and socioeconomic determinants in 11 European countries. *Vaccine*. (2009) 27:4018–24. doi: 10.1016/j.vaccine.2009.04.029

17. Zhao M, Liu H, Qu S, He L, Campy KS. Factors associated with parental acceptance of influenza vaccination for their children: the evidence from four cities of China. *Hum Vaccin Immunother*. (2021) 17:457–64. doi: 10.1080/21645515.2020.1771988

18. Li P, Qiu Z, Feng W, Zeng H, Chen W, Ke Z, et al. Analysis of factors influencing parents' willingness to accept the quadrivalent influenza vaccine for school-aged children in the Nanhai District, China. *Hum Vaccin Immunother*. (2020) 16:1078–85. doi: 10.1080/21645515.2019.1644881

19. Hofstetter AM, Opel DJ, Stockwell MS, Hsu C, de Hart MP, Zhou C, et al. Influenza-related knowledge, beliefs, and experiences among caregivers of hospitalized children. *Hosp Pediatr*. (2021) 11:815–32. doi: 10.1542/hpeds.2020-003459

20. Goldman RD, McGregor S, Marneni SR, Katsuta T, Griffiths MA, Hall JE, et al. Willingness to vaccinate children against influenza after the coronavirus disease 2019 pandemic. *J Pediatr*. (2021) 228:87–93.e2. doi: 10.1016/j.jpeds.2020.08.005

21. Ding X, Tian C, Wang H, Wang W, Luo X. Associations between family characteristics and influenza vaccination coverage among children. *J Public Health*. (2020) 42:e199–205. doi: 10.1093/pubmed/fdz101

22. Zhao X, Hu X, Wang J, Shen M, Zhou K, Han X, et al. A cross-sectional study on the understanding and attitudes toward influenza and influenza vaccines among different occupational groups in China. *Hum Vaccin Immunother*. (2024) 20:2397214. doi: 10.1080/21645515.2024.2397214

23. Flood EM, Rousculp MD, Ryan KJ, Beusterien KM, Divino VM, Toback SL, et al. Parents' decision-making regarding vaccinating their children against influenza: a web-based survey. *Clin Ther*. (2010) 32:1448–67. doi: 10.1016/j.clinthera.2010.06.020

24. Zeng Y, Yuan Z, Yin J, Han Y, Chu CI, Fang Y. Factors affecting parental intention to vaccinate kindergarten children against influenza: a cross-sectional survey in China. *Vaccine*. (2019) 37:1449–56. doi: 10.1016/j.vaccine.2019.01.071

25. Lv M, Fang R, Wu J, Pang X, Deng Y, Lei T, et al. The free vaccination policy of influenza in Beijing, China: the vaccine coverage and its associated factors. *Vaccine*. (2016) 34:2135–40. doi: 10.1016/j.vaccine.2016.02.032

26. Lau YL, Wong WHS, Hattangdi-Haridas SR, Chow CB. Evaluating impact of school outreach vaccination programme in Hong Kong influenza season 2018-2019. *Hum Vaccin Immunother*. (2020) 16:823–6. doi: 10.1080/21645515.2019.1678357

27. Yang J, Atkins KE, Feng L, Pang M, Zheng Y, Liu X, et al. Seasonal influenza vaccination in China: landscape of diverse regional reimbursement policy, and budget impact analysis. *Vaccine*. (2016) 34:5724–35. doi: 10.1016/j.vaccine.2016.10.013

28. Zhao HT, Peng ZB, Ni ZL, Yang XK, Guo QY, Zheng JD, et al. Investigation on influenza vaccination policy and vaccination situation during the influenza seasons of 2020-2021 and 2021-2022 in China. *Zhonghua Yu Fang Yi Xue Za Zhi*. (2022) 56:1560–4. doi: 10.3760/cma.j.cn112150-20220810-00802

frontiers | Frontiers in Public Health

TYPE Perspective
PUBLISHED 16 July 2025
DOI 10.3389/fpubh.2025.1613869

OPEN ACCESS

EDITED BY
Sneha Vishwanath,
University of Cambridge, United Kingdom

REVIEWED BY
Joanne Marie Montoya Del Rosario,
Diosynvax Ltd., United Kingdom

*CORRESPONDENCE
Cristina Possas
✉ cristina.possas@bio.fiocruz.br
Ernesto T. A. Marques
✉ marques@pitt.edu

RECEIVED 17 April 2025
ACCEPTED 04 July 2025
PUBLISHED 16 July 2025

CITATION
Possas C, Marques ETA, Oliveira A, Schumacher S, Siqueira MM, McCauley J, Antunes A and Homma A (2025) Highly pathogenic avian influenza: pandemic preparedness for a scenario of high lethality with no vaccines.
Front. Public Health 13:1613869.
doi: 10.3389/fpubh.2025.1613869

Highly pathogenic avian influenza: pandemic preparedness for a scenario of high lethality with no vaccines

Cristina Possas[1]*, Ernesto T. A. Marques[2,3]*, Alessandra Oliveira[4], Suzanne Schumacher[4], Marilda M. Siqueira[5], John McCauley[6], Adelaide Antunes[4,7] and Akira Homma[1]

[1]Bio-Manguinhos, Oswaldo Cruz Foundation, Rio de Janeiro, Brazil, [2]Aggeu Magalhães Institute, Oswaldo Cruz Foundation, Recife, Brazil, [3]Department of Infectious Diseases and Microbiology, University of Pittsburgh, Pittsburgh, PA, United States, [4]Chemical Industry Information System – SIQUIM, School of Chemistry, Federal University of Rio de Janeiro, Rio de Janeiro, Brazil, [5]Laboratory of Respiratory Viruses, Exanthematous Viruses, Enteroviruses, and Viral Emergencies, Oswaldo Cruz Foundation, Rio de Janeiro, Brazil, [6]Worldwide Influenza Centre, The Francis Crick Institute, London, United Kingdom, [7]Academy of Intellectual Property and Innovation, National Institute of Industrial Property, Rio de Janeiro, Brazil

Highly Pathogenic Avian Influenza (HPAI) viruses, particularly H5N1 and H7N9, have long been considered potential pandemic threats, despite the absence of sustained human-to-human transmission. However, recent outbreaks in previously unaffected regions, such as Antarctica, suggest we may be shifting from theoretical risk to a more imminent threat. These viruses are no longer limited to avian populations. Their increasing appearance in mammals, including dairy cattle and domestic animals, raises the likelihood of viral reassortment and mutations that could trigger a human pandemic. If such a scenario unfolds, the world may face a crisis marked by high transmissibility and lethality, without effective vaccines readily available. Unlike the COVID-19 pandemic, when vaccines were rapidly developed despite inequities in access, the current influenza vaccine production model, largely reliant on slow, egg-based technologies, is insufficient for a fast-moving outbreak. While newer platforms show promise, they remain in early stages and cannot yet meet global demand, which alerts to the urgent need for accelerating vaccine and drug development, especially universal vaccines, next-generation vaccine platforms designed to provide broad, long-lasting protection against a wide spectrum of HPAI virus subtypes and strains. Here we propose a paradigmatic shift toward a more integrated, digitalized One Health surveillance system that links human, animal, and environmental data, especially in high-risk spillover regions. We underscore that Artificial Intelligence can revolutionize pandemic preparedness strategies, from improving early detection to speeding up vaccine and drug development and access to medical care, but should not be considered a stand-alone solution.

KEYWORDS

HPAI, pandemic preparedness, mutation, spillover, vaccine governance, artificial intelligence

Introduction

Infections with zoonotic influenza viruses, including Highly Pathogenic Avian Influenza (HPAI) viruses pose a significant threat to global public health in scenarios where viruses could acquire the ability to transmit efficiently among humans and cause a pandemic. Particularly concerning are the avian influenza strains, such as H5N1 and H7N9, which can be, transmitted from birds to humans, with high case fatality rates (1), even considering that most of H7N9 zoonotic infections result from LPAI (Low Pathogenic Avian Influenza) viruses and not from HPAI viruses (2, 3). In addition, avian influenza viruses can mutate or reassort, potentially leading to more transmissible or lethal variants. Although to date there is no evidence of sustained human-to-human transmission of avian influenza viruses, this possibility of mutation or reassortment is concerning and requires urgent global strategies for preparedness (4, 5).

Understanding the epidemiological behavior of avian influenza viruses, the mechanisms underlying zoonotic spillover, and the potential public health ramifications of a highly lethal pandemic scenario is imperative for global preparedness. From a knowledge governance perspective, this calls for the urgent implementation of robust, integrated surveillance systems that encompass poultry farm environments, sylvatic animals, and human populations with high exposure risk. These systems must be complemented by the development and equitable distribution of rapid, point-of-care diagnostic tools and by the strategic deployment of non-pharmaceutical interventions aimed at slowing viral transmission in the absence of immediate pharmacological solutions.

In addition, we highlight the importance of international collaboration, risk communication, and equity considerations in resource allocation during vaccine and drug shortages (6). By addressing the unique challenges of this worst-case scenario, the article aims to contribute to a more resilient global preparedness framework, supported by quality data and Artificial Intelligence, capable of managing unprecedented public health crises. In a previous publication we emphasized the critical need for urgent and sustainable investments in vaccine innovation and global preparedness. The results of our publication warn that a future pandemic caused by avian influenza viruses could unfold in the absence of effective vaccines, given current technological and logistical limitations (7).

Key barriers include restricted access to vaccine patents, reliance on slow and labor-intensive egg-based production methods, and the insufficient advancement and technological limitation of the current mRNA platforms and universal influenza vaccine technologies. These challenges are particularly alarming in the context of viral evolution and adaptation within farmed animals and their human handlers, which heightens the risk of zoonotic spillover and widespread outbreaks. This potential vaccine gap underscores the urgent need for a comprehensive global pandemic preparedness framework. Such a model must prioritize the integration of genomic and antigenic surveillance within a unified One Health approach, while also fostering robust public-private partnerships and scaling up investment in innovative vaccine platforms. These efforts are essential not only for controlling highly pathogenic and low pathogenicity avian influenza viruses but also for anticipating and mitigating other emerging zoonotic threats (8).

Our article underscores the need for developing a universal influenza vaccine to reduce the risk of future pandemics, advocating for stronger international coordination led by organizations like World Health Organization (WHO) and Pan American Health Organization (PAHO) to improve vaccine accessibility and efficacy. Universal highly pathogenic avian influenza (HPAI) vaccines refer to next-generation vaccine platforms specifically designed to provide broad, long-lasting protection against a wide spectrum of HPAI virus subtypes and strains. Unlike conventional influenza vaccines that require frequent updates to match circulating strains, universal HPAI vaccines aim to target highly conserved viral regions—such as the hemagglutinin (HA) stalk domain, internal proteins (like NP and M1), or T-cell epitopes—that are less prone to antigenic drift and shift. By focusing on these conserved viral components, universal vaccines have the potential to induce cross-protective immune responses, reducing the need for strain-specific reformulation and offering a more effective tool for pandemic preparedness and control of both known and emerging HPAI variants (9, 10). Such vaccine candidates may utilize diverse platforms, including recombinant proteins, viral vectors, or mRNA technologies, and are under active investigation in both animal and early-phase human studies. Universal HPAI vaccines represent a critical innovation pathway toward overcoming the logistical and scientific limitations of current egg-based or strain-specific vaccines, especially in rapidly evolving outbreak scenarios (11, 12).

In this article we examine the epidemiological dynamics of HPAI and LPAI viruses, zoonotic spillover pathways, and societal and healthcare implications of a highly lethal pandemic. We emphasize the necessity of robust One Health surveillance systems, innovative vaccine technologies, international collaboration, and the role of Artificial Intelligence (AI) in bolstering preparedness and response mechanisms.

Epidemiological scenario: potential routes of zoonotic spillover

Avian influenza viruses, including HPAI viruses, are characterized by their ability to mutate rapidly, spreading and enabling them to adapt to new hosts. The primary zoonotic transmission routes include direct contact with infected birds and animals, exposure to contaminated environments, like faeces, etc., and the preparation of, and consumption of undercooked poultry (meat or other animal products). Further human activities, such as intensive farming and wildlife trade, amplify the risk of spillover events, events (by increasing the instances of human-animal interactions).

Avian influenza presents a critical global health threat, as indicated in Table 1. According to WHO, from January 1 2003 to December 12, 2024, 954 confirmed human cases of HPAI influenza A (H5N1) virus infection were reported across 24 countries, with 464 fatalities. Cases and fatalities related to other HPAI viruses are indicated in Table 1. While the global trend has been a decline in H5N1 human cases since 2015, recent reports (13, 14) indicate an increasing number of new human infections. For instance, as of January 6, 2025, the United States had reported 66 confirmed human cases of H5N1 since 2024, with one fatality. Historically, cattle were not considered natural hosts for H5N1, however recent cases (such as in the US in 2024) indicate that the virus can infect dairy cows, particularly spreading their mammary glands. In addition, in January 2025, a human case of H5N1 was detected in England, the second symptomatic case in the UK.

10.3389/fpubh.2025.1613869

TABLE 1 Zoonotic avian viruses: main characteristics and key concerns.

Viral subtype	HPAI/LPAI primary hosts	Main outbreaks	Key concerns
H5N1	Poultry, wild birds, mammals (4) Worldwide, the detection of A (H5N1) viruses in non-avian species, such as marine and terrestrial mammals (both domestic and wild), has increased in recent years (47)	1997 (Hong Kong) (48); 2003-Present (global) (49)	Human infections (over 890 confirmed human cases and more than 460 deaths as of 2024) (1, 4, 28, 50), pandemic potential, increased transmission to mammals, risk of viral reassortment in mammals
H5N6	Poultry, wild birds (51) Aquatic poultry (ducks and geese) and migratory birds (52)	2014-Present (China, Southeast Asia) (53)	Sporadic human cases (at least 84 confirmed human cases and 33 deaths reported globally by 2024) (54), possible reassortment with other flu viruses (52)
H5N8	Poultry, wild birds (51)	2014-Present (Europe, Asia, Africa) (51, 55, 56)	Highly contagious in birds, occasional mammal infections (no confirmed human cases to date, but multiple mammal infections in seals and foxes reported) (57, 58)
H7N9	Poultry (59)	2013–2019 (China) (59)	Mutations increasing human infectivity, pandemic potential. Over 1,500 laboratory-confirmed human cases and at least 615 deaths reported during epidemics (59, 60)
H10N3	Poultry, wild birds (61, 62)	2021 (China) (63)	Limited human infections (only 1 confirmed human case as of 2024), needs monitoring (63, 64)
H9N2	Poultry, wild birds (65)	Ongoing (Asia, Middle East) (63, 65)	Reassortment potential with other flu viruses. More than 90 sporadic human cases reported with low case fatality rate (66)

Sources: elaborated by the authors based on Refs. (1, 4, 28, 47–66).

It is important to note that although human cases have been relatively low, H5N1 has been spreading extensively among bird populations and has recently been increasingly detected in several mammalian species, including dairy cows and wild animals. For example, in the United States, since 2022, the United States Department of Agriculture Animal and Plant Health Inspection Service has reported HPAI A (H5N1) virus detections in more than 200 mammals (15).

Emerging evidence suggests that certain HPAI strains, particularly from clade 2.3.4.4b, have acquired mutations that may enhance their capacity to infect mammals. Among these, changes in the PB2 gene—such as E627K and D701N—have been identified as key molecular markers that improve viral replication efficiency in mammalian hosts. Although these mutations have been detected in sporadic cases, particularly in mammals exposed to infected birds, there is no conclusive evidence of sustained mammal-to-mammal transmission to date. Nonetheless, the detection of such adaptations underscores the need for heightened genomic surveillance at the human–animal interface, where the potential for zoonotic spillover is greatest.

Another critical genetic determinant in the adaptation of avian influenza viruses to mammalian hosts is the PB2 gene, which encodes one of the three polymerase subunits essential for viral replication. Specific mutations in PB2, notably E627K and D701N, have been repeatedly associated with enhanced viral replication efficiency at the lower temperatures found in the mammalian respiratory tract (16). These mutations can significantly increase the virulence and transmissibility of HPAI viruses in mammals, including humans. Studies following experimental infections and epidemiological investigations of zoonotic cases have consistently highlighted PB2 mutations as key markers for assessing pandemic potential. The capacity of these mutations to facilitate cross-species transmission underlines the importance of incorporating PB2 surveillance into global risk assessment frameworks for avian influenza viruses.

The transition of H7N9 from low pathogenic avian influenza (LPAI) to highly pathogenic avian influenza (HPAI) is marked by the acquisition of a polybasic cleavage site in the hemagglutinin (HA) protein, leading to increased virulence in poultry (17). However, this change does not necessarily enhance transmissibility or severity in humans. Notably, both LPAI and HPAI H7N9 strains have been linked to severe human infections, with case fatality rates around 40% (18).

HA cleavage site and receptor binding specificity

While the polybasic cleavage site facilitates systemic spread in avian hosts by enabling HA cleavage by ubiquitous proteases, human pathogenicity is more influenced by receptor-binding specificity and host factors than by the cleavage site alone.

Residue 226 mutation and receptor affinity

The Q226L amino acid substitution in the hemagglutinin (HA) protein shifts receptor-binding preference from avian-type (α-2,3-linked

sialic acids) to human-type (α-2,6-linked sialic acids), potentially increasing the risk of zoonotic transmission (19–21). Importantly, this substitution in the H7 HA does not eliminate affinity for avian receptors, allowing the virus to infect both avian and human hosts.

However, it is important to note that H1N1 viruses, including the 1918 pandemic strain and the 2009 H1N1 strain, do not follow this receptor-binding model. Structural and functional assessments of the 1918 virus indicate that its HA adapted for human transmission through distinct mechanisms rather than solely relying on the Q226L mutation (22). Previous studies, such as those by Gamblin et al. (23) have analyzed receptor binding affinity for the 1918 virus, providing insights into its human adaptation. Additionally, research on ferret-transmissible H5N1 viruses has examined similar receptor-binding changes, further informing our understanding of zoonotic transmission (24, 25).

Implications for zoonotic transmission

While the Q226L mutation may facilitate initial cross-species transmission, additional mutations are likely required for sustained human-to-human transmission. While the acquisition of a polybasic cleavage site is a defining feature of HPAI viruses and enhances their pathogenicity in birds, it does not necessarily correlate with increased or decreased zoonotic risk. Both LPAI and HPAI strains have demonstrated the capacity to cause severe disease in humans under certain exposure conditions. Continuous surveillance of these mutations is crucial to assess their impact on transmissibility and pathogenicity.

Zoonotic risks and mortality rates

In Figure 1, we compare the main high-risk HPAI subtypes considering zoonotic risks and mortality rates. The classification of zoonotic risk for HPAI viruses is based on factors such as the frequency and severity of human infections, potential for human-to-human transmission, and genetic characteristics of the virus. While there is not a universally standardized 1-to-5 scale, various health organizations assess these risks to inform public health responses.

The scores calculated in Figure 1 are scientifically based. We supported our classification of zoonotic risks based on two sources (26, 27). We supported our classification of zoonotic risks based on two sources, The Public Health Agency of Canada and WHO. The first one classifies certain influenza A virus subtypes, including H5N1, H5N6, and H7N9, as Risk Group 3 Human Pathogens due to their significant potential to cause serious human or animal disease (27). Similarly, WHO conducts risk assessments for specific HPAI and LPAI strains. In a 2022 assessment, the WHO evaluated the zoonotic risk of the A(H5N1) clade 2.3.4.4b viruses (28–30), considering factors like human cases, virus spread in wild and domestic animals, and genetic mutations. In Figure 1 we provide an indication of these zoonotic risks according to mortality rates, considering the possibility of overestimate of mortality rate due to underestimation of the number of infections especially.

These assessments, while not always presented on a numerical scale, provide a framework for scoring the relative zoonotic risks of different HPAI subtypes.

Accelerating HPAI vaccine innovation and development: technological gaps

Innovative approaches to vaccine development are urgently needed and key points include addressing technological development and production challenges to overcome technological gaps. Current

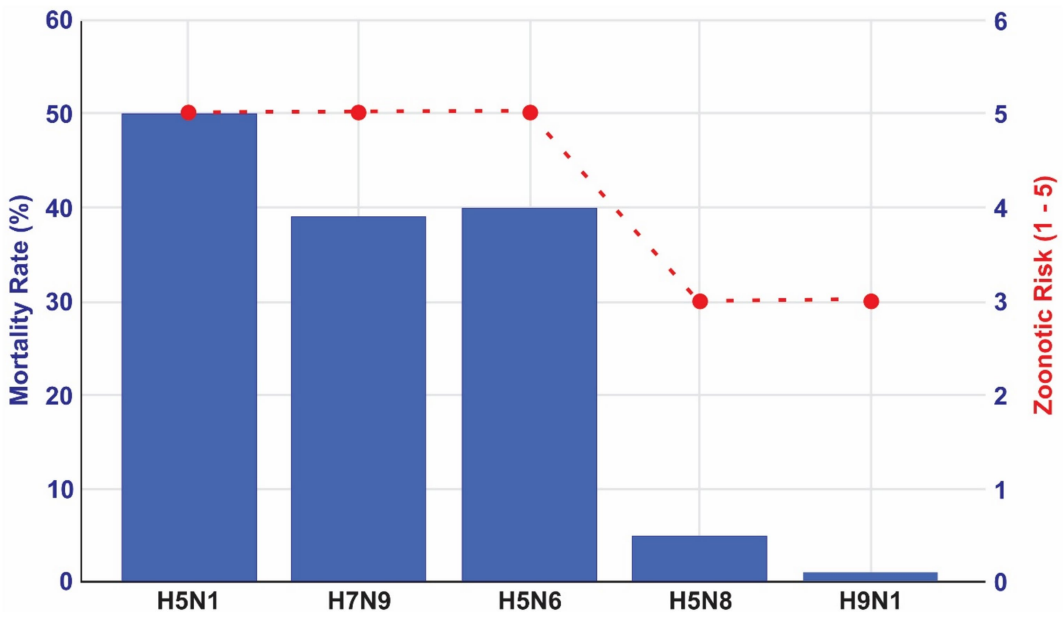

FIGURE 1
Zoonotic risks and mortality rates for the main HPAI viral subtypes. Source: elaborated by the authors based on World Health Organization (26) and Public Health Agency of Canada. Government of Canada (27).

egg-based vaccine production is slow and difficult to scale in an emergency, especially during an HPAI virus outbreak that could lead to massive animal culling. While mRNA technology shows promise, questions remain about the duration, breadth of protection and scalability (31). Due to these constraints, our previous study (7) provided evidence indicating that vaccine development for HPAI is lagging, with very few active patents and limited advancements in universal vaccines. This scenario hampers the global capacity to respond effectively to a potential pandemic. Substantial investment in universal influenza vaccines is crucial to address the limitations of current technologies.

In addition to the technological barriers previously discussed, a critical challenge in HPAI vaccine preparedness is the antigenic mismatch between stockpiled vaccines and the strain that causes a future outbreak. This scenario is increasingly likely given the accelerated antigenic drift and shift observed in H5Nx viruses. For example, while clade 2.3.4.4b viruses currently dominate outbreaks in Europe and North America, regions of Asia are still reporting circulation of other clades such as 2.3.2 and 2.3.3. This geographic heterogeneity in dominant clades increases the risk that existing vaccine stockpiles, often produced against earlier strains, will have reduced efficacy if deployed during a novel outbreak elsewhere. Moreover, regulatory and manufacturing timelines for updating avian influenza vaccines lag behind the pace of viral evolution, further compounding this gap. This underscores the urgency for next-generation HPAI vaccines that offer broader cross-clade protection, such as those targeting conserved viral epitopes or using novel platforms like mRNA and recombinant technologies (32, 33).

Broadly neutralizing antibodies: recent findings for potential universal flu vaccine

A recent breakthrough study by researchers from the University of Pittsburgh, in collaboration with the NIH Vaccine Research Center, demonstrated that monkeys pretreated with a moderate dose of the broadly neutralizing antibody MEDI8852[1] were universally protected against HPAI viruses. In addition to confirming the antibody's efficacy in preventing serious adverse health outcomes, the scientists established the minimum serum concentration required for protection in primate models (34) for further development of universal HPAI vaccines. For instance, deep learning approaches have been used to predict antigenic drift in H5N1 hemagglutinin variants, helping researchers anticipate viral escape mutations (35). Similarly, support vector machines and random forest algorithms have been applied to forecast epitope binding affinity and immunogenicity, enabling more targeted vaccine design (36). Recent studies have also demonstrated the use of neural network-based models to optimize mRNA vaccine sequences for enhanced expression and immunogenicity, which could be adapted for influenza vaccines in the future (37).

Pandemic preparedness and AI: enhancing genomic surveillance, knowledge governance and sustainability

Artificial Intelligence (AI) has begun to reshape the landscape of pandemic preparedness, particularly by enhancing the speed and precision of epidemiological surveillance and knowledge governance. In vaccine development, machine learning models can predict antigenic properties, simulate immune responses, and optimize candidate selection, accelerating preclinical pipelines (38, 39). In parallel, AI-powered epidemic intelligence systems can process diverse unstructured data—from genomic databases to wildlife surveillance—to detect abnormal patterns and emerging threats before they affect human populations.

These advances are especially relevant for HPAI, where rapid viral evolution and zoonotic spillover require integrated early warning systems. AI algorithms can assimilate real-time inputs from genomic sequencing, environmental monitoring, animal health records, and social behavior to anticipate outbreak hotspots. This predictive capacity enables health authorities to issue early alerts and prioritize surveillance resources more effectively.

Artificial Intelligence (AI) is emerging as a revolutionary tool, reshaping public health with advancements in analyzing and preventing future pandemic scenarios. Additionally, AI supports robust genomic and antigenic surveillance. Genomic analysis allows tracking of mutations and reassortments that enhance virulence or transmissibility, while antigenic assays assess how well existing immune responses recognize evolving HPAI strains. Integrating both approaches is critical to guide vaccine updates and antiviral strategies.

Beyond surveillance, AI offers transformative applications across operational domains of pandemic preparedness. When adequately designed and integrated within resilient health systems, AI can significantly enhance outbreak forecasting, optimize allocation of medical resources, and support rapid diagnostics. For example, deep learning models have been deployed to predict regional outbreak hotspots based on climatic and migratory bird data, as demonstrated during H5N1 outbreaks in Southeast Asia (40). AI-driven decision support systems have also been used to optimize stockpiling and distribution of antiviral medications and personal protective equipment in real-time emergency settings (41). Additionally, AI-powered diagnostic tools using image recognition and molecular data processing have accelerated point-of-care detection of avian influenza strains in field conditions (42). These efforts must also be grounded in the One Health framework, requiring international coordination and data sharing across human, animal, and environmental health domains to ensure comprehensive risk assessment (7, 26).

Designing AI to revolutionize pandemic preparedness

Artificial Intelligence (AI) is emerging as a revolutionary tool in public health, with its potential to analyze vast amounts of data,

1 MEDI8852 is a fully human monoclonal antibody that targets the highly conserved stem region of influenza A hemagglutinin (HA), offering robust protection in preclinical models of H5N1and H7N9, even when administered up to 72 h post-exposure, and outperforming oseltamivir in key measures of survival and disease severity. It neutralizes all 18 subtypes of influenza A, including both Group I (H5N1) and Group II (H7N9) strains (67).

identify trends, and enable informed decision-making. For HPAI, AI could help identify conserved viral epitopes across multiple subtypes, guiding the rational design of universal or broadly protective vaccines. Recent studies have used machine learning models to predict conserved B-cell and T-cell epitopes in H5N1 and H7N9 hemagglutinin and neuraminidase proteins, accelerating preclinical evaluation of cross-protective candidates (35, 43). In pharmacological pipelines, AI-based virtual screening platforms have been applied to search large chemical libraries for molecules with predicted binding affinity to influenza polymerase and neuraminidase targets, significantly reducing lead compound identification time (6). Notably, deep learning frameworks have also been used to repurpose existing antiviral drugs against emerging HPAI strains by predicting off-target antiviral activities (44).

One of the most critical roles of AI is accelerating vaccine and drug discovery. For HPAI, AI can help identify conserved viral epitopes across subtypes, guiding development of universal or broadly protective vaccines. In pharmacological pipelines, it can screen large chemical libraries to identify potential antiviral compounds, reducing the time from discovery to clinical testing. Inclusive governance, characterized by equitable decision-making and transparent data sharing across countries and regions, is fundamental to effective global pandemic preparedness. This includes open access to viral genomic sequences, real-time epidemiological reporting, and collaborative use of AI-driven surveillance platforms to ensure timely detection and response to HPAI threats (45).

AI also facilitates strategic decision-making in resource-constrained scenarios. Algorithms can integrate epidemiological data, health system capacity, and demographic variables to prioritize vaccine allocation, deploy health workers, and anticipate regional surges in infection. Logistics systems enhanced by AI can ensure timely distribution of critical supplies such as PPE, antivirals, and ventilators, especially in underserved areas.

Moreover, AI can support integration of epizootic surveillance with immunization efforts. By linking real-time data from wildlife and livestock with mutation tracking, AI enables targeted containment and adaptive vaccination strategies. This is crucial to prevent the emergence of vaccine-resistant strains or hidden transmission pathways.

However, the success of AI depends on high-quality data inputs, inclusive governance, and ethical frameworks. It must be implemented as part of a broader transdisciplinary preparedness strategy, not as a stand-alone solution. AI's greatest value lies in its ability to support rapid, data-driven action within a collaborative, globally coordinated response.

Beyond early warning and surveillance, AI also provides valuable tools for accelerating vaccine and drug development, optimizing resource-allocation, and integrating epizootic surveillance systems.

1 Accelerating vaccine and drug development

For HPAI, AI could help identify structurally conserved regions of viral proteins across multiple strains, supporting the development of vaccines that offer broad protection. In drug discovery, AI can analyze vast libraries of chemical compounds to identify potential antiviral candidates, drastically reducing the timeline from research to deployment.

2 Optimizing resource allocation

In a pandemic scenario marked by high lethality and scarce resources, AI supported by quality data could assist policymakers in making data-driven decisions about resource distribution. AI models could help a timely response to a broad range of indicators, such as population density, healthcare infrastructure, and disease transmission patterns to prioritize vaccine allocation, to deploy healthcare personnel, and to optimize hospital capacities.

AI-based logistics systems can predict areas likely to experience surges in cases, enabling timely delivery of critical supplies like personal protective equipment and ventilators. This proactive approach could ensure that even resource-limited regions are adequately supported.

3 Integrating epizootic surveillance and immunization

AI can play a critical role in supporting an integrated "big data" monitoring system that combines epizootic surveillance and immunization, if vaccines are not available. This integrated system can be a powerful tool to prevent and contain outbreaks, identifying viral circulation, monitoring mutations, and detecting early infections in domestic and wild birds. This information is essential for guiding targeted immunization programs and adjusting vaccine formulations to match emerging strains. Molecular diagnostics and genomic sequencing enhance the ability to track viral evolution, while international cooperation through organizations such as the World Organization for Animal Health (WOAH) and the Food and Agriculture Organization (FAO) facilitates data sharing and coordinated responses. Without comprehensive vaccine-oriented surveillance, immunization efforts may become ineffective due to the emergence of vaccine-resistant variants or undetected transmission routes. This AI strategy alongside stringent biosecurity measures and global cooperation, including geo-politically sensitive routes, is essential to mitigating the threat of HPAI and preventing future pandemics.

Conclusion

Global epidemiological reports indicate that we might be entering a new era of Avian Flu, with the H5N1 strain spreading more rapidly among mammals. Although cases have been linked to infected wild birds and livestock farms, the virus is now spreading not only among birds and domestic animals, but increasingly infecting mammals.

Indeed, H5N1 viruses have been found in both wild and captive mammals, and they can sometimes cause fatalities as well as severe illness. Additionally, H5N1 detections in domestic cats are gaining attention. The US Department of Agriculture's Animal and Plant Health Inspection Service reports that the HPAI H5N1 strain was found in a domestic cat in Colorado State on 2025/01/31 (15). Notably the B3.13 strain of the Eurasian 2.3.4.4b clade H5N1 virus has been spreading in animals not historically attributed as reservoirs for the HPAI virus (46). In relation to human infection, the World Health Organization (WHO) reported from 24 countries that between 2003 (beginning) and 2024 (2024/12/12), there were 954 human cases of H5N1, resulting in 464 fatalities, or 48.6% of the total zoonotic cases from avian influenza viruses (26).

A possible extreme scenario, in which a mutated strain becomes highly transmissible among humans, would create a global health crisis marked by significant morbidity and mortality. Preparing for a potential HPAI pandemic requires a multifaceted transdisciplinary approach that addresses epidemiological, technological, and societal challenges.

The possible absence of an effective HPAI vaccine for human in a highly lethal pandemic scenario, contrasting with rapid vaccine development in the COVID-19 pandemic, highlights the urgency of accelerating investment in innovative solutions and equitable global strategies. By leveraging AI strategies, fostering international collaboration and strengthening innovation funding mechanisms, the global health community can build a more resilient and sustainable innovation governance system capable of responding to unprecedented crises.

What is needed is a shift toward faster action and a coordinated, inclusive strategy that prioritizes preparedness before a next pandemic begins. The time to act is now.

Data availability statement

The original contributions presented in the study are included in the article/supplementary material, further inquiries can be directed to the corresponding author.

Author contributions

CP: Conceptualization, Formal analysis, Methodology, Writing – original draft, Writing – review & editing. EM: Formal analysis, Writing – review & editing. AO: Formal analysis, Writing – review & editing. SS: Formal analysis, Writing – review & editing. MS: Formal analysis, Writing – review & editing. JM: Formal analysis, Writing – review & editing. AA: Formal analysis, Writing – review & editing. AH: Formal analysis, Writing – review & editing.

Funding

The author(s) declare that financial support was received for the research and/or publication of this article. The authors thank the financial support of Bio-Manguinhos, Oswaldo Cruz Foundation Brazil, of the Chemical School of the Federal University of Rio de Janeiro, of the Brazilian National Institute of Industrial Property -INPI and of the University of Pittsburgh, US.

Acknowledgments

The authors thank Jose Viña for the technical support in the design of the Table 1 and Figure 1.

Conflict of interest

The authors declare that the research was conducted in the absence of any commercial or financial relationships that could be construed as a potential conflict of interest.

Generative AI statement

The authors declare that no Gen AI was used in the creation of this manuscript.

Publisher's note

All claims expressed in this article are solely those of the authors and do not necessarily represent those of their affiliated organizations, or those of the publisher, the editors and the reviewers. Any product that may be evaluated in this article, or claim that may be made by its manufacturer, is not guaranteed or endorsed by the publisher.

References

1. World Health Organization. (2025). Avian influenza weekly update number 997. Available online at: https://cdn.who.int/media/docs/default-source/wpro---documents/emergency/surveillance/avian-influenza/ai_20250516.pdf?download=true&sfvrsn=cf54905c_1 (accessed June 9, 2025).

2. Gao R, Cao B, Hu Y, Feng Z, Wang D, Hu W, et al. Human infection with a novel avian-origin influenza a (H7N9) virus. *N Engl J Med*. (2013) 368:1888–97. doi: 10.1056/NEJMoa1304459

3. Hou Y, Deng G, Cui P, Zeng X, Li B, Wang D, et al. Evolution of H7N9 highly pathogenic avian influenza virus in the context of vaccination. *Emerg Microbes Infect*. (2024) 13:2343912. doi: 10.1080/22221751.2024.2343912

4. Peacock TP, Moncla L, Dudas G, Vaninsberghe D, Sukhova K, Lloyd-Smith JO, et al. The global H5N1 influenza panzootic in mammals. *Nature*. (2025) 637:304–13. doi: 10.1038/s41586-024-08054-z

5. Caserta LC, Frye EA, Butt SL, Laverack M, Nooruzzaman M, Covaleda LM, et al. Spillover of highly pathogenic avian influenza H5N1 virus to dairy cattle. *Nature*. (2024) 634:669–76. doi: 10.1038/s41586-024-07849-4

6. Torreele E. Tackling vaccine inequity in 2023: have we made progress? *Expert Rev Vaccines*. (2024) 23:1–4. doi: 10.1080/14760584.2023.2292771

7. Possas C, Marques ET, Oliveira A, Schumacher S, Mendes FML, Siqueira MM, et al. Vaccine preparedness for highly pathogenic avian influenza: innovation and intellectual property issues In: C Keswani and C Possas, editors. Intellectual property issues in life sciences disputes and controversies. Boca Raton, FL: CRC Press (2025). 100–42.

8. Food and Agriculture Organization of the United Nations. World Organisation for Animal Health. (2024). Global strategy for the prevention and control of highly pathogenic avian influenza (2024–2033). Available online at: https://openknowledge.fao.org/server/api/core/bitstreams/6fff62da-80e1-43ab-94ee-3a5b69940b7c/content (accessed June 9, 2025).

9. Nachbagauer R, Krammer F. Universal influenza virus vaccines and therapeutic antibodies. *Clin Microbiol Infect*. (2017) 23:222–8. doi: 10.1016/j.cmi.2017.02.009

10. Sridhar S, Brokstad KA, Cox RJ. Influenza vaccination strategies: comparing inactivated and live attenuated influenza vaccines. *Vaccines*. (2015) 3:373–89. doi: 10.3390/vaccines3020373

11. Erbelding EJ, Post DJ, Stemmy EJ, Roberts PC, Augustine AD, Ferguson S, et al. A universal influenza vaccine: the strategic plan for the National Institute of Allergy and Infectious Diseases. *J Infect Dis*. (2018) 218:347–54. doi: 10.1093/infdis/jiy103

12. Krammer F. The human antibody response to influenza a virus infection and vaccination. *Nat Rev Immunol*. (2019) 19:383–97. doi: 10.1038/s41577-019-0143-6

13. Centers for Disease Control and Prevention. (2025). Avian influenza (bird flu). Past reported global human cases with highly pathogenic avian influenza a(H5N1) (HPAI H5N1) by country, 1997–2025. Available online at: https://www.cdc.gov/bird-flu/php/avian-flu-summary/chart-epi-curve-ah5n1.html (accessed June 9, 2025).

14. World Health Organization. (2025). Avian influenza weekly update number 983. Available online at: https://cdn.who.int/media/docs/default-source/wpro---documents/emergency/surveillance/avian-influenza/ai_20250131.pdf?sfvrsn=5f006f99_149 (accessed June 9, 2025).

15. Animal and Plant Health Inspection Service. U.S. department of agriculture. (2025). Detections of highly pathogenic influenza in mammals. Available online at: https://www.aphis.usda.gov/livestock-poultry-disease/avian/avian-influenza/hpai-detections/mammals (accessed June 9, 2025).

16. Mok CK, Lee HH, Lestra M, Nicholls JM, Chan MC, Sia SF, et al. Amino acid substitutions in polymerase basic protein 2 gene contribute to the pathogenicity of the novel a/H7N9 influenza virus in mammalian hosts. *J Virol*. (2014) 88:3568–76. doi: 10.1128/JVI.02740-13

17. Song W, Huang X, Guan W, Chen P, Wang P, Zheng M, et al. Multiple basic amino acids in the cleavage site of H7N9 hemagglutinin contribute to high virulence in mice. *J Thorac Dis*. (2021) 13:4650–60. doi: 10.21037/jtd-21-226

18. Chang P, Sadeyen JR, Bhat S, Daines R, Hussain A, Yilmaz H, et al. Risk assessment of the newly emerged H7N9 avian influenza viruses. *Emerg Microbes Infect*. (2023) 12:2172965. doi: 10.1080/22221751.2023.2172965

19. Lin TH, Zhu X, Wang S, Zhang D, McBride R, Yu W, et al. A single mutation in bovine influenza H5N1 hemagglutinin switches specificity to human receptors. *Science*. (2024) 386:1128–34. doi: 10.1126/science.adt0180

20. Vines A, Wells K, Matrosovich M, Castrucci MR, Ito T, Kawaoka Y. The role of influenza a virus hemagglutinin residues 226 and 228 in receptor specificity and host range restriction. *J Virol*. (1998) 72:7626–31. doi: 10.1128/JVI.72.9.7626-7631.1998

21. Liu WJ, Xiao H, Dai L, Liu D, Chen J, Qi X, et al. Avian influenza a (H7N9) virus: from low pathogenic to highly pathogenic. *Front Med*. (2021) 15:507–27. doi: 10.1007/s11684-020-0814-5

22. Taubenberger JK, Kash JC, Morens DM. The 1918 influenza pandemic: 100 years of questions answered and unanswered. *Sci Transl Med*. (2019) 11:502. doi: 10.1126/scitranslmed.aau5485

23. Gamblin SJ, Haire LF, Russell RJ, Stevens DJ, Xiao B, Ha Y, et al. The structure and receptor binding properties of the 1918 influenza hemagglutinin. *Science*. (2004) 303:1838–42. doi: 10.1126/science.1093155

24. Xiong X, Coombs PJ, Martin SR, Liu J, Xiao H, McCauley JW, et al. Receptor binding by a ferret-transmissible H5 avian influenza virus. *Nature*. (2013) 497:392–6. doi: 10.1038/nature12144

25. Herfst S, Schrauwen EJ, Linster M, Chutinimitkul S, de Wit E, Munster VJ, et al. Airborne transmission of influenza a/H5N1 virus between ferrets. *Science*. (2012) 336:1534–41. doi: 10.1126/science.1213362

26. World Health Organization. (2025). Avian influenza weekly update #986. Available online at: https://www.who.int/westernpacific/publications/m/item/avian-influenza-weekly-update---986--21-february-2025 (accessed June 9, 2025).

27. Public Health Agency of Canada. Government of Canada. (2024). Statement from the Public Health Agency of Canada: Update on avian influenza and risk to Canadians Available online at: https://www.canada.ca/en/public-health/news/2024/11/update-on-avian-influenza-and-risk-to-canadians.html (accessed June 9, 2025).

28. Food and Agriculture Organization of the United Nations, World Health Organization, & 418 World Organization for Animal Health. (2025). Updated joint FAO/WHO/WOAH public health assessment of recent influenza a(H5) virus events in animals and people. Assessment based on data as of 1 march 2025. Available online at: https://cdn.who.int/media/docs/default-source/influenza/human-animal-interface-risk-assessments/2025_04_17_fao-woah-who_h5n1_assessment.pdf?download=true&sfvrsn=9bc6cc8e_1 (accessed June 9, 2025).

29. World Health Organization. (2020). Tool for influenza pandemic risk assessment (TIPRA). Available online at: https://www.who.int/publications/i/item/tool-for-influenza-pandemic-risk-assessment-(tipra)-2nd-edition (accessed June 9, 2025).

30. Yamaji R, Zhang W, Kamata A, Adlhoch C, Swayne DE, Pereyaslov D, et al. Pandemic risk characterisation of zoonotic influenza a viruses using the tool for influenza pandemic risk assessment (TIPRA). *Lancet Microbe*. (2024) 6:100973. doi: 10.1016/j.lanmic.2024.100973

31. Possas C, Marques ETA, Oliveira A, Schumacher S, Mendes F, Siqueira MM, et al. Highly pathogenic avian influenza vaccines: challenges for innovation. *MedRxiv*. (2023). doi: 10.1101/2023.05.31.23290790

32. World Health Organization. (2025). Genetic and antigenic characteristics of zoonotic influenza a viruses and development of candidate vaccine viruses for pandemic preparedness. Available online at: https://cdn.who.int/media/docs/default-source/influenza/who-influenza-recommendations/vcm-northern-hemisphere-recommendation-2025-2026/202502_zoonotic_vaccinvirusupdatev2.pdf?sfvrsn=b7ee9689_13 (accessed June 9, 2025).

33. Le TH, Nguyen NT. Evolutionary dynamics of highly pathogenic avian influenza a/H5N1 HA clades and vaccine implementation in Vietnam. *Clin Exp Vaccine Res*. (2014) 3:117–27. doi: 10.7774/cevr.2014.3.2.117

34. Kanekiyo M, Gillespie RA, Cooper K, Canedo VG, Castanha PMS, Pegu A, et al. Pre-exposure antibody prophylaxis protects macaques from severe influenza. *Science*. (2025) 387:534–41. doi: 10.1126/science.ado6481

35. Yin R, Tran VH, Zhou X, Zheng J, Kwoh CK. Predicting antigenic variants of H1N1 influenza virus based on epidemics and pandemics using a stacking model. *PLoS One*. (2018) 13:e0207777. doi: 10.1371/journal.pone.0207777

36. Chen J, Liu H, Yang J, Chou KC. Prediction of linear B-cell epitopes using amino acid pair antigenicity scale. *Amino Acids*. (2007) 33:423–8. doi: 10.1007/s00726-006-0485-9

37. Rosa SS, Nunes D, Antunes L, Prazeres DMF, Marques MPC, Azevedo AM. Maximizing mRNA vaccine production with Bayesian optimization. *Biotechnol Bioeng*. (2022) 119:3127–39. doi: 10.1002/bit.28216

38. Syrowatka A, Kuznetsova M, Alsubai A, Beckman AL, Bain PA, Craig KJT, et al. Leveraging artificial intelligence for pandemic preparedness and response: a scoping review to identify key use cases. *NPJ Digit Med*. (2021) 4:96. doi: 10.1038/s41746-021-00459-8

39. Possas C, Marques ETA, Kuchipudi SV, Kumar P, Kim JH, Homma A. Disease X in the tropics, preventing the next pandemic: how to accelerate spillover prevention and vaccine preparedness? *Front in Tropical Dis*. (2024) 5:1417065. doi: 10.3389/fitd.2024.1417065

40. Kjær LJ, Kirkeby CT, Boklund AE, Hjulsager CK, Fox AD, Ward MP. Prediction models show differences in highly pathogenic avian influenza outbreaks in Japan and South Korea compared to Europe. *Sci Rep*. (2025) 15:6783. doi: 10.1038/s41598-025-91384-3

41. Koyuncu M, Erol R. Optimal resource allocation model to mitigate the impact of pandemic influenza: a case study for Turkey. *J Med Syst*. (2010) 34:61–70. doi: 10.1007/s10916-008-9216-y

42. Astill J, Dara R, Fraser EDG, Sharif S. Detecting and predicting emerging disease in poultry with the implementation of new technologies and big data: a focus on avian influenza virus. *Front Vet Sci*. (2018) 5:263. doi: 10.3389/fvets.2018.00263

43. Ton AT, Gentile F, Hsing M, Ban F, Cherkasov A. Rapid identification of potential inhibitors of SARS-CoV-2 main protease using deep docking of 1.3 billion compounds. *Mol Inform*. (2020) 39:28. doi: 10.1002/minf.202000028

44. Stokes JM, Yang K, Swanson K, Jin W, Cubillos-Ruiz A, Donghia NM, et al. A deep learning approach to antibiotic discovery. *Cell*. (2020) 180:688–702. doi: 10.1016/j.cell.2020.01.021

45. Jit M, Ananthakrishnan A, McKee M, Wouters OJ, Beutels P, Teerawattananon Y. Multi-country collaboration in responding to global infectious disease threats: lessons for Europe from the COVID-19 pandemic. *Lancet Reg Health Eur*. (2021) 9:100221. doi: 10.1016/j.lanepe.2021.100221

46. Colorado Veterinary Medical Association. (2024). Influenza a (highly pathogenic avian influenza H5N1) in domestic cats. Available online at: https://colovma.org/influenza-a-highly-pathogenic-avian-influenza-h5n1-in-domestic-cats/ (accessed June 9, 2025).

47. Pan American Health Organization. World Health Organization. (2025). Epidemiological update avian influenza a (H5N1) in the American regions. Available online at: https://www.paho.org/en/documents/epidemiological-update-avian-influenza-ah5n1-americas-region-24-january-2025#:~:text=24%20January%202025-,Epidemiological%20Update%20%2D20Avian20Influenza%20A(H5N1)%20in%20the,Americas%20Region%20%2D202420January%202025&text=Between%202022%20and20as20of,H5N1%20avian%20influenza%20to%20WOAH (accessed June 9, 2025).

48. Chan PKS. Outbreak of avian influenza a(H5N1) virus infection in Hong Kong in 1997. *Clin Infect Dis*. (2002) 34:S58–64. doi: 10.1086/338820

49. Centers for Disease Control and Prevention. (2023). Emergence and evolution of H5N1 bird flu. Available online at: https://archive.cdc.gov/www_cdc_gov/flu/avianflu/communication-resources/bird-flu-origin-infographic.html#:~:text=2003%2D2005%20H5N1%20Spreads,the%20Middle%20East%20and%20Europe (accessed June 9, 2025).

50. Kamel M, Aleya S, Almagharbeh WT, Aleya L, Abdel-Daim MM. The emergence of highly pathogenic avian influenza H5N1 in dairy cattle: implications for public health, animal health, and pandemic preparedness. *Eur J Clin Microbiol Infect Dis*. (2025) 14:1–17. doi: 10.1007/s10096025-05147-z

51. Kim S-H. Challenge for one health: co-circulation of zoonotic H5N1 and H9N2 avian influenza viruses in Egypt. *Viruses*. (2018) 10:121. doi: 10.3390/v10030121

52. Li H, Li Q, Li B, Guo Y, Xing J, Xu Q, et al. Continuous Reassortment of clade 2.3.4.4 H5N6 highly Pathogenetic avian influenza viruses demonstrating high risk to public health. *Pathogens*. (2020) 9:670. doi: 10.3390/pathogens9080670

53. Zhu W, Li X, Dong J, Bo H, Liu J, Yang J, et al. Epidemiologic, clinical, and genetic characteristics of human infections with influenza a(H5N6) viruses, China. *Emerg Infect Dis*. (2022) 28:1332–44. doi: 10.3201/eid2807.212482

54. Li Y, Li M, Li Y, Tian J, Bai X, Yang C, et al. Outbreaks of highly pathogenic avian influenza (H5N6) virus subclade 2.3.4.4h in swans, Xinjiang, Western China, 2020. *Emerg Infect Dis*. (2020) 26:2956–60. doi: 10.3201/eid2612.201201

55. Adlhoch C, Brown IH, Angelova SG, Bálint Á, Bouwstra R, Buda S, et al. Highly pathogenic avian influenza a(H5N8) outbreaks: protection and management of exposed people in Europe, 2014/15 and 2016. *Euro Surveill*. (2016) 21:30419. doi: 10.2807/1560-7917.ES.2016.21.49.30419

56. More S, Bicout D, Bøtner A, Butterworth A, Calistri P, Depner K, et al. Avian influenza. *EFSA J*. (2017) 15:e04991. doi: 10.2903/j.efsa.2017.4991

57. Graziosi G, Lupini C, Catelli E, Carnaccini S. Highly pathogenic avian influenza (HPAI) H5 clade 2.3.4.4b virus infection in birds and mammals. *Animals*. (2024) 14:372. doi: 10.3390/ani14091372

58. Rafique S, Rashid F, Mushtaq S, Ali A, Li M, Luo S, et al. Global review of the H5N8 avian influenza virus subtype. *Front Microbiol*. (2023) 14:1200681. doi: 10.3389/fmicb.2023.1200681

59. Zhang Z, Lei Z. The alarming situation of highly pathogenic avian influenza viruses in 2019–2023. *Glob Med Genet*. (2024) 11:200–13. doi: 10.1055/s-0044-1788039

60. Liu Y, Chen Y, Yang Z, Lin Y, Fu S, Chen J, et al. Evolution and antigenic differentiation of avian influenza a(H7N9) virus, China. *Emerg Infect Dis*. (2024) 30:1218–22. doi: 10.3201/eid3006.230530

61. Liu K, Qi X, Bao C, Wang X, Liu X. Novel H10N3 avian influenza viruses: a potential threat to public health. *Lancet Microbe*. (2024) 5:e417. doi: 10.1016/S26665247(23)00409-3

62. Ding S, Zhou J, Xiong J, Du X, Yang W, Huang J, et al. Continued evolution of H10N3 influenza virus with adaptive mutations poses an increased threat to mammals. *Virol Sin*. (2024) 39:546–55. doi: 10.1016/j.virs.2024.06.005

63. Alvarez J, Boklund A, Dippel S, Dórea F, Figuerola J, Herskin MS, et al. Preparedness, prevention and control related to zoonotic avian influenza. *EFSA J*. (2025) 23:e9191. doi: 10.2903/j.efsa.2025.9191

64. Zhu W, Yang L, Han X, Tan M, Zou S, Li X, et al. Origin, pathogenicity, and transmissibility of a human isolated influenza a (H10N3) virus from China. *Emerg Microbes Infect*. (2025) 14:2432364. doi: 10.1080/22221751.2024.2432364

65. Chrzastek K, Lee DH, Gharaibeh S, Zsak A, Kapczynski DR. Characterization of H9N2 avian influenza viruses from the Middle East demonstrates heterogeneity at amino acid position 226 in the hemagglutinin and potential for transmission to mammals. *Virology*. (2018) 518:195–201. doi: 10.1016/j.virol.2018.02.016

66. Gu M, Xu L, Wang X, Liu X. Current situation of H9N2 subtype avian influenza in China. *Vet Res*. (2017) 48:49. doi: 10.1186/s13567-017-0453-2

67. Paules CI, Lakdawala S, McAuliffe JM, Paskel M, Vogel L, Kallewaard NL, et al. The hemagglutinin a stem antibody MEDI8852 prevents and controls disease and limits transmission of pandemic influenza viruses. *J Infect Dis*. (2017) 216:356–65. doi: 10.1093/infdis/jix292

Frontiers in Public Health

Explores and addresses today's fast-moving healthcare challenges

One of the most cited journals in its field, which promotes discussion around inter-sectoral public health challenges spanning health promotion to climate change, transportation, environmental change and even species diversity.

Discover the latest Research Topics

See more →

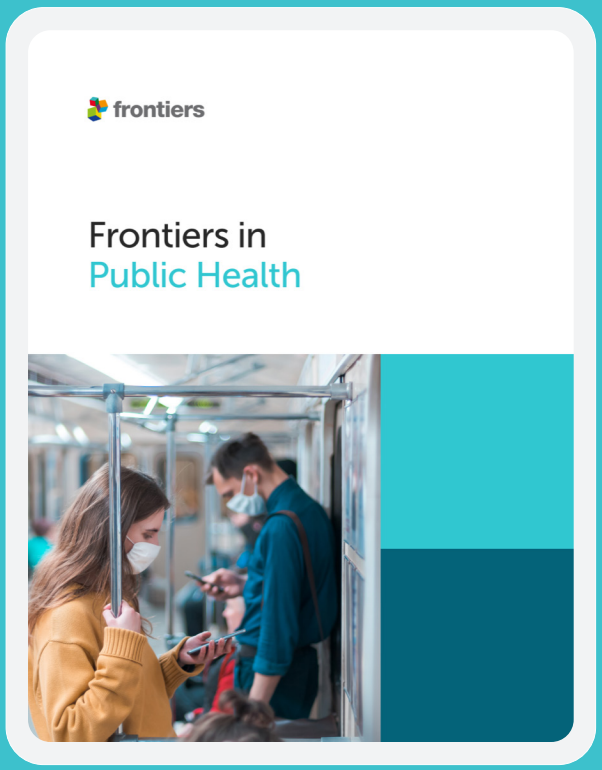

Frontiers

Avenue du Tribunal-Fédéral 34
1005 Lausanne, Switzerland
frontiersin.org

Contact us

+41 (0)21 510 17 00
frontiersin.org/about/contact